

Investigations in Two-Dimensional
Quantum Field Theory
by the Bootstrap and TCSA Methods

Ph.D. thesis

Gábor Zsolt Tóth

Supervisor: Professor László Palla, D.Sc.

Eötvös University, Budapest
Physics Doctoral School
Particle Physics and Astronomy program
Doctoral School leader: Zalán Horváth
Program leader: Ferenc Csikor

Theoretical Physics Research Group of the
Hungarian Academy of Sciences,
Theoretical Physics Department
Eötvös University, Budapest

2006

Contents

| | | |
|----------|---|-----------|
| 1 | Introduction | 5 |
| 1.1 | N=1 supersymmetric boundary bootstrap | 6 |
| 1.2 | Truncation effects in the boundary flows of the Ising model on a strip . . . | 10 |
| 1.3 | A nonperturbative study of phase transitions in the multi-frequency sine-Gordon model | 15 |
| 2 | On N=1 supersymmetric boundary bootstrap | 19 |
| 2.1 | Factorized scattering theory | 19 |
| 2.2 | Factorized scattering theory with a boundary | 33 |
| 2.3 | The bootstrap method | 46 |
| 2.4 | The supersymmetry algebra in 1+1 dimensions | 49 |
| 2.4.1 | Representations of the supersymmetry algebra | 50 |
| 2.5 | The boundary supersymmetry algebra in 1+1 dimensions | 55 |
| 2.5.1 | Representations of the boundary supersymmetry algebra | 57 |
| 2.6 | Supersymmetric factorized scattering | 58 |
| 2.6.1 | Ansatz for the supersymmetric scattering theory | 58 |
| 2.6.2 | Ansatz for the supersymmetric scattering theory in the presence of a boundary | 60 |
| 2.6.3 | Supersymmetric bootstrap | 62 |
| 2.6.4 | Supersymmetric S-matrix factors | 63 |
| 2.6.5 | Supersymmetric reflection matrix factors | 67 |
| 2.6.6 | Properties of the ground state reflection matrix factors | 71 |
| 2.6.7 | Higher level supersymmetric boundary states | 73 |
| 2.7 | Examples | 79 |
| 2.7.1 | Boundary sine-Gordon model | 79 |
| 2.7.2 | Boundary sinh-Gordon model | 81 |
| 2.7.3 | Free particle on the half-line | 82 |
| 2.7.4 | Boundary affine Toda field theories | 83 |

| | | |
|----------|--|------------|
| 2.8 | Discussion | 87 |
| 2.9 | Appendix | 89 |
| 3 | Truncation effects in the boundary flows of the Ising model on a strip | 91 |
| 3.1 | On the definition of field theories on the strip | 91 |
| 3.2 | Unitary representations of the Virasoro algebra | 93 |
| 3.2.1 | Primary fields | 94 |
| 3.2.2 | $c=1/2$ | 95 |
| 3.3 | Conformal field theory on the strip | 96 |
| 3.3.1 | Boundary conditions of the minimal models | 98 |
| 3.3.2 | Boundary flows | 99 |
| 3.4 | The Truncated Conformal Space Approach | 100 |
| 3.4.1 | TCSA for perturbed conformal field theory on the strip | 101 |
| 3.5 | Exact spectrum | 103 |
| 3.5.1 | Distributions on closed line segments | 103 |
| 3.5.2 | The free model | 105 |
| 3.5.3 | The perturbed model | 109 |
| 3.5.4 | Reverse description | 116 |
| 3.5.5 | Bethe-Yang equations | 119 |
| 3.6 | Exact spectrum in the Mode Truncated version | 121 |
| 3.6.1 | The free model | 121 |
| 3.6.2 | The perturbed model | 122 |
| 3.7 | Power series expansion of the energy levels | 124 |
| 3.8 | Perturbative results | 128 |
| 3.8.1 | Mode Truncation Scheme | 129 |
| 3.8.2 | TCS scheme | 130 |
| 3.9 | Numerical results | 131 |
| 3.9.1 | Mode Truncation Scheme | 131 |
| 3.9.2 | TCS scheme | 139 |
| 3.10 | Scaling properties of the s_1/s_0 , s_1 and s_0 functions | 147 |
| 3.11 | Discussion | 148 |
| 4 | A nonperturbative study of phase transitions in the multi-frequency sine-Gordon model | 151 |
| 4.1 | The multi-frequency sine-Gordon model | 151 |
| 4.2 | The Truncated Conformal Space Approach for the multi-frequency sine-Gordon model | 153 |

| | | |
|-------------------------|--|------------|
| 4.3 | Phase structure in the classical limit | 155 |
| 4.3.1 | Phase structure of the two-frequency model in the classical limit . . | 155 |
| 4.3.2 | Phase structure of the three-frequency model in the classical limit . | 157 |
| 4.3.3 | n -frequency model in the classical limit | 159 |
| 4.4 | Signatures of 1st and 2nd order phase transitions in finite volume | 159 |
| 4.5 | The phase diagram of the two-frequency model in the case $\frac{\alpha}{\beta} = \frac{1}{3}$, $\delta = \frac{\pi}{3}$. . | 161 |
| 4.6 | Phase diagram of the three-frequency model | 167 |
| 4.6.1 | The tricritical point | 168 |
| 4.6.2 | The critical line | 170 |
| 4.6.3 | The line of first order transition | 173 |
| 4.7 | Discussion | 176 |
| Acknowledgements | | 177 |
| Bibliography | | 179 |
| Abstract | | 191 |

Chapter 1

Introduction

Relativistic quantum field theory in two space-time dimensions has important role in physics, for example in the branches of string theory and statistical mechanics. It has also played important role in the development of a non-perturbative understanding of quantum field theory in general. In the latter respect massive integrable models and conformal field theory attract most interest, as they usually allow the exact determination of several physical quantities. Since W. Thirring proposed the first exactly solvable quantum field theoretical model in 1958 [1] and J. Schwinger presented the exact solution of Quantum Electrodynamics in 1+1 dimensions [2, 3], a remarkable complexity and richness of the non-perturbative structure of relativistic quantum field theories has been revealed. In the field of the two-dimensional models of statistical physics, which are closely related to two-dimensional quantum field theory, H. Bethe's results [4] in 1931 and L. Onsager's solution of the Ising model in 1943 [5] can be regarded as the beginning of the study of integrable models.

In massive integrable field theories the spectrum, S-matrix and the form factors of local operators can often be determined exactly, mainly by means of the bootstrap method. This is a feature that deserves high appreciation in itself, regarding the difficulty of making non-perturbative statements about these quantities in general.

The bootstrap programme for the spectrum and S-matrix proves to be manageable in integrable quantum field theory because the existence of higher spin conserved quantities, which is the criterion of integrability, severely constrains the scattering theory. The special kind of scattering theory related to integrable models is called factorized scattering theory. The bootstrap programme for form factors in integrable quantum field theory formulated in [6, 7, 8] is also based on factorized scattering.

Conformal field theory in two dimensions is a distinct branch of quantum field theory which has important role in string theory and in the description of physical systems at

critical points. A remarkable feature of the conformal symmetry algebra is that it is infinite dimensional in two space-time dimensions, therefore it imposes very severe constraints on the spectrum and correlation functions of conformally symmetric theories.

A link between massive integrable models and conformal field theory also exists: two dimensional quantum field theories can generally be regarded as conformal field theories perturbed by suitable operators [9, 10, 11]. Certain perturbations preserve a part of the conformal symmetry and render the perturbed theory integrable. This perturbed conformal field theory framework also serves as a basis for useful approximation methods like the conformal perturbation theory or the TCSA (truncated conformal space approach).

In this thesis we study problems in three areas of two-dimensional quantum field theory, especially integrable and conformal field theory. In accordance with this, the thesis is divided into three chapters, apart from the introduction. The investigations in the three chapters are largely independent, although certain connections between them exist.

The three areas, the particular problems and the contents of the chapters are introduced in the next sections.

The results of Chapter 2, 3 and 4 have been published in

- G.Zs. Tóth, N=1 boundary supersymmetric bootstrap, *Nucl. Phys.* **B676**, 2003, 497-536, hep-th/0308146
- G.Zs. Tóth, A Study of truncation effects in boundary flows of the Ising model on a strip, *J. Stat. Mech.* P04005, 2007, hep-th/0612256
- G.Zs. Tóth, A non-perturbative study of phase transitions in the multi-frequency sine-Gordon model, *J. Phys.* **A37**, 2004, 9631-9650, hep-th/0406139.

1.1 N=1 supersymmetric boundary bootstrap

The description of certain physical phenomena demands two-dimensional boundary quantum field theories, i.e. quantum field theories defined on manifolds with boundaries. Examples for such phenomena are impurity effects like the Kondo effect [14, 15], junctions in quantum wires, absorption of polymers on a surface and transport properties of Luttinger liquids [16]. (See also the introduction of [17] and [70]. A review can also be found in [18].) Boundary quantum field theory is important in open string theory as well.

In Chapter 2 we consider massive quantum field theories with one boundary, i.e. boundary quantum field theory defined on the space-time $(-\infty, 0] \times \mathbb{R}$. In these bound-

ary quantum field theories the role of the S-matrix is taken over by the reflection matrix (describing the bouncing back of the particles from the boundary) and in addition to the particles the spectrum contains states —called boundary bound states— which are localized at the boundary. The interior of the space $(-\infty, 0)$ is referred to as the bulk. Boundary field theories can usually be derived, especially at the classical level, from ordinary field theories by imposing a boundary condition. For integrable theories (without boundary) it is often possible to find boundary conditions which preserve the integrability in a sense described in [19]. In this case the scattering theory of the boundary model will be a factorized boundary scattering theory [19]. It should be noted that a factorized boundary scattering theory incorporates a (bulk) factorized scattering theory, the factorized scattering theory of the bulk part of the model under consideration. The complete procedure of the calculation of the S-matrix and reflection matrix and the full particle and boundary state spectrum of an integrable model (in the presence of a boundary) generally consists of several subsequent steps. Usually the bulk part is completed first, then the ground state reflection matrix is determined, and finally the spectrum of the higher level boundary states and the reflection matrix blocks on these boundary states are obtained.

The full reflection matrix and the spectrum of boundary states are known only for a few integrable models so far. The list of these models include the sine-Gordon model [20, 21, 22], $a_2^{(1)}$ and $a_4^{(1)}$ affine Toda field theories [23], the free boson on the half-line and the sinh-Gordon model [24, 25].

It is a further step to calculate the form factors of the local operators. The generalization of the form factor program to the boundary case has been proposed [26] (see also [27, 28, 29]) only recently. In [26] the minimal form factors of the boundary operators of the free boson, free fermion, Lee-Yang and sinh-Gordon models with certain boundary conditions have been investigated.

A formalism for constructing supersymmetric factorized scattering theories from non-supersymmetric factorized scattering theories is developed in [30, 31, 32, 33, 34]. This consists mainly of replacing the particles by supermultiplets and multiplying the S-matrix blocks by suitable supersymmetric factors. These supersymmetric S-matrix factors satisfy the axioms of factorized scattering theory in themselves with certain modifications.

An essential step in the construction is the choice of the supersymmetry representations in which the new particle multiplets will transform, this choice must be compatible with the fusion rules of the non-supersymmetric theory. If the possible representations in which the particles may transform are fixed, then by solving the axioms one can derive necessary and sufficient conditions that have to be satisfied by the particle spectrum and fusion rules of a non-supersymmetric theory to which one wants to apply the construction. Such

conditions have been obtained in the case when the possible representations are the kink and the boson-fermion representations [34], and several factorized scattering theories—the $a_{n-1}^{(1)}, d_n^{(1)}, (c_n^{(1)}, d_{n+1}^{(2)})$ and $(b_n^{(1)}, a_{2n-1}^{(2)})$ affine Toda theories and the sine-Gordon model—have been found to satisfy these conditions [34]. However, the Lagrangian field theories underlying the corresponding supersymmetric scattering theories are not known in every cases. The supersymmetric $SU(2)$ principal chiral model, the supersymmetric $O(2n)$ sigma model [34] and the multicomponent supersymmetric Yang-Lee minimal models (or supersymmetric FKM models) [35] have also been found to fit in the framework described in [34].

In Chapter 2 we study the construction above in the presence of a boundary. For this a concept of supersymmetry in the presence of a boundary is needed, the description of which is an important part of Chapter 2. Assuming that the supersymmetrization of the bulk part is already done, the first step of the construction is the choice of a representation of the boundary supersymmetry algebra for the ground state. Next the supersymmetric factors for the ground state one-particle reflection matrix should be determined using the boundary Yang-Baxter, unitarity and crossing symmetry equations, analyticity requirements and the supersymmetry condition for these factors. Finally the boundary bootstrap and fusion equations for supersymmetric factors can be used to obtain the representations in which the excited boundary bound states transform together with the supersymmetric factors of the one-particle reflection matrix on these states. The first and especially the second steps have been considered in the literature [36, 35, 37, 38, 39, 40], whereas the last step has been completed only in the case of the sine-Gordon model [36]. Our main purpose, motivated by [34] and [36], is to generalize the result of [36] and formulate rules that can be applied to any particular model. We assume that the particles in the bulk transform either in the kink or in the boson-fermion representation, mainly because this is the simplest and most natural choice, and this is the case for which the necessary results (concerning the bulk part and the first two steps) are sufficiently developed in the literature.

For the ground state we take the singlet representations with RSOS label $\frac{1}{2}$, this being the simplest case (see also Section 2.5.1). The general maximally analytic supersymmetric one-particle ground state reflection factors have been determined for this case in [38, 39, 40], but without imposing the supersymmetry condition. We rederive these reflection factors imposing the supersymmetry condition at the beginning, which simplifies the calculation considerably.

As the main result of Chapter 2 we present rules for the determination of the representations and supersymmetric one-particle reflection factors for excited boundary bound

states. It should be considered that in general there are several ways to generate a higher level boundary state by fusion, and it is not obvious that our rules give the same representations and supersymmetric factors for each way. We verify this statement in specific models and present an argument that it can be expected to hold generally. In particular, we complete the verification of the statement for the boundary sine-Gordon model started in [36]. The other examples to which we apply our rules are the boundary $a_2^{(1)}$ and $a_4^{(1)}$ affine Toda field theories [23], the free boson on the half-line and the boundary sinh-Gordon model [24, 25].

In Section 2.1 and 2.2 we review factorized scattering theory in the bulk and in the presence of a boundary. The main characteristics are presented as axioms, we refer the reader to other reviews [41, 42, 43, 21, 44, 45, 46] and the articles [47, 19] for their derivation or explanation. In our review we emphasize the linear algebraic structure of the axioms of factorized scattering theory. The main reason for this approach is that we found this linear algebraic form much more suitable for dealing with our problem than the component based form. Our review also includes a discussion of symmetries and the construction of representations on multi-particle states, i.e. the multiplication of representations. In the boundary case it is not entirely obvious what the proper algebraic formulation is. We adopt the structure described in [48, 49]. We remark that we describe the correspondence between the Coleman-Thun diagrams and the singularities of the S-matrix only briefly.

In Section 2.3 we outline the bootstrap procedure usually followed to find solutions to the axioms of factorized scattering theory.

In Section 2.4 we describe the supersymmetry algebra in 1+1 dimensions, the multiplication of representations and the construction of multi-particle representations from one-particle representations, and the one-particle representations which we use. We also discuss the vacuum representation and the decomposition of products of representations.

In Section 2.5 we describe the supersymmetry algebra in 1+1 dimensions in the presence of a boundary, the construction of multi-particle representations and the one-dimensional representations for the ground state. Our formulation differs from the formulations that can be found in the literature in that we apply the algebraic structure proposed in [48, 49].

In Section 2.6.1 we describe the ansatz for constructing supersymmetric factorized scattering theory.

In Section 2.6.2 we describe the extension of the construction to the case when a boundary is also present.

In Section 2.6.3 we describe the bootstrap procedure for the supersymmetric factors

briefly.

In Section 2.6.4 we discuss the particular supersymmetric S-matrix factors for kinks and boson-fermion states, their important linear algebraic properties, supersymmetry properties, the bootstrap structure and fusion rules. The discussion of the bootstrap structure and the fusion rules are based on the results of [34], which we have brought to a new form.

In Section 2.6.5 the supersymmetric ground state reflection matrix factors and their most important linear algebraic, singularity, supersymmetry and bootstrap properties are described.

In Section 2.6.7 we describe the boundary supersymmetric bootstrap structure, i.e. the supersymmetric boundary fusion rules and the supersymmetric reflection factors on higher level supersymmetric boundary states. These are the main results of Chapter 2.

In Section 2.7 we present examples for the application of the fusion rules described in Section 2.6.7.

The Appendix (Section 2.9) contains the normalization factors for the S-matrix and reflection matrix factors.

Chapter 2, especially the sections 2.4-2.9, is largely based on the paper [12], nevertheless several parts have been rewritten.

1.2 Truncation effects in the boundary flows of the Ising model on a strip

Chapter 3 is devoted to an investigation of the method called TCSA (truncated conformal space approach), which is a numerical method for the calculation of the spectra and eigenvectors of Hamiltonian operators of the form $H = H_0 + hH_I$, where H_0 has a known discrete spectrum, h is a coupling constant. This method is applied mainly to two-dimensional quantum field theories in finite volume formulated as perturbed conformal field theories. An advantage of the TCSA is that integrability is not necessary for its applicability. Application to theories in higher space-time dimensions is also possible in principle. The uses of the data obtained by TCSA include the verification of results obtained by other methods, example in [50], the extraction of resonance widths [51], the mapping of the phase structure of certain quantum field theories as in [52] and in Chapter 4, and the finding of renormalization group flow fixed points as in [53]. These last two uses are similar. Our investigation in this chapter is related to the use of TCSA for the study of renormalization group flows between minimal boundary conformal field theories.

Boundary conformal field theory is defined on surfaces with boundaries, e.g. on the

strip $[0, L] \times \mathbb{R}$, which is the case that we consider. A brief review of the areas where boundary conformal field theory plays important role can be found in [54]: it provides the framework for a world sheet analysis of D-branes in string theory, it also has applications to various systems of condensed matter physics such as the three-dimensional Kondo effect [15], fractional quantum Hall fluids (see e.g. [16]) and other quantum impurity problems.

A boundary flow is a one-parameter family of models, the parameter being the width (or volume) L of the strip. In the simplest case the parameter can be taken to be a coupling constant h instead of L and the models have the Hamiltonian operators $H = H_0 + hH_I$. H_0 is the Hamiltonian operator of a boundary conformal field theory, h is allowed to vary from 0 to ∞ or from 0 to $-\infty$. H_I is a relevant boundary field taken at a certain initial time. The study of such flows or deformations away from the critical point should provide some insight into the structure of the space of boundary theories. Such deformations are also important in string theory (see the introduction of [54]) and they may have applications in condensed matter physics. A particular problem of interest is that of finding values of h other than 0, called fixed points, where the model corresponding to $H_0 + hH_I$ is a conformal field theory, and identifying these conformal field theories. The TCSA can be used for this purpose if the Hilbert space of the conformal field theory corresponding to $h = 0$ consists of finitely many (or countably many) irreducible representations of the Virasoro algebra. Boundary conformal minimal models satisfy this condition. These boundary minimal models can be obtained from the usual (bulk) minimal models by imposing suitable conformal boundary conditions. Regarding the spectra at nonzero values of h , conformal symmetry can be recognized by the equal distances between neighbouring energy levels; the representation content can be identified by the degeneracy of the energy levels. It should be noted that perturbation theory and other methods can also be used [54, 55, 56, 57, 58] to explore flows. An important problem regarding the TCSA is that it gives approximate data, and our knowledge of the precise relation between this data and the exact spectrum is still limited (see [59] for already existing results). A good understanding of the effect of the truncation could be used to improve the TCSA data and to explain the qualitative features of TCSA pictures of flows, and generally it would make the results obtained using TCSA data better founded.

An idea proposed by G.M.T. Watts and K. Graham [60, 61] is that the effect of the truncation on the spectrum can be taken into consideration by a suitable change of the coefficients of the terms in H , i.e. the spectrum of H^{TCSA} (H^{TCSA} is the finite approximating Hamiltonian operator used in the TCSA method) is equal, in certain approximation at least, to the spectrum of

$$H^r = s_0(h, n_c)H_0 + s_1(h, n_c)H_I + s_2(h, n_c)H_{I,2} + \dots, \quad (1.1)$$

which we shall call renormalized Hamiltonian operator. n_c is the truncation parameter, s_0, s_1, \dots are suitable functions and $H_{I,2}, \dots$ are suitable operators. $H_{I,2}, \dots$ should be primary or descendant bulk or boundary operators. Our main purpose in Chapter 3 is to investigate the validity of this picture.

We consider the perturbed boundary conformal field theory on the strip $[0, L] \times \mathbb{R}$ with Hamiltonian operator

$$H = \frac{\pi}{L}L_0 + hL^{-1/2}\phi_{1/2}(x = L, t = 0) . \quad (1.2)$$

The unperturbed model is the $c = 1/2$ unitary conformal minimal model, i.e. the continuum limit of the critical Ising model, with the Cardy boundary condition 0 on the left and 1/16 on the right. $\frac{\pi}{L}L_0$ is the Hamiltonian operator of this model. L_0 is the ‘zero index’ Virasoro generator. L will be kept fixed at the value $L = 1$. The Hilbert space of the unperturbed model is the single $c = 1/2$, $h = 1/16$ irreducible highest weight representation of the Virasoro algebra. (Here and in Chapter 3 the coupling constant and the highest weight are both denoted by h , but it should be clear from the context which one is meant.) It should be noted that a whole series of similar boundary conformal minimal models exist, they can be obtained from other unitary minimal models by imposing boundary conditions. Imposing the 0 boundary condition on one side and another Cardy boundary condition on the other side always results in that the Hilbert space consists of a single irreducible representation. The field $\phi_{1/2}(L, t)$ is the weight 1/2 boundary primary field on the right boundary, which is also known in the literature as the boundary spin operator [62, 63, 19]. The normalization of $\phi_{1/2}$ is given by $\langle 1/16 | \phi_{1/2}(L, 0) | 1/16 \rangle = 1$, where $|1/16\rangle$ is the highest weight state, $\langle 1/16 | 1/16 \rangle = 1$. The coupling constant h can also be regarded as a constant external boundary magnetic field, which is coupled to the boundary spin operator. The model (1.2) is also referred to as the critical Ising model on a strip with boundary magnetic field. The perturbation $h\phi_{1/2}(L, t = 0)$ violates the conformal symmetry, which is nevertheless restored in the $h \rightarrow \pm\infty$ limit. It is known that in the $h \rightarrow \infty$ limit the $c = 1/2, h = 1/2$ representation is realized; in the $h \rightarrow -\infty$ limit the $c = 1/2, h = 0$ representation is realized (see e.g. [64, 19, 56, 55]). This can be written in a shorthand form as

$$(1/2, 1/16) + \phi_{1/2} \rightarrow (1/2, 1/2) \quad (1.3)$$

$$(1/2, 1/16) - \phi_{1/2} \rightarrow (1/2, 0) . \quad (1.4)$$

We have chosen the model (1.2) because it is integrable, furthermore it is relatively easy to handle; in particular the spectrum can be calculated analytically in terms of simple functions and the application of Rayleigh-Schrödinger perturbation theory is also relatively easy. Investigations in other perturbed conformal minimal models, especially in the

case of the tricritical Ising model and generally in the case of a perturbation by the field $\phi_{(13)}$, are carried out in [65] (see also [61]).

It should be noted that the Ising model with boundary magnetic field has been studied much, especially on the lattice and on the half-line. We refer the reader to [66, 17, 67, 19] and the references in them for further information.

To recognize conformal symmetry and to identify the representation content it is sufficient to look at the ratios of the energy gaps; therefore one often considers normalized spectra which are obtained by subtracting the ground state energy and dividing by the lowest energy gap. The normalized exact and TCSA spectra for the flows (1.3), (1.4) as a function of the logarithm of h can be seen in Figure 3.9. An interesting feature of these TCSA spectra is that they appear to correspond to the flows $(1/2, 1/16) \rightarrow (1/2, 1/2) \rightarrow (1/2, 1/16)$ and $(1/2, 1/16) \rightarrow (1/2, 0) \rightarrow (1/2, 1/16)$, i.e. second flows appear to be present after the normal flows. Flows in models similar to (1.2) mentioned above also show this behaviour. One application of the picture (1.1) could be the explanation of this phenomenon.

Following G.M.T. Watts' proposal based on the look of the TCSA spectra shown in Figure 3.9 we assume that only the first two terms are nonzero in (1.1):

$$H^r = s_0(h, n_c)H_0 + s_1(h, n_c)H_I . \quad (1.5)$$

In summary, in Chapter 3 we look for answers for the following questions: 1. Does the spectrum of (1.5) agree with the TCSA spectrum in some approximation with a suitable choice of the functions s_0 and s_1 ? 2. How can we explain the 'second' flows in the TCSA spectra?

The main difficulty we encounter is that it is hard to handle the TCSA spectra analytically even if the nontruncated model is exactly solvable. Therefore, hoping that we can gain some insight by looking at a similar but exactly solvable truncation method, we tried another truncation method which we call mode truncation. The mode truncated model can be solved exactly, but it turns out, rather unexpectedly, that the behaviour of the spectrum for large values of h is different from the behaviour of the TCSA spectrum, namely the qualitative behaviour of the mode truncated spectrum is very similar to that of the exact spectrum; the second flows are not present. This, besides leaving the second question open, raises the problem of finding the possible behaviours for large values of h and their dependence on the truncation method, and whether the mode truncation method can be generalized to other models.

We also applied the Rayleigh-Schrödinger perturbation theory to verify the validity of (1.5) for both the TCSA and mode truncation methods. In the mode truncation scheme, using the exact analytic expressions for the eigenvalues, we also obtained a result that is non-perturbative in h and perturbative in $1/n_c$.

The third calculation that we did is a numerical comparison of the exact and TCSA and the exact and mode truncated spectra. The TCSA calculation was done by a program written entirely by ourselves.

We determined the exact spectrum using an essentially known (see e.g. [19, 67, 66, 68, 69, 70]) quantum field theoretic representation of the operator (1.2). In this representation the operator (1.2) is a quadratic expression of fermionic fields. We extracted the spectrum from the field equations which are linear. Besides the spectrum we also considered the interacting fermion fields and their matrix elements, and certain other issues. The field theoretic approach also raises the problem of defining distributions (or similar objects) on a closed interval. We do not know of a systematic exposition of this subject (neither for a closed interval nor for the half-line), although it would be needed for boundary field theory. In this thesis we use distributions on closed intervals, nevertheless we restrict to the most necessary formulae only and do not work out a complete theory.

The field theoretic model mentioned above was studied in [68] and especially in [66] (at finite temperature). Our approach and aim are different, however, and the overlap between the results of [66] and our results is only partial. Our quantum field theoretic calculations are partially independent of the problem of the TCSA approximation. Some of these calculations are included only because we think that they are generally interesting from the point of view of quantum field theory.

We propose a description of (1.2) as a perturbation of the $\hbar \rightarrow \pm\infty$ limiting case, which cannot be found in the literature. An interesting feature of this description, which we call reverse description, is that the perturbing operator is non-relevant. We calculate the exact spectrum in a similar way as in the case of the standard description mentioned above.

We also present the description of the spectrum using the Bethe-Yang equations, which give the exact result in this case.

We treat the mode truncated model along the same lines as the nontruncated model, we restrict to the spectrum in this case, however.

We remark that our TCSA program relies on the conformal transformation properties only and does not make use of the representation mentioned above, therefore it can be used with other values of the central charge, highest weight and weight of the perturbing field.

The contents of Chapter 3 are the following:

In Sections 3.1-3.4 definitions and other introductory information are collected, which is followed by the presentation of the results in Sections 3.5-3.9.

In Section 3.1 the definition of quantum field theory on a strip is discussed briefly.

In Section 3.2 we describe certain well known results in conformal field theory which are important for our work.

In Section 3.3 we give a basic definition of conformal field theory on a strip. We restrict to those elements which are essential for our work. We refer the reader to [71, 72, 73] for more advanced exposition. In Subsection 3.3.2 we give a definition of flows.

In Section 3.4 we describe TCSA in general and its application to the type of models that we consider.

Section 3.5 contains the field theoretical description of the model (1.2), in particular the calculation of the exact spectrum. Results concerning the boundary conditions, the normalization of interacting creation and annihilation operators, the relation between free and interacting creation and annihilation operators, matrix elements of the interacting fields, nontrivial identities for the Dirac-delta and the expression of eigenstates in terms of the unperturbed eigenstates are obtained. The section also contains the reverse description of the model and the description of the spectrum using the Bethe-Yang equations. It is found that the latter gives exact result in this case.

Section 3.6 contains the description of the mode truncated model and the calculation of its spectrum.

Section 3.7 contains the power series for the exact, TCSA and mode truncated energy levels up to third order in \hbar obtained by the Rayleigh-Schrödinger perturbation theory.

Section 3.8 contains the perturbative results for the s_0 and s_1 functions.

Section 3.9 contains the results of the numerical test of the approximation by (1.5) for the TCSA and the mode truncation schemes.

Section 3.10 contains a description of the scaling properties, i.e. the truncation level dependence of the s_0 , s_1 , s_1/s_0 functions.

The results of Chapter 3 have been published in [74].

1.3 A nonperturbative study of phase transitions in the multi-frequency sine-Gordon model

In Chapter 4 we present an application of the TCSA to the mapping of the phase structure of the multi-frequency sine-Gordon model.

The sine-Gordon model has attracted interest long time ago for the reason that it appears in several areas of physics, and it is an integrable field theory. The areas of application include statistical mechanics of one-dimensional quantum spin chains and nonlinear optics among many others —see the introduction of [75] for a list with references.

The multi-frequency sine-Gordon model is a non-integrable extension of the sine-Gordon model in which the scalar potential consists of several cosine terms with different frequencies. It is suggested in [75] that this model can be used to give more refined approximation to some of the physical situations where the ordinary sine-Gordon model can be used. A feature of the multi-frequency model that is new compared to the usual sine-Gordon model is —apart from non-integrability— that phase transition can occur as the coupling constants are tuned. We concentrate our attention to this property. Such a phase transition is related to the evolution of the spectrum of the theory as the coupling constants vary. In accordance with this we shall use the massgap and other characteristics of the energy spectrum to identify the different phases.

Our investigation can be regarded as a continuation of the work done on the double-frequency case in [52]. We use the truncated conformal space approach (TCSA); the applicability and reliability of this method was thoroughly investigated in [52] and it was shown that the existence, nature and location of the phase transition can be established by this method, although rather large truncated space is needed for satisfactory precision. In particular, the existence and location of an Ising type transition was established in the double-frequency model (DSG) for the ratio $1/2$ of the frequencies, verifying a prediction by [75] based on perturbation theory and classical field theoretic arguments. We extend these investigations to the ratio $1/3$ and to the three-frequency model (at the ratio $1/2/3$ of the frequencies), in which a tricritical point and first order transition are expected to be found. The numerical nature of the TCSA makes it necessary to choose specific values for the frequencies.

We remark that the calculations of Chapter 4 were completed before the work presented in Chapter 3 was done.

The contents of Chapter 4 are the following:

In Section 4.1 we introduce the multi-frequency sine-Gordon model and describe basic properties of it.

In Section 4.2 we briefly review the formulation of the model in the perturbed conformal field theory framework (for the two-frequency case this can be found in [52], the extension to the multi-frequency model is straightforward), which is necessary for the application of the TCSA.

In Section 4.3 we give a description of the phase structure of the classical two- and three-frequency model, which serves as a reference for the investigations in quantum theory. The n -frequency case is also considered briefly. Exact and elementary analytic methods can be applied to the classical case, and the results are more general than in the quantum case.

Section 4.4 is devoted to theoretical considerations on the signatures of 1st and 2nd order phase transitions in the framework of perturbed conformal field theory in finite volume. Most of these considerations, which are necessary for the evaluation of the TCSA data, can also be found in [52].

In Section 4.5 and 4.6 we present the results we obtained by TCSA on the phase structure of the two- and three-frequency model, which are the main results of Chapter 4. The calculations were done by a program written by L. Palla, Z. Bajnok, G. Takács and F. Wágner on which we performed certain modifications.

Chapter 4 is based on the article [13].

Finally, we list a selection of books, articles and PhD theses which can be used as references:

- Two-dimensional quantum field theory: [43]
- Factorized scattering theory: [41, 42, 43, 21, 44, 45, 46, 47, 19]
- Factorized scattering theory in the presence of a boundary: [19, 21]
- Form factor bootstrap programme: [6, 76, 77, 44]
- Form factor bootstrap programme in the presence of a boundary: [26]
- Conformal field theory: [73, 46, 78]
- Boundary conformal field theory: [71, 73, 46, 62, 63, 79, 80, 81, 82, 83, 84, 85, 119]
- Flows: [86, 87, 88, 56, 42, 89]

Chapter 2

On $N=1$ supersymmetric boundary bootstrap

2.1 Factorized scattering theory

Factorized scattering theory describes collisions of quantum particles or particle-like quantum objects (e.g. solitons) which travel in $1+1$ dimensional space-time. We shall consider relativistic scattering theory of finitely many massive particles. Specific factorized scattering theories are usually associated to integrable relativistic quantum field theories which are characterized by the existence of higher spin conserved quantities.

The main constituents of scattering theory in general is a Hilbert space of asymptotic states of the particles, an operator S on the Hilbert space describing the scattering of particles, a representation of the Poincare group on the Hilbert space with respect to which S is equivariant, and representations of further possible symmetry algebras.

The characteristics of factorized scattering are listed and explicitly described below. Some of these properties are special to factorized scattering theory, others (like unitarity) are general properties of scattering theory applied to factorized scattering theory.

Factorized scattering theory is characterized by the following properties:

- 1) The particle number is conserved.
- 2) The sets of incoming and outgoing momenta are equal.

3) Factorization and Yang-Baxter equation: An arbitrary N -particle scattering process can be described as a sequence of 2-particle collisions, all possible descriptions (of which there are $N(N-1)/2$) are equivalent. The most interesting quantity in factorized

scattering theory is therefore the two-particle S-matrix block that describes the 2-particle collisions.

The momentum (p_0, p_1) of a free particle of mass m satisfies $p_0^2 - p_1^2 = m^2$, $p_0 > 0$. Instead of p_0 and p_1 one often uses m and the rapidity parameter Θ :

$$p_0 = m \cosh(\Theta) , \quad p_1 = m \sinh(\Theta) .$$

The physical values Θ are the real numbers, however it is useful to allow complex values (i.e. $\Theta \in \mathbb{C}$) unless there is a reason to restrict to real values.

The asymptotic in and out states are denoted in the following way:

$$|a_1(\Theta_1)a_2(\Theta_2)\dots a_N(\Theta_N)\rangle_{in/out} \quad (2.1)$$

where $\Theta_1 \geq \Theta_2 \geq \dots \geq \Theta_N$ for in states and $\Theta_1 \leq \Theta_2 \leq \dots \leq \Theta_N$ for out states.

The Hilbert space can be written as a sum of N -particle subspaces:

$$\mathcal{H} = \oplus_{N=0}^{\infty} \mathcal{H}_N$$

where \mathcal{H}_0 is the vacuum subspace, which is a finite dimensional space in general.

The N -particle Hilbert space can be written as

$$\mathcal{H}_N = \underbrace{\mathcal{H}_1 \otimes \mathcal{H}_1 \otimes \dots \otimes \mathcal{H}_1}_N .$$

\mathcal{H}_N can be decomposed into a (not direct) sum of spaces of in, out and intermediate states:

$$\mathcal{H}_N = \mathcal{H}_{N,in} + \mathcal{H}_{N,out} + \mathcal{H}_{N,intermed}$$

for $N \geq 3$, for $N = 0$ and $N = 1$ we have

$$\mathcal{H}_{0,in} = \mathcal{H}_{0,out} , \quad \mathcal{H}_{1,in} = \mathcal{H}_{1,out}$$

and there are no intermediate states for $N = 0, 1, 2$.

The space of intermediate states is spanned by those elements of the form (2.1) which do not satisfy the ordering prescription for in and out states.

The notation in (2.1) means

$$a_1(\Theta_1) \otimes a_2(\Theta_2) \otimes \dots \otimes a_N(\Theta_N) \quad (2.2)$$

where $a_i(\Theta_i) \in \mathcal{H}_1$ are one-particle states.

\mathcal{H}_1 can be written as

$$\mathcal{H}_1 = \int_{\Theta \in \mathbb{R}} d\Theta V(\Theta)$$

where $V(\Theta)$ is a finite dimensional vector space for any fixed value of Θ . $\Theta \in \mathbb{C}$ can also be allowed, but we do not introduce further notation for this case.

The action of a boost $B(\Theta)$ of rapidity Θ is

$$B(\Theta)a(\Theta_1) = a(\Theta_1 + \Theta) .$$

We introduce a finite dimensional vector space V with a basis labeled by a which also labels the particles, and the linear map $i_\Theta : V(\Theta) \rightarrow V$, $a(\Theta) \mapsto a$ for all Θ . V will be called internal space. The notation $a(\Theta)$ is used both for elements of \mathcal{H}_1 and for elements of $V(\Theta)$.

\mathcal{H}_1 , $V(\Theta)$ and V can also be decomposed into a sum of mass eigenspaces:

$$\mathcal{H}_1 = \oplus_m (\mathcal{H}_1)_m , \quad V(\Theta) = \oplus_m V(\Theta)_m , \quad V = \oplus_m V_m . \quad (2.3)$$

The normalization of the states is

$$\langle \Omega_i | \Omega_j \rangle = \delta_{ij}$$

and

$$\langle a_1(\Theta_1) | a_2(\Theta_2) \rangle = \delta(\Theta_1^* - \Theta_2) \delta_{a_1, a_2}$$

for \mathcal{H}_0 and \mathcal{H}_1 . The $*$ denotes complex conjugation. For multi-particle states the canonical normalization for tensor products is used. For V , $V(\Theta)$ and $V(\Theta^*)$ we have

$$\langle a_1 | a_2 \rangle = \delta_{a_1, a_2} , \quad \langle a_1(\Theta^*) | a_2(\Theta) \rangle = \delta_{a_1, a_2} , \quad V(\Theta)^\dagger = V(\Theta^*) . \quad (2.4)$$

The particles usually correspond to basis vectors in a distinguished orthonormal basis of V denoted by \mathcal{B} . V has a corresponding decomposition into one-dimensional subspaces:

$$V = \oplus_l V_l . \quad (2.5)$$

These basis vectors are mass eigenstates, i.e. the decomposition is a refinement of (2.3).

If some of the particles are soliton-like, then, assuming that we have chosen the appropriate basis, only part of the multi-particle states of the form (2.2) are physical states, and physical subspaces are spanned by these physical states. The physical states are usually selected by adjacency conditions: in a physical state of the form (2.2) only certain ordered pairs (a, b) may occur, i.e. if a pair (c, d) is not allowed, then a state of the form $\cdots \otimes c(\Theta_i) \otimes d(\Theta_{i+1}) \otimes \cdots$ is not physical. Physical and non-physical states of the form (2.2) are orthogonal, and one can introduce the orthogonal projector $P : V \otimes V \rightarrow V \otimes V$ that projects onto the physical subspace of $V \otimes V$. The physical subspace of $V \otimes V \otimes V$ can be obtained as $[P \otimes I][I \otimes P](V \otimes V \otimes V)$ where $P \otimes I$ and $I \otimes P$ commute, and

similar formulae can be written for general N -particle spaces. More general adjacency conditions are also possible, as we shall see in Section 2.4.1.

Instead of the physical S-operator one usually considers an auxiliary S-operator S_{aux} . The relation between S and S_{aux} is that the latter is defined for any complex value of the rapidities (although it can have singularities). The *aux* subscript is often omitted.

The \mathcal{H}_N are invariant subspaces of S_{aux} , the N -particle auxiliary S-operator S_N is obtained by restricting the full auxiliary S-operator to \mathcal{H}_N : $S_N : \mathcal{H}_N \rightarrow \mathcal{H}_N$. In particular

$$S_N(\mathcal{H}_{N,in}) = \mathcal{H}_{N,out}$$

and

$$S_0 = Id_{\mathcal{H}_0}, \quad S_1 = Id_{\mathcal{H}_1}.$$

For $N \geq 2$ the operators

$$\hat{S}_N(\Theta_1, \Theta_2, \dots, \Theta_N) : V(\Theta_1) \otimes V(\Theta_2) \otimes \dots \otimes V(\Theta_N) \rightarrow V(\Theta_N) \otimes V(\Theta_{N-1}) \otimes \dots \otimes V(\Theta_1)$$

can be introduced so that

$$\begin{aligned} \langle b_N(\Theta'_N) b_{N-1}(\Theta'_{N-1}) \dots b_1(\Theta'_1) | S_N | a_1(\Theta_1) a_2(\Theta_2) \dots a_N(\Theta_N) \rangle = \\ = \delta(\Theta_1 - \Theta_1^*) \delta(\Theta_2 - \Theta_2^*) \dots \delta(\Theta_N - \Theta_N^*) \times \\ \times \langle b_N(\Theta_N^*) b_{N-1}(\Theta_{N-1}^*) \dots b_1(\Theta_1^*) | \hat{S}_N(\Theta_1, \Theta_2, \dots, \Theta_N) | a_1(\Theta_1) a_2(\Theta_2) \dots a_N(\Theta_N) \rangle \end{aligned}$$

For the matrix elements of the \hat{S}_N -s the notation

$$\begin{aligned} (\hat{S}_N)_{a_1 a_2 \dots a_N}^{b_N b_{N-1} \dots b_1}(\Theta_1, \Theta_2, \dots, \Theta_N) = \\ = \langle b_N(\Theta_N^*) b_{N-1}(\Theta_{N-1}^*) \dots b_1(\Theta_1^*) | \hat{S}_N(\Theta_1, \Theta_2, \dots, \Theta_N) | a_1(\Theta_1) a_2(\Theta_2) \dots a_N(\Theta_N) \rangle \end{aligned}$$

is used. One can also introduce the operators

$$\tilde{S}_N(\Theta_{12}, \Theta_{13}, \dots, \Theta_{1N}) : \underbrace{V \otimes V \otimes \dots \otimes V}_N \rightarrow \underbrace{V \otimes V \otimes \dots \otimes V}_N$$

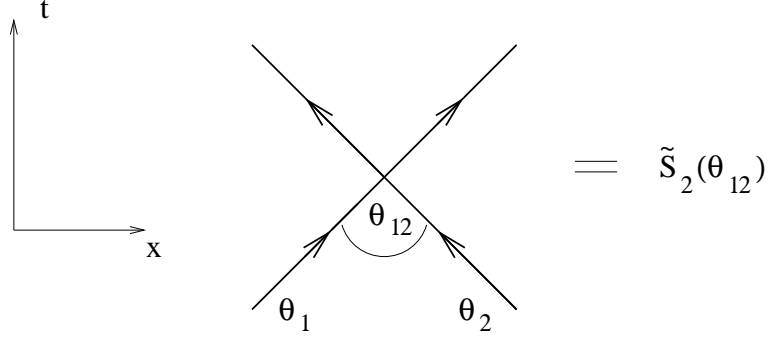
$$\tilde{S}_N(\Theta_{12}, \Theta_{13}, \dots, \Theta_{1N}) = [i_{\Theta_N} \otimes i_{\Theta_{N-1}} \otimes \dots \otimes i_{\Theta_1}] \hat{S}_N(\Theta_1, \Theta_2, \dots, \Theta_N) [i_{\Theta_1}^{-1} \otimes i_{\Theta_2}^{-1} \otimes \dots \otimes i_{\Theta_N}^{-1}]$$

where $\Theta_{ij} = \Theta_i - \Theta_j$. The matrix elements of the \tilde{S}_N -s are denoted as

$$(\tilde{S}_N)_{a_1 a_2 \dots a_N}^{b_N b_{N-1} \dots b_1}(\Theta_{12}, \Theta_{13}, \dots, \Theta_{1N}).$$

For the matrix elements of \hat{S}_N and \tilde{S}_N the equation

$$(\tilde{S}_N)_{a_1 a_2 \dots a_N}^{b_N b_{N-1} \dots b_1}(\Theta_{12}, \Theta_{13}, \dots, \Theta_{1N}) = (\hat{S}_N)_{a_1 a_2 \dots a_N}^{b_N b_{N-1} \dots b_1}(\Theta_1, \Theta_2, \dots, \Theta_N)$$

Figure 2.1: Two-particle S-matrix $\tilde{S}_2(\Theta_{12})$

holds.

One can also consider restrictions of \hat{S}_N and \tilde{S}_N to subspaces of states with definite mass of the particles:

$$(\tilde{S}_N)_{m_1 m_2 \dots m_N}(\Theta_{12}, \Theta_{13}, \dots, \Theta_{1N}) : V_{m_1} \otimes V_{m_2} \otimes \dots \otimes V_{m_N} \rightarrow V_{m_N} \otimes V_{m_{N-1}} \otimes \dots \otimes V_{m_1}$$

and similarly for \hat{S}_N . \hat{S}_N and \tilde{S}_N are composed of such blocks.

If

$$\tilde{S}_2(\Theta)(V_1 \otimes V_2) \subseteq V_2 \otimes V_1$$

for some subspaces $V_1 \subseteq V_{m_1}$, $V_2 \subseteq V_{m_2}$ with some masses m_1, m_2 , then we can use the notation $\tilde{S}_{V_1 V_2}(\Theta)$ for $\tilde{S}_2(\Theta)|_{V_1 \otimes V_2}$ and say that the multiplets V_1 and V_2 scatter on each other and the two-particle S matrix of the multiplets V_1 and V_2 is $\tilde{S}_{V_1 V_2}(\Theta)$.

If the particles satisfy adjacency conditions, they have to be observed in the formulae above, however we do not introduce explicit notation for this case.

If $\hat{S}_2(\Theta_1, \Theta_2)$ or $\tilde{S}_2(\Theta)$ is written in matrix form, i.e. as a table of entries, then the upper indices specify the rows and the lower indices specify the columns.

The graphical representation of $\tilde{S}_2(\Theta)$ is shown in Figure 2.1.

In the $N = 3$ case the factorization property is expressed by the equation

$$\tilde{S}_3(\Theta_{12}, \Theta_{13}) = [\tilde{S}_2(\Theta_{23}) \otimes I][I \otimes \tilde{S}_2(\Theta_{13})][\tilde{S}_2(\Theta_{12}) \otimes I]$$

or

$$\tilde{S}_3(\Theta_{12}, \Theta_{13}) = [I \otimes \tilde{S}_2(\Theta_{12})][\tilde{S}_2(\Theta_{13}) \otimes I][I \otimes \tilde{S}_2(\Theta_{23})] .$$

The two equations correspond to the two possible decompositions of the 3-particle scattering into 2-particle scatterings.

The equality of the two expressions on the right-hand side

$$[\tilde{S}_2(\Theta_{23}) \otimes I][I \otimes \tilde{S}_2(\Theta_{13})][\tilde{S}_2(\Theta_{12}) \otimes I] = [I \otimes \tilde{S}_2(\Theta_{12})][\tilde{S}_2(\Theta_{13}) \otimes I][I \otimes \tilde{S}_2(\Theta_{23})]$$

is called the Yang-Baxter equation. If the Yang-Baxter equations are satisfied, then the analogous equations expressing the equality of the possible factorizations of the N -particle scattering ($N > 3$) into 2-particle scatterings are also satisfied.

The above equations (with the obvious modifications) are also satisfied by S_2 , S_3 and \hat{S}_2 , \hat{S}_3 and by the appropriate blocks of them corresponding to definite masses. Similar statement applies to several formulae below. We shall usually write down the tilde versions only.

Most of the equations of factorized scattering theory for transition amplitudes like the Yang-Baxter equation admit a graphical representation which is very useful for grasping and handling these equations. The graphs representing these equations are similar to the Feynman graphs, their vertices correspond to tensors, especially to the two-particle S matrix or its blocks and to the fusion and decay tensors described below. Outgoing and incoming lines (distinguished by arrows) at a vertex correspond to the two type of indices (normal or upper and dual or lower), an outgoing line can be joined to an incoming line which corresponds to the contraction of the corresponding indices. We usually do not introduce a vertex for the identity tensor, although in the equations it can be useful to insert identity tensors explicitly. Momenta or rapidities are also associated to the lines. In several cases the graphs reflect the kinematical situation geometrically faithfully, i.e. the graphs can be regarded as geometrical pictures of scattering, fusion and decay processes. In the graphical formulation the Yang-Baxter and the bootstrap equations (described below) express the parallel shiftability of the individual lines in the diagrams. This shiftability is a consequence of the existence of higher spin conserved charges.

A graphical representation of the Yang-Baxter equation is shown in Figure 2.2.

4) Analytic properties: $\tilde{S}_2(\Theta)$ is an analytic function with possible pole singularities which are located in $i\mathbb{R}$. The domain $0 < \text{Im}(\Theta) < \pi$ is called the ‘physical strip’. The singular part of $\tilde{S}_2(\Theta)$ at a pole in the physical strip is generally a sum of various contributions related to bound states and anomalous thresholds.

5) Real analyticity

$$(\tilde{S}_2(\Theta^*))^\dagger = \tilde{S}_2(-\Theta) . \quad (2.6)$$

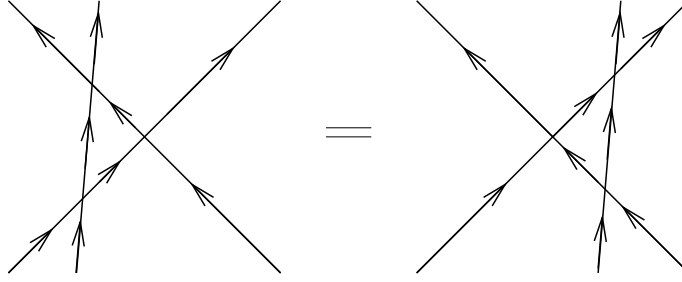


Figure 2.2: Yang-Baxter equation

For the blocks corresponding to definite masses, for example, this reads as

$$((\tilde{S}_2)_{m_1 m_2}(\Theta^*))^\dagger = (\tilde{S}_2)_{m_2 m_1}(-\Theta) .$$

6) Unitarity

$$(\tilde{S}_2(\Theta^*))^\dagger \tilde{S}_2(\Theta) = I . \quad (2.7)$$

This condition and the real analyticity condition imply

$$\tilde{S}_2(-\Theta) \tilde{S}_2(\Theta) = I . \quad (2.8)$$

It is usual in factorized scattering theory to refer to the latter condition rather than (2.7) as unitarity.

7) Bound states: at some poles of $(\tilde{S}_2)_{m_1 m_2}(\Theta)$ in the physical strip the singular part has a contribution corresponding to direct-channel (or s-channel) bound states:

$$(\tilde{S}_2)_{m_1 m_2}(\Theta) = \frac{\tilde{d}_{m_3}^{m_2 m_1} \tilde{f}_{m_1 m_2}^{m_3}}{\Theta - iu} + s(\Theta) + \text{reg}(\Theta) \quad (2.9)$$

where iu , $0 < u < \pi$, is the location of the pole, $\text{reg}(\Theta)$ is regular at iu , $s(\Theta)$ contains further possible singular terms. u is called fusion angle.

$$\tilde{d}_{m_3}^{m_2 m_1} : V_{m_3} \rightarrow V_{m_2} \otimes V_{m_1}$$

is the decay tensor,

$$\tilde{f}_{m_1 m_2}^{m_3} : V_{m_1} \otimes V_{m_2} \rightarrow V_{m_3}$$

is the fusion tensor. We also have the hatted versions

$$\hat{d}_{m_3}^{m_2 m_1} : V_{m_3}(\Theta) \rightarrow V_{m_2}(\Theta + iu_2) \otimes V_{m_1}(\Theta - iu_1)$$

and

$$\hat{f}_{m_1 m_2}^{m_3} : V_{m_1}(\Theta - iu_1) \otimes V_{m_2}(\Theta + iu_2) \rightarrow V_{m_3}(\Theta) ,$$

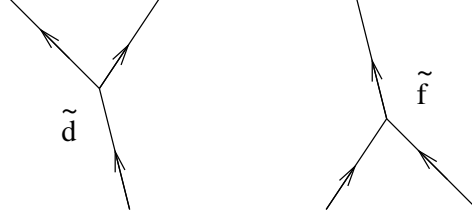


Figure 2.3: Fusion and decay tensors

where $0 < u_1$ and $0 < u_2$, $u_1 + u_2 = u$. u_1 and u_2 are determined in terms of m_1 , m_2 , m_3 by momentum conservation and by the mass shell condition. The fusion map projects onto the bound states in question.

Graphical representation of $\tilde{f}_{m_1 m_2}^{m_3}$ and $\tilde{d}_{m_3}^{m_2 m_1}$ can be seen in Figure 2.3. The graphical representation of the residue $\tilde{d}_{m_3}^{m_2 m_1} \tilde{f}_{m_1 m_2}^{m_3}$ is shown in Figure 2.4.

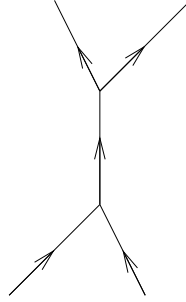


Figure 2.4: Contribution of bound states

The image space of $\tilde{f}_{m_1 m_2}^{m_3}$ has zero intersection with the kernel of $\tilde{d}_{m_3}^{m_2 m_1}$.

The image space of $\tilde{f}_{m_1 m_2}^{m_3}$ can usually be decomposed into a sum of some one-particle subspaces occurring in (2.5).

Generally if

$$V_1 = \oplus_{l_1} V_{l_1} , \quad V_2 = \oplus_{l_2} V_{l_2} , \quad V_3 = \oplus_{l_3} V_{l_3} ,$$

where l_1 , l_2 and l_3 take certain values from all possible values of l defined in (2.5) and the states in V_1 , V_2 , V_3 have mass m_1 , m_2 , m_3 and there exists a fusion tensor $\tilde{f}_{m_1 m_2}^{m_3}$ and

$$\tilde{f}_{m_1 m_2}^{m_3}(V_1 \otimes V_2) = V_3 ,$$

then we say that the particles labeled by l_3 (i.e. the particle multiplet V_3) are bound states of the particles labeled by l_1 and l_2 (i.e. of the particle multiplets V_1 and V_2). We can write

$$V_1 + V_2 \rightarrow V_3 \quad (u) , \quad (2.10)$$

where u is the fusion angle, and call this expression a fusion rule.

A rule denoted as

$$a + b \rightarrow c \quad (u) \quad (2.11)$$

can be written down and also called a fusion rule if there exists a fusion tensor \tilde{f} with fusion angle u with nonzero matrix element between the one-particle states $|a\rangle$, $|b\rangle$, $|c\rangle$: $\langle c|\tilde{f}(a \otimes b)\rangle \neq 0$.

8) Crossing symmetry

$$\langle c \otimes d|\tilde{S}_2(\Theta)(a \otimes b)\rangle = \langle d \otimes (\tilde{C}\tilde{P}\tilde{T}b)|\tilde{S}_2(i\pi - \Theta)((\tilde{C}\tilde{P}\tilde{T}c) \otimes a)\rangle \quad (2.12)$$

and

$$\langle c|\tilde{f}_{m_1 m_2}^{m_3}(a \otimes b)\rangle = \langle \tilde{C}\tilde{P}\tilde{T}a|\tilde{f}_{m_2 m_3}^{m_1}(b \otimes (\tilde{C}\tilde{P}\tilde{T}c))\rangle \quad (2.13)$$

$$\langle b \otimes c|\tilde{d}_{m_1}^{m_2 m_3}a\rangle = \langle (\tilde{C}\tilde{P}\tilde{T}a) \otimes b|\tilde{d}_{m_3}^{m_1 m_2}\tilde{C}\tilde{P}\tilde{T}c\rangle \quad (2.14)$$

$$\langle b \otimes c|\tilde{d}_{m_1}^{m_2 m_3}a\rangle = \langle \tilde{C}\tilde{P}\tilde{T}a|\tilde{f}_{m_3 m_2}^{m_1}((\tilde{C}\tilde{P}\tilde{T}c) \otimes (\tilde{C}\tilde{P}\tilde{T}b))\rangle . \quad (2.15)$$

$\tilde{C}\tilde{P}\tilde{T}$ will be discussed in 12).

9) Bootstrap equation

Let iu be the location of the pole of $(\tilde{S}_2)_{m_1 m_2}(\Theta)$ for some masses m_1 and m_2 that corresponds to a direct-channel bound state. The following equation called the bootstrap equation is satisfied:

$$(\tilde{S}_2)_{mm_3}(\Theta_{12})[I \otimes \tilde{f}_{m_1 m_2}^{m_3}] = [\tilde{f}_{m_1 m_2}^{m_3} \otimes I][I \otimes (\tilde{S}_2)_{mm_2}(\Theta_{12} + iu_2)][(\tilde{S}_2)_{mm_1}(\Theta_{12} - iu_1) \otimes I] \quad (2.16)$$

This equation is analogous to the Yang-Baxter equation and can be regarded as an equation expressing the parallel shiftability of lines in the diagrams corresponding to factorized scattering processes.

A graphical representation of (2.16) is shown in Figure 2.5.

10) Coleman-Thun diagrams

The poles of $(\tilde{S}_2)_{m_1 m_2}(\Theta)$ lying in the physical strip can be associated to bound states, as already mentioned in 4), and to anomalous thresholds [90]. The latter can also be related to on-shell diagrams, which are called Coleman-Thun diagrams in factorized scattering theory. The graphs corresponding to bound states can also be regarded as Coleman-Thun diagrams.

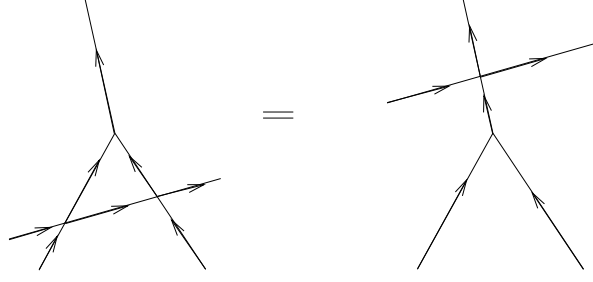


Figure 2.5: The bootstrap equation

If $(\tilde{S}_2)_{m_1 m_2}(\Theta)$ has a pole at iu in the physical strip, then the singular part of the Laurent series of $(\tilde{S}_2)_{m_1 m_2}(\Theta)$ around iu is the sum of the contributions of all possible Coleman-Thun diagrams.

The Coleman-Thun diagrams are planar geometrical graphs with oriented lines and can be drawn in the Euclidean space-time plane. Each diagram can be interpreted as a non-physical two-particle scattering process (and so has 4 external lines). The lines of the diagrams correspond to particles (or particle multiplets) which can be thought to be freely flying between pointlike events represented by the vertices. A mass and a momentum are associated with each line of the diagram. The momenta have real time components and imaginary space components. The ‘length’ of the momenta associated with the lines equals the masses assigned to the lines (i.e. the usual $p_0^2 - p_1^2 = m^2$ mass-shell condition is satisfied). Momentum is conserved at each vertex (i.e. $p_{in} = p_{out}$, where p_{in} is the sum of the incoming momenta, p_{out} is the sum of the outgoing momenta. Incoming and outgoing momenta are distinguished by the orientation of the lines with respect to the vertex.) The momenta are parallel to the lines with which they are associated. Either four or three lines can join in a vertex, the possible vertices are the two-particle scattering vertex as shown in Figure 2.1 and the fusion and decay vertices of Figure 2.3.

The possible angles in a diagram are completely determined by the mass spectrum, so if the mass spectrum is known, then it is a geometrical and combinatorial problem to find all possible Coleman-Thun diagrams.

In the simplest case the order of the pole of the term corresponding to a Coleman-Thun diagram is equal to the number of ‘degrees of freedom’, i.e. the number of internal lengths in the diagram which can be adjusted independently [21]. In the bound state diagram (Figure 2.4), for example, there is one internal line, the length of which can be set freely.

In general only the bound state diagram and its crossed version give first order pole, all other Coleman-Thun diagrams give higher order poles. This general rule is often mod-

ified, however.

11) Symmetries

Let \mathcal{A} be an associative algebra over \mathbb{R} . Representations of \mathcal{A} on multi-particle spaces are defined in the following way: as the multi-particle states are elements of tensor products of one-particle spaces, it is sufficient to construct representations on these tensor product spaces from the one-particle representations. The in, out and intermediate subspaces must be invariant, as well as the physical subspaces, if adjacency conditions are satisfied. On the tensor product of two one-particle spaces the construction is done by taking the tensor product of the two one-particle representations, which is a representation of $\mathcal{A} \otimes \mathcal{A}$, and then composing it with an algebra homomorphism $\Delta : \mathcal{A} \rightarrow \mathcal{A} \otimes \mathcal{A}$:

$$D_1 \times D_2 = (D_1 \otimes D_2) \circ \Delta$$

where D_1, D_2 are one-particle representations of \mathcal{A} on the spaces H_1 and H_2 , respectively:

$$D_1 : \mathcal{A} \rightarrow \text{End}(H_1) , \quad D_2 : \mathcal{A} \rightarrow \text{End}(H_2) .$$

$D_1 \times D_2$ is called the product of the representations D_1 and D_2 . This definition can be applied generally to any two representations, so it is also suitable to define products of several representations recursively. For the product of any three representations the following two definitions can be used:

$$\begin{aligned} D_1 \times D_2 \times D_3 &= D_1 \times (D_2 \times D_3) = [D_1 \otimes ((D_2 \otimes D_3) \circ \Delta)] \circ \Delta = \\ &= (D_1 \otimes D_2 \otimes D_3) \circ (id_{\mathcal{A}} \otimes \Delta) \circ \Delta \end{aligned}$$

and

$$\begin{aligned} D_1 \times D_2 \times D_3 &= (D_1 \times D_2) \times D_3 = [((D_1 \otimes D_2) \circ \Delta) \otimes D_3] \circ \Delta = \\ &= (D_1 \otimes D_2 \otimes D_3) \circ (\Delta \otimes id_{\mathcal{A}}) \circ \Delta . \end{aligned}$$

However, it is usually required that Δ be co-associative, i.e.

$$(id_{\mathcal{A}} \otimes \Delta) \circ \Delta = (\Delta \otimes id_{\mathcal{A}}) \circ \Delta ,$$

which implies that the two definitions above give identical results. Moreover, the analogous statement holds for products of more than three representations without further restriction on Δ , i.e. the multiplication of representations is associative if Δ is co-associative.

One expects that a representation D_Ω on the vacuum subspace has the property

$$D \times D_\Omega \simeq D_\Omega \times D \simeq D$$

for any one-particle representation D . \simeq denotes the equivalence of representations.

An element $A \in \mathcal{A}$ is a symmetry of the S operator if S_2 has the intertwining property

$$D(A)S_2 = S_2D(A) \quad (2.17)$$

where $D(A)$ is the representation of A on \mathcal{H}_2 . (2.17) implies that S_N has the intertwining property for the N -particle representation for any value of N . A symmetry of a fusion or a decay tensor is defined similarly. A symmetry of the factorized scattering theory is a symmetry of the S operator and all fusion and decay tensors.

In 1+1 dimensions the universal enveloping algebra of the Poincare algebra (supplemented with a unit element) is generated by the boost generator N , the time translation generator H , the space translation generator P , and the unit element I . They are subject to the relations

$$[N, H + P] = H + P, \quad [N, H - P] = -(H - P), \quad [H, P] = 0. \quad (2.18)$$

The co-product takes the standard form:

$$\begin{aligned} \Delta(H) &= H \otimes I + I \otimes H, & \Delta(N) &= N \otimes I + I \otimes N, \\ \Delta(P) &= P \otimes I + I \otimes P, & \Delta(I) &= I \otimes I. \end{aligned} \quad (2.19)$$

A local conserved quantity A of spin s has the properties

$$[A, H] = 0, \quad [A, P] = 0, \quad A(V(\Theta)) = V(\Theta), \quad (2.20)$$

$$A(a(\Theta)) = e^{s\Theta} q_A a(\Theta), \quad (2.21)$$

where q_A is a Θ -independent linear mapping, and

$$\begin{aligned} A[a_1(\Theta_1) \otimes a_2(\Theta_2) \otimes \cdots \otimes a_N(\Theta_N)] &= e^{s\Theta_1} (q_A a_1(\Theta_1)) \otimes a_2(\Theta_2) \otimes \cdots \otimes a_N(\Theta_N) + \\ &+ e^{s\Theta_2} a_1(\Theta_1) \otimes (q_A a_2(\Theta_2)) \otimes \cdots \otimes a_N(\Theta_N) + \cdots + \\ &+ e^{s\Theta_N} a_1(\Theta_1) \otimes a_2(\Theta_2) \otimes \cdots \otimes (q_A a_N(\Theta_N)). \end{aligned} \quad (2.22)$$

A commutes with the S operator as well.

In integrable models there exist commuting local higher spin (i.e. not spin 1) conserved quantities, their number is usually infinite. From this property of integrable models it is possible to derive the main factorization properties of factorized scattering theory.

12) Charge conjugation and reflections

The representation of some transformations do not always fit in the scheme described above in 11). For instance, the charge conjugation and space reflection are such transformations.

Charge conjugation C acts as a linear transformation and has the property $C(V(\Theta)) = V(\Theta)$ (the representation map is suppressed here and further on).

The space reflection P also acts as a unitary transformation, it has the property $P(V(\Theta)) = V(-\Theta)$ and it has a tilde-d version $\tilde{P} : V \rightarrow V$. $P(a(\Theta)) = (\tilde{P}a)(-\Theta)$. On multi-particle states it acts in the following way:

$$P(a_1(\Theta_1) \otimes a_2(\Theta_2) \otimes \cdots \otimes a_N(\Theta_N)) = P(a_N(\Theta_N)) \otimes P(a_{N-1}(\Theta_{N-1})) \otimes \cdots \otimes P(a_1(\Theta_1))$$

The time reflection T is represented by an antiunitary operator with the property $T(V(\Theta)) = V(-\Theta)$. It has a tilde-d version $\tilde{T} : V \rightarrow V$. On N -particle states it is given by

$$T_N = \underbrace{T_1 \otimes T_1 \otimes \cdots \otimes T_1}_N,$$

T_N denoting its restriction to N -particle states.

The product CPT of C , P and T is always represented (even if some of C , P and T are not represented) and it is always a symmetry. It is represented by an antiunitary operator. It has the property that $CPT(V(\Theta)) = V(\Theta)$ and it has a tilde-d version $\tilde{C}\tilde{P}\tilde{T} : V \rightarrow V$. On N -particle states it is given by

$$\begin{aligned} CPT(a_1(\Theta_1) \otimes a_2(\Theta_2) \otimes \cdots \otimes a_N(\Theta_N)) &= \\ &= CPT(a_N(\Theta_N)) \otimes CPT(a_{N-1}(\Theta_{N-1})) \otimes \cdots \otimes CPT(a_1(\Theta_1)). \end{aligned}$$

Energy and mass are invariant with respect to the C , P , T and CPT transformations.

The $\tilde{C}\tilde{P}\tilde{T}$ transformation usually has the property that $\tilde{C}\tilde{P}\tilde{T}(V_l) = V_{\bar{l}}$ where the V_l -s are the one-dimensional subspaces appearing in (2.5) and $\bar{l} = l$. The mapping $l \mapsto \bar{l}$ on the label of the particles is the particle-antiparticle correspondence. We also say that the particle \bar{l} is the conjugate of l .

Invariance of the S operator with respect to CPT transformation means

$$\tilde{C}\tilde{P}\tilde{T}\tilde{S}_2(\Theta) = (\tilde{S}_2(\Theta))^\dagger \tilde{C}\tilde{P}\tilde{T} \quad (2.23)$$

or equivalently

$$\langle a \otimes b | \tilde{S}_2(\Theta) (c \otimes d) \rangle = \langle \tilde{C}\tilde{P}\tilde{T}(c \otimes d) | \tilde{S}_2(\Theta) \tilde{C}\tilde{P}\tilde{T}(a \otimes b) \rangle, \quad (2.24)$$

which is the same as (2.12) applied twice. (2.23) implies that S_N also has the symmetry property for any value of N .

CPT-invariance of fusion and decay tensors means

$$\tilde{C}\tilde{P}\tilde{T}\tilde{d}_{m_1}^{m_2m_3} = (\tilde{f}_{m_3m_2}^{m_1})^\dagger \tilde{C}\tilde{P}\tilde{T} ,$$

which is the same as (2.15).

CPT-invariance of the factorized scattering theory means the CPT-invariance of the S operator and all fusion and decay tensors.

Space reflection invariance of the S -operator means

$$\tilde{P}\tilde{S}_2(\Theta) = \tilde{S}_2(\Theta)\tilde{P} .$$

Space reflection invariance of fusion and decay tensors means

$$\tilde{P}\tilde{d}_{m_1}^{m_2m_3} = \tilde{d}_{m_1}^{m_3m_2}\tilde{P} \quad \text{and} \quad \tilde{P}\tilde{f}_{m_1m_2}^{m_3} = \tilde{f}_{m_2m_1}^{m_3}\tilde{P} .$$

Time reflection invariance of the S -operator means

$$\tilde{T}\tilde{S}_2(\Theta) = (\tilde{S}_2(\Theta))^\dagger \tilde{T} .$$

Time reflection invariance of fusion and decay tensors means

$$\tilde{T}\tilde{d}_{m_1}^{m_2m_3} = (\tilde{f}_{m_2m_3}^{m_1})^\dagger \tilde{T} .$$

Charge conjugation invariance of the S -operator means

$$\tilde{C}\tilde{S}_2(\Theta) = \tilde{S}_2(\Theta)\tilde{C} .$$

Charge conjugation invariance of fusion and decay tensors means

$$\tilde{C}\tilde{d}_{m_1}^{m_2m_3} = \tilde{d}_{m_1}^{m_2m_3}\tilde{C} \quad \text{and} \quad \tilde{C}\tilde{f}_{m_1m_2}^{m_3} = \tilde{f}_{m_1m_2}^{m_3}\tilde{C} .$$

We remark, finally, that if a factorized scattering theory is given, then it is possible, in a straightforward way, to introduce particle groups or multiplets of particle groups and their scattering. A particle group is a multi-particle state with fixed (possible imaginary) relative rapidities of the constituting particles. These particle groups behave in the same way as single particles. They can be regarded as compound states. The S -matrix elements for these particle groups can be built from the two-particle S -matrix in straightforward way, they are certain multi-particle S matrix elements, in fact. The Yang-Baxter equation

and the bootstrap equation can be regarded as equations which express the isomorphism or homomorphism between certain particle groups or single particles, regarding their scattering and symmetry properties. The homomorphism maps are two-particle S-matrix blocks or fusion and decay tensors.

We also remark that the particle statistics has been left completely unspecified in this section, and the space of *in* and *out* and *intermediate* states were defined to be different. This, however, is only a minor deviation from the more usual formalism, in which both the *in* and the *out* states span the whole Hilbert space and the S-matrix elements are j conversion coefficients between the *in* and *out* bases. The more usual formalism corresponds to quotienting out the Hilbert space by the subspace defined by the relations $|v\rangle = \cdots \otimes I \otimes \cdots \otimes S_2 \otimes \cdots \otimes I \otimes \cdots |v\rangle$, where $|v\rangle$ is any multi-particle state with rapidities so that S_2 is nonsingular and has nonzero determinant. The statistics of the particles is then specified by the value of the two-particle S-matrix elements at zero relative rapidity.

It is possible to draw other figures which are similar to Figure 2.5, and to write down the corresponding bootstrap equations. For example, one can consider the mirror image of Figure 2.5. However, it can be shown that the new bootstrap equations obtained in this way can be derived from the axioms that have been written down.

2.2 Factorized scattering theory with a boundary

If the space is a half-line, then scattering theory describes interactions of particle-like objects and boundary states. The particle-like objects travel in the half space, whereas the boundary states are localized at the boundary of the (half) space. The ground states are boundary states. The scattering takes place in the following way: at the beginning particles far from each other and the boundary travel towards the boundary, then the particles scatter on each other and reflect from the boundary, and finally particles travel away from the boundary and each other. The boundary state participates in the reflection and generally changes. The scattering operator is called reflection operator and denoted by R .

The characteristics of factorized boundary scattering are listed and explicitly described below. Some of these properties are special to factorized boundary scattering theory, others (like unitarity) are general properties of boundary scattering theory applied to factorized boundary scattering theory.

Factorized scattering theory in the presence of a boundary is characterized by the following properties:

1) A factorized boundary scattering theory incorporates a standard (i.e. bulk) factorized scattering theory.

2) The particle number is conserved.

3) The outgoing rapidities equal -1 times the incoming rapidities.

4) Factorization and boundary Yang-Baxter equation: An arbitrary N -particle scattering process can be described as a sequence of 2-particle collisions and one-particle reflections, all possible descriptions are equivalent. The 2-particle collisions are described by the two-particle S-matrix block, the one-particle reflections are described by the one-particle reflection matrix block. These are the most interesting quantities in factorized boundary scattering theory.

The Hilbert space \mathcal{H}^b can be decomposed into a sum of N -particle subspaces:

$$\mathcal{H}^b = \oplus_{N=0}^{\infty} \mathcal{H}_N^b, \quad (2.25)$$

where

$$\mathcal{H}_N^b = \underbrace{\mathcal{H}_1 \otimes \cdots \otimes \mathcal{H}_1}_N \otimes \mathcal{H}_B$$

for $N \geq 1$, and

$$\mathcal{H}_0^b = \mathcal{H}_B.$$

\mathcal{H}_B is the space of boundary states, the space \mathcal{H}_{B0} of the ground states is a subspace of it. \mathcal{H}_{B0} is usually finite dimensional, most frequently one-dimensional.

\mathcal{H}_N^b can be decomposed into a (not direct) sum of spaces of in, out and intermediate states:

$$\mathcal{H}_N^b = \mathcal{H}_{N,in}^b + \mathcal{H}_{N,out}^b + \mathcal{H}_{N,intermed}^b$$

for $N \geq 1$, for $N = 0$ we have

$$\mathcal{H}_{0,in}^b = \mathcal{H}_{0,out}^b$$

and there are no intermediate states for $N = 0, 1$.

A multi-particle state of the form

$$a_1(\Theta_1) \otimes a_2(\Theta_2) \otimes \cdots \otimes a_N(\Theta_N) \otimes B$$

is an in state if $\Theta_1 \geq \Theta_2 \geq \dots \geq \Theta_N > 0$, an out state if $\Theta_1 \leq \Theta_2 \leq \dots \leq \Theta_N < 0$, and an intermediate state otherwise. We shall also use the ket notation for the multi-particle states.

\mathcal{H}_B can be decomposed into energy eigenspaces:

$$\mathcal{H}_B = \oplus_E \mathcal{H}_{B,E} . \quad (2.26)$$

The boundary states are normalized as

$$\langle B_i | B_j \rangle = \delta_{ij} .$$

It is often useful to consider a distinguished orthonormal basis of \mathcal{H}_B and the corresponding decomposition into a sum of one-dimensional subspaces:

$$\mathcal{H}_B = \oplus_{l^b} \mathcal{H}_{B,l^b} , \quad (2.27)$$

which should be a refinement of the decomposition (2.26).

Boundary states can also be involved in adjacency conditions.

Instead of the physical R-operator one usually uses an auxiliary R-operator R_{aux} , which is related to the physical R-operator in the same way as S_{aux} is related to S . The aux subscript will be suppressed. The \mathcal{H}_N^b are invariant subspaces of R_{aux} , the N -particle auxiliary R-operator R_N is obtained by restricting the full auxiliary R-operator to \mathcal{H}_N^b : $R_N : \mathcal{H}_N^b \rightarrow \mathcal{H}_N^b$. In particular

$$R_N^b(\mathcal{H}_{N,in}^b) = \mathcal{H}_{N,out}^b$$

and

$$R_0 = Id_{\mathcal{H}_0^b} .$$

For $N \geq 1$ the operators

$$\hat{R}_N(\Theta_1, \Theta_2, \dots, \Theta_N) :$$

$$V(\Theta_1) \otimes V(\Theta_2) \otimes \dots \otimes V(\Theta_N) \otimes \mathcal{H}_B \rightarrow V(-\Theta_1) \otimes V(-\Theta_2) \otimes \dots \otimes V(-\Theta_N) \otimes \mathcal{H}_B$$

can be introduced so that

$$\begin{aligned} & \langle b_1(\Theta'_1) b_2(\Theta'_2) \dots b_N(\Theta'_N) B_j | R_N | a_1(\Theta_1) a_2(\Theta_2) \dots a_N(\Theta_N) B_i \rangle = \\ & = \delta(\Theta_1 + \Theta_1^*) \delta(\Theta_2 + \Theta_2^*) \dots \delta(\Theta_N + \Theta_N^*) \times \\ & \times \langle b_1(-\Theta_1^*) b_2(-\Theta_2^*) \dots b_N(-\Theta_N^*) B_j | \hat{R}_N(\Theta_1, \Theta_2, \dots, \Theta_N) | a_1(\Theta_1) a_2(\Theta_2) \dots a_N(\Theta_N) B_i \rangle \end{aligned}$$

For the matrix elements of the \hat{R}_N -s the notation

$$\begin{aligned} (\hat{R}_N)_{a_1 a_2 \dots a_N, i}^{b_1 b_2 \dots b_N, j}(\Theta_1, \Theta_2, \dots, \Theta_N) = \\ = \langle b_1(-\Theta_1^*) b_2(-\Theta_2^*) \dots b_N(-\Theta_N^*) B_j | \hat{R}_N(\Theta_1, \Theta_2, \dots, \Theta_N) | a_1(\Theta_1) a_2(\Theta_2) \dots a_N(\Theta_N) B_i \rangle \end{aligned}$$

is used. One can also introduce the operators

$$\tilde{R}_N(\Theta_1, \Theta_2, \dots, \Theta_N) : \underbrace{V \otimes V \otimes \dots \otimes V}_N \otimes \mathcal{H}_B \rightarrow \underbrace{V \otimes V \otimes \dots \otimes V}_N \otimes \mathcal{H}_B$$

$$\tilde{R}_N(\Theta_1, \Theta_2, \dots, \Theta_N) = [i_{-\Theta_1} \otimes i_{-\Theta_2} \otimes \dots \otimes i_{-\Theta_N} \otimes I] \hat{R}_N(\Theta_1, \Theta_2, \dots, \Theta_N) [i_{\Theta_1}^{-1} \otimes i_{\Theta_2}^{-1} \otimes \dots \otimes i_{\Theta_N}^{-1} \otimes I] .$$

The matrix elements of the \tilde{R}_N -s are denoted as

$$(\tilde{R}_N)_{a_1 a_2 \dots a_N, i}^{b_1 b_2 \dots b_N, j}(\Theta_1, \Theta_2, \dots, \Theta_N) .$$

For the matrix elements of \hat{R}_N and \tilde{R}_N the equation

$$(\tilde{R}_N)_{a_1 a_2 \dots a_N, i}^{b_1 b_2 \dots b_N, j}(\Theta_1, \Theta_2, \dots, \Theta_N) = (\hat{R}_N)_{a_1 a_2 \dots a_N, i}^{b_1 b_2 \dots b_N, j}(\Theta_1, \Theta_2, \dots, \Theta_N)$$

holds.

One can introduce $(\tilde{R}_N)_{m_1 m_2 \dots m_N, E}(\Theta_1, \Theta_2, \dots, \Theta_N)$ and $(\hat{R}_N)_{m_1 m_2 \dots m_N, E}(\Theta_1, \Theta_2, \dots, \Theta_N)$ as in Section 2.1. \tilde{R}_N and \hat{R}_N are composed of these blocks.

Graphical representation of $\tilde{R}_1(\Theta)$ is shown in Figure 2.6.

If

$$\tilde{R}_1(\Theta)(V_1 \otimes \mathcal{H}_{B,2}) \subseteq V_1 \otimes \mathcal{H}_{B,2}$$

for some subspaces $V_1 \subseteq V_{m_1}$ and $\mathcal{H}_{B,2} \subseteq \mathcal{H}_{B,E_2}$ with some mass m_1 and energy E_2 , then we can introduce the notation $\tilde{R}_{V_1 \mathcal{H}_{B,2}}(\Theta) = \tilde{R}_1(\Theta)|_{V_1 \otimes \mathcal{H}_{B,2}}$ and say that $\tilde{R}_{V_1 \mathcal{H}_{B,2}}(\Theta)$ is the reflection matrix of the multiplet V_1 on the boundary multiplet $\mathcal{H}_{B,2}$. The case when $\mathcal{H}_{B,2}$ is \mathcal{H}_{B0} is considered frequently, the reflection matrix blocks with $\mathcal{H}_{B,2} = \mathcal{H}_{B0}$ are called ground state reflection matrices.

In the $N = 2$ case the factorization property is expressed by the equation

$$\tilde{R}_2(\Theta_1, \Theta_2) = [I \otimes \tilde{R}_1(\Theta_2)][\tilde{S}_2(\Theta_2 + \Theta_1) \otimes I][I \otimes \tilde{R}_1(\Theta_1)][\tilde{S}_2(\Theta_1 - \Theta_2) \otimes I]$$

or

$$\tilde{R}_2(\Theta_1, \Theta_2) = [\tilde{S}_2(\Theta_1 - \Theta_2) \otimes I][I \otimes \tilde{R}_1(\Theta_1)][\tilde{S}_2(\Theta_1 + \Theta_2) \otimes I][I \otimes \tilde{R}_1(\Theta_2)] .$$

The two equations correspond to the two possible decompositions of the 2-particle reflection into 2-particle scatterings and one-particle reflections.

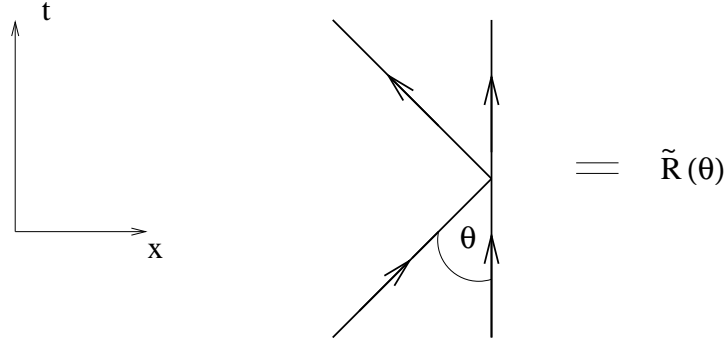
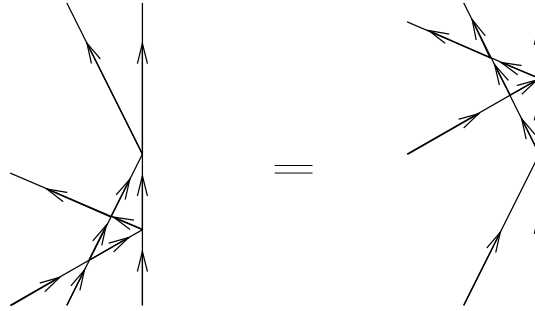
Figure 2.6: One-particle reflection matrix $\tilde{R}_1(\Theta)$ 

Figure 2.7: Boundary Yang-Baxter equation

The equality of the two expressions on the right-hand side

$$\begin{aligned}
 & [I \otimes \tilde{R}_1(\Theta_2)][\tilde{S}_2(\Theta_2 + \Theta_1) \otimes I][I \otimes \tilde{R}_1(\Theta_1)][\tilde{S}_2(\Theta_1 - \Theta_2) \otimes I] = \\
 & = [\tilde{S}_2(\Theta_1 - \Theta_2) \otimes I][I \otimes \tilde{R}_1(\Theta_1)][\tilde{S}_2(\Theta_1 + \Theta_2) \otimes I][I \otimes \tilde{R}_1(\Theta_2)] \quad (2.28)
 \end{aligned}$$

is called the boundary Yang-Baxter equation. A graphical representation of this equation is shown in Figure 2.7. If the boundary Yang-Baxter is satisfied, then the analogous equations expressing the equivalence of the possible factorizations of the N -particle reflection (for $N > 2$) into two-particle scatterings and one-particle reflections are also satisfied.

The above equations (with the obvious modifications) are also satisfied by R_2 , R_1 , S_2 and \hat{R}_2 , \hat{R}_1 , \hat{S}_2 and by the appropriate blocks of them corresponding to definite masses and energies.

5) Analytic properties: $\tilde{R}_1(\Theta)$ is an analytic function with possible pole singularities which are located in $i\mathbb{R}$. The ‘physical strip’ for $\tilde{R}_1(\Theta)$ is the domain $0 < \text{Im}(\Theta) < \pi/2$. The singular part of $\tilde{R}_1(\Theta)$ at a pole lying in the physical strip is generally a sum of various contributions related to bound states and anomalous thresholds.

6) Real analyticity

$$(\tilde{R}_1(\Theta^*))^\dagger = \tilde{R}_1(-\Theta) .$$

7) Unitarity

$$(\tilde{R}_1(\Theta^*))^\dagger \tilde{R}_1(\Theta) = I .$$

This condition and the real analyticity condition imply

$$\tilde{R}_1(-\Theta) \tilde{R}_1(\Theta) = I .$$

In factorized scattering theory usually the latter condition is referred to as unitarity.

8) Crossing symmetry

$$\begin{aligned} \langle c \otimes B_j | \tilde{R}_1(\Theta) (a \otimes B_i) \rangle = \\ = \sum_{b, d \in \mathcal{B}} \langle c \otimes d | \tilde{S}_2(2\Theta) (a \otimes b) \rangle \langle (\tilde{C} \tilde{P} \tilde{T} d) \otimes B_j | \tilde{R}_1(i\pi - \Theta) ((\tilde{C} \tilde{P} \tilde{T} b) \otimes B_i) \rangle \end{aligned} \quad (2.29)$$

(2.29) is called ‘boundary cross-unitarity’ condition. Any orthonormal basis could be used instead of \mathcal{B} .

9) Boundary bound states: at some poles of $(\tilde{R}_1)_{m,E}(\Theta)$ in the physical strip the singular part has a contribution corresponding to boundary bound states:

$$(\tilde{R}_1)_{m,E}(\Theta) = \frac{\tilde{h}_{E_1}^{m,E} \tilde{g}_{m,E}^{E_1}}{\Theta - iu} + s(\Theta) + reg(\Theta) \quad (2.30)$$

where iu , $0 < u < \pi/2$, is the location of the pole, $reg(\Theta)$ is regular at iu , $s(\Theta)$ contains further possible singular terms. u is called fusion angle. It will also be denoted by ν .

$$\tilde{h}_{E_1}^{m,E} : \mathcal{H}_{B,E_1} \rightarrow V_m \otimes \mathcal{H}_{B,E}$$

is the boundary decay tensor,

$$\tilde{g}_{m,E}^{E_1} : V_m \otimes \mathcal{H}_{B,E} \rightarrow \mathcal{H}_{B,E_1}$$

is the boundary fusion tensor. We also have the hatted versions

$$\hat{h}_{E_1}^{m,E} : \mathcal{H}_{B,E_1} \rightarrow V_m(-iu) \otimes \mathcal{H}_{B,E}$$

and

$$\hat{g}_{m,E}^{E_1} : V_m(iu) \otimes \mathcal{H}_{B,E} \rightarrow \mathcal{H}_{B,E_1} .$$

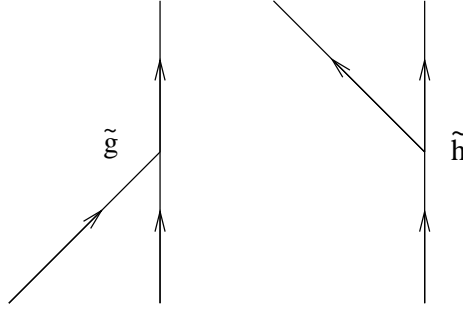


Figure 2.8: Boundary fusion and decay tensors



Figure 2.9: Contribution of boundary bound states

E , E_1 , m and u are related by energy conservation: $E_1 = E + m \cos(u)$.

Graphical representation of $\tilde{g}_{m,E}^{E_1}$ and $\hat{h}_{E_1}^{m,E}$ can be seen in Figure 2.8. The graphical representation of the residue $\tilde{h}_{E_1}^{m,E} \tilde{g}_{m,E}^{E_1}$ is shown in Figure 2.9.

The image space of $\tilde{g}_{m,E}^{E_1}$ has zero intersection with the kernel of $\tilde{h}_{E_1}^{m,E}$.

Generally if

$$V_1 = \oplus_{l_1} V_{l_1} , \quad \mathcal{H}_{B,1} = \oplus_{l_1^b} \mathcal{H}_{B,l_1^b} , \quad \mathcal{H}_{B,2} = \oplus_{l_2^b} \mathcal{H}_{B,l_2^b}$$

where l_1 , l_1^b and l_2^b take certain values from all possible values of l , l^b defined in (2.5) and (2.26) and the states in V_1 , $\mathcal{H}_{B,1}$, $\mathcal{H}_{B,2}$ have mass m and energy E , E_1 and there exists a fusion tensor $\tilde{g}_{m,E}^{E_1}$ and

$$\tilde{g}_{m,E}^{E_1}(V_1 \otimes \mathcal{H}_{B,1}) = \mathcal{H}_{B,2} ,$$

then we say that the boundary states labeled by l_2^b (i.e. the multiplet $\mathcal{H}_{B,2}$) are bound states of the particles and boundary states labeled by l_1 and l_1^b (i.e. of the multiplet V_1 and $\mathcal{H}_{B,1}$). We can write

$$V_1 + \mathcal{H}_{B,1} \rightarrow \mathcal{H}_{B,2} \quad (u) , \quad (2.31)$$

where u is the boundary fusion angle, and call this expression a boundary fusion rule.

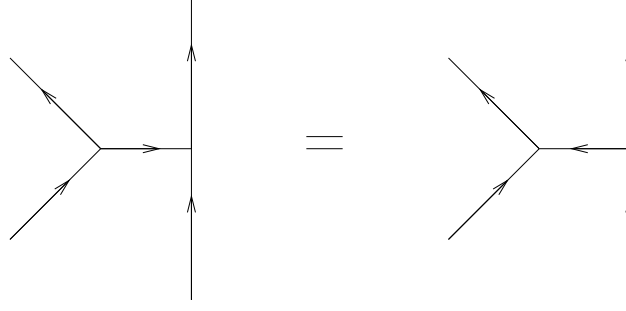


Figure 2.10: Graphical representation for (2.34)

A rule denoted as

$$a + B_1 \rightarrow B_2 \quad (u) \quad (2.32)$$

can be written down and also called a boundary fusion rule if there exists a boundary fusion tensor \tilde{g} with fusion angle u with nonzero matrix element between the one-particle states $|a\rangle$ and the boundary states $|B_1\rangle, |B_2\rangle$: $\langle B_2 | \tilde{g}(a \otimes B_1) \rangle \neq 0$.

10) At some poles the singular part of $(\tilde{R}_1)_{m,E}(\Theta)$ may have contributions related to the existence of a bulk fusion tensor $\tilde{f}_{mm'}^{m'}$. If such a fusion tensor exists, then $(\tilde{R}_1)_{m,E}(\Theta)$ can be written as

$$(\tilde{R}_1)_{m,E}(\Theta) = \frac{1}{2} \frac{[I \otimes \tilde{G}_{m',E}^E][\tilde{d}_m^{mm'} \otimes I]}{\Theta - iu} + s(\Theta) + \text{reg}(\Theta) , \quad (2.33)$$

where u is determined by the kinematical condition that

$$m(\cosh(iu), \sinh(iu)) = m(\cosh(-iu), \sinh(-iu)) + m'(\cosh(i\pi/2), \sinh(i\pi/2)) .$$

The residue can be written in another form as well:

$$[I \otimes \tilde{G}_{m',E}^E][\tilde{d}_m^{mm'} \otimes I] = [\tilde{f}_{mm'}^m \otimes I][I \otimes \tilde{H}_E^{m',E}] . \quad (2.34)$$

A diagrammatic representation is shown in Figure 2.10.

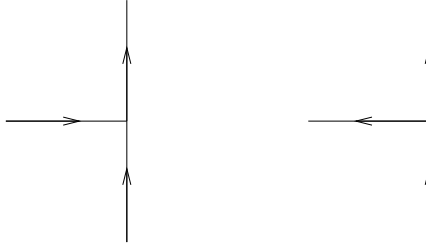
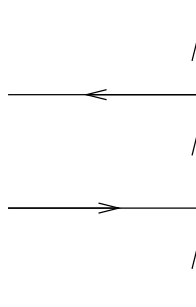
$$\tilde{H}_E^{m,E} : \mathcal{H}_{B,E} \rightarrow V_m \otimes \mathcal{H}_{B,E}$$

can be regarded as a decay tensor,

$$\tilde{G}_{m,E}^E : V_m \otimes \mathcal{H}_{B,E} \rightarrow \mathcal{H}_{B,E}$$

as a fusion tensor. We also have the hatted versions

$$\hat{H}_E^{m,E} : \mathcal{H}_{B,E} \rightarrow V_m(-i\pi/2) \otimes \mathcal{H}_{B,E}$$

Figure 2.11: $\tilde{G}_{m,E}^E$ and $\tilde{H}_E^{m,E}$ Figure 2.12: Graphical representation for $\tilde{H}_E^{m,E} \tilde{G}_{m,E}^E$

and

$$\hat{G}_{m,E}^E : V_m(i\pi/2) \otimes \mathcal{H}_{B,E} \rightarrow \mathcal{H}_{B,E} .$$

The graphical representation of $\tilde{G}_{m,E}^E$ and $\tilde{H}_E^{m,E}$ is shown in Figure 2.11.

The existence of $\tilde{f}_{mm}^{m'}$ does not necessarily imply that a contribution (2.33) really exists, as $\tilde{G}_{m',E}^E$ and $\tilde{H}_E^{m',E}$ may be zero.

If $\tilde{G}_{m',E}^E$ and $\tilde{H}_E^{m',E}$ are nonzero, then $(\tilde{R}_1)_{m',E}(\Theta)$ can be written as

$$(\tilde{R}_1)_{m,E}(\Theta) = \frac{1}{2} \frac{\tilde{H}_E^{m,E} \tilde{G}_{m,E}^E}{\Theta - i\pi/2} + s(\Theta) + \text{reg}(\Theta) \quad (2.35)$$

and so it usually has a pole at $i\pi/2$. The graphical representation of $\tilde{H}_E^{m,E} \tilde{G}_{m,E}^E$ is shown in Figure 2.12.

We remark that in some cases $\tilde{g}_{m',E}^E$ and $\tilde{h}_E^{m',E}$ exist and $s(\Theta)$ contains a contribution of the form (2.30).

The image space of $\tilde{G}_{m',E}^E$ has zero intersection with the kernel of $\tilde{H}_E^{m',E}$.

We also have the relation

$$\begin{aligned} (\tilde{R}_1)_{m',E}^{m'}(\Theta) [I \otimes \tilde{G}_{m,E}^E] [(\tilde{S}_2)_{mm'}(\frac{i\pi}{2} - \Theta) \otimes I] = \\ = [I \otimes \tilde{G}_{m,E}^E] [(\tilde{S}_2)_{mm'}(\frac{i\pi}{2} + \Theta) \otimes I] [I \otimes (\tilde{R}_1)_{m',E}(\Theta)] , \end{aligned} \quad (2.36)$$

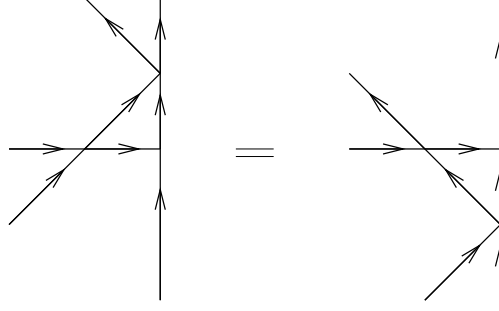


Figure 2.13: Graphical representation for (2.36)

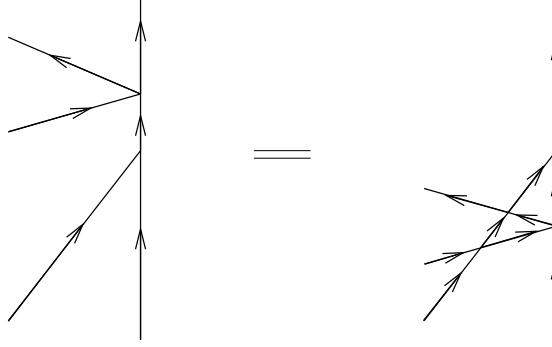


Figure 2.14: The first boundary bootstrap equation

which can be obtained from (2.28) and (2.16). Its graphical representation is shown in Figure 2.13.

11) Bootstrap equations

There are two kinds of bootstrap equations in the presence of a boundary. The first kind is related to reflections on boundary bound states: let iu be the location of the pole of $(\tilde{R}_1)_{m,E}(\Theta)$ for some mass m and energy E that corresponds to a boundary bound state. The following equation called the boundary bootstrap equation is satisfied:

$$[(\tilde{R}_1)_{m_1,E_1}(\Theta)][I \otimes \tilde{g}_{m,E}^{E_1}] = [I \otimes \tilde{g}_{m,E}^{E_1}][(\tilde{S}_2)_{m,m_1}(iu + \Theta) \otimes I][I \otimes (\tilde{R}_1)_{m_1,E}(\Theta)][(\tilde{S}_2)_{m_1,m}(\Theta - iu) \otimes I] . \quad (2.37)$$

We shall also call it first boundary bootstrap equation.

A graphical representation of (2.37) is shown in Figure 2.14.

The second kind is related to reflections of bound states of particles: let us assume that the underlying bulk factorized scattering theory has the property that if $(\tilde{S}_2)_{m_1 m_2}(\Theta)$

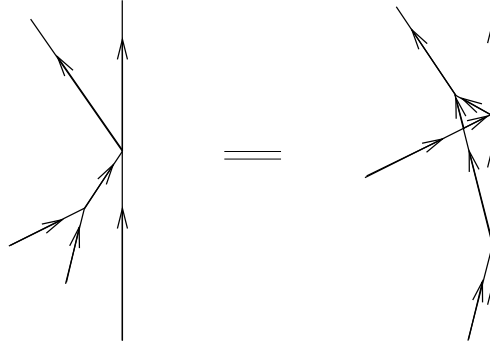


Figure 2.15: The second boundary bootstrap equation

has a pole at iu that corresponds to bound states, then $(\tilde{S}_2)_{m_2 m_1}(\Theta)$ also has a pole at iu corresponding to bound states. This property is ensured if, for example, the scattering is invariant with respect to space reflection. If $(\tilde{S}_2)_{m_1 m_2}(\Theta)$ has a pole that corresponds to a direct channel bound state, then the following equation is satisfied:

$$\begin{aligned}
 & [(\tilde{R}_1)_{m_3, E}(\Theta)][\tilde{f}_{m_1 m_2}^{m_3} \otimes I] = \\
 & = [\tilde{f}_{m_2 m_1}^{m_3} \otimes I][I \otimes (\tilde{R}_1)_{m_1, E}(\Theta + iu_1)][(\tilde{S}_2)_{m_1 m_2}(2\Theta + iu_1 - iu_2) \otimes I][I \otimes (\tilde{R})_{m_2, E}(\Theta - iu_2)] .
 \end{aligned} \tag{2.38}$$

We shall call it second boundary bootstrap equation. A graphical representation of (2.38) is shown in Figure 2.15.

12) Boundary Coleman-Thun diagrams

The statements made in 10) in Section 2.1 can be generalized for the singularities of $\tilde{R}_1(\Theta)$ in a straightforward way [91]. In general, first order poles correspond only to the diagrams shown in Figures 2.9, 2.10, 2.12. This general rule is often modified, however.

A more detailed description of boundary Coleman-Thun diagrams and the singularities of $\tilde{R}_1(\Theta)$ can be found in [21], for example. Applications can be found in [21, 22, 20, 23]. We remark that significant steps were made in [92] and [93] to develop perturbative quantum field theory in the presence of a boundary and to justify the generalization of the description of singularities to the boundary case.

13) Symmetries

Let \mathcal{A}^b be an associative algebra over \mathbb{R} . The representation of \mathcal{A}^b has the following

structure usually: \mathcal{A}^b is usually a remnant of a symmetry algebra \mathcal{A} of the underlying bulk scattering, so it is sufficient to have a representation $D_B : \mathcal{A}_B \rightarrow \text{End}(\mathcal{H}_B)$ of \mathcal{A}^b on \mathcal{H}_B and a co-product (an algebra-homomorphism) $\Delta_B : \mathcal{A}^b \rightarrow \mathcal{A} \otimes \mathcal{A}^b$ to define representations on the \mathcal{H}_N^b spaces. It is assumed that the representations of \mathcal{A} in the bulk scattering theory have the structure that is described in Section 2.1.

Generally the co-product Δ_B allows the definition of the product $D_1 \times D_2 \times \cdots \times D_N \times D_B$ of arbitrary representations D_1, D_2, \dots, D_N of \mathcal{A} and of an arbitrary representation D_B of \mathcal{A}^b , which will be a representation of \mathcal{A}^b . The definition of the product is analogous to that described in Section 2.1. For two representations

$$D_1 \times D_B = (D_1 \otimes D_B) \circ \Delta_B .$$

For D_1, D_2, D_B one can choose either

$$\begin{aligned} D_1 \times D_2 \times D_B &= D_1 \times (D_2 \times D_B) = [D_1 \otimes ((D_2 \otimes D_B) \circ \Delta_B)] \circ \Delta_B = \\ &= (D_1 \otimes D_2 \otimes D_B) \circ (Id_{\mathcal{A}} \otimes \Delta_B) \circ \Delta_B \end{aligned} \quad (2.39)$$

or

$$\begin{aligned} D_1 \times D_2 \times D_B &= (D_1 \times D_2) \times D_B = [((D_1 \otimes D_2) \circ \Delta) \otimes D_B] \circ \Delta_B = \\ &= (D_1 \otimes D_2 \otimes D_B) \circ (\Delta \otimes Id_{\mathcal{A}^b}) \circ \Delta_B . \end{aligned} \quad (2.40)$$

Δ_B is usually required to have the co-associativity property

$$(Id_{\mathcal{A}} \otimes \Delta_B) \circ \Delta_B = (\Delta \otimes Id_{\mathcal{A}^b}) \circ \Delta_B ,$$

where Δ is the co-product of \mathcal{A} , which implies that the two definitions (2.39) and (2.40) are equivalent. If Δ and Δ_B are both co-associative, then the multiplication of representations is associative.

Usually \mathcal{A}^b can be realized as a subalgebra of \mathcal{A} , i.e. there exists a monomorphism $i : \mathcal{A}^b \rightarrow \mathcal{A}$. i is not necessarily unique.

If $(\Delta \circ i)(\mathcal{A}^b) \subseteq \mathcal{A} \otimes \mathcal{A}^b$, then a co-product Δ_B can be defined in terms of Δ and i as follows:

$$\Delta_B = (Id_{\mathcal{A}} \otimes i)^{-1} \circ \Delta \circ i . \quad (2.41)$$

This co-product is co-associative if Δ is co-associative. The co-product Δ_B that actually appears in the definition of representations on multi-particle spaces often admits the form (2.41).

In the definition of a symmetry transformation we assume that \mathcal{A} is a symmetry algebra of the underlying bulk factorized scattering theory. An element $A_B \in \mathcal{A}^b$ is a symmetry of the R operator if R_1 has the intertwining property

$$D(A_B)R_1 = R_1D(A_B) , \quad (2.42)$$

where $D(A_B)$ is the representation of A_B on \mathcal{H}_1^b . (2.42) and the assumed symmetry property of \mathcal{A} imply that R_N has the intertwining property for the representation on \mathcal{H}_N^b for any value of N . A symmetry of a fusion or a decay tensor is defined similarly. A symmetry of the factorized scattering theory with boundary is a symmetry of the R operator and all fusion and decay tensors.

The remnant of the Poincare algebra is generated by the time translation generator H_B and the unit element I_B , the co-multiplication is

$$\Delta_B(H_B) = H \otimes I_B + I \otimes H_B, \quad \Delta_B(I_B) = I \otimes I_B. \quad (2.43)$$

We refer the reader to [19] for the discussion of higher spin conserved quantities. The special case of the boundary supersymmetry algebra will be discussed, however, in later sections.

14) Charge conjugation and reflections

Space reflection is not defined. It could be introduced as a transformation that relates distinct theories with boundaries on the left- and right-hand side, respectively.

The boundary charge conjugation and time reflection C_B and T_B , if their representation is defined in a theory, have the properties that $C_B(\mathcal{H}_{B,E}) = \mathcal{H}_{B,E}$ and $T_B(\mathcal{H}_{B,E}) = \mathcal{H}_{B,E}$. We also have

$$T_N = \underbrace{T_1 \otimes T_1 \otimes \cdots \otimes T_1}_N \otimes T_B$$

on \mathcal{H}_N^b . (Where T_B and T_N denote the restriction of T to \mathcal{H}_B and \mathcal{H}_N^b .)

Invariance of the R operator with respect to charge conjugation means invariance of the underlying bulk scattering theory as defined in 12) in Section 2.1 and

$$\tilde{C}\tilde{R}_1(\Theta) = \tilde{R}_1(\Theta)\tilde{C},$$

invariance of boundary fusion and decay tensors means

$$\tilde{C}\tilde{g}_{m,E}^{E_1} = \tilde{g}_{m,E}^{E_1}\tilde{C} \quad \text{and} \quad \tilde{C}\tilde{h}_{E_1}^{m,E} = \tilde{h}_{E_1}^{m,E}\tilde{C}.$$

Invariance of the R operator with respect to time reflection means invariance of the underlying bulk scattering theory as defined in 12) in Section 2.1 and

$$\tilde{T}\tilde{R}_1(\Theta) = (\tilde{R}_1(\Theta))^\dagger \tilde{T},$$

invariance of boundary fusion and decay tensors means

$$\tilde{T}\tilde{g}_{m,E}^{E_1} = (\tilde{h}_{E_1}^{m,E})^\dagger \tilde{T}.$$

Invariance of factorized scattering theory with boundary means that the R operator and the fusion and decay tensors are both invariant.

We remark, finally, that we assume that all boundary states are bound states, which implies that all boundary states can be generated in a few steps from the ground state by boundary fusion.

It is possible to introduce boundary particle groups, which are in fact multi-particle states (containing a boundary state) with fixed rapidities of the constituent particles. These ‘boundary particle groups’ behave in the same way as boundary states. They can also be regarded as compound boundary states. The reflection matrix elements on the boundary particle groups can be built from the two-particle S-matrix and one-particle reflection matrix in a straightforward way. One can also allow bulk ‘particle groups’ introduced in Section 2.1, their reflection matrix elements are also defined in a straightforward way. The boundary Yang-Baxter and bootstrap equations can be given a similar interpretation as in the bulk.

We also remark that the space of *in* and *out* and *intermediate* states were defined to be different, which is a minor deviation from the more standard formalism, in which both the *in* and the *out* states span the whole Hilbert space. This formalism corresponds to quotienting out the Hilbert space by the subspace defined by relations $|v\rangle = \cdots \otimes I \otimes \cdots \otimes S_2 \otimes \cdots \otimes I|v\rangle$, and $|v\rangle = \cdots \otimes I \otimes \cdots R_1|v\rangle$, where $|v\rangle$ is any multi-particle state with rapidities so that S_2 and R_1 is nonsingular and has nonzero determinant.

As in the bulk case, one can draw further figures which are similar to Figure 2.14 and Figure 2.15 and write down the corresponding bootstrap equations. These new equations, however, can be derived from the axioms written down and do not impose new restrictions.

2.3 The bootstrap method

The bootstrap method is a method for finding factorized scattering theories, i.e. solutions to the conditions described in Section 2.1. The boundary bootstrap method is a straightforward extension of the bootstrap method to the boundary case.

A description of the bootstrap method is the following: let us assume that we already know a part of the particle spectrum that is closed under scattering and the action of CPT, and this action is also known or can be guessed. The corresponding internal space is denoted by V^0 . In this case we solve the Yang-Baxter equation for $\tilde{S}_2(\Theta)|_{V^0 \otimes V^0}$. In some cases it is done by converting it into a linear differential equation by differentiation. If we look for theories with a given symmetry the action of which on V^0 is known, then

imposing it on $\tilde{S}_2(\Theta)|_{V^0 \otimes V^0}$ may also simplify the Yang-Baxter equations. The solution is obviously undetermined up to an overall scalar function multiplier $F(\Theta)$ and it can contain further undetermined parameters. Only analytic $F(\Theta)$ and $\tilde{S}_2(\Theta)|_{V^0 \otimes V^0}$ with possible pole singularities are considered. $F(\Theta)$ and the solution is further restricted by the real analyticity, unitarity and crossing symmetry conditions. After imposing these conditions $F(\Theta)$ is constrained to satisfy the equations $F(\Theta) = F(i\pi - \Theta)$, $F(\Theta)F(-\Theta) = 1$ and $F(\Theta^*)^* = F(-\Theta)$. The functions satisfying these equations are called CDD (Castillejo-Dalitz-Dyson, [94]) factors. $F(\Theta)$ is usually chosen so that $\tilde{S}_2(\Theta)|_{V^0 \otimes V^0}$ have the minimum or nearly minimum number of poles in the physical strip. After having determined $\tilde{S}_2(\Theta)|_{V^0 \otimes V^0}$, we check whether its poles lying in the physical strip can be related to bound states and Coleman-Thun diagrams as described in 4), 7), 10) in Section 2.1, and whether the bootstrap equations are satisfied. One often finds that not all simple poles can be explained in terms of bound states and Coleman-Thun diagrams, and in this case one extends V^0 by including new particles with masses prescribed by the location of the unexplained poles and kinematics. This extension of V^0 is denoted by V^1 . The bootstrap equations allow to calculate the still unknown parts of $\tilde{S}_2(\Theta)|_{V^1 \otimes V^1}$, they are linear algebraic equations for these parts. The action of possible symmetries is also determined on the extension of V^0 by demanding that the intertwining properties hold. The next step is to check again if the simple poles of $\tilde{S}_2(\Theta)|_{V^1 \otimes V^1}$ can be explained in terms of bound states and Coleman-Thun diagrams. If this is not the case, then one can continue by extending V^1 further into an internal space V^2 , calculate $\tilde{S}_2(\Theta)|_{V^2 \otimes V^2}$ and so on until no further extension is necessary. Finally it should be checked whether all poles can be explained in terms of bound states and Coleman-Thun diagrams. If they can, the procedure is finished ('the bootstrap is closed').

In case of the sine-Gordon model, for instance, V^0 can be chosen to be a two-dimensional space spanned by the soliton and anti-soliton, and the bootstrap is closed in one step. The space V^1 is spanned by the breathers together with the soliton and anti-soliton.

The choice of the CDD factor has an influence on the singularity structure of the S-matrix, so the consistency of the axioms of Section 2.1 imposes a constraint on the CDD factor, although in a complicated way.

It should also be noted that there is a large class of models (including the sinh-Gordon model, for example) in which the scattering is diagonal, and in this case the Yang-Baxter equation is automatically satisfied and cannot be used to constrain the S-matrix. However, the second part of the above method remains unaltered.

The boundary bootstrap method is the straightforward adaptation of the above de-

scribed steps to the boundary factorized scattering theory. One usually assumes that the ground state is unique and one starts with $\mathcal{H}_B^0 = \mathcal{H}_{B0}$. (The boundary analogue of V^0, V^1, \dots is denoted by $\mathcal{H}_B^0, \mathcal{H}_B^1, \dots$.) Then one determines the ground state reflection matrix $\tilde{R}_1(\Theta)|_{V \otimes \mathcal{H}_B^0}$ by the boundary Yang-Baxter equations, unitarity, crossing symmetry and real analyticity conditions and by the second boundary bootstrap equations. The second boundary bootstrap equation is a linear algebraic equation for the reflection matrix of bulk bound states on the the ground state boundary, so if the ground state reflection matrices of certain particles is already known, then the second boundary bootstrap equation generally allows one to compute the ground state reflection matrix of their bound states relatively easily.

If we multiply a reflection matrix which satisfies the Yang-Baxter equation by an overall scalar factor $F(\Theta)$, then the result also satisfies the Yang-Baxter equation. If the unitarity, crossing symmetry and real analyticity conditions are also taken into consideration, then $F(\Theta)$ is constrained exactly in the same way as in the bulk case described above. This $F(\Theta)$ is also referred to as a CDD factor.

Having obtained the ground state reflection matrix one considers the poles of this reflection matrix and determines $\mathcal{H}_B^1 < \mathcal{H}_B^2 < \dots$ and $\tilde{R}_1(\Theta)|_{V \otimes \mathcal{H}_B^0}, \tilde{R}_1(\Theta)|_{V \otimes \mathcal{H}_B^1}, \dots$ until the bootstrap is closed. In summary, in the boundary case all the excited boundary states are obtained by bootstrap from the ground state.

We remark that to perform the complete bootstrap procedure as described above can be rather laborious. In some cases the equations are best handled by a suitable computer algebra program. It is not uncommon in the literature that only certain parts, e.g. the solution of the Yang-Baxter equation or the verification of the pole structure and the actual bootstrap are considered, especially in the boundary case. Often the check of the correspondence between poles and Coleman-Thun diagrams is not performed completely.

The boundary bootstrap is usually harder than the bulk bootstrap, partially because it is built on the bulk part, partially because the equations themselves are larger and more difficult to handle, the structure of boundary states is more complex than the structure of bulk states, and much more Coleman-Thun diagrams exist than in the bulk.

It should be noted that if a solution to the axioms of factorized scattering theory has been found, then it is usually a further problem to link this solution to a model defined by a Lagrangian function, for instance, or to make sure that the solution is really right for the model that one investigates. In some cases the problem is only to find the mapping between the parameters of the Lagrangian function and the parameters of the solution. This matching of S matrices with field theoretical models is usually done by various other methods of quantum field theory.

In the rest of this chapter we shall generally omit the tilde and subscripts 2 and 1 from $\tilde{S}_2(\Theta)$ and $\tilde{R}_1(\Theta)$ and write $S(\Theta)$ and $R(\Theta)$, and we shall not use the other (e.g. hatted) versions of the two-particle S-matrix. Similar change in the notation applies to the fusion and decay tensors.

2.4 The supersymmetry algebra in 1+1 dimensions

The supersymmetry algebra \mathcal{A} is an associative algebra over \mathbb{R} , generated by $Q, \bar{Q}, \hat{Z}, H, P, N, \Gamma, I$. Q and \bar{Q} are called supercharges, \hat{Z} is the supersymmetric central charge, Γ is the fermionic parity operator, H and P are the time and space translation generators, N is the boost generator and I is the unit element of the algebra. These generators satisfy the following relations:

$$\begin{aligned}
\{\Gamma, \Gamma\} &= 2I & \{Q, \bar{Q}\} &= 2\hat{Z} \\
\{\Gamma, Q\} &= 0 & \{\Gamma, \bar{Q}\} &= 0 \\
\{Q, Q\} &= 2(H + P) & \{\bar{Q}, \bar{Q}\} &= 2(H - P) \\
[N, Q] &= \frac{1}{2}Q & [N, \bar{Q}] &= -\frac{1}{2}\bar{Q} \\
[N, \Gamma] &= 0 & & \\
[N, H + P] &= H + P & [N, H - P] &= -(H - P) .
\end{aligned} \tag{2.44}$$

The supersymmetric central charge commutes with all elements of the algebra. \mathcal{A} admits a \mathbb{Z}_2 -grading, generators of grade 0 are H, P, N, \hat{Z}, I , generators of grade 1 are Q, \bar{Q}, Γ .

One can also introduce the boosts: $B(\varphi) = e^{\varphi N}$.

The co-product Δ used to define the action of \mathcal{A} on multi-particle states is given by

$$\begin{aligned}
\Delta(Q) &= Q \otimes I + \Gamma \otimes Q & \Delta(\bar{Q}) &= \bar{Q} \otimes I + \Gamma \otimes \bar{Q} \\
\Delta(\Gamma) &= \Gamma \otimes \Gamma & \Delta(\hat{Z}) &= \hat{Z} \otimes I + I \otimes \hat{Z} \\
\Delta(H) &= H \otimes I + I \otimes H & \Delta(P) &= P \otimes I + I \otimes P \\
\Delta(N) &= N \otimes I + I \otimes N .
\end{aligned} \tag{2.45}$$

Δ satisfies the co-associativity property.

We call the algebra obtained by the omission of N the internal part of \mathcal{A} . We denote this internal part by $\tilde{\mathcal{A}}$. It has the property that $B(\varphi)\tilde{\mathcal{A}}B(-\varphi) = \tilde{\mathcal{A}}$ and $\Delta(\tilde{\mathcal{A}}) \subset \tilde{\mathcal{A}} \otimes \tilde{\mathcal{A}}$.

The latter property implies that the restriction of Δ to $\tilde{\mathcal{A}}$ will be a (co-associative) co-product for $\tilde{\mathcal{A}}$.

The one-particle representations of \mathcal{A} generally take the form of induced representations. A representation D of \mathcal{A} that is induced from a representation of $\tilde{\mathcal{A}}$ is characterized by the following properties: the representation space H can be written as

$$H = \int d\Theta W(\Theta) , \quad (2.46)$$

where the space $W(\Theta)$ at any fixed Θ is invariant with respect to $\tilde{\mathcal{A}}$ and contains states with rapidity Θ . The notation $W(D(\Theta))$, $W_{D(\Theta)}$, $W_D(\Theta)$ are also used instead of $W(\Theta)$. The representation of $\tilde{\mathcal{A}}$ on $W(\Theta)$ is denoted by $D(\Theta)$. We have

$$D(B(\varphi))D(\Theta)(\tilde{A})D(B(-\varphi)) = D(\Theta + \varphi)(B(\varphi)\tilde{A}B(-\varphi)) \quad (2.47)$$

for all $\tilde{A} \in \tilde{\mathcal{A}}$, this equation describes the relation between the representations $D(\Theta)$ at various values of Θ .

We can introduce the linear isomorphisms $i_\Theta : W(\Theta) \rightarrow W$, $a(\Theta) \mapsto a$, where the space W is called the internal space. The notation W_D or $W(D)$ is also used instead of W . The equation $D(B(\varphi))a(\Theta) = a(\Theta + \varphi)$ is satisfied. For any fixed Θ a representation of $\tilde{\mathcal{A}}$ on W can be defined in the following way: $\tilde{A} \mapsto i_\Theta D(\Theta)(\tilde{A})i_\Theta^{-1}$. We do not introduce new notation for these representations, we denote them by $D(\Theta)$.

The product of two representations $D_1(\Theta_1)$ and $D_2(\Theta_2)$ of $\tilde{\mathcal{A}}$ is obtained using the co-product $\Delta|_{\tilde{\mathcal{A}}}$. $D_1(\Theta_1) \times D_2(\Theta_2)$ is contained in $D_1 \times D_2$.

2.4.1 Representations of the supersymmetry algebra

We consider representations on Hilbert spaces. The Hermitian adjoints of the generators are

$$H^\dagger = H \quad P^\dagger = P \quad Q^\dagger = Q \quad \bar{Q}^\dagger = \bar{Q} \quad \hat{Z}^\dagger = \hat{Z} \quad \Gamma^\dagger = \Gamma \quad N^\dagger = -N . \quad (2.48)$$

On a one-particle supersymmetric multiplet $|a(\Theta)\rangle$ the action of the supersymmetry algebra takes the following general form:

$$Q|a(\Theta)\rangle = \sqrt{m}e^{\Theta/2}q|a(\Theta)\rangle \quad (2.49)$$

$$\bar{Q}|a(\Theta)\rangle = \sqrt{m}e^{-\Theta/2}\bar{q}|a(\Theta)\rangle \quad (2.50)$$

$$B(\varphi)|a(\Theta)\rangle = e^{\varphi N}|a(\Theta)\rangle = |a(\varphi + \Theta)\rangle , \quad (2.51)$$

where m is the mass of the multiplet and q and \bar{q} are Θ -independent matrices which act on the states of the supermultiplet and satisfy

$$q^2 = 1, \quad \bar{q}^2 = 1, \quad \{q, \bar{q}\} = 2Z ,$$

where $Z = \frac{1}{m}\hat{Z}$ on the multiplet. The action of Γ is independent of Θ and

$$\{\Gamma, q\} = \{\Gamma, \bar{q}\} = 0.$$

The boson-fermion representation P_m of mass m is defined by

$$q = \begin{pmatrix} 0 & \epsilon \\ \epsilon^* & 0 \end{pmatrix}, \quad \bar{q} = \begin{pmatrix} 0 & \epsilon^* \\ \epsilon & 0 \end{pmatrix}, \quad \Gamma = \begin{pmatrix} 1 & 0 \\ 0 & -1 \end{pmatrix} \quad (2.52)$$

in the basis $\{\phi(\Theta), \psi(\Theta)\}$, where $\epsilon = \exp(i\pi/4)$. The basis vectors $\phi(\Theta)$ and $\psi(\Theta)$ correspond to bosons and fermions, respectively. The central charge is zero in this representation. The action of CPT is $CPT\phi(\Theta) = \phi(\Theta)$, $CPT\psi(\Theta) = -\psi(\Theta)$. The boson-fermion representation will also be called particle representation and the boson-fermion states will also be called particle states. The word particle is used in the general sense as well, not referring to any particular representation.

Another representation \bar{P}_m is obtained if we multiply Γ in (2.52) by -1 . We call it pseudo-boson-fermion representation.

The kink representation K_m of mass m is given by

$$\begin{aligned} q &= \begin{pmatrix} 0 & i & 0 & 0 \\ -i & 0 & 0 & 0 \\ 0 & 0 & 1 & 0 \\ 0 & 0 & 0 & -1 \end{pmatrix}, & \bar{q} &= \begin{pmatrix} 0 & i & 0 & 0 \\ -i & 0 & 0 & 0 \\ 0 & 0 & -1 & 0 \\ 0 & 0 & 0 & 1 \end{pmatrix}, \\ \Gamma &= \begin{pmatrix} 0 & 1 & 0 & 0 \\ 1 & 0 & 0 & 0 \\ 0 & 0 & 0 & 1 \\ 0 & 0 & 1 & 0 \end{pmatrix}, & Z &= \begin{pmatrix} 1 & 0 & 0 & 0 \\ 0 & 1 & 0 & 0 \\ 0 & 0 & -1 & 0 \\ 0 & 0 & 0 & -1 \end{pmatrix} \end{aligned} \quad (2.53)$$

in the basis $\{K_{0\frac{1}{2}}(\Theta), K_{1\frac{1}{2}}(\Theta), K_{\frac{1}{2}0}(\Theta), K_{\frac{1}{2}1}(\Theta)\}$.

There are further representations \bar{K}_m called pseudo-kink representations, which are obtained by multiplying q and \bar{q} by -1 in (2.53), or by interchanging the labels $0 \leftrightarrow 1$.

It is also true that there exists a continuous family of (inequivalent) representations similar to the kink representation and interpolating between the kink and pseudo-kink representations.

Multi-kink states have to respect an adjacency condition: in the physical $|\dots K_{ab}(\Theta_1)K_{cd}(\Theta_2)\dots\rangle$ state $b = c$ must hold. Multi-kink states not satisfying this condition are set equal to zero (so $(\Gamma \otimes I)|K_{\frac{1}{2}1}(\Theta_1)K_{1\frac{1}{2}}(\Theta_2)\rangle = 0$, for example). This adjacency condition gives kinks a character rather different from that of usual particles.

CPT acts as follows: $K_{ab} \leftrightarrow K_{ba}$.

The following decomposition equations hold for two-particle states:

$$P_{m_1} \times P_{m_2} \simeq \sum_m (P_m + \bar{P}_m) , \quad \bar{P}_{m_1} \times \bar{P}_{m_2} \simeq \sum_m (P_m + \bar{P}_m) , \quad (2.54)$$

$$P_{m_1} \times \bar{P}_{m_2} \simeq \sum_m (P_m + \bar{P}_m) . \quad (2.55)$$

In (2.54) the first equation means, for example, that a two-particle state transforms in the sum of a boson-fermion and a pseudo-boson-fermion representation (of appropriate mass). One can write down the decomposition equations for the $P_{m_1}(\Theta_1)$ etc. representations of $\tilde{\mathcal{A}}$ as well:

$$P_{m_1}(\Theta_1) \times P_{m_2}(\Theta_2) \simeq P_m(\Theta) + \bar{P}_m(\Theta) , \quad \bar{P}_{m_1}(\Theta_1) \times \bar{P}_{m_2}(\Theta_2) \simeq P_m(\Theta) + \bar{P}_m(\Theta) , \quad (2.56)$$

$$P_{m_1}(\Theta_1) \times \bar{P}_{m_2}(\Theta_2) \simeq P_m(\Theta) + \bar{P}_m(\Theta) , \quad (2.57)$$

where m and Θ are determined by $m_1, m_2, \Theta_1, \Theta_2$ kinematically.

Multi-kink states containing even number of kinks can be arranged in two sectors: the first sector contains the states which have left and right label $\frac{1}{2}$, the second sector contains the states which have left and right labels 0 or 1. These two sectors will be called $\frac{1}{2}$ and 01 sector.

For two-kink states we have the decomposition equation

$$K_m \times K_m \simeq \sum_{m'} ([P_{m'}]_{\frac{1}{2}} + [P_{m'} + \bar{P}_{m'}]_{01}) . \quad (2.58)$$

The subscripts refer to the sectors in which the subspaces lie. The values of m' may have multiplicities higher than 1, this is not denoted explicitly. Similar equations as (2.56), (2.57) can also be written down.

It will become clear that it is reasonable to give the (reducible) representation $[P_{m'}]_{\frac{1}{2}} + [P_{m'} + \bar{P}_{m'}]_{01}$ appearing on the right-hand side of (2.58) a name of its own, which will be ‘two-kink-representation’ of mass m' , denoted by $K_{m'}^{(2)}$. The states transforming in this representation will be called two-kink-states.

The following combinations of two-kink states span the invariant subspaces (see also [33, 39]) :

$[P]_{\frac{1}{2}} :$

$$|\phi_1(\Theta; u)\rangle = |K_{\frac{1}{2}0}(\Theta + iu)K_{0\frac{1}{2}}(\Theta - iu)\rangle + |K_{\frac{1}{2}1}(\Theta + iu)K_{1\frac{1}{2}}(\Theta - iu)\rangle \quad (2.59)$$

$$|\psi_1(\Theta; u)\rangle = i\sqrt{\frac{\cos(\frac{\pi}{4} - \frac{u}{2})}{\cos(\frac{\pi}{4} + \frac{u}{2})}} (|K_{\frac{1}{2}0}(\Theta + iu)K_{0\frac{1}{2}}(\Theta - iu)\rangle - |K_{\frac{1}{2}1}(\Theta + iu)K_{1\frac{1}{2}}(\Theta - iu)\rangle) \quad (2.60)$$

$[P]_{01}$:

$$|\phi_2(\Theta; u)\rangle = |K_{0\frac{1}{2}}(\Theta + iu)K_{\frac{1}{2}0}(\Theta - iu)\rangle + |K_{1\frac{1}{2}}(\Theta + iu)K_{\frac{1}{2}1}(\Theta - iu)\rangle \quad (2.61)$$

$$|\psi_2(\Theta; u)\rangle = \sqrt{\frac{\cos(\frac{\pi}{4} - \frac{u}{2})}{\cos(\frac{\pi}{4} + \frac{u}{2})}} (|K_{1\frac{1}{2}}(\Theta + iu)K_{\frac{1}{2}0}(\Theta - iu)\rangle - |K_{0\frac{1}{2}}(\Theta + iu)K_{\frac{1}{2}1}(\Theta - iu)\rangle) \quad (2.62)$$

$[\bar{P}]_{01}$:

$$|\bar{\phi}(\Theta; u)\rangle = |K_{0\frac{1}{2}}(\Theta + iu)K_{\frac{1}{2}0}(\Theta - iu)\rangle - |K_{1\frac{1}{2}}(\Theta + iu)K_{\frac{1}{2}1}(\Theta - iu)\rangle \quad (2.63)$$

$$|\bar{\psi}(\Theta; u)\rangle = \sqrt{\frac{\cos(\frac{\pi}{4} - \frac{u}{2})}{\cos(\frac{\pi}{4} + \frac{u}{2})}} (|K_{1\frac{1}{2}}(\Theta + iu)K_{\frac{1}{2}0}(\Theta - iu)\rangle + |K_{0\frac{1}{2}}(\Theta + iu)K_{\frac{1}{2}1}(\Theta - iu)\rangle) \quad (2.64)$$

$|\phi_1(\Theta; u)\rangle, |\phi_2(\Theta; u)\rangle$ are boson states with $\Gamma = 1$, $|\psi_1(\Theta; u)\rangle$ and $|\psi_2(\Theta; u)\rangle$ are fermion states with $\Gamma = -1$. The two states in (2.63) and (2.64) span the pseudo-boson-fermion representation. The value of Γ on the pseudo-boson state $|\bar{\phi}(\Theta; u)\rangle$ is -1 , on $|\bar{\psi}(\Theta; u)\rangle$ it is 1 . In the basis (2.59), (2.60); (2.61), (2.62); (2.63), (2.64) the matrices of q and \bar{q} take the form written down above.

CPT acts on these states as follows:

$$CPT|\phi_1(\Theta; u)\rangle = |\phi_1(\Theta; u)\rangle \quad CPT|\psi_1(\Theta; u)\rangle = -|\psi_1(\Theta; u)\rangle \quad (2.65)$$

$$CPT|\phi_2(\Theta; u)\rangle = |\phi_2(\Theta; u)\rangle \quad CPT|\psi_2(\Theta; u)\rangle = -|\psi_2(\Theta; u)\rangle \quad (2.66)$$

$$CPT|\bar{\phi}(\Theta; u)\rangle = |\bar{\phi}(\Theta; u)\rangle \quad CPT|\bar{\psi}(\Theta; u)\rangle = |\bar{\psi}(\Theta; u)\rangle . \quad (2.67)$$

It should be noted that $|\phi_1(\Theta; u)\rangle, |\psi_1(\Theta; u)\rangle, |\phi_2(\Theta; u)\rangle, |\psi_2(\Theta; u)\rangle, |\bar{\phi}(\Theta; u)\rangle$ and $|\bar{\psi}(\Theta; u)\rangle$ are states which have zero norm and are not orthogonal. States transforming in the boson-fermion and pseudo-boson-fermion representations that are orthogonal and have nonzero scalar product with themselves are the following:

$$|\phi_1(\Theta; u)\rangle + |\phi_1(\Theta; -u)\rangle \quad |\psi_1(\Theta; u)\rangle + |\psi_1(\Theta; -u)\rangle \quad (2.68)$$

$$|\phi_2(\Theta; u)\rangle + |\phi_2(\Theta; -u)\rangle \quad |\psi_2(\Theta; u)\rangle + |\psi_2(\Theta; -u)\rangle \quad (2.69)$$

$$|\bar{\phi}(\Theta; u)\rangle + |\bar{\phi}(\Theta; -u)\rangle \quad |\bar{\psi}(\Theta; u)\rangle + |\bar{\psi}(\Theta; -u)\rangle \quad (2.70)$$

and

$$|\phi_1(\Theta; u)\rangle - |\phi_1(\Theta; -u)\rangle \quad |\psi_1(\Theta; u)\rangle - |\psi_1(\Theta; -u)\rangle \quad (2.71)$$

$$|\phi_2(\Theta; u)\rangle - |\phi_2(\Theta; -u)\rangle \quad |\psi_2(\Theta; u)\rangle - |\psi_2(\Theta; -u)\rangle \quad (2.72)$$

$$|\bar{\phi}(\Theta; u)\rangle - |\bar{\phi}(\Theta; -u)\rangle \quad |\bar{\psi}(\Theta; u)\rangle - |\bar{\psi}(\Theta; -u)\rangle . \quad (2.73)$$

Although $K^{(2)}$ can be decomposed into a sum of irreducible representations, the products of elements of $[P]_{\frac{1}{2}}$, $[P]_{01}$ and $[\bar{P}]_{01}$ satisfy certain relations because of the kink adjacency conditions. For example, $|\bar{\phi}\bar{\phi}\rangle = |\phi_2\phi_2\rangle$.

The eight particle-kink states $|p(\Theta_1)K(\Theta_2)\rangle$, where p stands for a boson or fermion and K stands for a kink, transform in the direct sum of a kink and a pseudo-kink representation if and only if

$$\Theta_1 - \Theta_2 = i(\pi - u) \quad \text{and} \quad m = 2M \cos(u) = 2M \sin(\pi/2 - u) , \quad (2.74)$$

where m is the mass of the particle and M is the mass of the kink. This is precisely the condition that the total mass of the particle-kink state is also M . If this condition is not satisfied, then the decomposition of the representation in which the particle-kink states transform contains the general kink-like representations mentioned above but does not contain the kink, pseudo-kink, particle or pseudo-particle representations. The same can be stated for the kink-particle states $|K(\Theta_1)p(\Theta_2)\rangle$. Similar statements can also be made if we replace the particle representation by the $K^{(2)}$ representations.

The simplest vacuum representations are one-dimensional, spanned by a state $|\Omega\rangle$. In a one-dimensional representation all operators act as a multiplication by a number, so Q , \bar{Q} , \hat{Z} , H , P have to be represented by zero. Γ can be either 1 or -1 . It is reasonable to require that a ground state representation D_Ω have the property

$$D_\Omega \times D \simeq D \quad (2.75)$$

for any one-particle representation D . This requirement eliminates the case $D_\Omega(\Gamma) = -1$. Different values for N yield inequivalent one-dimensional representations, all of which satisfy (2.75), nevertheless the scattering data does not depend on the eigenvalue of N on $|\Omega\rangle$, so it is chosen to be 0. The choice $D_\Omega(\Gamma) = -1$ would also leave the scattering data unaltered. CPT acts in the following way: $CPT|\Omega\rangle = |\Omega\rangle$.

Another natural vacuum representation $D_{01\frac{1}{2}}$ is 3-dimensional, the representation space is spanned by the vectors $|0\rangle$, $|1\rangle$, $|\frac{1}{2}\rangle$. The generators in this representation are $Q = \bar{Q} = \hat{Z} = H = P = N = 0$,

$$\Gamma = \begin{pmatrix} 0 & 1 & 0 \\ 1 & 0 & 0 \\ 0 & 0 & 1 \end{pmatrix} .$$

The states in this representation are subject to the the kink adjacency conditions. CPT acts in the following way: $CPT|0\rangle = |0\rangle$, $CPT|1\rangle = |1\rangle$, $CPT|\frac{1}{2}\rangle = |\frac{1}{2}\rangle$.

Taking into consideration the adjacency conditions we have

$$D_{01\frac{1}{2}} \times K_m \simeq K_m \times D_{01\frac{1}{2}} \simeq K_m ,$$

and the same equation holds for $[P_m]_{\frac{1}{2}}$, $[P_m]_{01}$, $[\bar{P}_m]_{01}$ and $K_m^{(2)}$, and also if a rapidity is specified and representations of $\tilde{\mathcal{A}}$ are considered. $D_{01\frac{1}{2}}$ is not used together with the P_m representations.

The representation $D_{01\frac{1}{2}}$ appears in the supersymmetric sine-Gordon model, for example (see [95]). It should be noted, however, that the vacuum does not appear to play a role in scattering theory.

The states

$$V_0(\Theta) = |K_{0\frac{1}{2}}(\Theta + \frac{i\pi}{2})K_{\frac{1}{2}0}(\Theta - \frac{i\pi}{2})\rangle \quad (2.76)$$

$$V_1(\Theta) = |K_{1\frac{1}{2}}(\Theta + \frac{i\pi}{2})K_{\frac{1}{2}1}(\Theta - \frac{i\pi}{2})\rangle \quad (2.77)$$

$$V_{\frac{1}{2}}(\Theta) = |K_{\frac{1}{2}0}(\Theta + \frac{i\pi}{2})K_{0\frac{1}{2}}(\Theta - \frac{i\pi}{2})\rangle + |K_{\frac{1}{2}1}(\Theta + \frac{i\pi}{2})K_{1\frac{1}{2}}(\Theta - \frac{i\pi}{2})\rangle \quad (2.78)$$

transform in a representation that differs from $D_{01\frac{1}{2}}$ only in the action of the boosts. Q and \bar{Q} are nilpotent on the states (2.59)-(2.64) at $u = \pi/2$. The kernel and image spaces of Q and \bar{Q} are both spanned by the boson and pseudo-boson states, or equivalently by $V_0, V_1, V_{\frac{1}{2}}$.

The adjacency condition for a multi-particle state containing both boson-fermions and kinks is the following: the usual condition applies for neighbouring kinks, and if in a state $|\dots K_{ab}p\dots p\dots pK_{cd}\dots\rangle$ where p stands for boson-fermions there are only boson-fermions between K_{ab} and K_{cd} , then either $b = c$ or $|b - c| = 1$.

We remark that P_m and \bar{P}_m as well as K_m and \bar{K}_m are equivalent as ray representations, and so are all the one-dimensional (vacuum) representations.

As we mentioned in the Introduction, we shall consider the boson-fermion (P_m) and kink (K_m) representations as representations in which bulk particle multiplets of supersymmetric theories can transform.

2.5 The boundary supersymmetry algebra in 1+1 dimensions

The boundary supersymmetry algebra \mathcal{A}_B is an associative algebra over \mathbb{R} . It is generated by a boundary supercharge Q_B , a boundary central charge Z_B , the time translation generator H_B and a unit element I_B . \mathcal{A}_B is commutative and the following relation is satisfied:

$$Q_B^2 = 2H_B + 2Z_B. \quad (2.79)$$

There are essentially two different co-products $\Delta_B^\pm : \mathcal{A}_B \rightarrow \mathcal{A} \otimes \mathcal{A}_B$:

$$\Delta_B^+(I_B) = I \otimes I_B \quad (2.80)$$

$$\Delta_B^+(H_B) = H \otimes I_B + I \otimes H_B \quad (2.81)$$

$$\Delta_B^+(Z_B) = \hat{Z} \otimes I_B + I \otimes Z_B \quad (2.82)$$

$$\Delta_B^+(Q_B) = (Q + \bar{Q}) \otimes I_B + \Gamma \otimes Q_B \quad (2.83)$$

and

$$\Delta_B^-(I_B) = I \otimes I_B \quad (2.84)$$

$$\Delta_B^-(H_B) = H \otimes I_B + I \otimes H_B \quad (2.85)$$

$$\Delta_B^-(Z_B) = -\hat{Z} \otimes I_B + I \otimes Z_B \quad (2.86)$$

$$\Delta_B^-(Q_B) = (Q - \bar{Q}) \otimes I_B + \Gamma \otimes Q_B . \quad (2.87)$$

They both satisfy the co-associativity property.

Δ_B^+ and Δ_B^- can be related by an automorphism j of \mathcal{A} that has the property $j^2 = Id$:

$$j(\bar{Q}) = -\bar{Q} \quad j(Q) = Q \quad j(N) = N \quad (2.88)$$

$$j(\hat{Z}) = -\hat{Z} \quad j(\Gamma) = \Gamma \quad (2.89)$$

$$(j \otimes Id) \circ \Delta_B^+ = \Delta_B^- . \quad (2.90)$$

Δ_B^+ and Δ_B^- can be written in the form (2.41) with the monomorphisms $i^+, i^- : \mathcal{A}_B \rightarrow \mathcal{A}$:

$$i^+(Q_B) = Q + \bar{Q} \quad i^+(H_B) = H \quad (2.91)$$

$$i^+(Z_B) = \hat{Z} \quad i^+(I_B) = I \quad (2.92)$$

$$i^-(Q_B) = Q - \bar{Q} \quad i^-(H_B) = H \quad (2.93)$$

$$i^-(Z_B) = -\hat{Z} \quad i^-(I_B) = I . \quad (2.94)$$

i^+ and i^- are also related by j : $j \circ i^+ = i^-$.

To describe situations when the fermionic parity is also conserved, \mathcal{A}_B can be supplemented with the boundary fermionic parity generator Γ_B . It satisfies the following relations:

$$\{\Gamma_B, \Gamma_B\} = 2I_B , \quad [\Gamma_B, Z_B] = 0 , \quad [\Gamma_B, H_B] = 0 , \quad (2.95)$$

and also

$$\{\Gamma_B, Q_B\} = 2gI_B , \quad (2.96)$$

where g is a parameter of the algebra. The co-product of Γ_B is

$$\Delta_B(\Gamma_B) = \Gamma \otimes \Gamma_B . \quad (2.97)$$

The co-associativity property remains valid.

Finally, as $\Delta_B^\pm(\tilde{\mathcal{A}}) \subset \tilde{\mathcal{A}} \otimes \mathcal{A}_B$, Δ_B^\pm can be used to multiply representations of $\tilde{\mathcal{A}}$ and one representation of \mathcal{A}_B .

2.5.1 Representations of the boundary supersymmetry algebra

As in Section 2.4.1, we consider representations on Hilbert spaces. The Hermitian adjoints of the generators are

$$H_B^\dagger = H_B \quad Q_B^\dagger = Q_B \quad Z_B^\dagger = Z_B \quad (\Gamma_B^\dagger = \Gamma_B) . \quad (2.98)$$

There are several different one-dimensional representations of the boundary supersymmetry algebra which can serve as representations in which the ground states of various models transform. Moreover, higher dimensional representations may also occur in some models. The adjacency condition between the ground state and the nearest kink is required to be satisfied, and we shall consider one-dimensional representations only, following [36], this being the simplest choice in the absence of other guiding information. In this case, as explained in [36], the supersymmetric kink label for the boundary must in general be $\frac{1}{2}$. We shall not consider the cases when the ground state is singlet with label 0 or 1.

The possible ground state representations form a one-parameter family. It is convenient to write this parameter in slightly different forms in the cases when Δ_B^+ and Δ_B^- is used. The representations are denoted by D_γ in the (+) case and $D_{e\gamma}$ in the (−) case, γ and $e\gamma$ being the two forms of the parameter. We shall also use the notation $B_{\frac{1}{2}}$ for the ground state representation, in this notation the parameters are not written explicitly. The representation space of $B_{\frac{1}{2}}$ will be denoted by $W(B_{\frac{1}{2}})$.

The action of the boundary supersymmetry generators on $|B_{\frac{1}{2}}\rangle$ in the (−) case is

$$Q_B|B_{\frac{1}{2}}\rangle = e\gamma|B_{\frac{1}{2}}\rangle , \quad Z_B|B_{\frac{1}{2}}\rangle = 0 , \quad e = \pm 1 , \quad (2.99)$$

where $\gamma \in \mathbb{R}$, $\gamma < 0$ and $|B_{\frac{1}{2}}\rangle$ is the basis vector for the representation space.

In the (+) case

$$Q_B|B_{\frac{1}{2}}\rangle = \gamma|B_{\frac{1}{2}}\rangle , \quad Z_B|B_{\frac{1}{2}}\rangle = 0 ,$$

where $\gamma \in \mathbb{R}$. $e\gamma$ or γ is a parameter of the model to be described and is expected to be expressible in terms of the parameters of the Lagrangian density. The reason for writing

the parameter in the form $e\gamma$ in the $(-)$ case will become clear in 2.6.5 when the ground state kink reflection amplitudes are discussed.

It is not necessary to set the eigenvalue of Z_B equal to zero, however the scattering data is completely independent of the eigenvalue of Z_B .

If Γ_B is also included in \mathcal{A}_B , then

$$\Gamma_B |B_{\frac{1}{2}}\rangle = \epsilon |B_{\frac{1}{2}}\rangle, \quad \epsilon = \pm 1$$

and $g = \epsilon e\gamma$ in the $(-)$ case and $g = e\gamma$ in the $(+)$ case.

2.6 Supersymmetric factorized scattering

2.6.1 Ansatz for the supersymmetric scattering theory

A formalism for constructing $N = 1$ supersymmetric factorizable bulk scattering theory is the following:

1) It is assumed that a known factorized scattering theory to be supersymmetrized is given as described in Section 2.1.

2) The internal space of the supersymmetrized theory will be

$$V_{tot} = \oplus_k (W_k \otimes V_k), \quad (2.100)$$

where the W_k -s are internal spaces of representations D_k of the supersymmetry algebra as described in Section 2.4, the V_k -s constitute a decomposition of V :

$$V = \oplus_k V_k, \quad (2.101)$$

and each V_k can be decomposed further into a sum of one-particle spaces appearing in (2.5), i.e. a specific value of k is assigned to each particle. The masses of the particles appearing in this decomposition of V_k are the same for specific values of k , i.e. the decomposition (2.101) is a refinement of (2.3), if two particles have the same value of k , then they also have the same mass. The V_k spaces must be invariant subspaces of $\tilde{C}\tilde{P}\tilde{T}$. The masses of the representations D_k are the same as the masses belonging to k in the non-supersymmetric theory.

The scalar product on V_{tot} is defined in the standard way. The representation of the supersymmetry algebra on the one-particle Hilbert space is also defined in a straightforward way, i.e. the generators, except for the boost generator, act trivially on the non-supersymmetric part.

The W_k -s will be referred to as supersymmetric parts.

$S(\Theta)$ must be block ‘diagonal’ with respect to the decomposition (2.101), i.e.

$$S(\Theta)(V_{k_1} \otimes V_{k_2}) \subseteq V_{k_2} \otimes V_{k_1} . \quad (2.102)$$

The fusion tensors must also have a similar property

$$f_{m_1 m_2}^{m_3}(V_{k_1} \otimes V_{k_2}) \subseteq V_{k_3}$$

where k_3 is uniquely determined by k_1 and k_2 and the fusion angle, which is denoted in the following way:

$$k_1 + k_2 \rightarrow k_3 \quad (u) .$$

Thus we can consider the blocks $S_{k_1 k_2}(\Theta)$, $f_{k_1 k_2}^{k_3}$ and $d_{k_3}^{k_2 k_1}$, which behave essentially in the same way as the blocks corresponding to definite masses.

We note that $V_{tot}(\Theta) = \oplus_k (W_k(\Theta) \otimes V_k(\Theta))$.

3) The full supersymmetric S-matrix will be ‘diagonal’ with respect to (2.100) and the blocks are given by

$$(S_{tot})_{k_1 k_2}(\Theta) = (S_{SUSY})_{k_1 k_2}(\Theta) \otimes S_{k_1 k_2}(\Theta) . \quad (2.103)$$

The $(S_{SUSY})_{k_1 k_2}(\Theta) : W_{k_1} \otimes W_{k_2} \rightarrow W_{k_2} \otimes W_{k_1}$ factors are called supersymmetric factors.

The fusion tensors also take similar form:

$$(f_{tot})_{k_1 k_2}^{k_3} = (f_{SUSY})_{k_1 k_2}^{k_3} \otimes f_{k_1 k_2}^{k_3} \quad (2.104)$$

$$(d_{tot})_{k_3}^{k_2 k_1} = (d_{SUSY})_{k_3}^{k_2 k_1} \otimes d_{k_3}^{k_2 k_1} . \quad (2.105)$$

$(f_{SUSY})_{k_1 k_2}^{k_3} : W_{k_1} \otimes W_{k_2} \rightarrow W_{k_3}$ and $(d_{SUSY})_{k_3}^{k_2 k_1} : W_{k_3} \rightarrow W_{k_2} \otimes W_{k_1}$ are also referred to as supersymmetric factors. The image space of $(f_{SUSY})_{k_1 k_2}^{k_3}$ should have zero intersection with the kernel of $(d_{SUSY})_{k_3}^{k_2 k_1}$.

The collection of the supersymmetry factors $(f_{SUSY})_{k_1 k_2}^{k_3}$ and $(d_{SUSY})_{k_3}^{k_2 k_1}$ and $(S_{SUSY})_{k_1 k_2}(\Theta)$ should satisfy every possible bootstrap equation of the form (2.16). This ensures that the full S-matrix and fusion and decay tensors will satisfy the bootstrap equations. The supersymmetry factors should also be invariant with respect to the supersymmetry algebra.

If $S_{k_1 k_2}(\Theta)$ has a pole at iu with a contribution corresponding to a direct channel bound state, then there will be such a contribution for $(S_{tot})_{k_1 k_2}(\Theta)$ with residue $(S_{SUSY})_{k_1 k_2}(iu) \otimes d_{k_3}^{k_1 k_2} f_{k_1 k_2}^{k_3}$ and the following equation is satisfied:

$$(S_{SUSY})_{k_1 k_2}(iu) = (d_{SUSY})_{k_3}^{k_1 k_2} (f_{SUSY})_{k_1 k_2}^{k_3} , \quad (2.106)$$

which is the version of (2.9) for the supersymmetric factor of the S-matrix. (2.106) is called fusion equation.

4) The supersymmetric factors $(S_{SUSY})_{k_1 k_2}(\Theta)$ are complex analytic functions. They satisfy the Yang-Baxter equation described in Section 2.1, the unitarity, real analyticity and crossing symmetry conditions. They do not have poles in the physical strip.

2.6.2 Ansatz for the supersymmetric scattering theory in the presence of a boundary

1) It is assumed that a known factorized scattering theory with boundary to be supersymmetrized is given as described in Section 2.2, and its underlying bulk factorized scattering theory is supersymmetrized in the way described in Section 2.6.1.

2) The space of boundary states of the supersymmetrized theory will be

$$\mathcal{H}_{B,tot} = \oplus_{k^b} (W_{B,k^b} \otimes \mathcal{H}_{B,k^b}) , \quad (2.107)$$

where the W_{B,k^b} -s are representation spaces of representations D_{k^b} of the boundary supersymmetry algebra. The \mathcal{H}_{B,k^b} -s constitute a decomposition of \mathcal{H}_B :

$$\mathcal{H}_B = \oplus_{k^b} \mathcal{H}_{B,k^b} , \quad (2.108)$$

which is a refinement of (2.26), i.e. if two states belong to the \mathcal{H}_{B,k^b} with a fixed value of k^b , then they also belong to a common energy eigenspace $\mathcal{H}_{B,E}$. The energy of the representations D_{k^b} is determined by the energy of the states belonging to k^b in the non-supersymmetric model. The scalar product on $\mathcal{H}_{B,tot}$ is defined in the standard way. The representation of the supersymmetry algebra on $W_{B,k^b} \otimes \mathcal{H}_{B,k^b}$ is also defined in a straightforward way, i.e. the generators act trivially on the non-supersymmetric part.

The W_{B,k^b} -s are referred to as supersymmetric parts.

$R(\Theta)$ must be diagonal with respect to (2.108) and (2.101):

$$R(\Theta)(V_k \otimes \mathcal{H}_{B,k^b}) \subseteq V_k \otimes \mathcal{H}_{B,k^b}$$

and the boundary fusion and decay tensors must also have a similar property:

$$g_{m,E_1}^{E_2}(V_k \otimes \mathcal{H}_{B,k_1^b}) \subseteq \mathcal{H}_{B,k_2^b} ,$$

where k_2^b is uniquely determined by k and k_1^b and the fusion angle, which is denoted in the following way:

$$k + k_1^b \rightarrow k_2^b \quad (u) .$$

Thus one can consider the blocks $R_{k,k_1^b}(\Theta)$, $g_{k,k_1^b}^{k_1^b}$, $h_{k_2^b}^{k,k_1^b}$, which behave essentially in the same way as the blocks corresponding to definite masses and energies.

3) The full supersymmetric R-matrix will be diagonal with respect to k and k^b and the blocks are

$$(R_{tot})_{k,k_1^b}(\Theta) = (R_{SUSY})_{k,k_1^b}(\Theta) \otimes R_{k,k_1^b}(\Theta) . \quad (2.109)$$

The boundary fusion and decay tensors also take similar form:

$$(g_{tot})_{k,k_1^b}^{k_2^b} = (g_{SUSY})_{k,k_1^b}^{k_2^b} \otimes g_{k,k_1^b}^{k_2^b} \quad (2.110)$$

$$(h_{tot})_{k_2^b}^{k,k_1^b} = (h_{SUSY})_{k_2^b}^{k,k_1^b} \otimes h_{k_2^b}^{k,k_1^b} \quad (2.111)$$

and

$$(G_{tot})_{k,k_1^b}^{k_1^b} = (G_{SUSY})_{k,k_1^b}^{k_1^b} \otimes G_{k,k_1^b}^{k_1^b} \quad (2.112)$$

$$(H_{tot})_{k_1^b}^{k,k_1^b} = (H_{SUSY})_{k_1^b}^{k,k_1^b} \otimes H_{k_1^b}^{k,k_1^b} . \quad (2.113)$$

The factors

$$(R_{SUSY})_{k,k_1^b}(\Theta) : W_k \otimes W_{B,k_1^b} \rightarrow W_k \otimes W_{B,k_1^b} ,$$

$$(g_{SUSY})_{k,k_1^b}^{k_2^b} : W_k \otimes W_{B,k_1^b} \rightarrow W_{B,k_2^b} , \quad (h_{SUSY})_{k_2^b}^{k,k_1^b} : W_{B,k_2^b} \rightarrow W_k \otimes W_{B,k_1^b} ,$$

$$(G_{SUSY})_{k,k_1^b}^{k_1^b} : W_k \otimes W_{B,k_1^b} \rightarrow W_{B,k_1^b} , \quad (H_{SUSY})_{k_1^b}^{k,k_1^b} : W_{B,k_1^b} \rightarrow W_k \otimes W_{B,k_1^b}$$

are called supersymmetry factors. The image spaces of $(g_{SUSY})_{k,k_1^b}^{k_2^b}$ and $(G_{SUSY})_{k,k_1^b}^{k_1^b}$ should have zero intersection with the kernel of $(h_{SUSY})_{k_2^b}^{k,k_1^b}$ and $(H_{SUSY})_{k_1^b}^{k,k_1^b}$.

The collection of all boundary supersymmetry factors together with the bulk supersymmetry factors should satisfy every possible bootstrap equation of the form (2.37) and (2.38). This ensures that the full R-matrix and fusion and decay tensors will satisfy the bootstrap equations. The supersymmetry factors should also be invariant with respect to the boundary supersymmetry algebra.

If $R_{k,k_1^b}(\Theta)$ has a pole at iu with a contribution corresponding to a boundary bound state, then there will be such a contribution for $(R_{tot})_{k,k_1^b}(\Theta)$ with residue $(R_{SUSY})_{k,k_1^b}(iu) \otimes h_{k_2^b}^{k,k_1^b} g_{k,k_1^b}^{k_2^b}$ and the following equation will be satisfied:

$$(R_{SUSY})_{k,k_1^b}(iu) = (h_{SUSY})_{k_2^b}^{k,k_1^b} (g_{SUSY})_{k,k_1^b}^{k_2^b} , \quad (2.114)$$

which is the version of (2.30) for the supersymmetric factor of the R-matrix. (2.114) is called boundary fusion equation.

If $R_{k,k_1^b}(\Theta)$ has a pole at iu with a contribution corresponding to the existence of a bulk fusion tensor $f_{kk'}^k$, then there will be such a contribution for $(R_{tot})_{k,k_1^b}(\Theta)$ with residue $(R_{SUSY})_{k,k_1^b}(iu) \otimes ([I \otimes G_{k',k_1^b}^{k_1^b}][d_k^{kk'} \otimes I])$. We require that

$$(R_{SUSY})_{k,k_1^b}(iu) = [I \otimes (G_{SUSY})_{k',k_1^b}^{k_1^b}][(d_{SUSY})_k^{kk'} \otimes I] , \quad (2.115)$$

which is the version of (2.33) for the supersymmetric factors, and

$$[I \otimes (G_{SUSY})_{k',k_1^b}^{k_1^b}][(d_{SUSY})_k^{kk'} \otimes I] = [(f_{SUSY})_{kk'}^k \otimes I][I \otimes (H_{SUSY})_{k_1^b}^{k',k_1^b}] , \quad (2.116)$$

which is the version of (2.34) for the supersymmetric factors.

Similar assumption is made about the pole at $i\pi/2$ and the version of (2.35) for the supersymmetry factors will be

$$(R_{SUSY})_{k,k_1^b}(i\pi/2) = (H_{SUSY})_{k_1^b}^{k,k_1^b}(G_{SUSY})_{k,k_1^b}^{k_1^b} . \quad (2.117)$$

4) The supersymmetric factors $(R_{SUSY})_{k,k_1^b}(\Theta)$ are complex analytic functions. They satisfy the boundary Yang-Baxter equation, the unitarity, real analyticity and crossing symmetry conditions described in Section 2.2. The supersymmetric factors $(R_{SUSY})_{k,k_1^b}(\Theta)$ should not have poles in the physical strip.

2.6.3 Supersymmetric bootstrap

The supersymmetric factors of the ansatz described in Sections 2.6.1 and 2.6.2 can be calculated in a way that is very similar to that described in Section 2.3. The main difference is that the fusion angles are not determined by poles but are taken from the non-supersymmetric theory, which is assumed to be known.

Supersymmetric fusion rules, which are related strictly to the supersymmetric factors only, can be defined in analogy with the non-supersymmetric fusion rules.

It is an interesting problem to find all the possible supersymmetric factors and supersymmetric fusion rules for a given set of representations for the bulk part, regardless of particular non-supersymmetric theories, and to find all the possible supersymmetric factors of the ground state reflection matrix for the given set of representations for the bulk particles and for the ground state, and finally to find the supersymmetric factors (including the reflection matrix factors) for higher level boundary states for arbitrary boundary fusion angles, and to describe the possible supersymmetric boundary fusion rules. Such results can then be applied to particular non-supersymmetric theories.

2.6.4 Supersymmetric S-matrix factors

The general solution of the Yang-Baxter equations that describes the (supersymmetric factor of the) scattering of two boson-fermion supermultiplets is

$$S_{PP}^{[i,j]}(\Theta, m_i, m_j, \alpha^{[i,j]}) = G^{[i,j]}(\Theta) \left[\frac{1}{2i} (q_1 - q_2)(\bar{q}_1 - \bar{q}_2) + \alpha^{[i,j]} F(\Theta) [1 - t(\Theta, m_i, m_j) q_1 q_2] [1 + t(\Theta, m_j, m_i) \bar{q}_1 \bar{q}_2] \right],$$

where

$$t(\Theta, m_i, m_j) = \tanh \left(\frac{\Theta + \log(m_i/m_j)}{4} \right), \quad F(\Theta) = \frac{m_i + m_j + 2\sqrt{m_i m_j} \cosh(\Theta/2)}{2i \sinh(\Theta)},$$

$$q_1 = q \otimes I, \quad q_2 = \Gamma \otimes q, \quad \bar{q}_1 = \bar{q} \otimes I, \quad \bar{q}_2 = \Gamma \otimes \bar{q}.$$

m_i and m_j are the masses of the multiplets, and $\alpha^{[i,j]}$ is a real constant, which is interpreted as the measure of the strength of Bose-Fermi mixing. $\alpha^{[i,j]} = 0$ corresponds to trivial scattering. i and j are indices of the type introduced in (2.101). $G^{[i,j]}(\Theta)$ is a scalar function. $S_{PP}^{[i,j]}(\Theta)/G^{[i,j]}(\Theta)$ can depend on the conserved quantities i, j through m_i, m_j and $\alpha^{[i,j]}$ only. It can be shown that the Yang-Baxter equation implies that the particles in a theory can be divided into disjoint sets with the property that any two particles in a set have the same nonzero α , and $\alpha = 0$ for two particles from different sets. To each particle in a theory we associate a value of α , which is the value that occurs in the scattering of the particle with itself. For simplicity we consider only theories which have only one such set and thus α is the same for any two-particle scattering (and the upper indices of α can be omitted). The scalar function $G^{[i,j]}(\Theta)$ is determined by unitarity and crossing symmetry up to CDD factors. It is important here that i, j are invariant under charge conjugation. It is also required that $S_{PP}^{[i,j]}(\Theta)$ should have minimal number of poles and overall zeroes in the physical strip, what fixes $G^{[i,j]}(\Theta)$ completely. An explicit expression for $G^{[i,j]}(\Theta)$ can be found in the Appendix. $G^{[i,j]}(\Theta)$ contains the parameters u_i, u_j for which

$$0 < \text{Re}(u_i), \text{Re}(u_j) \leq \pi/2, \quad m_i = 2M \sin(u_i), \quad m_j = 2M \sin(u_j), \quad (2.118)$$

where $M = |1/(2\alpha)|$. Consequently, we can assign an angle u to each particle. We shall consider only real values of u_i and u_j .

The supersymmetric factor that describes the scattering of two kinks of equal mass is

$$S_{KK}(\Theta) = K(\Theta) [\cosh(\gamma\Theta) - \sinh(\gamma\Theta) q_1 \bar{q}_1] [\cosh(\Theta/4) - \sinh(\Theta/4) q_1 q_2],$$

where $\gamma = (\log 2)/2\pi i$. This factor does not depend on any parameters. The scalar function $K(\Theta)$ is determined by unitarity and crossing symmetry and the condition that

$S_{KK}(\Theta)$ should have a minimal number of poles and zeroes in the physical strip. An explicit expression for $K(\Theta)$ can be found in the Appendix or [34]. There is no solution of the Yang-Baxter equation for the scattering of kinks of different mass, so all the kinks in a theory have to have the same mass.

The kink–boson-fermion S-matrix factors $S_{PK}(\Theta, \alpha, u_i)$ and $S_{KP}(\Theta, \alpha, u_i)$ will be considered later. They depend on the α parameter and on the u_i angle parameter of the boson-fermion representation.

The important common feature of these minimal S-matrix factors, including S_{PK} and S_{KP} , is that they have no poles and overall zeroes in the physical strip (although they can be degenerate at particular values of Θ).

In the light of (2.54), if it is decided that some particles and their bound states transform in the boson-fermion representation of the supersymmetry algebra, then the fusion equation (2.106) can be satisfied only if $S_{PP}(iu)$ is a projection onto the appropriate subspace carrying the boson-fermion representation. This is a nontrivial condition on $S_{PP}(iu)$, because $S_{PP}(\Theta)$ is bijective (of rank four) for general values of Θ . The other possible way to assure that only boson-fermion states (and no pseudo-boson-fermion states) are produced in the fusion is to quotient out the unwanted states by hand. We shall consider only the first, more natural possibility.

$S_{PP}^{[i,j]}(\Theta)$ is of rank two if $\Theta = iu_{ij}^k$, where

$$u_{ij}^k \in \{u_i + u_j, \pi - u_i + u_j, u_i + \pi - u_j\}. \quad (2.119)$$

Only two of these values can be in the physical strip, and $S_{PP}^{[i,j]}(\Theta)$ is nondegenerate at other values of Θ in the physical strip. The image space of $S_{PP}^{[i,j]}(iu_{ij}^k)$ carries the particle representation if and only if $\alpha < 0$, i.e. if $\alpha = -1/(2M)$. We remark that if $\alpha = 1/(2M)$, then the image space carries the pseudo-particle representation. The value of u_k (which is the angle parameter of the particle representation carried by the image space) is the following:

$$u_k = u_i + u_j \quad \text{if } u_{ij}^k = u_i + u_j < \pi/2, \quad (2.120)$$

$$u_k = \pi - (u_i + u_j) \quad \text{if } u_{ij}^k = u_i + u_j \geq \pi/2, \quad (2.121)$$

$$u_k = u_i - u_j \quad \text{if } u_{ij}^k = \pi - u_i + u_j, \quad (2.122)$$

$$u_k = u_j - u_i \quad \text{if } u_{ij}^k = u_i + \pi - u_j. \quad (2.123)$$

The conditions above are sufficient for the existence of unique fusion and decay tensors $f_{PP}^P(u_i, u_j, u_k, M)$, $d_{PP}^{PP}(u_i, u_j, u_k, M)$ which satisfy the fusion equation and have the required symmetry properties. Explicit expressions for them can be found in [34, 30].

We turn to the case of the fusion of two (supersymmetric) kinks of equal mass now. S_{KK} is bijective (of rank six) everywhere in the physical strip, so there is no natural degeneracy condition on $S_{KK}(iu)$ and no constraint arises on the fusion angle in this way, and unique fusion and decay tensors satisfying the fusion equation and having the required symmetry properties exist. Consequently, in the light of (2.58), if one insists that no pseudo-particles should be formed in kink fusion, then one has to quotient out the unwanted states from the Hilbert-space by hand. Even if states of the form (2.63) and (2.64) are quotiented out, kink fusion produces two types of particles corresponding to (2.59)-(2.62), i.e. to the $\frac{1}{2}$ and 01 sectors. The two types of particles will be referred to as type $\frac{1}{2}$ and type 01 particles.

There are adjacency conditions for particles produced in kink fusion, which follow from the adjacency conditions for kinks: type $\frac{1}{2}$ and type 01 particles cannot be adjacent in a multi-particle state, so they cannot scatter on each other. There are also appropriate adjacency conditions for kinks and particles. Bootstrap gives the result [33, 34] that the two types of particles have the same S-matrix factor which is equal to S_{PP} . Consequently, the two types of particles can be identified (which is the same as quotienting out certain combinations). If this identification is made, then only the following adjacency condition applies: if in a state $|\dots K_{ab}p\dots p\dots pK_{cd}\dots\rangle$ (where p stands for a particle and the rapidities are suppressed) there are only particles (at least one) between K_{ab} and K_{cd} , then either $b = c$, or $|b - c| = 1$. For adjacent kinks K_{ab} and K_{cd} the condition $b = c$ applies as before.

The elimination of the pseudo-particle states and the identification of 01 and $\frac{1}{2}$ states as described above is usually done in the literature (e.g. [34, 33]), despite of its unnatural character. It is more natural to accept that the fusion of two kinks produces states that transform in the two-kink-representations $K_m^{(2)}$, and recent numerical calculations [95] in finite volume for the supersymmetric sine-Gordon model also seem to support this version. These calculations suggest that the breathers of the supersymmetric sine-Gordon model transform in the $K_m^{(2)}$ representations. To conform to the literature we shall use the boson-fermion representations (i.e. the P_m -s). Switching to two-kink-representation, however, is in most cases straightforward.

$S_{KK}(\Theta)$ is bijective (of rank six) everywhere in the physical strip. However, it is degenerate at $\Theta = \pm i\pi$, and at this point it projects onto the subspace spanned by the states (2.76)-(2.78).

The supersymmetry factors $S_{PK}(\Theta)$ and $S_{KP}(\Theta)$ for the scattering of a particle with $\alpha < 0$ and a kink of mass $M = -1/(2\alpha)$ can be obtained from S_{KK} by bootstrap [33, 34] applied to the $kink + kink \rightarrow particle$ vertex. It turns out that $S_{PK}(\Theta)$ and $S_{KP}(\Theta)$ are

also minimal and have neither poles nor zeroes in the physical strip.

It is expected that a kink is produced in the kink-particle fusion. The transformation properties of the kink-particle states discussed earlier show that in this case it is necessary that (2.74) is satisfied. We checked that S_{PK} (and S_{KP}) is bijective (of rank eight) everywhere in the physical strip, except when (2.74) is satisfied. In the latter case it is a projection onto the four dimensional kink subspace. The *kink + particle* \rightarrow *kink* fusion is thus possible, and there are no restrictions other than (2.74). The *kink + particle* \rightarrow *kink* fusion is a crossed version of *kink + kink* \rightarrow *particle* fusion. The produced kink is of the same mass as the incoming one, so the fusion angle is in the domain $[\pi/2, \pi]$. The fusion tensor (regarded as a linear mapping) is a projection.

Finally, there are bootstrap equations for S_{PP} , S_{KK} , S_{PK} , S_{KP} and f_{PP}^P , d_P^{PP} , f_{KK}^P , d_P^{KK} , f_{KP}^K , d_K^{PK} , f_{PK}^K , d_K^{KP} which were found to be satisfied [34, 30]. The fusion of two particles with $\alpha < 0$ produces a particle with the same value of α . The fusion of two kinks of mass M produces a particle with $\alpha = -1/(2M)$, and if the fusion angle is ρ , then the angle parameter u of the produced particle is $u = \pi/2 - \rho/2$. The fusion of a kink of mass M and a particle with $\alpha = -1/(2M)$ produces a kink of mass M . In the diagrammatic representation there are essentially two types of vertices: the kink-kink-particle and the three-particle vertices.

To a supersymmetric boson-fermion multiplet $W_P(\Theta)$ with definite rapidity and mass $m = 2M \cos(\rho/2)$ we assign the following (not ordered) set of rapidities:

$$L[W_P(\Theta)] = \{\Theta - i\rho/2, \Theta + i\rho/2\} ,$$

where it is not required that $\Theta \pm i\rho/2$ be in the physical strip. The elements of the set are the rapidities of those kink multiplets which fuse into the boson-fermion multiplet $W_P(\Theta)$. $L[W_P(\Theta)]$ and M determines $W_P(\Theta)$ uniquely. The set $L[W_K(\Theta)] = \{\Theta\}$ is assigned to a kink multiplet $W_K(\Theta)$. In terms of these sets the fusion rule of two boson-fermion multiplets takes the form

$$\{\Theta_1, \Theta_2\} + \{\Theta_3, \Theta_1 \pm i\pi\} \rightarrow \{\Theta_2, \Theta_3\} , \quad (2.124)$$

where $\Theta_1, \Theta_2, \Theta_3$ are appropriate complex rapidities. Similarly, the fusion of a kink and a particle takes the form

$$\{\Theta_1\} + \{\Theta_2, \Theta_1 \pm i\pi\} \rightarrow \{\Theta_2\} . \quad (2.125)$$

A kink-kink fusion takes the form

$$\{\Theta_1\} + \{\Theta_2\} \rightarrow \{\Theta_1, \Theta_2\} . \quad (2.126)$$

In these fusions the set of rapidities corresponding to the final state is obtained in the following way: the disjoint union of the two sets of rapidities corresponding to the fusing particles/kinks is formed and the pair of rapidities differing by $\pm i\pi$ is deleted (if there is any such pair). It is important that we allow here and further on that a set contains certain elements several times, i.e. the elements of the sets we consider have multiplicity. Such sets denoted by $L[\dots]$ will be used in the boundary case as well and they will be called labeling sets.

The rules (2.124)-(2.126) follow from the fact that S_{KK} is bijective (of rank 6) in the physical strip but is of rank 3 at $\Theta = i\pi$. The bijectivity of the fusion tensor $f_{KK}^{K(2)}$ together with the bootstrap equations and the symmetry properties of $f_{KK}^{K(2)}$ implies that a multiplet of two-kink-states $W_{K(2)}(\Theta)$ has the same scattering and transformation properties as the multiplet of two-kink states $(\hat{f}_{KK}^{K(2)})^{-1}(W_{K(2)}(\Theta))$. Similar statement applies if we use the boson-fermion states. The kinks can be considered as elementary states, whereas boson-fermions or two-kink-states as composite states (mentioned at the end of Section 2.1) constituted by two kinks with fixed rapidity difference.

In summary, the supersymmetric factors are characterized by a single mass parameter M which is the common mass of the kinks, and each particle multiplet has a mass $m \leq 2M$ and a parameter $0 < u \leq \pi/2$ so that $m = 2M \sin(u)$ (see (2.118)). The fusion rules satisfy the constraint $u_{ij}^k \in \{u_i + u_j, \pi - u_i + u_j, u_i + \pi - u_j\}$ for the fusion angle of a $particle_i + particle_j \rightarrow particle_k$ fusion (this constraint is equivalent to (2.124)), $u_k = \pi/2 - u_{ij}^k/2$ for a $kink_i + kink_j \rightarrow particle_k$ fusion (which is equivalent to (2.126)), and $u_{ij}^k = \pi/2 + u_i$ for a $particle_i + kink_j \rightarrow kink_k$ fusion (this constraint is equivalent to (2.125)). These constraints are nontrivial, because the fusion angle is not restricted kinematically in general by the masses of the fusing particles. The supersymmetric factors are $S_{PP}(\Theta, u_i, u_j, M)$, $S_{KK}(\Theta)$, $S_{PK}(\Theta, M, u_i)$, $S_{KP}(\Theta, M, u_i)$ and $f_{PP}^P(u_i, u_j, u_k, M)$, $d_{PP}^{PP}(u_i, u_j, u_k, M)$, $f_{KK}^P(u_k)$, $d_P^{KK}(u_k)$, $f_{KP}^K(u_j)$, $d_K^{PK}(u_j)$, $f_{PK}^K(u_i)$, $d_K^{KP}(u_i)$. (Assuming that the boson-fermion representation is used, not the two-kink-representation.)

2.6.5 Supersymmetric reflection matrix factors

We consider one-particle kink reflection matrix factors R_K on ground state boundary first. As the left and right RSOS labels should be conserved, $\{R_K\}_{K_{1\frac{1}{2}}}^{K_{0\frac{1}{2}}}(\Theta) = \{R_K\}_{K_{0\frac{1}{2}}}^{K_{1\frac{1}{2}}}(\Theta) = 0$ must hold, i.e. R_K is diagonal. The general solution of the boundary Yang-Baxter equation, unitarity condition and crossing equation without imposing supersymmetry is [38, 40]

$$\{R_K\}_{K_{0\frac{1}{2}}}^{K_{0\frac{1}{2}}}(\Theta) = (1 + A \sinh(\Theta/2))M(\Theta) ,$$

$$\{R_K\}_{K_{1\frac{1}{2}}}^{K_{1\frac{1}{2}}}(\Theta) = (1 - A \sinh(\Theta/2))M(\Theta) ,$$

where $M(\Theta)$ is restricted by unitarity and crossing symmetry. After imposing the boundary supersymmetry condition one finds that in the (+) case [36, 37]

$$\{R_K^{(+)}\}_{K_{0\frac{1}{2}}}^{K_{0\frac{1}{2}}}(\Theta) = \{R_K^{(+)}\}_{K_{1\frac{1}{2}}}^{K_{1\frac{1}{2}}}(\Theta) = 2^{-\Theta/(\pi i)}P(\Theta), \quad A = 0 .$$

(A formula for $P(\Theta)$ can be found in the Appendix.) In the (−) case there are two distinct solutions for a given γ corresponding to the two values of the sign e :

$$\{R_{K,e}^{(-)}\}_{K_{0\frac{1}{2}}}^{K_{0\frac{1}{2}}}(\Theta) = (\cos \frac{\xi}{2} + ei \sinh \frac{\Theta}{2})K(\Theta - i\xi)K(i\pi - \Theta - i\xi)2^{-\Theta/(\pi i)}P(\Theta) , \quad (2.127)$$

$$\{R_{K,e}^{(-)}\}_{K_{1\frac{1}{2}}}^{K_{1\frac{1}{2}}}(\Theta) = (\cos \frac{\xi}{2} - ei \sinh \frac{\Theta}{2})K(\Theta - i\xi)K(i\pi - \Theta - i\xi)2^{-\Theta/(\pi i)}P(\Theta) , \quad (2.128)$$

where $\gamma = -2\sqrt{M} \cos \frac{\xi}{2}$ and $0 \leq \xi \leq \pi$, M is the kink mass. (2.127) and (2.128) are invariant under $\xi \leftrightarrow -\xi$. These reflection amplitudes are minimal, they have no poles and zeroes in the physical strip. The sign e seems to have a correspondence here with the 0 and 1 RSOS vacua. It should be noted that $R_K^{(+)}(\Theta)$ is independent of γ . Furthermore, as symmetry under Γ_B requires $R_{K_{0\frac{1}{2}}}^{K_{0\frac{1}{2}}}(\Theta) = R_{K_{1\frac{1}{2}}}^{K_{1\frac{1}{2}}}(\Theta)$, the $R_K^{(+)}(\Theta)$ is automatically Γ_B -symmetric, although this is not required a priori. On the other hand, $R_{K,e}^{(-)}(\Theta)$ are not Γ_B -symmetric. However, $\{R_{K,e}^{(-)}\}_{K_{0\frac{1}{2}}}^{K_{0\frac{1}{2}}}(\Theta) = -\{R_{K,e}^{(-)}\}_{K_{1\frac{1}{2}}}^{K_{1\frac{1}{2}}}(\Theta)$ if $\gamma = 0$ ($A \rightarrow \infty$). We also remark that $\{R_K\}_{K_{1\frac{1}{2}}}^{K_{1\frac{1}{2}}}(\Theta)/\{R_K\}_{K_{0\frac{1}{2}}}^{K_{0\frac{1}{2}}}(\Theta)$ is determined by the supersymmetry condition, i.e. if we impose the condition of invariance under supersymmetry, then we do not need to solve the Yang-Baxter equation.

We determined the general solution of the Yang-Baxter equation for the boundary supersymmetric particle reflection matrix factor (on the ground state boundary). We imposed the supersymmetry condition first. The resulting forms of the reflection amplitude in the (+) and (−) cases are

$$R_P^{(+)}(\Theta) = Z^{(+)}(\Theta) \frac{1}{\sqrt{m}} \times \begin{pmatrix} (X^{(+)}(\Theta) + e\gamma Y^{(+)}(\Theta))c(\frac{\Theta}{2} - \frac{i\pi}{4}) & \sqrt{m}Y^{(+)}(\Theta)c(\Theta) \\ \sqrt{m}Y^{(+)}(\Theta)c(\Theta) & (X^{(+)}(\Theta) - e\gamma Y^{(+)}(\Theta))c(\frac{\Theta}{2} + \frac{i\pi}{4}) \end{pmatrix}, \quad (2.129)$$

$$R_P^{(-)}(\Theta) = Z^{(-)}(\Theta) \frac{1}{\sqrt{m}} \times \begin{pmatrix} (X^{(-)}(\Theta) + e\gamma Y^{(-)}(\Theta))c(\frac{\Theta}{2} + \frac{i\pi}{4}) & i\sqrt{m}Y^{(-)}(\Theta)c(\Theta) \\ -i\sqrt{m}Y^{(-)}(\Theta)c(\Theta) & (X^{(-)}(\Theta) - e\gamma Y^{(-)}(\Theta))c(\frac{\Theta}{2} - \frac{i\pi}{4}) \end{pmatrix}, \quad (2.130)$$

where c stands for \cosh and X , Y and Z are functions not determined by supersymmetry. Now two cases can be distinguished depending on whether Γ_B is a symmetry or not: in the first case, which is the Γ_B -symmetric case, $Y(\Theta) \equiv 0$, $X(\Theta)$ can be absorbed into the prefactor, and the structure of the reflection amplitude is completely determined and does not contain free parameters:

$$R_{P1}^{(\pm)}(\Theta) = \frac{1}{\sqrt{m}} Z X^{(\pm)}(\Theta) \begin{pmatrix} \cosh(\frac{\Theta}{2} \mp \frac{i\pi}{4}) & 0 \\ 0 & \cosh(\frac{\Theta}{2} \pm \frac{i\pi}{4}) \end{pmatrix}.$$

This case is discussed in [35], the explicit form of $ZX^{(\pm)}$ can be found in the Appendix, see also [36, 35, 39]. We checked that the boundary Yang-Baxter equation for incoming particles of arbitrary masses is satisfied by this reflection amplitude. $R_{P1}^{(\pm)}(\Theta)$ can also be obtained from $R_K^{(+)}(\Theta)$ and $R_K^{(-)}(\Theta)$ at $\gamma = 0$ by bootstrap [36, 39].

In the second case, when Γ_B is not conserved, $Y(\Theta)$ is not identically zero, and it can be absorbed into the prefactor, so one free function $y^{(\pm)}(\Theta) = X^{(\pm)}(\Theta)/Y^{(\pm)}(\Theta)$ remains in the reflection amplitude, which is to be determined by the boundary Yang-Baxter equation. To obtain $y^{(\pm)}(\Theta)$ we solved the Yang-Baxter equation first in the case when the conserved quantum numbers introduced in (2.108) have the same values for the two incoming particles. Although the boundary Yang-Baxter equation is quadratic in general, in this case it is inhomogeneous linear in the variables $y^{(\pm)}(\Theta_1)$ and $y^{(\pm)}(\Theta_2)$. The coefficient of the quadratic term $y^{(\pm)}(\Theta_1)y^{(\pm)}(\Theta_2)$ vanishes precisely because $R_{P1}^{(\pm)}(\Theta)$ satisfies the Yang-Baxter equation. The Yang-Baxter equation consists of 16 scalar equations in our case. Some of them are trivial ($0=0$), and the remaining n equations are of the form

$$a_q^{(\pm)}(\Theta_1, \Theta_2)y^{(\pm)}(\Theta_1) + b_q^{(\pm)}(\Theta_1, \Theta_2)y^{(\pm)}(\Theta_2) + c_q^{(\pm)}(\Theta_1, \Theta_2) = 0, \quad q = 1..n.$$

It is possible to choose two inequivalent equations from this set. Two such equations can be solved for the numbers $y^{(\pm)}(\Theta_1)$ and $y^{(\pm)}(\Theta_2)$. The solution turns out to be of the form $y^{(\pm)}(\Theta_1) = g^{(\pm)}(\Theta_1)$, $y^{(\pm)}(\Theta_2) = g^{(\pm)}(\Theta_2)$ (for general coefficients $d_{q1}, e_{q1}, f_{q1}; d_{q2}, e_{q2}, f_{q2}$ instead of $a_{q1}, b_{q1}, c_{q1}; a_{q2}, b_{q2}, c_{q2}$ it would be of the form $y(\Theta_1) = g_1(\Theta_1, \Theta_2)$, $y(\Theta_2) = g_2(\Theta_1, \Theta_2)$, which does not define a function $y(\Theta)$), where $g^{(\pm)}$ is a function that depends also on m, α, γ , but has no other parameters. Consequently, the reflection amplitude depends on the conserved quantum numbers introduced in (2.108) through these parameters only. We checked that the solution obtained in this way satisfies the other $n-2$ equations as well. In the next step we checked that the solutions $R_{P2,e}^{(\pm)}(\Theta)$ satisfy the Yang-Baxter equation for incoming particles of different masses as well. The two functions $y^{(+)}(\Theta)$ and $y^{(-)}(\Theta)$ have very similar form.

The solutions that we obtained can be brought to the following form:

$$\begin{aligned} \{R_{P2,e}^{(\pm)}\}_b^b(\Theta) &= A_+^{(\pm)}(\Theta) & \{R_{P2,e}^{(\pm)}\}_f^f(\Theta) &= A_-^{(\pm)}(\Theta) \\ \{R_{P2,e}^{(\pm)}\}_b^f(\Theta) &= \pm B^{(\pm)}(\Theta) & \{R_{P2,e}^{(\pm)}\}_f^b(\Theta) &= B^{(\pm)}(\Theta) \end{aligned}$$

$$A_{\pm}^{(-)}(\Theta) = \tilde{Z}^{(-)}(\Theta) \left\{ \cosh\left(\frac{\Theta}{2}\right) \left(\frac{\gamma^2}{4M} - \left[\sin^2\left(\frac{\rho}{4}\right) + \sinh^2\left(\frac{\Theta}{2}\right) \right] \right) \right. \\ \left. \mp i \sinh\left(\frac{\Theta}{2}\right) \left(\frac{\gamma^2}{4M} + \left[\sin^2\left(\frac{\rho}{4}\right) + \sinh^2\left(\frac{\Theta}{2}\right) \right] \right) \right\}$$

$$A_{\pm}^{(+)}(\Theta) = \tilde{Z}^{(+)}(\Theta) \left\{ -i \cosh\left(\frac{\Theta}{2}\right) \left(\frac{\gamma^2}{4M} - \left[\sin^2\left(\frac{\rho}{4}\right) - \cosh^2\left(\frac{\Theta}{2}\right) \right] \right) \right. \\ \left. \pm \sinh\left(\frac{\Theta}{2}\right) \left(\frac{\gamma^2}{4M} + \left[\sin^2\left(\frac{\rho}{4}\right) - \cosh^2\left(\frac{\Theta}{2}\right) \right] \right) \right\}$$

$$B^{(\pm)}(\Theta) = \tilde{Z}^{(\pm)}(\Theta) \frac{e\gamma}{2\sqrt{M}} \sqrt{\cos(\rho/2)} \sinh(\Theta),$$

where

$$m = 2M \cos\left(\frac{\rho}{2}\right), \quad \frac{\rho}{2} = \frac{\pi}{2} - u, \quad \alpha = -\frac{1}{2M}, \quad (2.131)$$

$0 \leq \rho < \pi$, $e = \pm 1$ in the $(-)$ case and $e = 1$ in the $(+)$ case. Note that $R_{P2,e}^{(\pm)}$ depends on two parameters: γ^2/M and ρ only. $R_{P2,e}^{(-)}$ has the same structure as the particle reflection amplitude obtained in [36] for the case of the boundary supersymmetric sine-Gordon model from the kink reflection amplitude by bootstrap. Consequently, there is no need now to solve the crossing and unitarity equations for $\tilde{Z}^{(-)}(\Theta)$, we take it from [36]. We determined $\tilde{Z}^{(+)}(\Theta)$ using the unitarity and crossing equations and exploiting the fact that these equations take a similar form for $\tilde{Z}^{(-)}(\Theta)$. Explicit formulae for these prefactors can be found in the Appendix.

In the $(+)$ case we introduce the parameter ξ in the following way: $\gamma = -2\sqrt{M}i \sin(\xi/2)$, $\xi \in [-\pi, \pi]$. It should be noted, however, that if $\xi \neq 0$, then the condition $Q_B^\dagger = Q_B$ is violated. If we choose ξ so that $\gamma \in \mathbb{R}$, then, as we can see from the formula for $\tilde{Z}^{(+)}(\Theta)$, the condition 5) in Section 2.2 requiring that the poles should be in $i\mathbb{R}$ is not satisfied. We also note that if $\xi = 0$, then $R_{P2,e}^{(+)}(\Theta) = R_{P1}^{(+)}(\Theta)$.

To summarize, we have the supersymmetric reflection matrix factors

$$\begin{aligned} &R_K^{(+)}(\Theta) \\ &R_{K,e}^{(-)}(\Theta, \xi) & \xi \in [0, \pi], \quad e = \pm 1 \\ &R_{P1}^{(\pm)}(\Theta) & \\ &R_{P2,e}^{(-)}(\Theta, M, \rho, \xi) & M > 0, \quad 0 \leq \rho < \pi, \quad \xi \in [0, \pi], \quad e = \pm 1 \\ &R_{P2,e}^{(+)}(\Theta, M, \rho, \xi) & M > 0, \quad 0 \leq \rho < \pi, \quad \xi \in [-\pi, \pi], \quad e = 1. \end{aligned} \quad (2.132)$$

The same set of kink and particle reflection matrix factors can be obtained by solving the Yang-Baxter equations without imposing the boundary supersymmetry condition [38, 39, 40]. The supersymmetry condition relates the parameters of the reflection matrix factors obtained in this way to the parameters of the representations of the supersymmetry algebra. The results described above show that the task of solving the Yang-Baxter equations is greatly simplified if one imposes the supersymmetry condition first.

2.6.6 Properties of the ground state reflection matrix factors

In this section various important properties of the ground state reflection matrix factors are collected.

$R_{P2,e}^{(\pm)}$ are not symmetric with respect to Γ_B , $R_{P1}^{(\pm)}$ are symmetric with respect to Γ_B . $R_{P1}^{(\pm)}$ and $R_{P2,e}^{(\pm)}$ do not satisfy the Yang-Baxter equation together. It is also important to note that $\lim_{\gamma \rightarrow 0} R_{P2,e}^{(\pm)} = R_{P1}^{(\pm)}$. We shall assume that $\gamma \neq 0$ when we mention $R_{P2,e}^{(\pm)}$.

The second boundary bootstrap equation applied to the *kink + kink* \rightarrow *particle* bulk fusion determines reflection matrix factors for boson-fermions on ground state boundary. They turn out [36, 39] to be the same as those obtainable by solving the boundary Yang-Baxter, crossing and unitarity equations. In terms of the reflection matrix factors

$$R_K^{(+)} + R_K^{(+)} \rightarrow R_{P1}^{(+)} \quad (2.133)$$

and

$$R_{K,e}^{(-)}(\xi) + R_{K,e}^{(-)}(\xi) \rightarrow R_{P2,e}^{(-)}(\xi) \quad (2.134)$$

with appropriate values of the parameters. Similarly, it can be checked that the second boundary bootstrap equation is also satisfied for the *particle + particle* \rightarrow *particle*, *kink + particle* \rightarrow *kink* fusions with the reflection matrix factors

$$R_{P1}^{(\pm)} + R_{P1}^{(\pm)} \rightarrow R_{P1}^{(\pm)} \quad (2.135)$$

$$R_{P2,e}^{(\pm)}(\xi) + R_{P2,e}^{(\pm)}(\xi) \rightarrow R_{P2,e}^{(\pm)}(\xi) \quad (2.136)$$

$$R_K^{(+)} + R_{P1}^{(+)} \rightarrow R_K^{(+)} \quad (2.137)$$

$$R_{K,e}^{(-)}(\xi) + R_{P2,e}^{(-)}(\xi) \rightarrow R_{K,e}^{(-)}(\xi) \quad (2.138)$$

respectively. These relations are nontrivial, although it is clear that they are satisfied up to CDD factors. It is remarkable that $R_{P2,e}^{(+)}$ cannot be obtained by bootstrap from kink reflection matrix factors, while the other particle reflection matrix factors $R_{P1}^{(\pm)}$ and $R_{P2,e}^{(-)}$ can be obtained in this way.

$R_K^{(+)}(\Theta)$ is bijective (of rank two) in the physical strip. $\{R_{K,+1}^{(-)}\}_{K_{0\frac{1}{2}}}^{K_{0\frac{1}{2}}}(\Theta)$ and $\{R_{K,-1}^{(-)}\}_{K_{1\frac{1}{2}}}^{K_{1\frac{1}{2}}}(\Theta)$ have a zero at $\Theta = i(\pi - \xi)$, so $R_{K,e}^{(-)}$ is of rank one at this angle. This

Table 2.1: Degeneracy properties of reflection factors

| | |
|----------------------------|---|
| $R_K^{(+)}(\Theta)$: | bijjective (rank two) |
| $R_{K,e}^{(-)}(\Theta)$: | degenerate (rank one) at $\Theta = i(\pi - \xi)$, which is in the physical strip if $\pi > \xi > \pi/2$. |
| $R_{P1}^{(\pm)}(\Theta)$: | bijjective (rank two) |
| $R_{P2,e}^{(-)}(\Theta)$: | degenerate (rank one) at $\Theta = i(\pi - \xi \pm \rho/2)$, one or both of these angles can be in the physical strip. $\pi - \xi \geq \rho/2$ is necessary and sufficient for $R_{P2,e}^{(-)}$ not to have any poles in the physical strip. |
| $R_{P2,e}^{(+)}(\Theta)$: | degenerate (rank one) at $\Theta = i(\pi - \xi \pm \rho/2)$, $\Theta = i(\pi + \xi \pm \rho/2)$. Some of these angles can be in the physical strip. $\pi - \xi \geq \rho/2$ is necessary and sufficient for $R_{P2,e}^{(+)}$ not to have any poles in the physical strip. |

zero is in the physical strip if $\pi > \xi > \pi/2$, any other zeroes of the kink amplitudes are outside the physical strip.

Consequently, the relations $R_K^{(+)} + R_K^{(+)} \rightarrow R_{P1}^{(+)}$, and $R_{K,e}^{(-)} + R_{K,e}^{(-)} \rightarrow R_{P2,e}^{(-)}$ together with the bijectivity of the kink-kink fusion tensor and S_{KK} imply that $R_{P1}^{(+)}$ is of rank two (bijjective) and has no poles in the physical strip, and $R_{P2,e}^{(-)}(\Theta)$ is also bijective for generic values of Θ , but it is of rank one if $\Theta = i(\pi - \xi \pm \rho/2)$. It is possible for these angles to be in the physical strip and on the imaginary axis. $(\pi - \xi - \rho/2) > -\pi/2$ holds, so if $(\pi - \xi - \rho/2)$ is negative, then there is a pole in the physical strip at $i(\rho/2 + \xi - \pi)$ because of unitarity. If $(\pi - \xi - \rho/2) > 0$, then $R_{P2,e}^{(-)}(\Theta)$ has no poles and zeroes in the physical strip, and within the physical strip it is of rank 1 if and only if $\Theta = i(\pi - \xi \pm \rho/2)$. We therefore impose the following condition on ξ :

$$\pi - \xi \geq \rho/2 . \quad (2.139)$$

$R_{P1}^{(-)}$ is also bijective and has no poles in the physical strip. It can be verified by direct calculation that $R_{P2,e}^{(+)}(\Theta)$ is degenerate (of rank two) at $\Theta = i(\pi - \xi \pm \rho/2)$ and $\Theta = i(\pi + \xi \pm \rho/2)$, therefore the condition (2.139) reads in this case as

$$\pi - |\xi| \geq \rho/2 . \quad (2.140)$$

(Note that the relation between ξ and γ is different in the (+) and (−) cases).

A particular boundary scattering theory is characterized by the M parameter of the underlying bulk theory and by the sign (+) or (−), and also by the parameters ξ and e . Considering the properties of the supersymmetric factors the following three cases can be distinguished:

1. The boundary co-multiplication is Δ_B^+ , the theory may contain kinks as well as particles, the supersymmetric reflection matrix factors on ground state boundary are $R_K^{(+)}$ and $R_{P_1}^{(+)}$.
2. The boundary co-multiplication is Δ_B^+ , the theory may contain particles only, the supersymmetric reflection matrix factor on ground state boundary is $R_{P_{2,e}}^{(+)}$. $\gamma \neq 0$ is assumed.
3. The boundary co-multiplication is Δ_B^- , the theory may contain kinks as well as particles, the supersymmetric reflection matrix factors on ground state boundary are $R_{K,e}^{(-)}$ and $R_{P_{2,e}}^{(-)}$. In this case we allow $\gamma = 0$.
4. The boundary co-multiplication is Δ_B^- , the theory may contain particles only, the supersymmetric reflection matrix factor on ground state boundary is $R_{P_1}^{(-)}$. In this case it is assumed that $\gamma \neq 0$.

(2.139) imply that if $R_{P_{2,e}}^{(-)}$ describes the ground state reflections of the particles in a theory (and $\gamma \neq 0$), then

$$\pi - |\xi| \geq \rho_{max}/2, \quad \rho_{max} = \max_i(\rho_i), \quad (2.141)$$

where i runs over all particles in a particular theory, is necessary and sufficient for all $R_{P_{2,e}}^{(-)}$ and $R_{P_{2,e}}^{(+)}$ factors (in a particular theory) not to have poles in the physical strip.

2.6.7 Higher level supersymmetric boundary states

Cases 1 and 3

In case 1. and 3. of Section 2.6.6 the supersymmetric part of any boundary multiplet can be labeled as

$$W(\nu_1, \nu_2, \dots, \nu_n, B_{\frac{1}{2}}) \quad (2.142)$$

where

$$\pi > \nu_1 > \nu_2 > \dots > \nu_n > 0 \quad (2.143)$$

$$\nu_i + \nu_j \neq \pi \quad \forall i, j = 1 \dots n, \quad i \neq j. \quad (2.144)$$

We assume here and below that $\nu_i \neq \pi - \xi \quad \forall i$. The special situation when $\pi - \xi$ is also allowed and the situation when equalities are also allowed in (2.143) will be discussed after the description of the general case.

$W(\nu_1, \nu_2, \dots, \nu_n, B_{\frac{1}{2}})$ stands for a linear space which is spanned by the states belonging to the (supersymmetric part of the) multiplet,

$$v = W(\nu_1, \nu_2, \dots, \nu_n, B_{\frac{1}{2}}) = W_K \otimes W_K \otimes \dots \otimes W_K \otimes W(B_{\frac{1}{2}}) , \quad (2.145)$$

where W_K stands for the internal space of the kink representation of mass M . The second equality is, strictly speaking, an equality up to an isomorphism. The space v , taking into consideration the kink adjacency conditions, has dimension

$$\dim v = 2^{\lceil n/2 \rceil} . \quad (2.146)$$

The representation of \mathcal{A}_B on v is

$$K(\nu_1, \nu_2, \dots, \nu_n, B_{\frac{1}{2}}) = K_M(i\nu_1) \times K_M(i\nu_2) \times \dots \times K_M(i\nu_n) \times B_{\frac{1}{2}} . \quad (2.147)$$

Strictly speaking, this equality is an equivalence of representations, the intertwining map being the isomorphism mentioned above. We assign a labeling set to a boundary multiplet in the following way:

$$L[W(\nu_1, \nu_2, \dots, \nu_n, B_{\frac{1}{2}})] = \{i\nu_1, i\nu_2, \dots, i\nu_n\} . \quad (2.148)$$

The reflection factors on v have no poles and zeroes on the imaginary axis in the physical strip if and only if

$$\nu_i < \pi - \rho_{max}/2 \quad \forall i = 1 \dots n . \quad (2.149)$$

(Note that ρ was defined in (2.131).) Let $p + v \rightarrow y$ be a boundary fusion where p is either a kink or a particle multiplet with appropriate rapidity and v and y are boundary multiplets, $L[v] = \{i\nu_1, \dots, i\nu_n\}$. $L[y]$ can be obtained from $L[p]$ and $L[v]$:

If p is a kink multiplet, $L[p] = \{iw\}$, and $w + \nu_i \neq \pi$, $i = 1 \dots n$, then

$$\{iw\} + \{i\nu_1, i\nu_2, \dots, i\nu_n\} \rightarrow \{i\nu_1, \dots, i\nu_k, iw, i\nu_{k+1}, \dots, i\nu_n\} , \quad (2.150)$$

if $w + \nu_k = \pi$, then

$$\{iw\} + \{i\nu_1, i\nu_2, \dots, i\nu_n\} \rightarrow \{i\nu_1, \dots, i\nu_{k-1}, i\nu_{k+1}, \dots, i\nu_n\} . \quad (2.151)$$

If p is a particle multiplet, $L[p] = \{iw_1, iw_2\}$, and $|w_1| > |w_2|$ and $|w_1| + \nu_i \neq \pi$, $i = 1 \dots n$, $|w_2| + \nu_i \neq \pi$, $i = 1 \dots n$, then

$$\{iw_1, iw_2\} + \{i\nu_1, i\nu_2, \dots, i\nu_n\} \rightarrow \{i\nu_1, \dots, i\nu_k, i|w_1|, i\nu_{k+1}, \dots, i\nu_l, i|w_2|, i\nu_{l+1}, \dots, i\nu_n\}, \quad (2.152)$$

if $|w_1| + \nu_k = \pi$, $|w_2| + \nu_i \neq \pi$, $i = 1 \dots n$, then

$$\{iw_1, iw_2\} + \{i\nu_1, i\nu_2, \dots, i\nu_n\} \rightarrow \{i\nu_1, \dots, i\nu_{k-1}, i\nu_{k+1}, \dots, i\nu_l, i|w_2|, i\nu_{l+1}, \dots, i\nu_n\}, \quad (2.153)$$

if $|w_1| + \nu_i \neq \pi$, $i = 1 \dots n$, $|w_2| + \nu_l = \pi$, then

$$\{iw_1, iw_2\} + \{i\nu_1, i\nu_2, \dots, i\nu_n\} \rightarrow \{i\nu_1, \dots, i\nu_k, i|w_1|, i\nu_{k+1}, \dots, i\nu_{l-1}, i\nu_{l+1}, \dots, i\nu_n\}, \quad (2.154)$$

if $|w_1| + \nu_k = \pi$, $|w_2| + \nu_l = \pi$, then

$$\{iw_1, iw_2\} + \{i\nu_1, i\nu_2, \dots, i\nu_n\} \rightarrow \{i\nu_1, \dots, i\nu_{k-1}, i\nu_{k+1}, \dots, i\nu_{l-1}, i\nu_{l+1}, \dots, i\nu_n\}. \quad (2.155)$$

In other words, $L[y]$ is obtained in the following way: we form the union $b = L[p] \cup L[v]$ (the elements may have multiplicities), replace iw_1 , iw_2 by $i|w_1|$, $i|w_2|$, and remove all the pairs of elements $i\Theta_1, i\Theta_2$ satisfying $\Theta_1 + \Theta_2 = \pi$. This rule is analogous to the bulk fusion rules, but the amplitudes $i\Theta$ and $-i\Theta$ ($\Theta \in \mathbb{R}$) are identified.

The reflection matrix factor of a particle or kink on the boundary multiplet $W(\nu_1, \nu_2, \dots, \nu_n, B_{\frac{1}{2}})$ is

$$R_{XW(\nu_1, \nu_2, \dots, \nu_n, B_{\frac{1}{2}})}(\Theta) = U_1 U_2 \dots U_n R T_n T_{n-1} \dots T_1 \quad (2.156)$$

where

$$T_k = \underbrace{I \otimes \dots \otimes I}_{k-1} \otimes S_{XK}(\Theta - i\nu_k) \otimes \underbrace{I \otimes \dots \otimes I}_{n-k} \otimes I \quad (2.157)$$

$$R = \underbrace{I \otimes \dots \otimes I}_n \otimes R_X(\Theta) \quad (2.158)$$

$$U_k = \underbrace{I \otimes \dots \otimes I}_{k-1} \otimes S_{KX}(\Theta + i\nu_k) \otimes \underbrace{I \otimes \dots \otimes I}_{n-k} \otimes I \quad (2.159)$$

and X stands either for K (kink) or P (particle). A graphical illustration is given in Figure 2.16.

We consider now the special case when kink rapidities $i(\pi - \xi)$ are also allowed and case 3. of Section 2.6.6 applies. The speciality of $i(\pi - \xi)$ is that at this rapidity the ground state reflection factor $R_{K,e}^{(-)}$ is degenerate. The rules above are modified in the following way: there is no change in the rules for the labeling sets, but if the labeling set contains $i(\pi - \xi)$, i.e. $L = \{i\nu_1, i\nu_2, \dots, i(\pi - \xi), \dots, i\nu_n\}$, then the linear space of the multiplet is denoted as $W(\nu_1, \nu_2, \dots, \nu_n, B_0)$ or $W(\nu_1, \nu_2, \dots, \nu_n, B_1)$ and $v = W(\nu_1, \nu_2, \dots, \nu_n, B_0) = W_K \otimes W_K \otimes \dots \otimes W_K \otimes W(B_0)$, $v = W(\nu_1, \nu_2, \dots, \nu_n, B_1) = W_K \otimes W_K \otimes \dots \otimes W_K \otimes W(B_1)$, where $W(B_0)$ or $W(B_1)$ is the one-dimensional space spanned by $|B_0\rangle$ or $|B_1\rangle$, which are

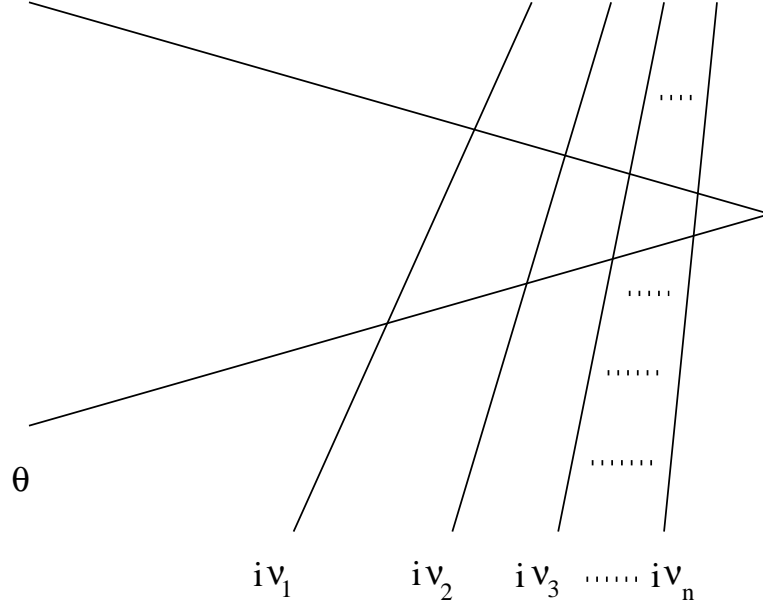


Figure 2.16: Graphical representation for (2.156)-(2.159)

the boundary states created by the fusion of $K_{0\frac{1}{2}}(i(\pi - \xi))$ and $|B_{\frac{1}{2}}\rangle$ of $K_{1\frac{1}{2}}(i(\pi - \xi))$ and $|B_{\frac{1}{2}}\rangle$, respectively. ‘0’ should be taken in these and the following formulae if $e = -1$, ‘1’ if $e = +1$. The dimension of v is $2^{\lceil n/2 \rceil - 1}$. $W(B_0)$ or $W(B_1)$ is invariant with respect to the action of \mathcal{A}_B , the representation on $W(B_0)$ or $W(B_1)$ is denoted by B_0 or B_1 . The representation of \mathcal{A}_B on v is $K(i\nu_1) \times K(i\nu_2) \times \cdots \times K(i\nu_n) \times B_0$ or $K(i\nu_1) \times K(i\nu_2) \times \cdots \times K(i\nu_n) \times B_1$. The formulae (2.156)-(2.159) apply with the modification that $R_X(\Theta)$ should be replaced by the reflection matrix factor on $W(B_0)$ or $W(B_1)$, which can be calculated by the bootstrap equation.

The only modification if equalities between the ν ’s (i.e. in (2.143)) are also allowed is that the labeling sets can contain certain elements with multiplicities greater than 1. If $i(\pi - \xi)$ has multiplicity greater than 1 in the labeling set, then only one copy of it is absorbed to form the label B_0 or B_1 .

It can be verified that the labeling (2.142) of the boundary multiplets is unambiguous, i.e. if two multiplets have different labels, then they have different transformation and scattering properties. This can be seen from the dimensions of the multiplets and from the singularity properties of the reflection factors on them.

It is also possible that (2.149) is not satisfied for certain bound states, but the poles of the supersymmetric reflection factors on them are canceled by zeroes of the corresponding non-supersymmetric reflection factor, so the poles of the supersymmetric reflection factors do not introduce new singularity. The fusion rules above apply in this case as well.

We remark that the above characterization of the supersymmetric factors for higher level boundary bound states can be interpreted as a characterization in terms of ‘boundary particle groups’. In this interpretation we can say, in particular, that the supersymmetric parts of the boundary bound states can be described as supersymmetric boundary particle groups in which the boundary is in the ground state.

We refer the reader to [20] for a detailed justification of the statements in this section. Here we remark only that the degeneracy properties of the two-particle S-matrix factors, the bulk supersymmetric fusion rules and the degeneracy properties of the one-particle ground state reflection matrix factors play very important role.

It should be noted that we have not assumed particular statistical properties of the particles.

As we mentioned in Section 2.6.4, the boson-fermion representation can be replaced by the two-kink-representation without difficulty.

Cases 2 and 4

In cases 2. and 4. of Section 2.6.6 the supersymmetric part of any boundary multiplet can be labeled as

$$W(\nu_1, \nu_2, \dots, \nu_n, B_{\frac{1}{2}}) \quad (2.160)$$

where n is even,

$$\pi > \nu_1 > \nu_2 > \dots > \nu_{n-1} > 0, \quad \nu_n > -\pi \quad (2.161)$$

$$\nu_{n-1} > |\nu_n| \quad (2.162)$$

$$\nu_i + \nu_j \neq \pi \quad \forall i, j = 1 \dots n, \quad i \neq j \quad (2.163)$$

$$\nu_i \neq -\nu_n \quad \forall i = 1 \dots n-1. \quad (2.164)$$

We assume here and below that $\nu_i \neq \pi - |\xi| \quad \forall i$. The special situation when $\pi - |\xi|$ is also allowed and the situation when equalities are also allowed in (2.161), (2.162) will be discussed after the description of the general case.

$$v = W(\nu_1, \nu_2, \dots, \nu_n, B_{\frac{1}{2}}) = W_K \otimes W_K \otimes \dots \otimes W_K \otimes W(B_{\frac{1}{2}}). \quad (2.165)$$

The dimension of v is

$$\dim v = 2^{\lceil n/2 \rceil}. \quad (2.166)$$

The representation on v is

$$K(\nu_1, \nu_2, \dots, \nu_n, B_{\frac{1}{2}}) = K(i\nu_1) \times K(i\nu_2) \times \dots \times K(i\nu_n) \times B_{\frac{1}{2}}. \quad (2.167)$$

We assign a labeling set to a boundary multiplet as in the previous section:

$$L[W(\nu_1, \nu_2, \dots, \nu_n, B_{\frac{1}{2}})] = \{i\nu_1, i\nu_2, \dots, i\nu_n\} . \quad (2.168)$$

The reflection factors on v have no poles and zeroes on the imaginary axis in the physical strip if and only if (2.149) is satisfied.

Let $p + v \rightarrow y$ be a boundary fusion where p is a particle multiplet with appropriate rapidity and v and y are boundary multiplets, $L[p] = \{iw_1, iw_2\}$, $L[v] = \{i\nu_1, i\nu_2, \dots, i\nu_n\}$. $L[y]$ is obtained in the following way: we form the union $b = L[p] \cup L[v]$ (the elements may have multiplicities), then delete (zero, two or four) elements in a few steps applying the following algorithm: 1. if $\Theta - \Theta_2 = i\pi$ for two elements, then they are removed, 2. the sign of any even number of elements of b can be changed freely, 3. sign changes are done until no more deletions can be done. Finally if b is not yet of the form (2.160)-(2.164), then we bring it to this form by changing the sign of an even number (usually two) of appropriate elements of b . The b obtained in this way equals to $L[y]$.

The formulae (2.156) - (2.159) apply in this case as well, X should be replaced by P .

We consider now the special case when kink rapidities $i(\pi - |\xi|)$ are also allowed and case 2. of Section 2.6.6 applies. The speciality of $i(\pi - |\xi|)$ is related to the degeneracy properties of the reflection factor $R_{P2}^{(+)}$. The rules above are modified in the following way: if the labeling set contains $i(\pi - |\xi|)$, i.e. $L = \{i\nu_1, i\nu_2, \dots, i(\pi - |\xi|), \dots, i\nu_n\}$, then the linear space of the multiplet is denoted as $W(\nu_1, \nu_2, \dots, \nu_{n-1}, B'_{\frac{1}{2}})$ and $v = W(\nu_1, \nu_2, \dots, \nu_{n-1}, B'_{\frac{1}{2}}) = W_K \otimes W_K \otimes \dots \otimes W_K \otimes W(B'_{\frac{1}{2}})$, where $W(B'_{\frac{1}{2}})$ is the one-dimensional space of the boundary state arising in the fusion of a particle composed of the kink multiplets $K(i(\pi - |\xi|))$ and $K(i\nu_n)$ and $|B'_{\frac{1}{2}}\rangle$. The dimension of v is $2^{\lceil n/2 \rceil - 1}$. The representation on v is $K(i\nu_1) \times K(i\nu_2) \times \dots \times K(i\nu_{n-1}) \times B'_{\frac{1}{2}}$. The formulae (2.156)-(2.159) apply with the modification that $R_P(\Theta)$ should be replaced by the (particle) reflection factor on $B'_{\frac{1}{2}}$ which can be computed using the bootstrap equation.

The modification in the above rules if equalities between the ν 's (in (2.161), (2.162)) are also allowed is that the labeling sets can contain certain elements with multiplicities greater than 1. If $i(\pi - |\xi|)$ has multiplicity greater than 1 in the labeling set, then only one copy of it is absorbed to form the label $B'_{\frac{1}{2}}$. If the last element ν_n is negative, it can have multiplicity 1 only.

It can be verified that the labeling (2.160) of the boundary multiplets is unambiguous, i.e. if two multiplets have different labels, then they have different transformation and scattering properties.

The remarks made at the end of the previous section apply to the present section as well.

We consider now the situation when a boundary state (or multiplet) in the non-supersymmetric theory arises as a bound state in more than one way. In this case the question that arises is whether the supersymmetric parts obtained by the rules of this section give the same result in each way of creating the boundary bound state. In the non-supersymmetric theory the diagrams corresponding to the different ways of creation can usually be transformed into each other by shifting lines using the bootstrap and Yang-Baxter equations and by splitting or merging vertices. It is natural to expect that these transformations are usually applicable to the supersymmetric parts as well, and so the answer to the question above is positive. This should nevertheless be checked in specific models. If the answer is negative, then one has to take direct sums of the multiplets (2.142) or (2.160) as supersymmetric parts of the boundary multiplets.

2.7 Examples

In this section we present examples for the application of the fusion rules written down in Section 2.6.7. The sinh-Gordon model and the free particle will be discussed only briefly, restricting mainly to the dimension of the boundary multiplets. The reason for this is that in these cases not all the assumptions that we have made are satisfied. The sine-Gordon model and the $a_2^{(1)}$ and $a_4^{(1)}$ affine Toda models will be discussed in more detail.

2.7.1 Boundary sine-Gordon model

It was argued in [96, 19] that the boundary version of sine-Gordon model which has the action

$$S = \int_{-\infty}^{\infty} dt \int_{-\infty}^0 dx \mathcal{L}_{SG} - \int_{-\infty}^{\infty} dt V_B(\Phi_B) , \quad (2.169)$$

where

$$\mathcal{L}_{SG} = \frac{1}{2}(\partial_\mu \Phi)^2 - \frac{m^2}{\beta^2}(1 - \cos(\beta\Phi)) \quad (2.170)$$

is the Lagrangian density of the sine-Gordon model, $\Phi(x, t)$ is a real scalar field, β is a real dimensionless coupling constant and $\Phi_B(t) = \Phi(x, t)|_{x=0}$, preserves the integrability of the bulk theory if the boundary potential is chosen as

$$V_B(\Phi_B) = M_0 \left(1 - \cos \left(\frac{\beta}{2}(\Phi_B - \phi_0) \right) \right) , \quad (2.171)$$

Table 2.2: Fusion rules of the boundary sine-Gordon model

| Initial state | Particle | Rapidity | Final state |
|---|--------------|--|---|
| $ n_1, \dots, n_{2k}\rangle$ | s, \bar{s} | $i\nu_n$ | $ n_1, \dots, n_{2k}, n\rangle$ |
| $ n_1, \dots, n_{2k-1}\rangle$ | s, \bar{s} | iw_n | $ n_1, \dots, n_{2k-1}, n\rangle$ |
| $ n_1, \dots, n_{2k}, n_{2k+1}, \dots\rangle$ | B_n | $i\frac{1}{2}(\nu_l - w_{n-l})$ | $ n_1, \dots, n_{2k}, l, n-l, n_{2k+1}, \dots\rangle$ |
| $ n_1, \dots, n_{2k-1}, n_{2k}, \dots\rangle$ | B_n | $i\frac{1}{2}(w_l - \nu_{n-l})$ | $ n_1, \dots, n_{2k-1}, l, n-l, n_{2k}, \dots\rangle$ |
| $ n_1, \dots, n_{2k}, \dots\rangle$ | B_n | $i\frac{1}{2}(\nu_{-n_{2k}} - w_{n+n_{2k}})$ | $ n_1, \dots, n_{2k} + n, \dots\rangle$ |
| $ n_1, \dots, n_{2k-1}, \dots\rangle$ | B_n | $i\frac{1}{2}(w_{-n_{2k-1}} - \nu_{n+n_{2k-1}})$ | $ n_1, \dots, n_{2k-1} + n, \dots\rangle$ |

where M_0 and ϕ_0 are free parameters. As a result of the boundary potential the scalar field satisfies the boundary condition

$$\partial_x \Phi|_{x=0} = -M_0 \frac{\beta}{2} \sin\left(\frac{\beta}{2}(\Phi_B - \phi_0)\right). \quad (2.172)$$

The particle spectrum of the bulk sine-Gordon theory (SG) contains a soliton s and an anti-soliton \bar{s} of mass M and the breathers B_n of mass $m_n = 2M \sin(u_n)$, where $u_n = \pi n/(2\lambda)$, $n = 1, \dots, [\lambda]$, $\lambda = \frac{8\pi}{\beta^2} - 1$. M can be expressed in terms of β, m . The breathers are self-conjugate, and the conjugate of s is \bar{s} . The fusions (given in the form *process, (fusion angle)*) are the following: $s + \bar{s} \rightarrow B_n, (\pi - 2u_n)$; $B_n + B_m \rightarrow B_{n+m}, (u_n + u_m)$ provided $n + m \leq [\lambda]$; and the crossed versions of these rules. These rules are consistent with the following decomposition (see (2.101)): $\langle s, \bar{s} \rangle \oplus \langle b_1 \rangle \oplus \dots \oplus \langle b_{[\lambda]} \rangle$, where $\langle v, \dots \rangle$ denotes the linear space spanned by the vectors v, \dots . One can associate kink representations to $\langle s, \bar{s} \rangle$ and particle or ‘two-kink-representations’ with $\alpha = -1/(2M)$ to the breathers (see also (2.102)). The labeling sets corresponding to the supersymmetric parts W_s, W_n of $\langle s, \bar{s} \rangle, \langle B_n \rangle$ are $L[W_s(\Theta)] = \{\Theta\}$, $L[W_n(\Theta)] = \{\Theta + i(\pi/2 - u_n), \Theta - i(\pi/2 - u_n)\}$.

The boundary sine-Gordon model (BSG) has the boundary spectrum containing the states $|n_1, n_2, \dots, n_k\rangle$, where n_1, n_2, \dots, n_k are nonnegative integers satisfying the condition $\pi/2 \geq \nu_{n_1} > w_{n_2} > \nu_{n_3} > \dots \geq 0$, where $\nu_n = \eta/\lambda - u_{2n+1}$, $w_n = \pi - \eta/\lambda - u_{2n-1}$, and $0 < \eta \leq \frac{\pi}{2}(\lambda + 1)$ is a boundary parameter which can be expressed in terms of ϕ_0, M_0, β, m (see [20]). The fusion rules [20, 21] are listed in Table 2.2.

The first and second columns contain the initial boundary state and the incoming bulk particle, the fusion angle times i is shown in the third column and the final state is shown in the fourth column.

Because of the presence of the kinks, only the cases 1 and 3 of Section 2.6.6 can apply.

In the decomposition (2.108) every subspace is one-dimensional and is spanned by the boundary bound states introduced above.

The first two lines show that the whole boundary spectrum can be generated by kinks. Correspondingly, we associate to the BSG state $|n_1, n_2, \dots, n_k\rangle$ the supersymmetric part $W(\nu_{n_1}, w_{n_2}, \nu_{n_3}, \dots, B_{\frac{1}{2}})$ (using the notation introduced earlier). Now we have to verify whether the fusion rules given in the 3-6th lines are also valid for these supersymmetric parts. This is easily done using the rules given in Section 2.6.7. Let us consider the 3rd line first. Let $v = W(\nu_{n_1}, \dots, w_{n_{2k}}, \nu_{n_{2k+1}}, \dots, B_{\frac{1}{2}})$, $p = W_P(i\frac{1}{2}(\nu_l - w_{n-l}))$ with mass parameter u_n , and $w_{2k} > \nu_l > w_{n-l} > \nu_{2k+1}$ and $p + v \rightarrow y$. In this case $L[p] = \{i\nu_l, -iw_{n-l}\}$, so $L[y] = \{i\nu_{n_1}, \dots, iw_{n_{2k}}, i\nu_{n_{2k+1}}, \dots, i\nu_l, iw_{n-l}\}$. The 4th line is similar. Turning to the 5th line, let $v = W(\nu_{n_1}, \dots, w_{n_{2k}}, \dots, B_{\frac{1}{2}})$, $p = W_P(i\frac{1}{2}(\nu_{-n_{2k}} - w_{n+n_{2k}}))$ with mass parameter u_n , and $p + v \rightarrow y$. Now $L[p] = \{i\nu_{-n_{2k}}, -iw_{n+n_{2k}}\}$, and because of $\nu_{-n_{2k}} + w_{n_{2k}} = \pi$ we have $L[y] = \{i\nu_{n_1}, \dots, iw_{n+n_{2k}}, \dots\}$. The 6th line is similar to the 5th line.

Condition (2.149) is clearly satisfied for all boundary bound states, so the supersymmetric factors of the reflection matrix blocks do not have poles on the imaginary axis in the physical strip.

The Lagrangian function and also the one-particle reflection matrix blocks and two-particle S-matrix blocks of the BSG model contain two bulk and two boundary parameters. A Lagrangian function for the boundary supersymmetric sine-Gordon model was written down in [97] (it can also be found in [36]), this Lagrangian function also contains four parameters only. The supersymmetric reflection matrix constructed above (and in [36]), however, contains the parameter γ (see (2.99)) in addition, therefore one can expect that γ can be related to the other four parameters. This relation is not yet known. In particular, it is not known whether any of the angles ν_n and w_n coincides with $\pi - \xi$ or not. The supersymmetric transformation and scattering properties and in particular the dimensions of the boundary bound state multiplets are modified by such a coincidence.

We remark that this section confirms the results of [36].

2.7.2 Boundary sinh-Gordon model

The classical equation of motion for the sinh-Gordon field Φ , which is a real field, is

$$\partial_t^2 \Phi - \partial_x^2 \Phi + \frac{\sqrt{8}m^2}{\beta} \sinh(\sqrt{2}\beta\Phi) = 0, \quad (2.173)$$

where m and β are parameters.

The sinh-Gordon model (ShG) can be restricted to the left half-line $-\infty \leq x \leq 0$ without losing integrability by imposing the boundary condition

$$\partial_x \Phi|_0 = \frac{\sqrt{2}m}{\beta} \left(\epsilon_0 e^{-\frac{\beta}{\sqrt{2}}\Phi(0,t)} - \epsilon_1 e^{\frac{\beta}{\sqrt{2}}\Phi(0,t)} \right), \quad (2.174)$$

Table 2.3: Fusion rules of the boundary sinh-Gordon model

| Initial state | Particle | Rapidity | Final state |
|---------------|----------|--|-------------|
| b_n | P | $i(\frac{\eta}{\lambda} - \frac{\pi}{2} + \frac{\pi}{\lambda}n)$ | b_{n+1} |

where ϵ_0 and ϵ_1 are two additional parameters [19, 98].

Some quantities of the sinh-Gordon and the boundary sinh-Gordon (BShG) model can be obtained from those of the sine-Gordon and boundary sine-Gordon model by analytic continuation of their coupling constant β to the imaginary axis.

The particle spectrum of the ShG model contains only one self-conjugate particle P with a two-particle S-matrix and reflection matrix that can be obtained from the corresponding matrices of the first SG breather (B_1) by the analytic continuation mentioned above. The BShG model also contains a series of finitely many boundary bound states b_n found in [25] (see also [24]). These states correspond to the BSG states $|\nu_0, w_n\rangle$, $n = 1 \dots$ which are precisely those states that can be generated using B_1 only. b_0 is the ground state. The boundary fusion rules are listed in Table 2.3. The parameter η is determined by $\epsilon_0, \epsilon_1, \beta$. For a more detailed description we refer the reader to [25, 24].

Some quantities (the Lagrangian densities and the scattering and reflection matrices, for example) of the supersymmetric BShG model are also obtained by the analytic continuation above [99]. This, however, implies $\lambda < 0$ and $M < 0$, $u < 0$ in the formula $m = 2M \sin(u)$ for the particle mass, i.e. the values of these parameters are not in the range that we have considered. One consequence of this, for example, is that the supersymmetric factor of the two-particle S-matrix has a pole in the physical strip (canceled by a zero of the non-supersymmetric factor) [99]. Applying the rules of Section 2.6.7 (cases 1 and 3) formally we can nevertheless obtain supersymmetric parts W_n for the states b_n , and corresponding reflection matrix factors. In this way the multiplets W_n turn out to be two-dimensional in the supersymmetric BShG model if the value of ξ is generic.

2.7.3 Free particle on the half-line

The supersymmetric factors of the scattering and ground state reflection matrices of a massive real free boson can be obtained by taking the limit $\alpha \rightarrow 0$, which implies $M \rightarrow \infty$, $u \rightarrow 0$, $\rho \rightarrow \pi$; in the $(-)$ case $\xi \rightarrow \pi$, $R_{P2,e}^{(-)} \rightarrow R_{P1}^{(-)}$, and in the $(+)$ case $\xi \rightarrow 0$, $R_{P2,e}^{(+)} \rightarrow R_{P1}^{(+)}$. The same result can be obtained by solving the Yang-Baxter equations. S_{PP} is also bijective in the physical strip.

The dimension of a boundary bound state multiplet created from the ground state in n steps will be 2^n irrespectively of the particular boundary fusion rules. The reflection

matrix factors on the boundary bound states are also free from physical strip poles for any values of the fusion angles. However, if some value of the boundary fusion angles occurs several times and we take into consideration the statistical properties of the particles, then the dimensions of the boundary bound state multiplets are modified. In particular, if all the boundary fusion angles are the same (see [24]), then the all excited boundary bound state multiplets are 2-dimensional. This is consistent with the multiplicities obtained by taking the zero bulk coupling limit of the boundary sinh-Gordon model.

The boundary condition for the real scalar field Φ of mass m considered in [24] is

$$\partial_x \Phi|_0 = -m\lambda\Phi ,$$

where λ is a coupling constant. The spectrum of boundary states consists of an infinite tower of states b_n , $n = 1, 2, \dots$, the boundary fusion rules are $P + b_n \rightarrow b_{n+1}$, and the fusion angle is independent of n (P denotes the bulk boson). In this case the dimension of the supersymmetric parts of the b_n -s is 2.

2.7.4 Boundary affine Toda field theories

As in [23], only $a_n^{(1)}$ Toda theory will be considered. The classical equation of motion for the n -component bosonic field ϕ of $a_n^{(1)}$ Toda theory is

$$\partial_t^2 \phi - \partial_x^2 \phi + \frac{m^2}{\beta} \sum_{i=0}^n \alpha_i e^{\beta \alpha_i \cdot \phi} = 0 . \quad (2.175)$$

The α_i , $i = 1, \dots, n$ are the simple roots of the Lie algebra $a_n = \mathfrak{sl}_{n+1}$ and α_0 is minus the highest root. The coupling constant β could be removed from the equations of motion by rescaling the field and therefore the coupling constant plays a role only in the quantum theory. We shall use the notation

$$B = \frac{1}{2\pi} \frac{\beta^2}{1 + \frac{\beta^2}{4\pi}} .$$

It was discovered [100, 101] that this equation of motion can be restricted to the left half-line $x < 0$ without losing integrability if one imposes a boundary condition at $x = 0$ of the form

$$\beta \partial_x \phi + \sum_{i=0}^n C_i \alpha_i e^{\beta \alpha_i \cdot \phi/2} \Big|_{x=0} = 0 , \quad (2.176)$$

where the boundary parameters C_i satisfy either

$$C_i = 0 , \quad (i = 0, 1, \dots, n) , \quad (2.177)$$

Table 2.4: Fusion rules of the boundary $a_2^{(1)}$ affine Toda field theory

| Initial state | Particle | Rapidity | Final state |
|----------------------|----------|--|----------------|
| $b_{n,m}$ | 1 | $i\frac{\pi}{6} - i\frac{\pi}{6}B(2n+1)$ | $b_{n+1,m}$ |
| $b_{n,m}$ | 2 | $i\frac{\pi}{6} - i\frac{\pi}{6}B(2m+1)$ | $b_{n,m+1}$ |
| $b_{-n,n}, 0 \leq n$ | 1 | $i\frac{\pi}{2} - i\frac{\pi}{6}B(2n+1)$ | $b_{-n-1,n+1}$ |
| $b_{n,-n}, 0 \leq n$ | 2 | $i\frac{\pi}{2} - i\frac{\pi}{6}B(2n+1)$ | $b_{n+1,-n-1}$ |

which is the Neumann boundary condition, or

$$C_i = \pm 1, \quad (i = 0, 1, \dots, n), \quad (2.178)$$

which will be denoted as the $(++\dots - \dots)$ boundary conditions.

Boundary $a_2^{(1)}$ affine Toda field theory

The bulk spectrum of this model contains two particles 1 and 2 of equal mass $m_1 = m_2$. Their fusion rules are $1 + 1 \rightarrow 2$ ($\pi/3$) and $2 + 2 \rightarrow 1$ ($\pi/3$). The anti-particle of 1 is 2. These rules are easily seen to be consistent with the decomposition (see (2.101)) consisting of a single term $\langle 1, 2 \rangle$ and with associating supersymmetric particle representation to $\langle 1, 2 \rangle$ with $\alpha = -1/(2M)$, $m_1 = m_2 = 2M \sin(\pi/3)$ [34]. The labeling set for the supersymmetric part of 1 and 2 denoted by W_{12} is $L[W_{12}(\Theta)] = \{\Theta - \frac{i\pi}{6}, \Theta + \frac{i\pi}{6}\}$. M is determined by β and m .

The boundary version of this model with any of the solitonic boundary conditions $(+--)$, $(-+-)$ or $(-+)$ contains the boundary states $b_{n,m}$ for all $n, m \in \mathbb{Z}$, $n+m \geq 0$, $-\frac{1}{2B} - \frac{1}{2} < n, m < \frac{1}{2B} + \frac{1}{2}$, and the states $b_{-n,n}$ and $b_{n,-n}$ for all $n \in \mathbb{Z}$, $0 \leq \frac{3}{2B} + \frac{1}{2}$, as described in [23]. We consider only generic values of B and only the domain $0 < B < 1$, as in [23]. $b_{0,0}$ is the ground state. The fusion rules are shown in Table 2.4.

The decomposition (2.108) is $\oplus_{n,m} \langle b_{n,m}, b_{m,n} \rangle$, where $n \geq m$. The supersymmetric part associated to $\langle b_{n,m}, b_{m,n} \rangle$ is denoted by $W_{n,m}$. We assume, for the sake of simplicity, that the cases 1 and 3 of Section 2.6.6 apply. It is straightforward to verify that the fusion rules above imply that the labeling sets $L[W_{n,m}]$ are the following:

$$L[W_{n,m}] = Abs\{i(\frac{\pi}{3} - \frac{\pi}{6}B(2j+1)), i(\frac{\pi}{6}B(2j+1)), i(\frac{\pi}{3} - \frac{\pi}{6}B(2l+1)), i(\frac{\pi}{6}B(2l+1)) \mid j = 0 \dots n-1, l = 0 \dots m-1\} \quad \text{if } n, m \geq 0, \quad (2.179)$$

$$L[W_{n,-n}] = Abs\{i(\frac{2\pi}{3} - \frac{\pi}{6}B(2j+1)), i(\frac{\pi}{3} - \frac{\pi}{6}B(2j+1)) \mid j = 0 \dots n-1\} \quad (2.180)$$

$$L[W_{n,m}] = \text{Abs}\{i(\frac{2\pi}{3} - \frac{\pi}{6}B(2j+1)), i(\frac{\pi}{3} - \frac{\pi}{6}B(2l+1)), i(\frac{\pi}{6}B(2r+1)) \mid j = 0 \dots (-m-1), \\ l = 0 \dots n-1, r = (-m) \dots n-1\} \quad \text{if } m < 0, \quad (2.181)$$

where $\text{Abs}(ix) = i|x|$ if $x \in \mathbb{R}$, and the limit for the running variables given on the left-hand side of the dots is always assumed to be lower than or equal to the limit given on the right-hand side, if this condition is not satisfied, then the set of allowed values is empty. These conventions apply below as well. The dimension of $W_{n,m}$ is 2^{n+m} if $n, m \geq 0$ and 2^n if $m < 0$, provided that there is no coincidence between $\pi - \xi$ and the rapidities above. $\pi - \rho_{\max}/2 = 5\pi/6$, so condition (2.149) is satisfied and the supersymmetric reflection matrix factors do not have poles on the imaginary axis in the physical strip.

Boundary $a_4^{(1)}$ affine Toda field theory

The bulk spectrum of this model contains four particles 1, 2, 3, 4 of mass $m_1 = m_4 = 2M \sin(\pi/5)$, $m_2 = m_3 = 2M \sin(2\pi/5)$. The fusion rules are $a + b \rightarrow c$, where either $c = a + b$ or $c = a + b - 5$. The corresponding fusion angles are $\frac{\pi}{5}(a + b)$ if $c = a + b$ and $\frac{\pi}{5}(10 - a - b)$ if $c = a + b - 5$. The anti-particle of 1 and 2 is 4 and 3. These rules are easily seen to be consistent with the decomposition (see (2.101)) $\langle 1, 4 \rangle \oplus \langle 2, 3 \rangle$ and with associating supersymmetric particle representations to $\langle 1, 4 \rangle$ and $\langle 2, 3 \rangle$ with $\alpha = -1/(2M)$ [34]. The labeling sets corresponding to the supersymmetric parts of $\langle 1, 4 \rangle$ and $\langle 2, 3 \rangle$ denoted by W_{14} and W_{23} are $L[W_{14}(\Theta)] = \{\Theta - i\frac{3\pi}{10}, \Theta + i\frac{3\pi}{10}\}$, $L[W_{23}(\Theta)] = \{\Theta - i\frac{\pi}{10}, \Theta + i\frac{\pi}{10}\}$.

The boundary version of this model described in [23] has two classes of inequivalent solitonic boundary conditions to which different boundary spectra belong. The first class contains the boundary conditions $(- + + + -)$, $(+ + + - -)$, $(+ + - - +)$, $(- - + + +)$ and $(+ - - + +)$, the second class contains the boundary conditions $(- + + - +)$, $(- + - + +)$, $(+ + - + -)$, $(- + - - -)$, $(+ - + + -)$, $(+ - + - +)$, $(- - + - -)$, $(- - - + -)$, $(- - - - +)$ and $(+ - - - -)$.

If the boundary condition belongs to the first class, then there are the boundary states b_{n_2, n_3} , $n_2, n_3 \in \mathbb{Z}$, $n_2 + n_3 \geq 0$, $-\frac{1}{2B} - \frac{1}{2} < n_2, n_3 < \frac{1}{2B} + \frac{1}{2}$, and $b_{n, -n}$ and $b_{-n, n}$ for all $n \in \mathbb{Z}$, $0 \leq n < \frac{5}{2B} + \frac{1}{2}$, where B is a parameter of the bulk model. Generic values of B are considered in the domain $0 < B < 1$. The fusion rules, which are analogous to those of the $a_2^{(1)}$ model, are listed in Table 2.5.

The decomposition (2.108) is $\oplus_{n_2, n_3} \langle b_{n_2, n_3}, b_{n_3, n_2} \rangle$, where $n_2 \geq n_3$. The supersymmetric part associated to $\langle b_{n_2, n_3}, b_{n_3, n_2} \rangle$ is denoted by W_{n_2, n_3} . Again, we assume for the sake of

Table 2.5: Fusion rules of the $a_4^{(1)}$ affine Toda field theory with first class boundary conditions

| Initial state | Particle | Rapidity | Final state |
|-----------------------|----------|--|------------------|
| b_{n_2, n_3} | 2 | $i\frac{\pi}{10} - i\frac{\pi}{10}B(2n_2 + 1)$ | b_{n_2+1, n_3} |
| b_{n_2, n_3} | 3 | $i\frac{\pi}{10} - i\frac{\pi}{10}B(2n_3 + 1)$ | b_{n_2, n_3+1} |
| $b_{-n, n}, 0 \leq n$ | 1 | $i\frac{\pi}{2} - i\frac{\pi}{10}B(2n + 1)$ | $b_{-n-1, n+1}$ |
| $b_{n, -n}, 0 \leq n$ | 4 | $i\frac{\pi}{2} - i\frac{\pi}{10}B(2n + 1)$ | $b_{n+1, -n-1}$ |

simplicity that the cases 1 and 3 of Section 2.6.6 apply. We have

$$L[W_{n_2, n_3}] = Abs\{i(\frac{\pi}{5} - \frac{\pi}{10}B(2j + 1)), i(\frac{\pi}{10}B(2j + 1)), i(\frac{\pi}{5} - \frac{\pi}{10}B(2l + 1)), i(\frac{\pi}{10}B(2l + 1)) | j = 0 \dots n_2 - 1, l = 0 \dots n_3 - 1\} \quad \text{if } n_2, n_3 \geq 0, \quad (2.182)$$

$$L[W_{n, -n}] = Abs\{i(\frac{4\pi}{5} - \frac{\pi}{10}B(2j + 1)), i(\frac{\pi}{5} - \frac{\pi}{10}B(2j + 1)) | j = 0 \dots n - 1\}, \quad (2.183)$$

$$L[W_{n_2, n_3}] = Abs\{i(\frac{4\pi}{5} - \frac{\pi}{10}B(2j + 1)), i(\frac{\pi}{5} - \frac{\pi}{10}B(2l + 1)), i(\frac{\pi}{10}B(2r + 1)) | j = 0 \dots (-n_3 - 1), l = 0 \dots n_2 - 1, r = -n_3 \dots n_2 - 1\} \quad \text{if } n_3 < 0. \quad (2.184)$$

The dimension of W_{n_2, n_3} is $2^{n_2+n_3}$ if $n_2, n_3 \geq 0$ and 2^{n_2} if $n_3 < 0$, provided that there is no coincidence between $i(\pi - \xi)$ and the rapidities above.

If B is sufficiently small, then $W_{1, -1}, W_{2, -2}, \dots$ violate condition (2.149), so the supersymmetric factor of the reflection matrix of particle 1 on these states have poles on the imaginary axis in the physical strip.

If the boundary condition belongs to the second class, then there are the boundary states b_{n_1, n_2, n_3, n_4} , $n_1, n_2, n_3, n_4 \in \mathbb{Z}$, $n_1 + n_2 \geq 0$, $n_2 + n_3 \geq 0$, $n_3 + n_4 \geq 0$. The ground state is $b_{0,0,0,0}$. The fusion rules are listed in Table 2.6.

The decomposition (2.108) is $\oplus_{n_1, n_2, n_3, n_4} \langle b_{n_1, n_2, n_3, n_4}, b_{n_4, n_2, n_3, n_1}, b_{n_1, n_3, n_2, n_4}, b_{n_4, n_3, n_2, n_1} \rangle$, where $n_1 \leq n_4$, $n_2 \geq n_3$, and $b_{k, l, m, n} = 0$ if the condition $k + l \geq 0$ and $l + m \geq 0$ and $m + n \geq 0$ is not satisfied. The supersymmetric part associated to b_{n_1, n_2, n_3, n_4} is denoted by W_{n_1, n_2, n_3, n_4} . Assuming, for the sake of simplicity, that the cases 1 and 3 of Section 2.6.6 apply, using our rules we get

$$L[W_{n_1, n_2, n_3, n_4}] = Abs\{i(\frac{2\pi}{5} - \frac{\pi}{10}B(2l_1 + 1)), i(\frac{\pi}{5} + \frac{\pi}{10}B(2l_1 + 1)), i(\frac{2\pi}{5} - \frac{\pi}{10}B(2l_4 + 1)), i(\frac{\pi}{5} + \frac{\pi}{10}B(2l_4 + 1)), i(\frac{\pi}{5} - \frac{\pi}{10}B(2l_2 + 1)), i(\frac{\pi}{10}B(2l_2 + 1)), i(\frac{\pi}{5} - \frac{\pi}{10}B(2l_3 + 1)), i(\frac{\pi}{10}B(2l_3 + 1)) | l_i = 0 \dots n_i - 1\} \quad \text{if } n_1, n_2, n_3, n_4 \geq 0, \quad (2.185)$$

Table 2.6: Fusion rules of the $a_4^{(1)}$ affine Toda field theory with second class boundary conditions

| Initial state | Particle | Rapidity | Final state |
|---------------------------------------|----------|---|-------------------------------|
| b_{n_1, n_2, n_3, n_4} | 1 | $i\frac{\pi}{10} - i\frac{\pi}{10}B(2n_1 + 1)$ | b_{n_1+1, n_2, n_3, n_4} |
| b_{n_1, n_2, n_3, n_4} | 2 | $i\frac{\pi}{10} - i\frac{\pi}{10}B(2n_2 + 1)$ | b_{n_1, n_2+1, n_3, n_4} |
| b_{n_1, n_2, n_3, n_4} | 3 | $i\frac{\pi}{10} - i\frac{\pi}{10}B(2n_3 + 1)$ | b_{n_1, n_2, n_3+1, n_4} |
| b_{n_1, n_2, n_3, n_4} | 4 | $i\frac{\pi}{10} - i\frac{\pi}{10}B(2n_4 + 1)$ | b_{n_1, n_2, n_3, n_4+1} |
| $b_{-n_2, n_2, n_3, n_4}, 0 \leq n_2$ | 1 | $i\frac{3\pi}{10} - i\frac{\pi}{10}B(2n_2 + 1)$ | $b_{-n_2-1, n_2+1, n_3, n_4}$ |
| $b_{n_1, n_2, n_3, -n_3}, 0 \leq n_3$ | 4 | $i\frac{3\pi}{10} - i\frac{\pi}{10}B(2n_3 + 1)$ | $b_{n_1, n_2, n_3+1, n_3-1}$ |

$$\begin{aligned}
L[W_{n_1, n_2, n_3, n_4}] = Abs\{ & i(\frac{\pi}{5} - \frac{\pi}{10}B(2l_3 + 1)), i(\frac{\pi}{10}B(2l_3 + 1)), i(\frac{2\pi}{5} - \frac{\pi}{10}B(2l_4 + 1)), \\
& i(\frac{\pi}{5} + \frac{\pi}{10}B(2l_4 + 1)), i(\frac{6\pi}{10} - \frac{\pi}{10}B(2j_1 + 1)), i(\frac{\pi}{10}B(2j_2 + 1)), \\
& i(\frac{\pi}{5} - \frac{\pi}{10}B(2j_3 + 1)) \mid l_3 = 0 \dots n_3 - 1, l_4 = 0 \dots n_4 - 1, j_2 = 0 \dots n_2 - 1, \\
& j_1 = 0 \dots (-n_1 - 1), j_3 = -n_1 \dots n_2 - 1\} \quad \text{if } n_3, n_4, n_2 \geq 0, n_1 < 0, \quad (2.186)
\end{aligned}$$

$$\begin{aligned}
L[W_{n_1, n_2, n_3, n_4}] = Abs\{ & i\frac{\pi}{10}B(2l_1 + 1), i(\frac{6\pi}{10} - \frac{\pi}{10}B(2l_1 + 1)), i\frac{\pi}{10}B(2l_4 + 1), \\
& i(\frac{6\pi}{10} - \frac{\pi}{10}B(2l_4 + 1)), i(\frac{\pi}{5} - \frac{\pi}{10}B(2l_2 + 1)), i\frac{\pi}{10}B(2l_2 + 1), \\
& i(\frac{\pi}{5} - \frac{\pi}{10}B(2l_2 + 1)), i\frac{\pi}{10}B(2l_2 + 1) \mid l_1 = 0 \dots (-n_1 - 1), l_4 = 0 \dots (-n_4 - 1), \\
& l_2 = -n_1 \dots n_2 - 1, l_3 = -n_4 \dots n_3 - 1\} \quad \text{if } n_1, n_4 < 0. \quad (2.187)
\end{aligned}$$

The dimension of W_{n_1, n_2, n_3, n_4} is $2^{n_1+n_2+n_3+n_4}$ if $n_1, n_2, n_3, n_4 \geq 0$, $2^{n_2+n_3+n_4}$ if $n_1 < 0$, $n_2, n_3, n_4 \geq 0$ and $2^{n_2+n_3}$ if $n_1, n_4 < 0$ provided that there is no coincidence between $\pi - \xi$ and the rapidities above. Condition (2.149) is satisfied in this case, so the supersymmetric factors of the reflection matrix blocks do not have poles on the imaginary axis in the physical strip.

2.8 Discussion

We studied the boundary supersymmetric bootstrap programme in a special framework in which the blocks of the full two-particle S-matrix and the blocks of the full one-particle reflection matrix take a factorized form. We assumed that the ground state is a singlet with RSOS label $\frac{1}{2}$ and the bulk particles transform in the kink and boson-fermion representations.

We introduced the boundary supersymmetry algebra in the framework proposed by [49, 48], which requires that the boundary supersymmetry algebra be a co-ideal of the bulk supersymmetry algebra. It is a remarkable feature of the boundary supersymmetry algebra that it admits essentially two possible boundary co-multiplications — the corresponding two cases are denoted by $(+)$ and $(-)$. The two co-multiplications lead to different supersymmetric ground state reflection matrix factors. We found that these factors are essentially the same as those given in [38, 39, 40]. Although the two co-multiplications appear to play symmetric role algebraically, the corresponding kink reflection matrix factors turn out to be significantly different. A further important difference between the two cases is that in the $(+)$ case the boson-fermion reflection matrix factor can be obtained by bootstrap from the kink reflection matrix factor only at special values of its parameters [39]. We also found that the kink and boson-fermion reflection factors can be degenerate at particular rapidities depending on a parameter γ of the ground state representation.

We presented supersymmetric boundary fusion rules by which the representations and reflection matrix factors for excited boundary bound states can be easily determined in specific models. The main difficulty of the problem of finding such rules is to handle the degeneracies of the boundary fusion tensors that occur at particular rapidities (resulting from the degeneracies of the one-particle reflection matrix factors). These degeneracies are closely related to the degeneracies of the bulk two-particle S-matrix factors and of the ground state one-particle reflection matrix factors. We found that the boundary fusion rules are analogous to the bulk rules of [34, 30], and that it is useful to characterize the boson-fermion multiplets by their constituent kinks. The kink representation appears to be an elementary object.

For the sake of simplicity we assumed that the two-particle S-matrix factors and ground state reflection matrix factors have no poles and overall zeroes on the imaginary axis in the physical strip and there is no interplay between the poles and zeroes of the supersymmetric and non-supersymmetric factors of the S-matrix and reflection matrix. We found, regarding the boundary part, that the main restriction on the applicability of the described framework follows from this condition.

We applied our rules to the sine-Gordon model, to the $a_2^{(1)}$ and $a_4^{(1)}$ affine Toda field theories, to the free particle and to the sinh-Gordon model. We found that in the case of the $a_4^{(1)}$ model with first class boundary condition the supersymmetric reflection matrix factors on some excited boundary states have poles in the physical strip.

It is a further problem to consider the axioms in 10) of Section 2.2. Initial steps in this direction were made in [35]. The possible Coleman-Thun diagrams could be considered as well, although we think that it is less likely that they yield further constraints. Writing

down formulae for the fusion and decay tensors is also a task for the future.

At the present stage it is an open problem to tell how large class of non-supersymmetric theories can be supersymmetrized under the assumption that the bulk particles transform in the kink and boson-fermion representation and the ground state is a singlet with label $1/2$, and, generally, how uniquely supersymmetric theories are characterized by the one-particle representations and the ground state representation occurring in them.

In general, representations beyond the kink and boson-fermion for the bulk particles and other (possibly non-singlet) ground state representations are also relevant to some models. We think that at least two lessons can be learned from our investigation which are relevant for cases with other representations: the first one is that the degeneracy properties of the supersymmetric ground state reflection matrix factor and the supersymmetric two-particle S-matrix factor have very important role in the fusion rules, the second one is that one should find ‘elementary’ representations for which the mentioned degeneracies show a simple pattern and from which one can build the other representations of interest by multiplication.

2.9 Appendix

$$G^{[i,j]}(\Theta) = R^{[i,j]}(\Theta)R^{[i,j]}(\pi i - \Theta)$$

$$R^{[i,j]}(\Theta) = \frac{1}{\Gamma(\frac{\Theta}{2\pi i})\Gamma(\frac{\Theta}{2\pi i} + \frac{1}{2})} \prod_{k=1}^{\infty} \frac{\Gamma(\frac{\Theta}{2\pi i} + \Delta_1 + k + 1)\Gamma(\frac{\Theta}{2\pi i} - \Delta_1 + k)}{\Gamma(\frac{\Theta}{2\pi i} + \Delta_1 + k - \frac{1}{2})\Gamma(\frac{\Theta}{2\pi i} - \Delta_1 + k + \frac{1}{2})} \times \\ \times \frac{\Gamma(\frac{\Theta}{2\pi i} + \Delta_2 + k - \frac{1}{2})\Gamma(\frac{\Theta}{2\pi i} - \Delta_2 + k - \frac{1}{2})}{\Gamma(\frac{\Theta}{2\pi i} + \Delta_2 + k)\Gamma(\frac{\Theta}{2\pi i} - \Delta_2 + k)},$$

where $\Delta_1 = (u_i + u_j)/(2\pi)$, $\Delta_2 = (u_i - u_j)/(2\pi)$.

$$K(\Theta) = \frac{1}{\sqrt{\pi}} \prod_{k=1}^{\infty} \frac{\Gamma(k - \frac{1}{2} + \frac{\Theta}{2\pi i})\Gamma(k - \frac{\Theta}{2\pi i})}{\Gamma(k + \frac{1}{2} - \frac{\Theta}{2\pi i})\Gamma(k + \frac{\Theta}{2\pi i})}$$

$$P(\Theta) = \prod_{k=1}^{\infty} \left[\frac{\Gamma(k - \frac{\Theta}{2\pi i})^2}{\Gamma(k - \frac{1}{4} - \frac{\Theta}{2\pi i})\Gamma(k + \frac{1}{4} - \frac{\Theta}{2\pi i})} \right] / \{\Theta \leftrightarrow -\Theta\}$$

$$ZX^{(+)}(\Theta) = \sqrt{m}P(\Theta + i\rho/2)P(\Theta - i\rho/2)\sqrt{2}K(2\Theta)2^{-\Theta/(i\pi)},$$

where $m = 2M \cos(\frac{\rho}{2})$, $0 \leq \rho < \pi$, $M = -1/\alpha$.

$$\begin{aligned}\tilde{Z}^{(-)}(\Theta) &= K(2\Theta)2^{-\Theta/(i\pi)}F(\Theta - i\rho/2)F(\Theta + i\rho/2) \\ F(\Theta) &= P(\Theta)K(\Theta + i\xi)K(\Theta - i\xi) ,\end{aligned}$$

where $\gamma = -2\sqrt{M}\cos\frac{\xi}{2}$.

$$ZX^{(-)}(\Theta) = \sqrt{m}\tilde{Z}^{(-)}(\Theta)\frac{1}{\sqrt{2}}(\cos(\rho/2) - \cosh(\Theta)) ,$$

where $\xi = \pi$.

$$\begin{aligned}\tilde{Z}^{(+)}(\Theta) &= iK(2\Theta)2^{-\Theta/(i\pi)}F(\Theta - i\rho/2)F(\Theta + i\rho/2)U(\Theta) \\ F(\Theta) &= P(\Theta)K(\Theta + i\xi)K(\Theta - i\xi) ,\end{aligned}$$

where $\gamma = -2\sqrt{M}i\sin(\xi/2)$,

$$\begin{aligned}U(\Theta) &= f(\Theta)/f(-\Theta) \\ \frac{U(i\Theta)}{U(i\Theta - i\pi)} &= -\frac{\cos(\Theta) - \cos(\rho/2)}{\cos(\Theta) + \cos(\rho/2)}\end{aligned}$$

$$f(\Theta) = \prod_{k=1}^{\infty} \frac{\Gamma(\frac{\rho}{4\pi} - \frac{\Theta}{2\pi i} - \frac{1}{2} + k)\Gamma(\frac{\rho}{4\pi} + \frac{\Theta}{2\pi i} + k)\Gamma(-\frac{\rho}{4\pi} - \frac{\Theta}{2\pi i} - \frac{1}{2} + k)\Gamma(-\frac{\rho}{4\pi} + \frac{\Theta}{2\pi i} + k)}{\Gamma(\frac{\rho}{4\pi} - \frac{\Theta}{2\pi i} + k)\Gamma(\frac{\rho}{4\pi} + \frac{\Theta}{2\pi i} + \frac{1}{2} + k)\Gamma(-\frac{\rho}{4\pi} - \frac{\Theta}{2\pi i} + k)\Gamma(-\frac{\rho}{4\pi} + \frac{\Theta}{2\pi i} + \frac{1}{2} + k)} .$$

Chapter 3

Truncation effects in the boundary flows of the Ising model on a strip

3.1 On the definition of field theories on the strip

By quantum field theory on the strip $[0, L] \times \mathbb{R}$ we generally mean a collection of the following elements: a Hilbert space \mathcal{H}_B of states, a Hamiltonian operator H_B acting on the Hilbert space, a set of fields $\Phi_B(x, t)$ which satisfy the time evolution equation

$$\Phi_B(x, t) = \exp(iH_B t) \Phi_B(x, 0) \exp(-iH_B t) , \quad (3.1)$$

a set of fields $\phi_B(t, 0)$ defined on the left boundary $\{0\} \times \mathbb{R}$ which satisfy the time evolution equation

$$\phi_B(0, t) = \exp(iH_B t) \phi_B(0, 0) \exp(-iH_B t) \quad (3.2)$$

and a set of fields $\phi_B(t, L)$ defined on the right boundary $\{L\} \times \mathbb{R}$ which satisfy the time evolution equation

$$\phi_B(L, t) = \exp(iH_B t) \phi_B(L, 0) \exp(-iH_B t) . \quad (3.3)$$

The factor $[0, L]$ in $[0, L] \times \mathbb{R}$ represents the space, \mathbb{R} represents the time. Fields defined on one of the boundaries only are often called boundary fields. We assume that the strip $[0, L] \times \mathbb{R}$ is equipped with Minkowski metric.

New boundary theories can be obtained from old ones by perturbing the Hamiltonian operator:

$$\hat{H}_B = H_B + H_{I,B} , \quad (3.4)$$

where the perturbation $H_{I,B}$ is often a sum of various kinds of terms. A bulk term in the

perturbation takes the form

$$H_{I,B} = g_1 \int_0^L dx \Psi_B(x, 0) , \quad (3.5)$$

a boundary perturbation takes the form

$$H_{I,B} = g_2 \psi_B(L, 0) \quad \text{or} \quad H_{I,B} = g_3 \psi_B(0, 0) , \quad (3.6)$$

where $\Psi_B(x, t)$, $\psi_B(L, t)$ and $\psi_B(0, t)$ are certain fields of the unperturbed theory and g_1, g_2, g_3 are coupling constants.

The fields of the perturbed theory, which are distinguished by a hat, are defined by the equations

$$\hat{\Phi}_B(x, t) = \exp(i\hat{H}_B t) \Phi_B(x, 0) \exp(-i\hat{H}_B t) \quad (3.7)$$

$$\hat{\phi}_B(0, t) = \exp(i\hat{H}_B t) \phi_B(0, 0) \exp(-i\hat{H}_B t) \quad (3.8)$$

$$\hat{\phi}_B(L, t) = \exp(i\hat{H}_B t) \phi_B(L, 0) \exp(-i\hat{H}_B t) . \quad (3.9)$$

In particular,

$$\hat{\Phi}_B(x, 0) = \Phi_B(x, 0) , \quad \hat{\phi}_B(0, 0) = \phi_B(0, 0) , \quad \hat{\phi}_B(L, 0) = \phi_B(L, 0) . \quad (3.10)$$

The calculations of Section 3.5 are done in this perturbed Hamiltonian operator framework.

We remark that to define a quantum (and classical) field theory on a strip it is usual in the literature to take a classical Lagrangian function of the form

$$\mathcal{L} = \int_0^L \mathcal{L}_{bulk}(x) dx + \mathcal{L}_{b,1}(x=0) + \mathcal{L}_{b,2}(x=L) , \quad (3.11)$$

which contains a bulk term and boundary terms (the notation of the dependence of \mathcal{L}_{bulk} , $\mathcal{L}_{b,1}$ and $\mathcal{L}_{b,2}$ on the fields is suppressed). The classical equations of motion are derived from (3.11) via a variational principle. These equations of motion usually consist of bulk partial differential equations and certain boundary conditions. Finally a quantization is carried out (see for example [19, 66, 17]).

It is also possible to remain in the framework of the standard Lagrangian formalism without boundaries on the full Minkowski space, in this case the presence of boundaries is taken into consideration in the Lagrangian function by step functions and Dirac-deltas (see [102]). One can also start with a classical Hamiltonian function (see e.g. [103, 104]) instead of a Lagrangian function.

Boundary conditions usually play an important role in the literature in the definition of boundary field theories.

We remark finally that as far as we know, a complete, systematic and definitive discussion of the definition and basic formalism of classical and quantum field theory with boundaries cannot be found in the literature.

3.2 Unitary representations of the Virasoro algebra

The Virasoro algebra with central charge c is generated by the elements L_n , $n \in \mathbb{Z}$ and the identity element I and the relations

$$[L_n, L_m] = (n - m)L_{n+m} + \frac{c}{12}(n^3 - n)\delta_{n+m,0}I . \quad (3.12)$$

A unitary highest weight representation is characterized by the following properties: there exists a unitary highest weight vector $|h\rangle$ which satisfies the relations

$$L_n|h\rangle = 0 \quad \forall n > 0 \quad (3.13)$$

$$L_0|h\rangle = h|h\rangle , \quad (3.14)$$

and the scalar product is related to the generators by the following relation:

$$L_n^\dagger = L_{-n} . \quad (3.15)$$

A highest weight unitary representation $M(c, h)$ is uniquely specified by the numbers c and h . h is called the weight of the representation. The positive definiteness of the scalar product and the above requirements do not permit any values for (c, h) . For $0 \leq c < 1$ only the following discrete set is allowed:

$$c(m) = 1 - \frac{6}{m(m+1)} \quad (3.16)$$

$$h_{p,q}(m) = \frac{[(m+1)p - mq]^2 - 1}{4m(m+1)} \quad (3.17)$$

where m, p, q are integers, $m = 2, 3, 4, 5, 6, \dots$, $1 \leq p < m$, $1 \leq q < m+1$. The pair of numbers (p, q) is called Kac-label. Each weight appears twice since $h(p, q) = h(m-p, m+1-q)$.

We restrict to conformal field theories the Hilbert space of which is a finite sum $\mathcal{H} = \oplus_i M(c, h_i)$, where (c, h_i) belongs to the above discrete series.

A construction for these representations is the following: we take a vector $|h\rangle$ with the properties $\langle h|h\rangle = 1$, (3.13), (3.14), and we take the vectors

$$L_{-n_1} L_{-n_2} \dots L_{-n_k} |h\rangle \quad n_1 \geq n_2 \geq \dots \geq n_k > 0 \quad (3.18)$$

which are assumed to be linearly independent. These vectors (including $|h\rangle$) form a basis of a representation $V(c, h)$ of the Virasoro algebra. They are also eigenvectors of L_0 with eigenvalue

$$h + n_1 + n_2 + \cdots + n_k . \quad (3.19)$$

We say that the level of the vector $L_{-n_1}L_{-n_2}\cdots L_{-n_k}|h\rangle$ is $n_1 + n_2 + \cdots + n_k$. The space spanned by the eigenvectors of level i is denoted by $V_i(c, h)$. $V(c, h)$ can be written as

$$V(c, h) = \oplus_{i=0}^{\infty} V_i(c, h) . \quad (3.20)$$

A unique scalar product is determined on the representation $V(c, h)$ by (3.13), (3.14), (3.15) and (3.12), in particular the scalar product of any two basis vectors can be calculated recursively using these formulae. The strategy for this calculation is to use the commutation relations (3.12) to move L -s with positive index to the right and L -s with negative index to the left. This scalar product is not guaranteed to be positive definite for general values of (c, h) . For the above discrete values of (c, h) it is positive semidefinite, there is a unique maximal subspace $V^{null}(c, h)$ which is orthogonal to the whole $V(c, h)$. $V^{null}(c, h)$ decomposes as

$$V^{null}(c, h) = \oplus_{i=0}^{\infty} V_i^{null}(c, h) \quad (3.21)$$

where $V_i^{null}(c, h) = 0$ may hold for some values of i . The unitary irreducible representation $M(c, h)$ is obtained by quotienting out $V^{null}(c, h)$,

$$M(c, h) = V(c, h)/V^{null}(c, h) = \oplus_{i=0}^{\infty} (V_i(c, h)/V_i^{null}(c, h)) . \quad (3.22)$$

The corresponding projection is denoted by $q : V(c, h) \rightarrow M(c, h)$. The scalar product on $M(c, h)$ is defined in the standard way, i.e. by the requirement that $\langle v|w\rangle = \langle q(v)|q(w)\rangle$.

3.2.1 Primary fields

A (chiral) Virasoro primary field of weight l is a field $\Phi(z)$, $z \in \mathbb{C}$ that satisfies the property

$$[L_m, \Phi(z)] = l(m+1)z^m\Phi(z) + z^{m+1}\frac{\partial\Phi}{\partial z}(z) . \quad (3.23)$$

The matrix elements of a primary field satisfy the relation

$$\langle A|\Phi(z)|B\rangle = \frac{\langle A|\Phi(1)|B\rangle}{z^{l+h_B-h_A}} , \quad (3.24)$$

where l is the weight of $\Phi(z)$, $|A\rangle$ and $|B\rangle$ are eigenvectors of L_0 with eigenvalues h_A , h_B .

Equations (3.13), (3.14), (3.15), (3.12), (3.23), (3.24) determine $\frac{\langle A|\Phi(1)|B\rangle}{\langle h_1|\Phi(1)|h_2\rangle}$ uniquely, where $|A\rangle$, $|B\rangle$ are vectors of the form (3.18) with h_1 and h_2 , respectively. It is assumed

here that $\langle h_1|\Phi(1)|h_2\rangle \neq 0$, if $\langle h_1|\Phi(1)|h_2\rangle = 0$, then $\langle A|\Phi(1)|B\rangle = 0 \forall |A\rangle \in V(c, h_1)$, $|B\rangle \in V(c, h_2)$. $\frac{\langle A|\Phi(1)|B\rangle}{\langle h_1|\Phi(1)|h_2\rangle}$ can be calculated recursively using the equations (3.13), (3.14), (3.15), (3.12), (3.23), (3.24), the strategy of the calculation being again to use (3.12) and (3.23) to move L -s with positive index to the right and L -s with negative index to the left.

Although the matrix elements $\frac{\langle A|\Phi(1)|B\rangle}{\langle h_1|\Phi(1)|h_2\rangle}$, where $|A\rangle \in V(c, h_1)$, $|B\rangle \in V(c, h_2)$, are determined uniquely, they determine the matrix elements $\frac{\langle q(A)|\Phi(1)|q(B)\rangle}{\langle h_1|\Phi(1)|h_2\rangle}$ unambiguously only if $\langle A|\Phi(1)|B\rangle = 0$ whenever $|A\rangle \in V^{null}(c, h_1)$ or $|B\rangle \in V^{null}(c, h_2)$. This condition restricts the value of l if c, h_1, h_2 are fixed. If l has other value, then $\langle A|\Phi(1)|B\rangle = 0 \forall |A\rangle \in M(c, h_1)$ and $|B\rangle \in M(c, h_2)$.

The permitted values of l are given by the Verlinde fusion rule. If $h_1 = h_{r,s}(m)$ and $h_2 = h_{p,n}(m)$, then the permitted values are $h_{k,j}(m)$, where the numbers k and j take the values given by the following equations:

$$k = 1 + |r - p| \dots k_{max}, \quad k + r + p = 1 \mod 2 \quad (3.25)$$

$$j = 1 + |s - n| \dots j_{max}, \quad j + s + n = 1 \mod 2 \quad (3.26)$$

$$k_{max} = \min(r + p - 1, 2m - 1 - r - p) \quad (3.27)$$

$$j_{max} = \min(s + n - 1, 2m + 1 - s - n) . \quad (3.28)$$

It is usual to write the Verlinde fusion rules as

$$h_a(m) \times h_b(m) = \sum_c n_{ab}^c h_c(m), \quad (3.29)$$

where the Verlinde fusion numbers n_{ab}^c are either 0 or 1; a, b, c stand for Kac labels, e.g. $a = (r, s)$, $b = (p, n)$, $c = (k, j)$. The summation is done over the possible Kac labels modulo the relation $(p, q) \sim (m - p, m + 1 - q)$. The values of c for which n_{ab}^c is 1 are determined by (3.25)-(3.28).

We refer the reader to the literature on conformal field theory (e.g. [73]) for the description of descendant fields.

3.2.2 $c=1/2$

The value of the central charge that is relevant for the model (1.2) is $c = 1/2$, this corresponds to $m = 3$. The values of the weights $h_{p,q}(3)$ are

$$h_{1,1}(3) = 0 \quad h_{1,2}(3) = 1/16 \quad h_{1,3}(3) = 1/2 \quad (3.30)$$

$$h_{2,1}(3) = 1/2 \quad h_{2,2}(3) = 1/16 \quad h_{2,3}(3) = 0, \quad (3.31)$$

Table 3.1: Dimensions of levels of $c = 1/2$ unitary representations of the Virasoro algebra

| | Level | 0 | 1 | 2 | 3 | 4 | 5 | 6 | 7 | 8 | 9 | 10 | 11 | 12 | 13 | 14 | 15 |
|------------|-----------|---|---|---|---|---|---|---|---|---|---|----|----|----|----|----|----|
| $h = 0$ | dimension | 1 | 0 | 1 | 1 | 2 | 2 | 3 | 3 | 5 | 5 | 7 | 8 | 11 | 12 | 16 | 18 |
| $h = 1/2$ | dimension | 1 | 1 | 1 | 1 | 2 | 2 | 3 | 4 | 5 | 6 | 8 | 9 | 12 | 14 | 17 | 20 |
| $h = 1/16$ | dimension | 1 | 1 | 1 | 2 | 2 | 3 | 4 | 5 | 6 | 8 | 10 | 12 | 15 | 18 | 22 | 27 |

i.e. there are three different unitary highest weight representations of the Virasoro algebra, the weights of these representations are $0, 1/2, 1/16$. The dimensions of the subspaces of definite level of these representations are listed in Table 3.1 (taken from [46]) up to level 15.

The fusion rule (3.25)-(3.28) written in the usual form is

$$0 \times 0 = 0 \quad 0 \times 1/2 = 1/2 \quad 0 \times 1/16 = 1/16 \quad (3.32)$$

$$1/2 \times 1/2 = 0 \quad 1/2 \times 1/16 = 1/16 \quad 1/16 \times 1/16 = 0 + 1/2 \quad (3.33)$$

in this case.

3.3 Conformal field theory on the strip

In this section we discuss some basic properties of boundary conformal field theory on the strip $[0, L] \times \mathbb{R}$. We restrict to those elements which are necessary for our work.

The Hilbert space is a sum of irreducible unitary highest weight representations of the Virasoro algebra (3.12) with common central charge c . We restrict to the cases when the Hilbert space is a finite sum of the Virasoro algebra representations belonging to the unitary minimal series described in Section (3.2).

The Hamiltonian operator of the theory is $\frac{\pi}{L}L_0$, where L_0 is the L_0 element of the Virasoro algebra. A term proportional to the identity operator may also be added.

One can have right and left moving primary fields $\Phi_R(x, t)$, $\Phi_L(x, t)$ which depend only on $t - x$ or $t + x$, respectively, and satisfy the equations

$$[L_n, \Phi_R(x, t)] = D_n(l)\Phi_R(x, t) \quad (3.34)$$

$$[L_n, \Phi_L(x, t)] = \bar{D}_n(l)\Phi_L(x, t) . \quad (3.35)$$

l is the weight of these fields, and $D_n(l)$ and $\bar{D}_n(l)$ are operators on functions on the strip:

$$D_n(l) = \frac{-iL}{2\pi} e^{i\frac{n\pi}{L}(t-x)} \partial_- + l n e^{i\frac{n\pi}{L}(t-x)} \quad (3.36)$$

$$\bar{D}_n(l) = \frac{-iL}{2\pi} e^{i\frac{n\pi}{L}(t+x)} \partial_+ + l n e^{i\frac{n\pi}{L}(t+x)} , \quad (3.37)$$

where $\partial_- = \partial_t - \partial_x$, $\partial_+ = \partial_t + \partial_x$.

A boundary primary field of weight l on the left boundary is a field $\Phi_B(0, t)$ that is defined on the left boundary and satisfies

$$[L_n, \Phi_B(0, t)] = D_n^0(l) \Phi_B(0, t) = \left[\frac{-iL}{\pi} e^{i\frac{n\pi}{L}t} \partial_t + l n e^{i\frac{n\pi}{L}t} \right] \Phi_B(0, t) . \quad (3.38)$$

Similarly, a boundary primary field of weight l on the right boundary is a field $\Phi_B(L, t)$ that is defined on the right boundary and satisfies

$$[L_n, \Phi_B(L, t)] = D_n^L(l) \Phi_B(L, t) = (-1)^n \left[\frac{-iL}{\pi} e^{i\frac{n\pi}{L}t} \partial_t + l n e^{i\frac{n\pi}{L}t} \right] \Phi_B(L, t) . \quad (3.39)$$

The restriction of left or right moving primary fields of weight l to any one of the boundaries will be boundary fields of weight l .

$D_n(l)$, $\bar{D}_n(l)$, $D_n^0(l)$ and $D_n^L(l)$ satisfy the identities

$$[D_n(l), \bar{D}_m(l)] = 0 \quad (3.40)$$

$$[D_n(l), D_m(l)] = -(n-m) D_{n+m}(l) \quad (3.41)$$

$$[\bar{D}_n(l), \bar{D}_m(l)] = -(n-m) \bar{D}_{n+m}(l) \quad (3.42)$$

$$[D_n^0(l), D_m^0(l)] = -(n-m) D_{n+m}^0(l) \quad (3.43)$$

$$[D_n^L(l), D_m^L(l)] = -(n-m) D_{n+m}^L(l) \quad (3.44)$$

which are compatible with (3.12) and (3.34), (3.35), (3.38), (3.39).

The matrix elements of the right and left moving primary fields and boundary primary fields of weight l satisfy the equations

$$\langle A | \Phi_R(x, t) | B \rangle = \langle A | \Phi_R(0, 0) | B \rangle \exp[(h_A - h_B) \frac{i\pi}{L} (t - x)] \quad (3.45)$$

$$\langle A | \Phi_L(x, t) | B \rangle = \langle A | \Phi_L(0, 0) | B \rangle \exp[(h_A - h_B) \frac{i\pi}{L} (t + x)] \quad (3.46)$$

$$\langle A | \Phi_B(0, t) | B \rangle = \langle A | \Phi_B(0, 0) | B \rangle \exp[(h_A - h_B) \frac{i\pi}{L} t] \quad (3.47)$$

$$\langle A | \Phi_B(L, t) | B \rangle = \langle A | \Phi_B(L, 0) | B \rangle \exp[(h_A - h_B) \frac{i\pi}{L} t] , \quad (3.48)$$

where $|A\rangle$ and $|B\rangle$ are eigenstates of L_0 with eigenvalues h_A and h_B .

Introducing the new variables $z = e^{i\frac{\pi}{L}(t-x)}$, $\bar{z} = e^{i\frac{\pi}{L}(t+x)}$, $y = e^{i\frac{\pi}{L}t}$ and the operators $\hat{\Phi}_R(z) = z^{-l} \Phi_R(z)$, $\hat{\Phi}_L(\bar{z}) = \bar{z}^{-l} \Phi_L(\bar{z})$, $\hat{\Phi}_B(0, y) = y^{-l} \Phi_B(0, y)$, $\hat{\Phi}_B(L, y) = y^{-l} \Phi_B(L, y)$, and allowing z , \bar{z} and y to take any values from \mathbb{C} , we have

$$[L_n, \hat{\Phi}_R(z)] = (z^{n+1} \partial_z + l(n+1) z^n) \hat{\Phi}_R(z) \quad (3.49)$$

$$[L_n, \hat{\Phi}_L(\bar{z})] = (\bar{z}^{n+1} \partial_{\bar{z}} + l(n+1) \bar{z}^n) \hat{\Phi}_L(\bar{z}) \quad (3.50)$$

$$[L_n, \hat{\Phi}_B(0, y)] = (y^{n+1} \partial_y + l(n+1) y^n) \hat{\Phi}_B(0, y) \quad (3.51)$$

$$[L_n, \hat{\Phi}_B(L, y)] = (-1)^n [y^{n+1} \partial_y + l(n+1) y^n] \hat{\Phi}_B(L, y) \quad (3.52)$$

$$\langle A|\hat{\Phi}_R(z)|B\rangle = \langle A|\hat{\Phi}_R(1)|B\rangle z^{h_A-h_B-l} \quad (3.53)$$

$$\langle A|\hat{\Phi}_L(\bar{z})|B\rangle = \langle A|\hat{\Phi}_L(1)|B\rangle \bar{z}^{h_A-h_B-l} \quad (3.54)$$

$$\langle A|\hat{\Phi}_B(0, y)|B\rangle = \langle A|\hat{\Phi}_B(0, 1)|B\rangle y^{h_A-h_B-l} \quad (3.55)$$

$$\langle A|\hat{\Phi}_B(L, y)|B\rangle = \langle A|\hat{\Phi}_B(L, 1)|B\rangle y^{h_A-h_B-l}, \quad (3.56)$$

which are the standard formulae for chiral primary fields in conformal field theory.

3.3.1 Boundary conditions of the minimal models

Certain conformal field theories on the strip can be obtained by imposing so called conformal boundary conditions on conformal minimal models. J. Cardy investigated this construction and introduced a certain type of elementary boundary conditions often called ‘Cardy boundary conditions’. A complete classification of possible Cardy boundary conditions of minimal models has been given in [83, 84, 85]; see also [86]. For the A-type unitary minimal models these boundary conditions are in one-one correspondence with the irreducible representations of the Virasoro algebra belonging to the unitary discrete series and so we can label both boundary conditions and representations from the same set, e.g. the set of Kac labels.

The Hilbert space of a model with boundary condition α on the left-hand side and boundary condition β on the right-hand side decomposes into the following sum of Virasoro algebra representations:

$$\mathcal{H}_{\alpha\beta} = \oplus_c n_{c\alpha}^\beta R_c \quad (3.57)$$

where $n_{c\alpha}^\beta$ are Verlinde fusion numbers (see Section 3.2.1). R_c denotes the representation belonging to the label c .

In particular, if the boundary condition is 0 on one side and h on the other side, then the Hilbert space will consist of the single representation $0 \times h = h$. The possible primary boundary fields are $h \times h$. In the case that we will investigate $c = 1/2$, $h = 1/16$, and we have $1/16 \times 1/16 = 0 + 1/2$, i.e. two nonzero boundary primary fields exist (up to normalization), one has weight 0 (this is the constant identity field), the other has weight $1/2$.

The $1/16$ Cardy boundary condition is also known as the ‘free’ boundary condition, the 0 and $1/2$ boundary conditions are known as ‘fixed up’ and ‘fixed down’ boundary conditions [62]. These boundary conditions correspond to letting the boundary spins free or to fix them in the two possible directions.

3.3.2 Boundary flows

The flows we shall consider are trajectories of the form

$$H = g_0(t)H_0 + g_1(t)H_1 + g_2(t)H_2 + \dots \quad (3.58)$$

in the space of possible Hamiltonian operators, where the g_i coupling constants are functions of a parameter t . Often $g_0(t) = 1$, t varies from 0 to ∞ , and in the simplest situations there is only one perturbing term on the right-hand side of (3.58) and $g_1(t) = t$.

In the context of perturbed conformal field theory on a strip a boundary renormalization group (RG) flow is a trajectory of the form

$$H = \frac{\pi}{L}L_0 + g_1L^{-l_1}\phi_1(t=0) + g_2L^{-l_2}\phi_2(t=0) + \dots \quad (3.59)$$

where the length of the line segment L plays the role of the parameter of the trajectory, ϕ_1, ϕ_2, \dots are boundary perturbations with definite weights l_1, l_2, \dots . Such flows are associated with changing the width of the strip.

A perturbation is called relevant if $l < 1$, irrelevant if $l > 1$, marginal if $l = 1$. Relevant operators generate RG flows away from boundary conformal field theory, irrelevant operators generate RG flows into boundary conformal field theory at small values of L . In case of marginal operators a more detailed investigation is required to determine whether they generate flows away from or into boundary conformal field theory or whether they generate a flow within the space of boundary conformal field theories.

A massless RG flow is an RG flow in which nontrivial conformal symmetry is restored in the endpoint (e.g. $L \rightarrow \infty$). Values of L at which the theory described by (3.59) has conformal symmetry are called fixed points.

In the simplest case when there is only one perturbation, e.g. in the case of (1.2), one can keep L fixed and use the coupling constant instead as a parameter of the flow.

As we mentioned in the Introduction, a problem of interest, e.g. in string theory, is to find the possible RG flows, i.e. to find the triplets consisting of a BCFT (boundary conformal field theory) which is the starting point of the flow, a boundary perturbation which generates the flow and which is usually a relevant boundary operator of the starting BCFT, and a boundary BCFT which is the endpoint of the flow.

One can also include bulk perturbation terms into H , in this chapter, however, we shall consider boundary flows only. In Chapter 4 we shall see an example for renormalization group flows of models defined on the cylinder, where the perturbations will be bulk perturbations.

3.4 The Truncated Conformal Space Approach

The method called Truncated Conformal Space Approach (TCSA) is a numerical method for the computation of the eigenvalues and eigenvectors of Hamiltonian operators of perturbed conformal field theories.

It was introduced by Yurov and Al. Zamolodchikov in 1990 in [105] to study bulk perturbations of conformal field theories, and it was first applied to boundary perturbations by Dorey et al in [106]. A modified version applied to a perturbed massive free field theory can be found in [107]. In this section we describe the TCSA method in a general form that is not tied to conformal field theory.

The idea is to compute the matrix of the Hamiltonian operator in a suitable basis, to take a finite corner of it and to calculate the eigenvectors and eigenvalues numerically.

A detailed description of the method is the following: let us assume that we want to obtain the eigenvalues and eigenvectors of a Hamiltonian operator of the form $H_0 + \lambda H_I$, where λ is a coupling constant, H_0 is a Hamiltonian operator with known discrete spectrum $E_0 < E_1 < E_2 < \dots$ and the eigenspaces \mathcal{H}_i belonging to the eigenvalues are finite dimensional. We also assume that a basis (which is not necessarily orthonormal) of each eigenspace is given, the elements of which are denoted by v_i^n , $n = 1 \dots \dim \mathcal{H}_i$ for \mathcal{H}_i . We assume that the matrix elements $h_{I,ij}^{nm} = \langle v_i^n | H_I | v_j^m \rangle$ of H_I and the scalar product matrix $g_{ij}^{nm} = \langle v_i^n | v_j^m \rangle$ are also known (in particular, g is block-diagonal: $g_{ij}^{nm} = 0$ if $i \neq j$).

The entries of the matrix of H_I with respect to the basis $\{v_i^n\}$ are determined by the above data in the following way:

$$H_I |v_j^m\rangle = \sum_{i=0}^{\infty} \sum_{n=1}^{\dim \mathcal{H}_i} \tilde{h}_{I,ij}^{nm} |v_i^n\rangle, \quad (3.60)$$

where $\tilde{h}_{I,ij}^{nm}$ denotes the entries of the matrix of H_I we are looking for,

$$h_{I,kj}^{lm} = \langle v_k^l | H_I | v_j^m \rangle = \sum_{i=0}^{\infty} \sum_{n=1}^{\dim \mathcal{H}_i} \tilde{h}_{I,ij}^{nm} \langle v_k^l | v_i^n \rangle = \sum_{i=0}^{\infty} \sum_{n=1}^{\dim \mathcal{H}_i} g_{ki}^{ln} \tilde{h}_{I,ij}^{nm}, \quad (3.61)$$

so

$$\tilde{h}_{I,sj}^{rm} = \sum_{k=0}^{\infty} \sum_{l=1}^{\dim \mathcal{H}_k} (g^{-1})_{sk}^{rl} h_{I,kj}^{lm}, \quad (3.62)$$

where g^{-1} is the inverse matrix of g :

$$\sum_{k=0}^{\infty} \sum_{l=1}^{\dim \mathcal{H}_k} (g^{-1})_{sk}^{rl} g_{ki}^{ln} = \delta_{si} \delta_{rn}. \quad (3.63)$$

g^{-1} is block-diagonal, the block $(g^{-1})_{ii}^{nm}$ (where i is fixed) is the inverse of the block g_{ii}^{nm} . The blocks of g^{-1} have finite sizes $\dim \mathcal{H}_1, \dim \mathcal{H}_2, \dots$, so they can be calculated numerically by a computer.

The entries of the matrix of the operator

$$H^{TCSA}(n_c) = P_{n_c}(H_0 + \lambda H_I)P_{n_c}|_{\mathcal{H}(n_c)} \quad (3.64)$$

are

$$\tilde{h}_{0,ij}^{nm} + \lambda \tilde{h}_{I,ij}^{nm} = E_i \delta_{ij} \delta_{nm} + \lambda \tilde{h}_{I,ij}^{nm} = E_i \delta_{ij} \delta_{nm} + \lambda \sum_{k=0}^{\infty} \sum_{l=1}^{\dim \mathcal{H}_k} (g^{-1})_{ik}^{nl} h_{I,kj}^{lm}, \quad (3.65)$$

where $i, j \leq n_c$, P_{n_c} is the orthogonal projector onto the finite dimensional subspace $\mathcal{H}(n_c) = \oplus_{i=0}^{n_c} \mathcal{H}_i$ and $\tilde{h}_{0,ij}^{nm} = E_i \delta_{ij} \delta_{nm}$ are the entries of the matrix of H_0 (as well as of $P_{n_c} H_0 P_{n_c}|_{\mathcal{H}(n_c)}$ for $i, j \leq n_c$). n_c is called truncation level. Using the property that $g_{ij}^{nm} = 0$ if $i \neq j$ we can also write

$$\tilde{h}_{0,ij}^{nm} + \lambda \tilde{h}_{I,ij}^{nm} = E_i \delta_{ij} \delta_{nm} + \lambda \sum_{k=0}^{n_c} \sum_{l=1}^{\dim \mathcal{H}_k} (g^{-1})_{ik}^{nl} h_{I,kj}^{lm}. \quad (3.66)$$

The second term on the right-hand side is just a product of two finite matrices which are obtained by simply taking the $\dim \mathcal{H}(n_c) \times \dim \mathcal{H}(n_c)$ corner of the infinite matrices g^{-1} and h_I . Therefore the right-hand side of (3.66) can be calculated and diagonalized numerically by a computer. In this way we obtain the eigenvalues of $P_{n_c}(H_0 + \lambda H_I)P_{n_c}|_{\mathcal{H}(n_c)}$ and the expansion coefficients of its eigenvectors with respect to the basis $\{v_i^n, i \leq n_c\}$. These eigenvalues and expansion coefficients approximate those of $H_0 + \lambda H_I$. The approximation is generally better and applies to more eigenvectors if n_c is larger. One also expects that the approximation gets worse as λ is increased.

We remark that the above truncation method also serves as a regularization for possible ultraviolet divergences.

3.4.1 TCSA for perturbed conformal field theory on the strip

In this section we describe the application of the TCSA to a quantum field theory on a strip with the Hamiltonian operator

$$H = \frac{\pi}{L} L_0 + \lambda L^{-l} \Phi(t=0), \quad (3.67)$$

where $\frac{\pi}{L} L_0$ is the Hamiltonian operator of a conformal field theory on the strip with Hilbert space $\mathcal{H} = \oplus_j M(c, h_j)$, Φ is a boundary primary field of weight l of this conformal field theory, λ is a coupling constant and L is the width of the strip.

The Hilbert space at truncation level n_c will be $\mathcal{H}(n_c) = \oplus_j (\oplus_{i=0}^{n_c} M_i(c, h_j))$. A basis for $M_i(c, h)$ is obtained in the following way: we take the vectors

$$L_{-n_1} L_{-n_2} \dots L_{-n_k} |h\rangle \quad n_1 \geq n_2 \geq \dots \geq n_k > 0 \quad n_1 + n_2 + \dots + n_k = i \quad (3.68)$$

which are linearly independent and form a basis of $V_i(c, h)$. We compute the scalar product matrix as described in Section 3.2, this calculation can be done by computer. Then we use a simple linear algebraic algorithm (which is not specific to conformal field theory, and which we do not describe here) to eliminate elements from the above basis so that the image of the remaining vectors by the mapping q (see Section 3.2) will constitute a basis for $M_i(c, h)$. The elimination is also done by computer.

The matrix elements of a chiral primary field $\Psi(z)$ between the basis vectors can also be calculated algorithmically by computer as described in Section 3.2.1 if all the matrix elements $\langle h_1 | \Psi(1) | h_2 \rangle$ between highest weight states are known. Therefore the matrix elements of $\Phi(t=0)$ can also be calculated.

In summary, a TCSA calculation consists of the following steps:

1. Fixing the data specifying the model under investigation (the representations appearing in the decomposition of the Hilbert space into irreducible representations of the Virasoro algebra, weight of the perturbation, normalizations).
2. Fixing the truncation level n_c .
3. Taking a basis for $V_i(c, h_j)$ for all values of i and j and computing the inner product matrix for the generated basis.
4. Generating a basis for $M_i(c, h_j)$ for all values of i and j as described above, storing \tilde{h}_0 (which is a diagonal matrix with entry $\frac{\pi}{L}(h_j + i)$ for a basis vector in $M_i(c, h_j)$), storing the inner product matrix g for $\mathcal{H}(n_c)$ and computing its inverse.
5. Computing h_I , i.e. the matrix of the matrix elements of the perturbing primary field $\Phi(t=0)$ between the basis vectors of $\mathcal{H}(n_c)$.
6. Computing the product matrix $g^{-1}h_I$.
7. Computing the eigenvalues and eigenvectors of the matrix $\tilde{h}_0 + \lambda L^{-l} g^{-1} h_I$, which is the matrix of $H^{TCSA}(n_c)$, at the values of λ which are of interest.

These steps can obviously be extended to the case when the perturbation consists of more than one terms.

An application of the TCSA is to locate RG fixed points and identify the representation of the Virasoro algebra at these points. When one deals with spectra, the representations of the Virasoro algebra can be identified from the dimensions of the energy eigenspaces at various levels (see Section 3.2.2).

3.5 Exact spectrum

In this section we present a quantum field theoretic description of the model (1.2) introduced in Chapter 1. Regarding that the TCSA consists in the (approximate) diagonalization of the operator (1.2) given by its matrix elements, the main goal is to realize this Hamiltonian operator explicitly in the field theoretic framework and to calculate its spectrum. This is what determined the choice of the approach that we take in this section. In particular, the framework for our calculation will be the one introduced in Section 3.1 as the perturbed Hamiltonian operator framework, because in this framework the perturbed Hamiltonian operator structure, on which the TCSA is based, is explicit. In a calculation using the Bethe-Yang equations (which we also present, nevertheless) or in the approach of [66] where boundary conditions play central role the link with the TCSA formulation would not be entirely obvious. Furthermore, the formulation presented in this section is also suitable for Rayleigh-Schrödinger perturbation theory and for the treatment of the mode truncated version in the subsequent sections. We do not consider the classical level of the field theoretic model, mainly because it is irrelevant to our problem. We remark that the same model with massive unperturbed part (see e.g. [17]) could be studied along the same lines.

3.5.1 Distributions on closed line segments

We shall use distributions on the closed line segment (interval) $[0, L] \subset \mathbb{R}$. The necessary formulae for the Dirac-delta $\delta(x)$ and step function $\Theta(x)$ distributions on this interval are the following:

$$\int_0^L \delta(x-a)f(x) dx = f(a) \quad \text{if } a \in (0, L) \quad (3.69)$$

$$\int_0^L \delta(x-a)f(x) dx = \frac{1}{2}f(0) \quad \text{if } a = 0 \quad (3.70)$$

$$\int_0^L \delta(x-a)f(x) dx = \frac{1}{2}f(L) \quad \text{if } a = L \quad (3.71)$$

$$\int_0^L \delta(x-a)f(x) dx = 0 \quad \text{if } a \notin [0, L] , \quad (3.72)$$

where f is a function defined on $[0, L]$, and $x \in [0, L]$.

$$\Theta(x-a) = 0 \quad \text{if } x < a \quad (3.73)$$

$$\Theta(x-a) = 1 \quad \text{if } x \geq a , \quad (3.74)$$

where $a \in \mathbb{R}$,

$$\partial_x \Theta(x-L) = 2\delta(x-L) \quad (3.75)$$

$$\partial_x \Theta(x) = 0 \quad (3.76)$$

$$\partial_x \Theta(x-a) = \delta(x-a) \quad \text{if } a \in (0, L) \quad (3.77)$$

$$\partial_x \Theta(x-a) = 0 \quad \text{if } a \notin [0, L] , \quad (3.78)$$

where $x \in [0, L]$.

$$\sum_{k \in \frac{\pi\mathbb{Z}}{L}} \exp[ik(x-x')] = 2L\delta(x-x') \quad (3.79)$$

$$\sum_{k \in \frac{\pi\mathbb{Z}}{L}} \exp[ik(x+x')] = 2L[\delta(x+x') + \delta(x+x'-2L)] , \quad (3.80)$$

where $x, x' \in [0, L]$.

3.5.2 The free model

The defining constituents of the unperturbed model are the following: two fermion fields $\Psi_1(x, t)$ and $\Psi_2(x, t)$ and a fermionic operator $A_2(t)$ with the anticommutators

$$\{\Psi_1(x, t), \Psi_1(y, t)\} = 4L\delta(x - y) \quad (3.81)$$

$$\{\Psi_2(x, t), \Psi_2(y, t)\} = 4L\delta(x - y) \quad (3.82)$$

$$\{\Psi_1(x, t), \Psi_2(y, t)\} = -4L[\delta(x + y) + \delta(x + y - 2L)] \quad (3.83)$$

$$\{A_2(t), \Psi_1(x, t)\} = 0 \quad (3.84)$$

$$\{A_2(t), \Psi_2(x, t)\} = 0 \quad (3.85)$$

$$\{A_2(t), A_2(t)\} = 2 \quad (3.86)$$

and the relations

$$\Psi_1(x, t)^\dagger = \Psi_1(x, t) \quad \Psi_2(x, t)^\dagger = \Psi_2(x, t) \quad A_2(t)^\dagger = A_2(t) , \quad (3.87)$$

the Hamiltonian operator

$$H_0 = -\frac{i}{8L} \int_0^L dx \Psi_1(x, 0) \partial_x \Psi_1(x, 0) + \frac{i}{8L} \int_0^L dx \Psi_2(x, 0) \partial_x \Psi_2(x, 0) , \quad (3.88)$$

the equations of motion

$$\frac{d}{dt} A_2(t) = [iH_0, A_2(t)] = 0 , \quad (3.89)$$

$$\begin{aligned} \partial_t \Psi_1(x, t) &= [iH_0, \Psi_1(x, t)] = \\ &= -\partial_x \Psi_1(x, t) + \frac{1}{2} [\Theta(-x) + \Theta(x - L)] [-\partial_x \Psi_2(x, t) + \partial_x \Psi_1(x, t)] + \\ &\quad + \frac{1}{2} [-\Psi_1(0, t) - \Psi_2(0, t)] \delta(x) + \frac{1}{2} [\Psi_1(L, t) + \Psi_2(L, t)] \delta(x - L) , \end{aligned} \quad (3.90)$$

$$\begin{aligned} \partial_t \Psi_2(x, t) &= [iH_0, \Psi_2(x, t)] = \\ &= \partial_x \Psi_2(x, t) + \frac{1}{2} [\Theta(-x) + \Theta(x - L)] [-\partial_x \Psi_2(x, t) + \partial_x \Psi_1(x, t)] + \\ &\quad + \frac{1}{2} [\Psi_1(0, t) + \Psi_2(0, t)] \delta(x) + \frac{1}{2} [-\Psi_1(L, t) - \Psi_2(L, t)] \delta(x - L) . \end{aligned} \quad (3.91)$$

The fermion fields, which can be regarded as one-component real fermion fields with zero mass, have the following expansion:

$$\Psi_1(x, t) = \sum_{k \in \frac{\pi}{L}\mathbb{Z}, k>0} \sqrt{2} [a(k) e^{ik(t-x)} + a^\dagger(k) e^{-ik(t-x)}] + A_1 \quad (3.92)$$

$$\Psi_2(x, t) = \sum_{k \in \frac{\pi}{L}\mathbb{Z}, k>0} \sqrt{2} [-a(k) e^{ik(t+x)} - a^\dagger(k) e^{-ik(t+x)}] - A_1 \quad (3.93)$$

$$a(k)^\dagger = a(-k) \quad A_1^\dagger = A_1 \quad (3.94)$$

$$\{a(k_1), a(k_2)\} = \delta_{k_1, -k_2} \quad \{a(k), A_1\} = 0 \quad (3.95)$$

$$\{A_2, A_1\} = 0 \quad \{A_1, A_1\} = 2 \quad (3.96)$$

$$\{A_2, a(k)\} = 0 \quad (3.97)$$

The fermion fields and A_2 are dimensionless.

A unitary representation for the above operator algebra is defined by the following formulae: an orthonormal basis of the Hilbert space is

$$|a(k_1)a(k_2)a(k_3)\dots a(k_n)u\rangle \quad |a(k_1)a(k_2)a(k_3)\dots a(k_n)v\rangle, \quad (3.98)$$

where $k_1 > k_2 > k_3 > \dots > k_n > 0$, $k_i \in \frac{\pi\mathbb{Z}}{L}$ and $n \geq 0$,

$$A_1|a(k_1)a(k_2)a(k_3)\dots a(k_n)u\rangle = (-1)^n|a(k_1)a(k_2)a(k_3)\dots a(k_n)v\rangle \quad (3.99)$$

$$A_1|a(k_1)a(k_2)a(k_3)\dots a(k_n)v\rangle = (-1)^n|a(k_1)a(k_2)a(k_3)\dots a(k_n)u\rangle \quad (3.100)$$

$$A_2|a(k_1)a(k_2)a(k_3)\dots a(k_n)u\rangle = (-1)^n(-i)|a(k_1)a(k_2)a(k_3)\dots a(k_n)v\rangle \quad (3.101)$$

$$A_2|a(k_1)a(k_2)a(k_3)\dots a(k_n)v\rangle = (-1)^n(+i)|a(k_1)a(k_2)a(k_3)\dots a(k_n)u\rangle. \quad (3.102)$$

The condition $k_1 > k_2 > k_3 > \dots > k_n > 0$, $k_i \in \frac{\pi\mathbb{Z}}{L}$ and $n \geq 0$ also applies below if not stated otherwise. $a(k)|u\rangle = 0$, $a(k)|v\rangle = 0$ if $k < 0$.

The Hamiltonian operator can be written as

$$H_0 = \sum_{k \in \frac{\pi\mathbb{Z}}{L}, k > 0} k[a(k)a^\dagger(k)], \quad (3.103)$$

where an infinite constant is subtracted, by normal ordering for example, which is not denoted explicitly. The energy eigenvalue of a basis vector $|a(k_1)a(k_2)a(k_3)\dots a(k_n)u\rangle$ is

$$E_{\{k_1, k_2, \dots, k_n, u\}} = \sum_{i=1}^n k_i, \quad (3.104)$$

and the same applies if u is replaced by v .

The following boundary conditions are satisfied by the fermion fields:

$$\langle E_1|\Psi_1(0, t) + \Psi_2(0, t)|E_2\rangle = 0 \quad \langle E_1|\Psi_1(L, t) + \Psi_2(L, t)|E_2\rangle = 0, \quad (3.105)$$

where $|E_1\rangle$ and $|E_2\rangle$ are energy eigenstates.

A representation of the Virasoro algebra can also be defined on the Hilbert space in the following way (which is well known essentially in conformal field theory; see [73, 78]):

$$a(0) = \frac{1}{\sqrt{2}}A_1 \quad (3.106)$$

$$L_N = \frac{L}{2\pi} \sum_{k \in \frac{\pi}{L}\mathbb{Z}} -ka(-k)a(k - \frac{N\pi}{L}) \quad (3.107)$$

where $N = 1, 2, 3, 4, \dots$,

$$L_{-N} = (L_N)^\dagger \quad (3.108)$$

$$L_0 = \frac{L}{2\pi} \sum_{k \in \frac{\pi}{L}\mathbb{Z}} [-k : a(-k)a(k) :] + \frac{1}{16} , \quad (3.109)$$

where $::$ denotes the normal ordering for fermionic creation and annihilation operators, $: a(-k)a(k) := a(-k)a(k)$ if $k < 0$, $: a(-k)a(k) := -a(k)a(-k)$ if $k > 0$. L_N , $N \in \mathbb{Z}$ will be the generators of the Virasoro algebra. They satisfy the relations

$$[L_N, L_M] = (N - M)L_{N+M} \quad \text{if } N + M \neq 0 \quad (3.110)$$

and

$$\begin{aligned} [L_N, L_{-N}] &= \\ &= \frac{L^2}{4\pi^2} \sum_{k \in \frac{\pi}{L}\mathbb{Z}} [-k(-2k + \frac{N\pi}{L})a(-k)a(k) + k(-2k + \frac{N\pi}{L})a(-k + \frac{N\pi}{L})a(k - \frac{N\pi}{L})] \end{aligned} \quad (3.111)$$

if $N > 0$. It can be verified that in the above representation of the creation and annihilation operators the right-hand side of the equation (3.111) is equal to

$$2NL_0 + \frac{1}{24}N(N-1)(N+1) , \quad (3.112)$$

and so the operators L_N satisfy the (usual) relations of the generators of the Virasoro algebra with central charge $c = 1/2$. A_2 commutes with the L_N -s. $|v\rangle$ and $|u\rangle$ are highest weight states with weight $1/16$ and the Hilbert space decomposes into two copies of the $M(c = 1/2, h = 1/16)$ unitary highest weight representation of the Virasoro algebra. The invariant subspace belonging to u is spanned by the vectors $|a(k_1)a(k_2)\dots a(k_n)u\rangle$ with n even and $|a(k_1)a(k_2)\dots a(k_n)v\rangle$ with n odd. The invariant subspace belonging to v is spanned by the vectors $|a(k_1)a(k_2)\dots a(k_n)u\rangle$ with n odd and $|a(k_1)a(k_2)\dots a(k_n)v\rangle$ with n even. These subspaces will be called u and v sectors.

The relation between H_0 and L_0 is

$$H_0 = \frac{\pi}{L}L_0 - \frac{1}{16}\frac{\pi}{L} . \quad (3.113)$$

The fields Ψ_1 and Ψ_2 can be written as

$$\Psi_1(x, t) = \sqrt{2} \sum_{k \in \frac{\pi}{L}\mathbb{Z}} a(k) e^{ik(t-x)} \quad (3.114)$$

$$\Psi_1(z) = \sqrt{2} \sum_{n \in \mathbb{Z}} \tilde{a}(n) z^n \quad (3.115)$$

$$\Psi_2(x, t) = \sqrt{2} \sum_{k \in \frac{\pi}{L}\mathbb{Z}} -a(k) e^{ik(t+x)} \quad (3.116)$$

$$\Psi_2(\bar{z}) = \sqrt{2} \sum_{n \in \mathbb{Z}} -\tilde{a}(n) \bar{z}^n, \quad (3.117)$$

where $\tilde{a}(n) = a(k)$, $k = n\frac{\pi}{L}$, $z = e^{i\frac{\pi}{L}(t-x)}$, $\bar{z} = e^{i\frac{\pi}{L}(t+x)}$.

The following commutation relations are satisfied:

$$[L_N, \Psi_1(x, t)] = \frac{-iL}{2\pi} e^{i\frac{N\pi}{L}(t-x)} [\partial_t - \partial_x] \Psi_1(x, t) + \frac{N}{2} e^{i\frac{N\pi}{L}(t-x)} \Psi_1(x, t) \quad (3.118)$$

$$[L_N, \Psi_1(z)] = z^{N+1} \frac{d\Psi_1}{dz}(z) + \frac{1}{2} N z^N \Psi_1(z) \quad (3.119)$$

$$[L_N, \Psi_2(x, t)] = \frac{-iL}{2\pi} e^{i\frac{N\pi}{L}(t+x)} [\partial_t + \partial_x] \Psi_2(x, t) + \frac{N}{2} e^{i\frac{N\pi}{L}(t+x)} \Psi_2(x, t) \quad (3.120)$$

$$[L_N, \Psi_2(\bar{z})] = \bar{z}^{N+1} \frac{d\Psi_2}{d\bar{z}}(\bar{z}) + \frac{1}{2} N \bar{z}^N \Psi_2(\bar{z}). \quad (3.121)$$

In the equations (3.119) and (3.121) the domains of z and \bar{z} are extended to the whole complex plane and the differentiation with respect to z and \bar{z} is the usual complex differentiation.

For $\epsilon(z) = \frac{\Psi_1(z)}{\sqrt{z}}$ we have

$$[L_N, \epsilon(z)] = z^{N+1} \frac{d\epsilon}{dz}(z) + \frac{1}{2} (N+1) z^N \epsilon(z) \quad (3.122)$$

and for $\bar{\epsilon}(\bar{z}) = \frac{\Psi_2(\bar{z})}{\sqrt{\bar{z}}}$

$$[L_N, \bar{\epsilon}(\bar{z})] = \bar{z}^{N+1} \frac{d\bar{\epsilon}}{d\bar{z}}(\bar{z}) + \frac{1}{2} (N+1) \bar{z}^N \bar{\epsilon}(\bar{z}), \quad (3.123)$$

i.e. $\epsilon(z)$ and $\bar{\epsilon}(\bar{z})$ are chiral Virasoro primary fields of weight $1/2$. The same relations apply to the fields $A_2\Psi_1$, $A_2\Psi_2$, $A_2\epsilon$ and $A_2\bar{\epsilon}$, in particular $A_2\epsilon$ and $A_2\bar{\epsilon}$ are also chiral primary fields of weight $1/2$. $A_2\epsilon$ and $A_2\bar{\epsilon}$ have zero matrix elements between the u and v sector, whereas $\epsilon(z)$ and $\bar{\epsilon}(\bar{z})$ have zero matrix elements within the u and v sectors.

The operator A_2 is an auxiliary operator and if it is omitted, then it is possible to represent the fields so that the Hilbert space is a single Virasoro module $(1/2, 1/16)$. It is the next section where the presence of A_2 will be really useful.

We remark that if we demand the equations of motion $\partial_t \Psi_1(x, t) = -\partial_x \Psi_1(x, t)$, $\partial_t \Psi_2(x, t) = \partial_x \Psi_2(x, t)$ for $x \in [0, L]$, the fermionic nature of the mode creating and annihilating operators and the boundary conditions

$$\langle E_1 | \Psi_1(0, t) + \Psi_2(0, t) | E_2 \rangle = 0 \quad \langle E_1 | \Psi_1(L, t) + \Psi_2(L, t) | E_2 \rangle = 0 \quad (3.124)$$

or

$$\langle E_1 | \Psi_1(0, t) - \Psi_2(0, t) | E_2 \rangle = 0 \quad \langle E_1 | \Psi_1(L, t) - \Psi_2(L, t) | E_2 \rangle = 0, \quad (3.125)$$

where $|E_1\rangle$ and $|E_2\rangle$ are energy eigenstates, then the $(c = 1/2, h = 1/16)$ representation of the Virasoro algebra can be defined on the Hilbert space (without A_2 and considering the simplest possibility). If we demand the boundary conditions

$$\langle E_1 | \Psi_1(0, t) + \Psi_2(0, t) | E_2 \rangle = 0 \quad \langle E_1 | \Psi_1(L, t) - \Psi_2(L, t) | E_2 \rangle = 0 \quad (3.126)$$

or

$$\langle E_1 | \Psi_1(0, t) - \Psi_2(0, t) | E_2 \rangle = 0 \quad \langle E_1 | \Psi_1(L, t) + \Psi_2(L, t) | E_2 \rangle = 0, \quad (3.127)$$

then the representation of the Virasoro algebra on the Hilbert space will be $(c = 1/2, h = 1/2) \oplus (c = 1/2, h = 0)$. The anticommutation relations of the fields are slightly different in these four cases.

3.5.3 The perturbed model

The Hamiltonian operator is

$$H = -\frac{i}{8L} \int_0^L \Psi_1(x, 0) \partial_x \Psi_1(x, 0) dx + \frac{i}{8L} \int_0^L \Psi_2(x, 0) \partial_x \Psi_2(x, 0) dx + \\ + h i A_2(0) [\Psi_2(L, 0) - \Psi_1(L, 0)] , \quad (3.128)$$

where h is a coupling constant of dimension *mass*. The perturbing term $hH_I = h i A_2(0) [\Psi_2(L, 0) - \Psi_1(L, 0)]$ has zero matrix elements between vectors belonging to different sectors, which means that H can be restricted to the u and v sectors separately. These restrictions are denoted by $H|_u$ and $H|_v$. H_I is also a primary boundary field of weight $1/2$ with respect to the Virasoro algebra defined in the previous section taken at $t = 0$. The matrix elements of H_I , i.e. of $H_I|_u$ and $H_I|_v$, are uniquely determined by this property and by the values of the matrix elements $\langle u | H_I | u \rangle$ and $\langle v | H_I | v \rangle$. It is easy to verify that $2 = \langle u | H_I | u \rangle = -\langle v | H_I | v \rangle$, and there exists an intertwiner Y of the Virasoro algebra representations on the u and v sectors so that $Y u = v$, $Y H_0|_u Y^{-1} = H_0|_v$. This also implies that $Y H_I|_u Y^{-1} = -H_I|_v$. This means finally that we can restrict to $0 \leq h \leq \infty$, and the u sector and $H|_u$ will correspond to the $h \geq 0$ case of (1.2) and to

(1.3), the v sector and $H|_v$ will correspond to the $h \leq 0$ case of (1.2) and to (1.4). For $0 \leq h \leq \infty$ the operator (3.128) describes in the two sectors the two flows mentioned in the Introduction. The precise relation between the h in (1.2) in the Introduction and the h in (3.128) is the following: $h_{Introd} = 2L^{1/2}h$ in the u sector, $h_{Introd} = -2L^{1/2}h$ in the v sector. Further on we shall assume that $0 < h < \infty$.

The eigenvalues of the Hamiltonian operator (3.128) are ultraviolet divergent in perturbation theory; the divergence can be removed by adding a term ch^2I with appropriate value of the logarithmically divergent (as a function of the cutoff energy) coefficient c . This means that the differences of the eigenvalues of H are not ultraviolet divergent. We shall assume that the ground state energy is set to zero by the renormalization, and the ch^2I term will not be written explicitly.

The equations of motion are obtained by adding the following terms to the right-hand side of the unperturbed equations of motion (3.89), (3.90), (3.91):

$$[ihH_I, \Psi_1(x, t)] = 8LhA_2(t)\delta(x - L) \quad (3.129)$$

$$[ihH_I, \Psi_2(x, t)] = -8LhA_2(t)\delta(x - L) \quad (3.130)$$

$$[ihH_I, A_2(t)] = 2h(\Psi_2(L, t) - \Psi_1(L, t)) . \quad (3.131)$$

These terms are linear in the fermion fields and A_2 , so the equations of motion for the perturbed theory are linear and by sandwiching these equations between energy eigenstates we get a system of three first-order differential equations for the expectation values of the fields and A_2 . These expectation values can be assumed to take the form

$$\langle E_1 | \Psi_1(x, t) | E_2 \rangle = -e^{ik(t-x)} - \Theta(x - L)C_1(k)e^{ikt} \quad (3.132)$$

$$\langle E_1 | \Psi_2(x, t) | E_2 \rangle = e^{ik(t+x)} - \Theta(x - L)C_2(k)e^{ikt} \quad (3.133)$$

$$\langle E_1 | A_2(t) | E_2 \rangle = C_3(k)e^{ikt} , \quad (3.134)$$

where $C_1(k)$, $C_2(k)$, $C_3(k)$ are finite constants, $|E_1\rangle$ and $|E_2\rangle$ are eigenstates of H and $k = E_1 - E_2$. $|E_1\rangle$ and $|E_2\rangle$ are not necessarily normalized to 1 here.

Substituting (3.132)-(3.134) into the equations of motion we get algebraic equations for $C_1(k)$, $C_2(k)$, $C_3(k)$, which have the following solution:

$$kL \tan(kL) = 16L^2h^2 \quad (3.135)$$

$$\psi_1(k)(x, t) = \langle E_1 | \Psi_1(x, t) | E_2 \rangle = -e^{ik(t-x)} - \Theta(x - L)i \sin(kL)e^{ikt} \quad (3.136)$$

$$\psi_2(k)(x, t) = \langle E_1 | \Psi_2(x, t) | E_2 \rangle = e^{ik(t+x)} - \Theta(x - L)i \sin(kL)e^{ikt} \quad (3.137)$$

$$a_2(k)(t) = \langle E_1 | A_2(t) | E_2 \rangle = -\frac{i \sin(kL)}{4Lh}e^{ikt} . \quad (3.138)$$

(3.135) is the formula that determines the possible values of k at a given value of h and L and so the spectrum of H up to an undetermined additive overall constant.

The assumption (3.132), (3.133) is motivated by the fact that the equations of motion for $x \in (0, L)$ are $(\partial_t + \partial_x)\Psi_1(x, t) = 0$, $(\partial_t - \partial_x)\Psi_2(x, t) = 0$. We remark that the equations of motion could also be solved directly without making any assumptions on the form of the expectation values.

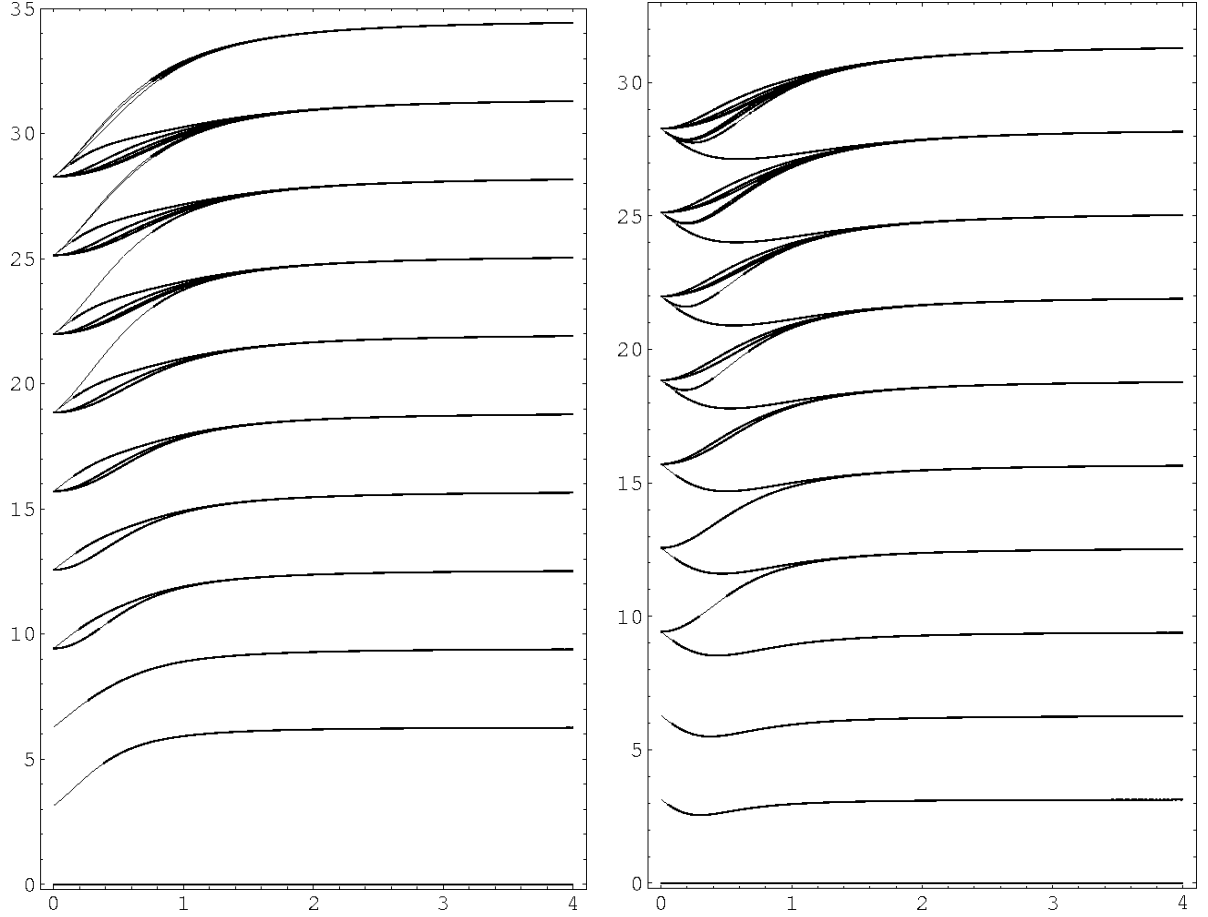


Figure 3.1: Exact energy gaps in the v and u sectors as a function of h

Introducing the notation

$$n(k) = (\psi_1(k), \psi_2(k), a_2(k)) \quad (3.139)$$

the mode expansion of (Ψ_1, Ψ_2, A_2) is

$$(\Psi_1, \Psi_2, A_2) = \sum_{k \in S} b(k) n(k) , \quad (3.140)$$

where the $b(k)$ are creation/annihilation operators and the summation is done over the set S of all real solutions of (3.135).

The anticommutation relation of the $b(k)$ -s can be obtained in the following way: we define a scalar product on the classical complex valued solutions of the equations of motion:

$$\langle \psi_1, \psi_2, a_2 | \phi_1, \phi_2, b_2 \rangle = \int_0^L [\psi_1^* \phi_1 + \psi_2^* \phi_2] dx + 2La_2^* b_2 . \quad (3.141)$$

This product should be calculated at a fixed time. Using the equations of motion it can be shown that the product is independent of this time.

The essential properties of this scalar product are that it is defined by a local expression and that the $n(k)$ -s are orthogonal with respect to it:

$$\langle n(k_1) | n(k_2) \rangle = \delta_{k_1-k_2,0} (2L + \frac{\sin(2k_1 L)}{k_1}) . \quad (3.142)$$

The creation/annihilation operators can be expressed in the following way:

$$\langle n(k) | (\Psi_1, \Psi_2, A_2) \rangle = b(k) \langle n(k) | n(k) \rangle \quad (3.143)$$

Using the formula (3.141) and the anticommutation relations (3.81)-(3.86) we get

$$\{b(k_1), b(k_2)\} = \delta_{k_1+k_2,0} \frac{4Lk_1}{2Lk_1 + \sin(2Lk_1)} . \quad (3.144)$$

The equation

$$b(k)^\dagger = b(-k) \quad (3.145)$$

is also satisfied.

The expansion (3.140) and (3.81)-(3.86) imply that the following nontrivial formulae hold:

$$\sum_{k \in S} f(k) \psi_1(k)(x, 0) \psi_1(-k)(y, 0) = 4L \delta(x - y) \quad (3.146)$$

$$\sum_{k \in S} f(k) \psi_2(k)(x, 0) \psi_2(-k)(y, 0) = 4L \delta(x - y) \quad (3.147)$$

$$\sum_{k \in S} f(k) \psi_1(k)(x, 0) \psi_2(-k)(y, 0) = -4L [\delta(x + y) + \delta(x + y - 2L)] \quad (3.148)$$

$$\sum_{k \in S} f(k) a_2(k)(0) \psi_1(-k)(x, 0) = 0 \quad (3.149)$$

$$\sum_{k \in S} f(k) a_2(k)(0) \psi_2(-k)(x, 0) = 0 \quad (3.150)$$

$$\sum_{k \in S} f(k) a_2(k)(0) a_2(-k)(0) = 2 , \quad (3.151)$$

where

$$f(k) = \frac{4Lk}{2Lk + \sin(2Lk)} . \quad (3.152)$$

These formulae are generalizations of (3.79), (3.80).

Using the formulae

$$a(k) = \frac{1}{2\sqrt{2}L} \left[\int_0^L e^{ikx} \Psi_1(x, 0) dx - \int_0^L e^{-ikx} \Psi_2(x, 0) dx \right] \quad (3.153)$$

$$A_1 = \frac{1}{2L} \left[\int_0^L \Psi_1(x, 0) dx - \int_0^L \Psi_2(x, 0) dx \right] \quad (3.154)$$

and (3.140) and (3.10) we obtain the following relations:

$$a(k) = \frac{-1}{\sqrt{2}L} \sum_{k' \in S} b(k') \frac{\sin[(k - k')L]}{k - k'} \quad (3.155)$$

$$A_1 = \frac{-1}{L} \sum_{k' \in S} b(k') \frac{\sin[k'L]}{k'} \quad (3.156)$$

$$A_2(0) = \sum_{k \in S} b(k) \frac{-i \sin(kL)}{4Lh} = -i \sum_{k \in S} b(k) \frac{\sin(kL)}{\sqrt{kL \tan(kL)}}. \quad (3.157)$$

Using (3.143) we get the relation

$$b(k) \left(2L + \frac{\sin(2kL)}{k} \right) = \sqrt{2} \sum_{k' \in \frac{\pi}{L}\mathbb{Z}} a(k') \frac{-2 \sin[(k' - k)L]}{k' - k} + \frac{i \sin(kL)}{2h} A_2(0). \quad (3.158)$$

(3.155)-(3.158) can be regarded as Bogoliubov transformation formulae for this model.

We remark that the above scalar product technique is also suitable for free fields on the half-line or in the usual full Minkowski space without boundaries in arbitrary spacetime dimensions.

We also remark that we have not given a mathematically completely rigorous proof that (3.140) satisfies (3.81)-(3.86), but we think that this would be possible.

The Hilbert space is spanned by the orthogonal eigenstates $|b(k_1)b(k_2)b(k_3) \dots b(k_n)0_h\rangle$ where $k_1 > k_2 > \dots > k_n > 0$, $|0_h\rangle$ is the ground state, which is unique, and $b(k)|0_h\rangle = 0$ if $k < 0$. The eigenvalues of these states are

$$E_{\{k_1, k_2, \dots, k_n\}} = \sum_{i=1}^n k_i. \quad (3.159)$$

The eigenvector $|b(k_1)b(k_2) \dots b(k_n)0_h\rangle$ belongs to the v sector if n is even and to the u sector if n is odd. The first few energy gaps (i.e. energies relative to the lowest energy) within the two sectors are shown in Figure 3.1 as functions of h with $L = 1$.

In the $h \rightarrow 0$ limit

$$b(k(n, h)) \rightarrow -\sqrt{2}a(k(n, 0)) \quad n \geq 1 \quad (3.160)$$

$$b(k(0, h)) + b(k(0, h))^\dagger \rightarrow -A_1 \quad (3.161)$$

$$i(b(k(0, h))^\dagger - b(k(0, h))) \rightarrow A_2(0) \quad (3.162)$$

$$|0_h\rangle \rightarrow |v\rangle, \quad (3.163)$$

where $k(n, h)$ is the n -th nonnegative root of (3.135) as a function of h , $k(n, 0) = n\pi/L$, $n = 0, 1, 2, \dots$.

The nonzero matrix elements of the fields are

$$\frac{\langle P | (\Psi_1(x, t), \Psi_2(x, t), A_2(t)) | Q \rangle}{\sqrt{|\langle P | P \rangle \langle Q | Q \rangle|}} = n(k) (-1)^m \sqrt{f(k)} \quad (3.164)$$

$$\frac{\langle Q | (\Psi_1(x, t), \Psi_2(x, t), A_2(t)) | P \rangle}{\sqrt{|\langle P | P \rangle \langle Q | Q \rangle|}} = n(-k) (-1)^m \sqrt{f(k)} , \quad (3.165)$$

where $Q = |b(k_1)b(k_2) \dots b(k_n)0_h\rangle$, $P = |b(k_1), \dots, b(k_m), b(k), b(k_{m+1}), \dots, b(k_n)0_h\rangle$,

$$\langle Q | Q \rangle = \prod_{i=1}^n f(k_i) . \quad (3.166)$$

The Hamiltonian operator can be written as

$$H = \sum_{k \in S, k > 0} \frac{k}{f(k)} b(k) b(-k) . \quad (3.167)$$

The following formula can be written for $|0_h\rangle$:

$$N|0_h\rangle = \lim_{\alpha \rightarrow \infty} e^{-\alpha H} |v\rangle = \prod_{k \in S, k > 0} \left(1 - \frac{1}{f(k)} b(k) b(-k)\right) |v\rangle \quad (3.168)$$

where N is a normalization factor. The second equation on the right-hand side can be verified directly using the following formulae:

$$[b(k_1)b(-k_1), b(k_2)b(-k_2)] = 0 \quad (3.169)$$

if $k_1 \neq k_2$ (and $k_1, k_2 > 0$) and

$$(b(k)b(-k))^n = f(k)^{n-1} b(k)b(-k) . \quad (3.170)$$

The following boundary conditions are satisfied:

$$\langle E_1 | \Psi_1(0, t) + \Psi_2(0, t) | E_2 \rangle = 0 \quad (3.171)$$

$$\langle E_1 | \Psi_1(L, t) + \Psi_2(L, t) | E_2 \rangle = 0 \quad (3.172)$$

and

$$\lim_{x \rightarrow 0} \langle E_1 | \Psi_1(x, t) + \Psi_2(x, t) | E_2 \rangle = 0 \quad (3.173)$$

$$\lim_{x \rightarrow L} \langle E_1 | \partial_x \Psi_1(x, t) - \partial_x \Psi_2(x, t) | E_2 \rangle = 16Lh^2 \langle E_1 | \Psi_2(L, t) - \Psi_1(L, t) | E_2 \rangle \quad (3.174)$$

$$\lim_{h \rightarrow \infty} \lim_{x \rightarrow L} \langle E_1 | \Psi_1(x, t) - \Psi_2(x, t) | E_2 \rangle = 0 \quad (3.175)$$

$$\lim_{h \rightarrow \infty} \lim_{x \rightarrow L} \langle E_1 | \Psi_1(x, t) + \Psi_2(x, t) | E_2 \rangle \neq 0 , \quad (3.176)$$

where $|E_1\rangle$ and $|E_2\rangle$ are eigenstates of H . The boundary conditions (3.171) and (3.172) are the same as those satisfied by the free fields and they are also in agreement with the definition (3.7)-(3.9). On the other hand, (3.173) and (3.174) are similar to the boundary conditions written down in [19, 67, 66]. The equations (3.175), (3.176) show that in the $h : 0 \rightarrow \infty$ limit the boundary condition (3.126) is realized. From the point of view of the boundary conditions one can say that the perturbation H_I induces a flow from the boundary condition $\lim_{x \rightarrow L} \langle E_1 | \Psi_1(x, t) + \Psi_2(x, t) | E_2 \rangle = 0$ to the boundary condition $\lim_{x \rightarrow L} \langle E_1 | \Psi_1(x, t) - \Psi_2(x, t) | E_2 \rangle = 0$ and the boundary condition on the left-hand side remains constant, which is in accordance with the literature (see e.g. [19]). The boundary condition $\langle E_1 | \Psi_1(L, t) + \Psi_2(L, t) | E_2 \rangle = 0$ is called free spin boundary condition in the literature (e.g. [19]) and $\langle E_1 | \Psi_1(L, t) - \Psi_2(L, t) | E_2 \rangle = 0$ is called fixed spin boundary condition. One also has the physical picture of these boundary conditions that at zero magnetic field (i.e. $h = 0$) the direction of the spin at the boundary is free, whereas at infinite magnetic field it is completely fixed to one of the two directions (depending on the sign of the boundary magnetic field).

We remark that from (3.173) and (3.174) and the bulk equations of motion $(\partial_t + \partial_x)\Psi_1 = 0$, $(\partial_t - \partial_x)\Psi_2 = 0$ the equation (3.135) can be recovered.

In the $h : 0 \rightarrow \infty$ limit

$$k(n, h) \rightarrow k(n, 0) + \frac{1}{2} \frac{\pi}{L} = \frac{n\pi}{L} + \frac{1}{2} \frac{\pi}{L} \quad (3.177)$$

and

$$\{b(k_i), b(k_j)\} \rightarrow 2\delta_{k_i+k_j, 0} . \quad (3.178)$$

It can be verified that in the $h \rightarrow \infty$ limit the $(c = 1/2, h = 0)$ representation of the Virasoro algebra can be introduced in the v sector and the $(c = 1/2, h = 1/2)$ representation can be introduced in the u sector. One can write expressions (which are well known essentially, see [73, 78]) for the generators in terms of the $b(k)$ -s similar to (3.107), (3.109). Therefore $h : 0 \rightarrow \infty$ corresponds to the $(1/2, 1/16) \rightarrow (1/2, 0)$ flow in the v sector and to the $(1/2, 1/16) \rightarrow (1/2, 1/2)$ flow in the u sector. We remark that the easiest way to determine which representations are realized in the $h \rightarrow \infty$ limit is to count the degeneracies of the first few energy levels (separately in the two sectors) and compare the result with Table 3.1.

We define the fields

$$\Phi_1(x, t) = \sum_{k \in S} -b(k) e^{ik(t-x)} \quad (3.179)$$

$$\Phi_2(x, t) = \sum_{k \in S} b(k) e^{ik(t+x)} . \quad (3.180)$$

They satisfy the following equations:

$$(\Psi_1 - \Psi_2)(L, t) = \frac{1}{16Lh^2} \partial_x (\Phi_2 - \Phi_1)(L, t) \quad (3.181)$$

$$A_2(t) = -\frac{1}{8Lh} (\Phi_1 + \Phi_2)(L, t) \quad (3.182)$$

$$H_0 = -\frac{i}{8L} \int_0^L dx \Phi_1(x, 0) \partial_x \Phi_1(x, 0) + \frac{i}{8L} \int_0^L dx \Phi_2(x, 0) \partial_x \Phi_2(x, 0) - \frac{1}{2} h H_I . \quad (3.183)$$

Note that the energies of the modes are not in $\frac{\pi}{L}\mathbb{Z}$, so one cannot conclude that the sum of the first two terms in (3.183) equals to H .

The above equations suggest how to describe the model discussed in this section as a perturbation of the $h \rightarrow \infty$ limiting model. This description will be given in the next section.

3.5.4 Reverse description

In this section we propose the description of the model (3.128) as a perturbation of its $h \rightarrow \infty$ limit. It should be noted that the meaning of the notation H_0 or H_I etc. differs from that in the previous section. The precise correspondence between the quantities in this section and in the previous section will be given explicitly for the coupling constant and for the spectrum.

The free model

The fundamental objects of the model at $h = \infty$ are two one-component real fermion fields $\Phi_1(x, t)$, $\Phi_2(x, t)$ with the anticommutation relations

$$\{\Phi_1(x, t), \Phi_1(y, t)\} = 4L\delta(x - y) \quad (3.184)$$

$$\{\Phi_2(x, t), \Phi_2(y, t)\} = 4L\delta(x - y) \quad (3.185)$$

$$\{\Phi_1(x, t), \Phi_2(y, t)\} = -4L[\delta(x + y) - \delta(x + y - 2L)] \quad (3.186)$$

and reality property

$$\Phi_1(x, t)^\dagger = \Phi_1(x, t) \quad \Phi_2(x, t)^\dagger = \Phi_2(x, t) . \quad (3.187)$$

Φ_1 and Φ_2 are dimensionless.

The Hamiltonian operator is

$$H_0 = -\frac{i}{8L} \int_0^L dx \Phi_1(x, 0) \partial_x \Phi_1(x, 0) + \frac{i}{8L} \int_0^L dx \Phi_2(x, 0) \partial_x \Phi_2(x, 0) . \quad (3.188)$$

The equations of motion are

$$\begin{aligned} \partial_t \Phi_1(x, t) &= [iH_0, \Phi_1(x, t)] = -\partial_x \Phi_1(x, t) + \\ &\quad + \frac{1}{2} \delta(x - L) [\Phi_1(L, t) - \Phi_2(L, t)] + \frac{1}{2} \delta(x) [-\Phi_1(0, t) - \Phi_2(0, t)] + \\ &\quad + \frac{1}{2} \Theta(-x) [\partial_x \Phi_1(x, t) - \partial_x \Phi_2(x, t)] + \frac{1}{2} \Theta(x - L) [\partial_x \Phi_1(x, t) + \partial_x \Phi_2(x, t)] \end{aligned} \quad (3.189)$$

$$\begin{aligned} \partial_t \Phi_2(x, t) &= [iH_0, \Phi_2(x, t)] = \partial_x \Phi_2(x, t) + \\ &\quad + \frac{1}{2} \delta(x - L) [\Phi_1(L, t) - \Phi_2(L, t)] + \frac{1}{2} \delta(x) [\Phi_1(0, t) + \Phi_2(0, t)] + \\ &\quad + \frac{1}{2} \Theta(-x) [\partial_x \Phi_1(x, t) - \partial_x \Phi_2(x, t)] + \frac{1}{2} \Theta(x - L) [-\partial_x \Phi_1(x, t) - \partial_x \Phi_2(x, t)] . \end{aligned} \quad (3.190)$$

The fermion fields have the following mode expansion:

$$\Phi_1(x, t) = \sum_{k \in \frac{\pi}{L}\mathbb{Z} + \frac{\pi}{2L}} \sqrt{2} a(k) e^{ik(t-x)} \quad (3.191)$$

$$\Phi_2(x, t) = \sum_{k \in \frac{\pi}{L}\mathbb{Z} + \frac{\pi}{2L}} -\sqrt{2} a(k) e^{ik(t+x)} \quad (3.192)$$

$$\{a(k_1), a^\dagger(k_2)\} = \delta_{k_1, k_2} \quad a(k)^\dagger = a(-k) . \quad (3.193)$$

An orthonormal basis for the Hilbert space is formed by the vectors

$$|a(k_1)a(k_2) \dots a(k_n)0\rangle , \quad (3.194)$$

where $k_i > 0$, $k_i \in \frac{\pi}{L}\mathbb{Z} + \frac{\pi}{2L}$, $n \geq 0$. $a(k)|0\rangle = 0$ if $k < 0$. The Hamiltonian operator can be written as

$$H_0 = \sum_{k>0, k \in \frac{\pi}{L}\mathbb{Z} + \frac{\pi}{2L}} k [a(k)a^\dagger(k)] \quad (3.195)$$

after subtracting an infinite constant, by normal ordering for example, which is not denoted explicitly. The eigenvalue of the eigenvector $|a(k_1)a(k_2) \dots a(k_n)0\rangle$ is

$$E_{\{k_1, k_2, \dots, k_n, 0\}} = \sum_{i=1}^n k_i . \quad (3.196)$$

The fermion fields satisfy the following boundary conditions:

$$\langle E_1 | \Phi_1(0, t) + \Phi_2(0, t) | E_2 \rangle = 0 \quad \langle E_1 | \Phi_1(L, t) - \Phi_2(L, t) | E_2 \rangle = 0 , \quad (3.197)$$

where $|E_1\rangle, |E_2\rangle$ are eigenstates of H_0 .

One can define a representation of the Virasoro algebra on the Hilbert space in the same way as in Section 3.5.2 (see also [73, 78]). This representation is $(1/2, 0) \oplus (1/2, 1/2)$. The fields $\Phi_1(x, t)$ and $\Phi_2(x, t)$ can be converted to right and left moving weight 1/2 primary fields by multiplying them by a suitable simple exponential factor.

The perturbed model

The Hamilton operator is

$$H = -\frac{i}{8L} \int_0^L dx \Phi_1(x, 0) \partial_x \Phi_1(x, 0) + \frac{i}{8L} \int_0^L dx \Phi_2(x, 0) \partial_x \Phi_2(x, 0) + \\ + g[i(\Phi_1 + \Phi_2)(L, 0) \lim_{x \rightarrow L} \partial_x (\Phi_2 - \Phi_1)(x, 0)] , \quad (3.198)$$

where g is a dimensionless coupling constant. In the same way as in Section 3.5.3, the perturbing term has zero matrix elements between vectors belonging to different irreducible representations.

The limit prescription in the perturbing term is important, and the limit $\lim_{x \rightarrow L}$ should be taken at the end of any calculation. It should be assumed that $\lim_{x \rightarrow L} \delta(x - L) = 0$, for example, and similarly for the derivatives of $\delta(x - L)$.

It should be noted that the only primary field in the 0 or in the $1/2$ representation is the identity operator, all other fields are descendant and non-relevant fields.

The equations of motion are obtained by adding the following terms to the right-hand side of the unperturbed equations of motion (3.189), (3.190):

$$[igH_I, \Phi_1(x, t)] = g8L\delta(x - L) \lim_{x \rightarrow L} \partial_x (\Phi_2 - \Phi_1)(x, t) \quad (3.199)$$

$$[igH_I, \Phi_2(x, t)] = g8L\delta(x - L) \lim_{x \rightarrow L} \partial_x (\Phi_2 - \Phi_1)(x, t) \quad (3.200)$$

where

$$H_I = [i(\Phi_1 + \Phi_2)(L, 0) \lim_{x \rightarrow L} \partial_x (\Phi_2 - \Phi_1)(x, 0)] . \quad (3.201)$$

We remark that we used the following formulae in the computation of (3.199), (3.200):

$$\{\Phi_1(x, t), \lim_{y \rightarrow L} \partial_y (\Phi_2 - \Phi_1)(y, t)\} = 0 \quad (3.202)$$

$$\{\Phi_2(x, t), \lim_{y \rightarrow L} \partial_y (\Phi_2 - \Phi_1)(y, t)\} = 0 . \quad (3.203)$$

Similar steps to those in Section 3.5.3 can now be taken to obtain $\langle E_1 | \Phi_1(x, t) | E_2 \rangle$ and $\langle E_1 | \Phi_2(x, t) | E_2 \rangle$. In the same way as in Section 3.5.3, the forms

$$\langle E_1 | \Phi_1(x, t) | E_2 \rangle = e^{ik(t-x)} + \Theta(x - L) D_1(k) e^{ikt} \quad (3.204)$$

$$\langle E_1 | \Phi_2(x, t) | E_2 \rangle = -e^{ik(t+x)} + \Theta(x - L) D_2(k) e^{ikt} \quad (3.205)$$

can be assumed, where $D_1(k)$ and $D_2(k)$ are finite constants, $|E_1\rangle$ and $|E_2\rangle$ are eigenstates of H and $k = E_1 - E_2$.

Solving the equations of motion for $D_1(k)$, $D_2(k)$, we get

$$D_2(k) = \cos(kL) \quad (3.206)$$

$$D_1(k) = -\cos(kL) \quad (3.207)$$

and

$$(kL) \tan(kL) = \frac{-1}{16g} . \quad (3.208)$$

(3.208) is the formula that determines the spectrum of H up to an overall additive constant. The eigenvalues of H are

$$k_1 + k_2 + \cdots + k_n , \quad (3.209)$$

where $n \geq 0$, $k_i \geq 0$, $k_i \neq k_j$ if $i \neq j$, the k_i -s are real roots of (3.208) and the lowest eigenvalue is assumed to be set to zero by adding a constant which is not written explicitly. The substitution

$$g = \frac{-1}{256L^2h^2} \quad (3.210)$$

converts (3.208) into (3.135). Thus $g : 0 \rightarrow -\infty$ corresponds to the flow $(0 \rightarrow 1/16) \oplus (1/2 \rightarrow 1/16)$.

The following boundary conditions are satisfied:

$$\langle E_1 | \Phi_1(0, t) + \Phi_2(0, t) | E_2 \rangle = 0 \quad (3.211)$$

$$\langle E_1 | \Phi_1(L, t) - \Phi_2(L, t) | E_2 \rangle = 0 \quad (3.212)$$

and

$$\lim_{x \rightarrow 0} \langle E_1 | \Phi_1(x, t) + \Phi_2(x, t) | E_2 \rangle = 0 \quad (3.213)$$

$$\lim_{x \rightarrow L} \langle E_1 | \partial_x \Phi_1(x, t) - \partial_x \Phi_2(x, t) | E_2 \rangle = \frac{1}{16Lg} \langle E_1 | \Phi_1(L, t) - \Phi_2(L, t) | E_2 \rangle \quad (3.214)$$

$$\lim_{g \rightarrow \infty} \lim_{x \rightarrow L} \langle E_1 | \Phi_1(x, t) + \Phi_2(x, t) | E_2 \rangle = 0 \quad (3.215)$$

$$\lim_{g \rightarrow \infty} \lim_{x \rightarrow L} \langle E_1 | \Phi_1(x, t) - \Phi_2(x, t) | E_2 \rangle \neq 0 , \quad (3.216)$$

where $|E_1\rangle$ and $|E_2\rangle$ are eigenstates of H .

In perturbation theory there are divergences if we take $x = L$ at the beginning. However, if one allows x to take general values, then in Rayleigh-Schrödinger perturbation theory for the differences of the energy levels one can expect to get sums at any fixed order which are possible to evaluate. We expect that the evaluation yields, besides non-singular parts, $\Theta(x - L)$, $\delta(x - L)$ and its derivatives, and taking the $x \rightarrow L$ limit gives finite result eventually.

3.5.5 Bethe-Yang equations

The Bethe-Yang equations can be used to give a description of the spectrum of models in finite volume which have factorized scattering in their infinite volume limit. The Bethe-Yang equations for models defined on a cylinder are exposed, for example, in [108, 109,

110]; for models defined on a strip they were written down in [111, 112]. It should be noted that the Bethe-Yang equations usually give approximate result only.

In the case of the model that we study the ingredients of the Bethe-Yang description are the following: there is a single massless particle with fermionic statistics, the two-particle S-matrix is a constant scalar $S(k) = -1$, where k is the relative momentum. The reflection matrix on the left-hand side can be read from (3.173), it is $R_L(k) = -1$, the reflection matrix on the right-hand side can be read from (3.174), it is

$$R_R(k) = \frac{16Lh^2 + ik}{16Lh^2 - ik} . \quad (3.217)$$

The transfer matrices for N -particle states are scalars:

$$\begin{aligned} T_i(k_1, k_2, \dots, k_N) &= \\ &= R_L(k_i) R_R(k_i) \prod_{j, j \neq k} S(k_i + k_j) \prod_{j, j \neq k} S(k_i - k_j) = -R_R(k_i) , \quad i = 1 \dots N , \end{aligned} \quad (3.218)$$

where $k_1 > k_2 > \dots k_N \neq 0$. This very simple form is the consequence of the simplicity of the S-matrix. The Bethe-Yang equations for the momenta $k_1, k_2, \dots k_N$ of the N -particle states take the form

$$e^{2ik_i L} T_i(k_1, k_2, \dots, k_N) = e^{2ik_i L} \frac{ik_i + 16Lh^2}{ik_i - 16Lh^2} = 1 , \quad i = 1 \dots N . \quad (3.219)$$

The total energy of an N -particle state in the Bethe-Yang framework is

$$E = \sum_{i=1}^N k_i . \quad (3.220)$$

(3.219) can be rewritten as

$$k_i L \tan(k_i L) = 16L^2 h^2 , \quad i = 1 \dots N , \quad (3.221)$$

which has the same form as (3.135). This means that the Bethe-Yang description reproduces the result of Section 3.5.3 for the spectrum exactly.

The ‘reverse’ model is similar, one can read from (3.213) and (3.214) that

$$R_L(k) = -1 , \quad R_R(k) = \frac{1 - ik16Lg}{1 + ik16Lg} , \quad (3.222)$$

and the Bethe-Yang equations for the momenta can be written as

$$k_i L \tan(k_i L) = \frac{-1}{16g} , \quad i = 1 \dots N , \quad (3.223)$$

which has the same form as (3.208), i.e. the result of Section 3.5.4 for the spectrum is reproduced exactly.

3.6 Exact spectrum in the Mode Truncated version

3.6.1 The free model

Let n_c , called the truncation level, be a positive integer. The mode truncated version of the free model described in Section 3.5.2 is the following:

$$\{\Psi_1(x, t), \Psi_1(y, t)\} = 2[1 + 2 \sum_{k \in \frac{\pi}{L}\{1 \dots n_c\}} \cos(k(x - y))] \quad (3.224)$$

$$\{\Psi_2(x, t), \Psi_2(y, t)\} = 2[1 + 2 \sum_{k \in \frac{\pi}{L}\{1 \dots n_c\}} \cos(k(x - y))] \quad (3.225)$$

$$\{\Psi_1(x, t), \Psi_2(y, t)\} = -2[1 + 2 \sum_{k \in \frac{\pi}{L}\{1 \dots n_c\}} \cos(k(x + y))] \quad (3.226)$$

$$\{A_2(t), \Psi_1(x, t)\} = 0 \quad (3.227)$$

$$\{A_2(t), \Psi_2(x, t)\} = 0 \quad (3.228)$$

$$\{A_2(t), A_2(t)\} = 2 \quad (3.229)$$

$$\Psi_1(x, t)^\dagger = \Psi_1(x, t) \quad \Psi_2(x, t)^\dagger = \Psi_2(x, t) \quad A_2(t)^\dagger = A_2(t) \quad (3.230)$$

$$\Psi_1(x, t) = \sum_{k \in \frac{\pi}{L}\{1 \dots n_c\}} \sqrt{2}[a(k)e^{ik(t-x)} + a^+(k)e^{-ik(t-x)}] + A_1 \quad (3.231)$$

$$\Psi_2(x, t) = \sum_{k \in \frac{\pi}{L}\{1 \dots n_c\}} \sqrt{2}[-a(k)e^{ik(t+x)} - a^+(k)e^{-ik(t+x)}] - A_1 \quad (3.232)$$

The equations (3.94)-(3.97) apply unchanged.

The Hamiltonian operator is

$$H_0 = \sum_{k \in \frac{\pi}{L}\{1 \dots n_c\}} k[a(k)a^+(k)] \quad (3.233)$$

The equations of motion are

$$\partial_t \Psi_1(x, t) = [iH_0, \Psi_1(x, t)] = -\partial_x \Psi_1(x, t) \quad (3.234)$$

$$\partial_t \Psi_2(x, t) = [iH_0, \Psi_2(x, t)] = \partial_x \Psi_2(x, t) \quad (3.235)$$

$$\partial_t A_2(t) = [iH_0, A_2(t)] = 0 \quad (3.236)$$

The Hilbert space and the energy eigenstates are similar to those in Section 3.5.2, but

$$k \in \frac{\pi}{L}\{-n_c, -n_c + 1, \dots, n_c - 1, n_c\} \quad (3.237)$$

applies instead of $k \in \pi\mathbb{Z}/L$. The Hilbert space is 2×2^{n_c} dimensional.

3.6.2 The perturbed model

The perturbed Hamiltonian operator is $H_0 + hH_I$, where

$$H_I = iA_2(0)[\Psi_2(L, 0) - \Psi_1(L, 0)] . \quad (3.238)$$

The equations of motion are

$$\partial_t \Psi_1(x, t) = [i(H_0 + hH_I), \Psi_1(x, t)] = -\partial_x \Psi_1(x, t) - hA_2(t)C_1(x) \quad (3.239)$$

$$\partial_t \Psi_2(x, t) = [i(H_0 + hH_I), \Psi_2(x, t)] = \partial_x \Psi_2(x, t) - hA_2(t)C_2(x) \quad (3.240)$$

$$\frac{d}{dt}A_2(t) = [i(H_0 + hH_I), A_2(t)] = 2h(\Psi_2(L, t) - \Psi_1(L, t)) , \quad (3.241)$$

where

$$C_1(x) = \{\Psi_1(x, t), \Psi_2(L, t) - \Psi_1(L, t)\} = -4[1 + 2 \sum_{k \in \frac{\pi}{L}\{1 \dots n_c\}} \cos(k(x + L))] \quad (3.242)$$

$$C_2(x) = \{\Psi_2(x, t), \Psi_2(L, t) - \Psi_1(L, t)\} = -C_1(x) . \quad (3.243)$$

These equations are linear as in the non-truncated case, so sandwiching them between energy eigenstates gives a system of 3 first-order linear partial differential equations for the expectation values. The analogue of (3.135) can be obtained from these equations in the following way: we can eliminate A_2 :

$$\partial_t^2 \Psi_1(x, t) = -\partial_{xt} \Psi_1(x, t) - 2h^2(\Psi_2(L, t) - \Psi_1(L, t))C_1(x) \quad (3.244)$$

$$\partial_t^2 \Psi_2(x, t) = \partial_{xt} \Psi_1(x, t) - 2h^2(\Psi_2(L, t) - \Psi_1(L, t))C_2(x) \quad (3.245)$$

and introduce the functions $f_1(x)$, $f_2(x)$:

$$\langle E_1 | \Psi_1(x, t) | E_2 \rangle = f_1(x) e^{ikt} \quad (3.246)$$

$$\langle E_1 | \Psi_2(x, t) | E_2 \rangle = f_2(x) e^{ikt} , \quad (3.247)$$

where $k = E_1 - E_2$ and the dependence of f_1 and f_2 on k is not denoted explicitly. Equations (3.244) and (3.245) give

$$-k^2 f_1(x) = -ik f_1'(x) - 2h^2(f_2(L) - f_1(L))C_1(x) \quad (3.248)$$

$$-k^2 f_2(x) = ik f_2'(x) - 2h^2(f_2(L) - f_1(L))C_2(x) . \quad (3.249)$$

We also have the boundary conditions

$$f_1(0) = -f_2(0) \quad (3.250)$$

$$f_1(L) = -f_2(L) \quad (3.251)$$

so

$$-k^2 f_1(x) = -ik f_1'(x) + 4h^2 C_1(x) f_1(L) \quad (3.252)$$

$$-k^2 f_2(x) = ik f_2'(x) - 4h^2 C_2(x) f_2(L) . \quad (3.253)$$

These are almost first-order inhomogeneous linear ordinary differential equations, the difference is that the inhomogeneity depends on the unknown functions. The method of undetermined coefficients can nevertheless be applied:

$$f_1(x) = C(x) e^{-ikx} \quad (3.254)$$

$$C'(x) = \frac{4h^2}{ik} e^{ikx} C_1(x) f_1(L) \quad (3.255)$$

$$C(x) = C(0) + \int_0^x dx' \frac{4h^2}{ik} e^{ikx'} C_1(x') f_1(L) = C(0) + I_1(x) \quad (3.256)$$

$$f_1(L) = C(L) e^{-ikL} = [C(0) + \int_0^L dx' \frac{4h^2}{ik} e^{ikx'} C_1(x') f_1(L)] e^{-ikL} \quad (3.257)$$

$$C(0) = f_1(0) , \quad (3.258)$$

$$f_2(x) = D(x) e^{ikx} \quad (3.259)$$

$$D'(x) = \frac{4h^2}{ik} e^{-ikx} C_2(x) f_2(L) \quad (3.260)$$

$$D(x) = D(0) + \int_0^x dx' \frac{4h^2}{ik} e^{-ikx'} C_2(x') f_2(L) = D(0) + I_2(x) \quad (3.261)$$

$$f_2(L) = D(L) e^{ikL} = [D(0) + \int_0^L dx' \frac{4h^2}{ik} e^{-ikx'} C_2(x') f_2(L)] e^{ikL} \quad (3.262)$$

$$D(0) = f_2(0) . \quad (3.263)$$

In particular

$$f_1(L) e^{ikL} = C(0) + I_1(L) \quad (3.264)$$

$$f_2(L) e^{-ikL} = D(0) + I_2(L) . \quad (3.265)$$

Using the boundary condition $C(0) + D(0) = 0$:

$$I_1(L) + I_2(L) = f_1(L) e^{ikL} + f_2(L) e^{-ikL} , \quad (3.266)$$

and then the boundary condition $f_1(L) + f_2(L) = 0$:

$$\int_0^L dx' \frac{4h^2}{ik} [e^{ikx'} C_1(x') - e^{-ikx'} C_2(x')] = e^{ikL} - e^{-ikL} . \quad (3.267)$$

Simplifying this equation we finally obtain

$$16h^2 \left[\frac{1}{k^2} + \sum_{k_0 \in \frac{\pi}{L}\{1 \dots n_c\}} \frac{2}{k^2 - k_0^2} \right] = 1, \quad (3.268)$$

which is the analogue of (3.135) and determines the energy of the modes as functions of h .

(3.268) as an algebraic equation for k has finitely many real roots, and if k is a root, then $-k$ is a root as well. All real roots converge to finite values as $h \rightarrow \infty$ except for the pair with the largest absolute value. This pair of roots diverges linearly as $h \rightarrow \infty$. This pair has the largest absolute value already at $h = 0$. A consequence of this behaviour is that the lower half of the spectrum, namely those states which do not contain the mode with the highest energy, remains finite as $h \rightarrow \infty$, whereas the higher half of the spectrum, i.e. the states which contain the mode with the highest energy, diverges linearly as $h \rightarrow \infty$ with a common slope. Here it is assumed that the ground state energy is set to zero. In the subsequent sections we shall consider the lower half of the spectrum. The look of this half as a function of h is very similar to that shown in Figure 3.1. We remark that it is not hard to see that the two halves of the spectrum are mirror symmetric with respect to a horizontal line, if the ground state energy is set appropriately.

Applying the formula

$$1 + \sum_{n=1}^{\infty} \frac{2k^2}{k^2 - 4n^2\pi^2} = \frac{k/2}{\tan(k/2)} \quad (3.269)$$

we can easily verify that the limit of (3.268) as $n_c \rightarrow \infty$ is (3.135).

3.7 Power series expansion of the energy levels

The eigenvectors of H_0 suitable for Rayleigh-Schrödinger perturbation theory are those introduced in (3.98). Degenerate perturbation theory has to be used.

The nonzero matrix elements of H_I in Section 3.5.3 are the following:

$$\langle Qu | H_I | Qu \rangle = 2 \quad (3.270)$$

$$\langle Qv | H_I | Qv \rangle = -2 \quad (3.271)$$

$$\langle Qu | H_I | Pv \rangle = \langle Pv | H_I | Qu \rangle = 2\sqrt{2}(-1)^{n+m}(-1)^{kL/\pi} \quad (3.272)$$

$$\langle Qv | H_I | Pu \rangle = \langle Pu | H_I | Qv \rangle = -2\sqrt{2}(-1)^{n+m}(-1)^{kL/\pi}, \quad (3.273)$$

where

$$P = a(k_1)a(k_2) \dots a(k_m)a(k)a(k_{m+1}) \dots a(k_n) \quad (3.274)$$

$$Q = a(k_1)a(k_2) \dots a(k_n). \quad (3.275)$$

We remark that certain perturbative calculations were also done in [113].

Non-truncated case: The eigenvalue of the state starting from $|a(\frac{N_1\pi}{L})a(\frac{N_2\pi}{L})\dots a(\frac{N_r\pi}{L})v\rangle$ at $h = 0$ is

$$E_{\{N_1, N_2, \dots, N_r, v\}}(h) = \frac{(N_1 + N_2 + \dots + N_r)\pi}{L} - 2h + \left(\frac{16L}{\pi}\left(\frac{1}{N_1} + \frac{1}{N_2} + \dots + \frac{1}{N_r}\right) - \sum_{n=1}^{\infty} \frac{8L}{n\pi}\right)h^2 + \left(\sum_{n=1}^{\infty} \frac{32L^2}{n^2\pi^2}\right)h^3 + \dots \quad (3.276)$$

and the eigenvalue of the state starting form $|a(\frac{N_1\pi}{L})a(\frac{N_2\pi}{L})\dots a(\frac{N_r\pi}{L})u\rangle$ at $h = 0$ is

$$E_{\{N_1, N_2, \dots, N_r, u\}}(h) = \frac{(N_1 + N_2 + \dots + N_r)\pi}{L} + 2h + \left(\frac{16L}{\pi}\left(\frac{1}{N_1} + \frac{1}{N_2} + \dots + \frac{1}{N_r}\right) - \sum_{n=1}^{\infty} \frac{8L}{n\pi}\right)h^2 + \left(-\sum_{n=1}^{\infty} \frac{32L^2}{n^2\pi^2}\right)h^3 + \dots \quad (3.277)$$

In particular

$$E_{\{v\}}(h) = 0 - 2h - \sum_{n=1}^{\infty} \frac{8L}{n\pi}h^2 + h^3 \sum_{n=1}^{\infty} \frac{32L^2}{n^2\pi^2} + \dots \quad (3.278)$$

$$E_{\{u\}}(h) = 0 + 2h - \sum_{n=1}^{\infty} \frac{8L}{n\pi}h^2 - h^3 \sum_{n=1}^{\infty} \frac{32L^2}{n^2\pi^2} + \dots \quad (3.279)$$

We note that the coefficient of h^2 is ultraviolet divergent and should be regularized. The TCSA and the mode truncation both provide a regularization.

The energy differences corresponding to the creation operators $b(k(n, h))$ are the following: for $n = 0$

$$\Delta E_0(h) = E_{\{u\}}(h) - E_{\{v\}}(h) = 0 + 4h + 0 + h^3 \left(-\sum_{n=1}^{\infty} \frac{64L^2}{n^2\pi^2}\right) + \dots \quad (3.280)$$

and for $n = N > 0$

$$\Delta E_N = E_{\{N, u\}}(h) - E_{\{v\}}(h) = \frac{N\pi}{L} + 0 + h^2 \frac{16L}{N\pi} + 0 + \dots \quad (3.281)$$

Generally

$$E_{\{N_1, N_2, \dots, N_r, v\}}(h) - E_{\{v\}}(h) = \frac{(N_1 + N_2 + \dots + N_r)\pi}{L} + 0 \cdot h + \frac{16L}{\pi}\left(\frac{1}{N_1} + \frac{1}{N_2} + \dots + \frac{1}{N_r}\right)h^2 + 0 \cdot h^3 + \dots \quad (3.282)$$

$$E_{\{N_1, N_2, \dots, N_r, v\}}(h) - E_{\{u\}}(h) = \frac{(N_1 + N_2 + \dots + N_r)\pi}{L} - 4h + \frac{16L}{\pi} \left(\frac{1}{N_1} + \frac{1}{N_2} + \dots + \frac{1}{N_r} \right) h^2 + \left(\sum_{n=1}^{\infty} \frac{64L^2}{n^2\pi^2} \right) h^3 + \dots \quad (3.283)$$

$$E_{\{N_1, N_2, \dots, N_r, u\}}(h) - E_{\{u\}}(h) = \frac{(N_1 + N_2 + \dots + N_r)\pi}{L} + 0 \cdot h + \frac{16L}{\pi} \left(\frac{1}{N_1} + \frac{1}{N_2} + \dots + \frac{1}{N_r} \right) h^2 + 0 \cdot h^3 + \dots \quad (3.284)$$

$$E_{\{N_1, N_2, \dots, N_r, u\}}(h) - E_{\{v\}}(h) = \frac{(N_1 + N_2 + \dots + N_r)\pi}{L} + 4h + \frac{16L}{\pi} \left(\frac{1}{N_1} + \frac{1}{N_2} + \dots + \frac{1}{N_r} \right) h^2 - \left(\sum_{n=1}^{\infty} \frac{64L^2}{n^2\pi^2} \right) h^3 + \dots \quad (3.285)$$

MT scheme:

$$E_{\{N_1, N_2, \dots, N_r, v\}}(h) = \frac{(N_1 + N_2 + \dots + N_r)\pi}{L} - 2h + \left(\frac{16L}{\pi} \left(\frac{1}{N_1} + \frac{1}{N_2} + \dots + \frac{1}{N_r} \right) - \sum_{n=1}^{n_c} \frac{8L}{n\pi} \right) h^2 + \left(\sum_{n=1}^{n_c} \frac{32L^2}{n^2\pi^2} \right) h^3 + \dots \quad (3.286)$$

$$E_{\{N_1, N_2, \dots, N_r, u\}}(h) = \frac{(N_1 + N_2 + \dots + N_r)\pi}{L} + 2h + \left(\frac{16L}{\pi} \left(\frac{1}{N_1} + \frac{1}{N_2} + \dots + \frac{1}{N_r} \right) - \sum_{n=1}^{n_c} \frac{8L}{n\pi} \right) h^2 + \left(- \sum_{n=1}^{n_c} \frac{32L^2}{n^2\pi^2} \right) h^3 + \dots \quad (3.287)$$

$$E_{\{v\}}(h) = 0 - 2h - \sum_{n=1}^{n_c} \frac{8L}{n\pi} h^2 + h^3 \sum_{n=1}^{n_c} \frac{32L^2}{n^2\pi^2} + \dots \quad (3.288)$$

$$E_{\{u\}}(h) = 0 + 2h - \sum_{n=1}^{n_c} \frac{8L}{n\pi} h^2 - h^3 \sum_{n=1}^{n_c} \frac{32L^2}{n^2\pi^2} + \dots \quad (3.289)$$

$$\Delta E_0(h) = E_{\{u\}}(h) - E_{\{v\}}(h) = 0 + 4h + 0 + h^3 \left(- \sum_{n=1}^{n_c} \frac{64L^2}{n^2\pi^2} \right) + \dots \quad (3.290)$$

$$\Delta E_N = E_{\{N, u\}}(h) - E_{\{v\}}(h) = \frac{N\pi}{L} + 0 + h^2 \frac{16L}{N\pi} + 0 + \dots \quad (3.291)$$

In these formulae n_c is the truncation level introduced in Section 3.6.1.

Generally

$$E_{\{N_1, N_2, \dots, N_r, v\}}(h) - E_{\{v\}}(h) = \frac{(N_1 + N_2 + \dots + N_r)\pi}{L} + 0 \cdot h + \frac{16L}{\pi} \left(\frac{1}{N_1} + \frac{1}{N_2} + \dots + \frac{1}{N_r} \right) h^2 + 0 \cdot h^3 + \dots \quad (3.292)$$

$$E_{\{N_1, N_2, \dots, N_r, v\}}(h) - E_{\{u\}}(h) = \frac{(N_1 + N_2 + \dots + N_r)\pi}{L} - 4h + \frac{16L}{\pi} \left(\frac{1}{N_1} + \frac{1}{N_2} + \dots + \frac{1}{N_r} \right) h^2 + \left(\sum_{n=1}^{n_c} \frac{64L^2}{n^2\pi^2} \right) h^3 + \dots \quad (3.293)$$

$$E_{\{N_1, N_2, \dots, N_r, u\}}(h) - E_{\{u\}}(h) = \frac{(N_1 + N_2 + \dots + N_r)\pi}{L} + 0 \cdot h + \frac{16L}{\pi} \left(\frac{1}{N_1} + \frac{1}{N_2} + \dots + \frac{1}{N_r} \right) h^2 + 0 \cdot h^3 + \dots \quad (3.294)$$

$$E_{\{N_1, N_2, \dots, N_r, u\}}(h) - E_{\{v\}}(h) = \frac{(N_1 + N_2 + \dots + N_r)\pi}{L} + 4h + \frac{16L}{\pi} \left(\frac{1}{N_1} + \frac{1}{N_2} + \dots + \frac{1}{N_r} \right) h^2 - \left(\sum_{n=1}^{n_c} \frac{64L^2}{n^2\pi^2} \right) h^3 + \dots \quad (3.295)$$

TCS scheme:

$$E_{\{N_1, N_2, \dots, N_r, v\}}(h) = \frac{(N_1 + N_2 + \dots + N_r)\pi}{L} - 2h + \left(\frac{16L}{\pi} \left(\frac{1}{N_1} + \frac{1}{N_2} + \dots + \frac{1}{N_r} \right) - \sum_{n=1}^{n_m} \frac{8L}{n\pi} \right) h^2 + \left(\sum_{n=1}^{n_m} \frac{32L^2}{n^2\pi^2} \right) h^3 + \dots \quad (3.296)$$

$$E_{\{N_1, N_2, \dots, N_r, u\}}(h) = \frac{(N_1 + N_2 + \dots + N_r)\pi}{L} + 2h + \left(\frac{16L}{\pi} \left(\frac{1}{N_1} + \frac{1}{N_2} + \dots + \frac{1}{N_r} \right) - \sum_{n=1}^{n_m} \frac{8L}{n\pi} \right) h^2 + \left(- \sum_{n=1}^{n_m} \frac{32L^2}{n^2\pi^2} \right) h^3 + \dots \quad (3.297)$$

where $n_m = n_c - (N_1 + N_2 + \dots + N_r)$, n_c is the conformal truncation level.

$$E_{\{v\}}(h) = 0 - 2h - \sum_{n=1}^{n_c} \frac{8L}{n\pi} h^2 + h^3 \sum_{n=1}^{n_c} \frac{32L^2}{n^2\pi^2} + \dots \quad (3.298)$$

$$E_{\{u\}}(h) = 0 + 2h - \sum_{n=1}^{n_c} \frac{8L}{n\pi} h^2 - h^3 \sum_{n=1}^{n_c} \frac{32L^2}{n^2\pi^2} + \dots \quad (3.299)$$

$$\Delta E_0(h) = E_{\{u\}}(h) - E_{\{v\}}(h) = 0 + 4h + 0 + h^3 \left(- \sum_{n=1}^{n_c} \frac{64L^2}{n^2\pi^2} \right) + \dots \quad (3.300)$$

$$\Delta E_N = E_{\{N,u\}}(h) - E_{\{v\}}(h) = \frac{N\pi}{L} + 0 + h^2 \left(\frac{16L}{N\pi} + \sum_{n=n_m+1}^{n_c} \frac{8L}{n\pi} \right) + h^3 \sum_{n=n_m+1}^{n_c} \frac{32L^2}{n^2\pi^2} + \dots \quad (3.301)$$

Generally

$$\begin{aligned} E_{\{N_1, N_2, \dots, N_r, v\}}(h) - E_{\{v\}}(h) &= \frac{(N_1 + N_2 + \dots + N_r)\pi}{L} + 0 + \\ &+ \left(\frac{16L}{\pi} \left(\frac{1}{N_1} + \frac{1}{N_2} + \dots + \frac{1}{N_r} \right) + \sum_{n=n_m+1}^{n_c} \frac{8L}{n\pi} \right) h^2 - \sum_{n=n_m+1}^{n_c} \frac{32L^2}{n^2\pi^2} h^3 + \dots \end{aligned} \quad (3.302)$$

$$\begin{aligned} E_{\{N_1, N_2, \dots, N_r, v\}}(h) - E_{\{u\}}(h) &= \frac{(N_1 + N_2 + \dots + N_r)\pi}{L} - 4h + \\ &+ \left(\frac{16L}{\pi} \left(\frac{1}{N_1} + \frac{1}{N_2} + \dots + \frac{1}{N_r} \right) + \sum_{n=n_m+1}^{n_c} \frac{8L}{n\pi} \right) h^2 + \left(\sum_{n=n_1}^{n_m} \frac{32L^2}{n^2\pi^2} + \sum_{n=1}^{n_c} \frac{32L^2}{n^2\pi^2} \right) h^3 + \dots \end{aligned} \quad (3.303)$$

$$\begin{aligned} E_{\{N_1, N_2, \dots, N_r, u\}}(h) - E_{\{u\}}(h) &= \frac{(N_1 + N_2 + \dots + N_r)\pi}{L} + 0 + \\ &+ \left(\frac{16L}{\pi} \left(\frac{1}{N_1} + \frac{1}{N_2} + \dots + \frac{1}{N_r} \right) + \sum_{n=n_m+1}^{n_c} \frac{8L}{n\pi} \right) h^2 + \sum_{n=n_m+1}^{n_c} \frac{32L^2}{n^2\pi^2} h^3 + \dots \end{aligned} \quad (3.304)$$

$$\begin{aligned} E_{\{N_1, N_2, \dots, N_r, u\}}(h) - E_{\{v\}}(h) &= \frac{(N_1 + N_2 + \dots + N_r)\pi}{L} + 4h + \\ &+ \left(\frac{16L}{\pi} \left(\frac{1}{N_1} + \frac{1}{N_2} + \dots + \frac{1}{N_r} \right) + \sum_{n=n_m+1}^{n_c} \frac{8L}{n\pi} \right) h^2 - \left(\sum_{n=n_1}^{n_m} \frac{32L^2}{n^2\pi^2} + \sum_{n=1}^{n_c} \frac{32L^2}{n^2\pi^2} \right) h^3 + \dots \end{aligned} \quad (3.305)$$

We remark that the above formulae show that the truncated energy gaps converge to the non-truncated energy gaps as $1/n_c$.

3.8 Perturbative results

The renormalized Hamiltonian operator is

$$H^r = s_0(h, n_c)H_0 + s_1(h, n_c)H_I, \quad (3.306)$$

where the functions $s_0(h, n_c)$ and $s_1(h, n_c)$ are determined by the renormalization condition, n_c is the truncation level. The renormalization condition in the present case is the following: the differences of those eigenvalues of H^r that are low compared to the truncation level should be equal to those of the truncated Hamiltonian operator $H^t(n_c)$. $H^t(n_c)$ is, in particular, the TCSA Hamiltonian operator $H^{TCSA}(n_c)$, or the Hamiltonian operator $H^{MT}(n_c)$ of the mode truncated model. This condition applies separately and independently within the u and v sectors, and we have in fact a pair s_0^u, s_1^u for the u sector and another pair s_0^v, s_1^v for the v sector.

The renormalization condition is a very strong condition on s_0 and s_1 and generally we cannot expect that it can be satisfied. It is possible, however, that it can be satisfied in certain approximations.

3.8.1 Mode Truncation Scheme

Using the equations (3.292)-(3.295) in Section 3.7 we can obtain the following results:

The renormalization conditions have a solution if the eigenfunctions are expanded into a power series in h and terms that are of order higher than 3 are omitted:

$$s_0(h, n_c) = 1 + x_1 h^2 + O(h^4) \quad (3.307)$$

$$s_1(h, n_c) = h + x_2 h^3 + O(h^4) \quad (3.308)$$

$$x_1 = 0 \quad x_2 = \frac{1}{2}(S - S(n_c))L^2 \quad (3.309)$$

where

$$S = \sum_{n=1}^{\infty} \frac{32}{n^2 \pi^2} \quad S(n_c) = \sum_{n=1}^{n_c} \frac{32}{n^2 \pi^2} . \quad (3.310)$$

This solution applies to both the u and v sectors and it is exact in n_c . We remark that

$$S - S(n_c) = \frac{32}{\pi^2 n_c} + O(1/n_c^2) . \quad (3.311)$$

In the MT scheme we can obtain another result that is not perturbative in h : doing power series expansion we obtain the formula

$$\frac{1}{k^2} + \sum_{n=1}^{n_c} \frac{2}{k^2 - \frac{\pi^2}{L^2} n^2} = \frac{L}{k \tan(kL)} + \frac{2L^2}{\pi^2} + \frac{1}{n_c} + O(1/n_c^2) . \quad (3.312)$$

Omitting the terms which are of second or higher order in $1/n_c$, equation (3.268) takes the form

$$1 = 16h^2 \left(\frac{L}{k \tan(kL)} + \frac{2L^2}{\pi^2} + \frac{1}{n_c} \right) \quad (3.313)$$

or

$$kL \tan(kL) = 16L^2 h^2 \frac{1}{1 - \frac{32L^2 h^2}{\pi^2 n_c}} \quad (3.314)$$

which takes the form of (3.135) if

$$h_{\text{eff}} = \frac{h}{\sqrt{1 - \frac{32L^2 h^2}{\pi^2 n_c}}} = h + 16h^3 \frac{L^2}{\pi^2} \frac{1}{n_c} + O(1/n_c^2) \quad (3.315)$$

is introduced:

$$kL \tan(kL) = 16L^2 h_{\text{eff}}^2 . \quad (3.316)$$

This means that rescaling by

$$s_0(h, n_c) = 1 + O(1/n_c^2) \quad (3.317)$$

$$s_1(h, n_c) = h + 16h^3 \frac{L^2}{\pi^2} \frac{1}{n_c} + O(1/n_c^2) \quad (3.318)$$

improves the convergence of the mode truncated energy gaps to the exact energy gaps from order $1/n_c$ to order $1/n_c^2$, i.e. the difference between the energy gaps of $s_0(h, n_c)H_0 + s_1(h, n_c)H_I$ and the energy gaps of $(H_0 + hH_I)^{MT}$ tends to zero as $1/n_c^2$ for any fixed finite value of h , whereas the difference between the energy gaps of $H_0 + hH_I$ and $(H_0 + hH_I)^{MT}$ tends to zero as $1/n_c$.

3.8.2 TCS scheme

Using the equations (3.302)-(3.305) in Section 3.7 we obtain the following results:

The renormalization conditions have a solution if the eigenfunctions are expanded into a power series in h and in $1/n_c$ and terms that are of order higher than 3 in h and 1 in $1/n_c$ are omitted:

$$s_0(h, n_c) = 1 + x_1 h^2 + y_1 h^3 + O(h^4) \quad (3.319)$$

$$s_1(h, n_c) = h + y_2 h^2 + x_2 h^3 + O(h^4) \quad (3.320)$$

$$x_1 = \frac{8L^2}{\pi^2 n_c} + O(1/n_c^2) \quad y_1 = 0 + O(1/n_c^2) \quad (3.321)$$

$$x_2 = \frac{1}{2}(S - S(n_c))L^2 + O(1/n_c^2) \quad y_2 = 0 + O(1/n_c^2) . \quad (3.322)$$

This solution applies to both sectors. If terms of order $1/n_c^2$ are also taken into consideration, then the renormalization conditions do not have a solution.

Calculating $s_0(h, n_c)$ and $s_1(h, n_c)$ from the three lowest energy levels gives the result

$$s_0^u(h, n_c) = 1 + h^2 \frac{8L^2}{(n_c - 1)\pi^2} - h^3 \frac{32L^3}{(n_c - 1)^2 n_c \pi^3} + O(h^4) \quad (3.323)$$

$$s_1^u(h, n_c) = h + \frac{2L}{(n_c^2 - n_c)\pi} h^2 + \left[\frac{16L^2(1 - 5n_c + 3n_c^2)}{2(n_c - 1)^2 n_c^2 \pi^2} + \frac{1}{2}(S - S(n_c))L^2 \right] h^3 + O(h^4) \quad (3.324)$$

in the u sector and

$$s_0^v(h, n_c) = 1 + h^2 \frac{8L^2}{(n_c - 1)\pi^2} + h^3 \frac{32L^3}{(n_c - 1)^2 n_c \pi^3} + O(h^4) \quad (3.325)$$

$$s_1^v(h, n_c) = h - \frac{2L}{(n_c^2 - n_c)\pi} h^2 + \left[\frac{16L^2(1 - 5n_c + 3n_c^2)}{2(n_c - 1)^2 n_c^2 \pi^2} + \frac{1}{2}(S - S(n_c))L^2 \right] h^3 + O(h^4) \quad (3.326)$$

in the v sector. These formulae are exact in n_c . In this case $s_0(h, n_c)$ and $s_1(h, n_c)$ are given by the following formulae:

$$\frac{s_1}{s_0}(h) = \left(\frac{E_2 - E_0}{E_1 - E_0} \right)^{-1} \left(\left(\frac{E_2 - E_0}{E_1 - E_0} \right)^{TCSA} (h) \right) \quad (3.327)$$

$$s_0(h) = \frac{(E_1 - E_0)^{TCSA}(h)}{(E_1 - E_0)(\frac{s_1}{s_0}(h))}, \quad (3.328)$$

where the superscriptless quantities are the non-truncated ones. E_0, E_1, E_2 denote the three lowest energy eigenvalues.

The coefficient y_1 of h^3 in $s_0(h)$ and the coefficient y_2 of h^2 in $s_1(h)$ depend on which three energy levels one uses to calculate them, and the same applies to that part of x_1 and x_2 which is beyond first order in $1/n_c$.

3.9 Numerical results

In the numerical calculations described in this section the value of L was set equal to 1. This does not affect the generality of the results. In the calculations we used the same normalizations as in Section 3.5.

3.9.1 Mode Truncation Scheme

Figure 3.2 shows the exact and mode truncated spectra as a function of the logarithm of the coupling constant. The truncation level is $n_c = 9$, and the dimension of the Hilbert space is 512 in each sector. It is remarkable that there is a good qualitative agreement

between the mode truncated and exact spectra for all values of h . Numerical values are listed in Table 3.3 for the fifth energy gap $k(3, h) + k(0, h)$ of the v sector and in Table 3.5 for the fifth energy gap $k(4, h) - k(0, h)$ of the u sector. The number of digits presented do not exceed the numerical precision.

Figure 3.3 shows the same spectra, but the lowest gap is normalized to 1, i.e. the functions $\frac{E_i(h) - E_0(h)}{E_1(h) - E_0(h)}$ are shown. It is remarkable that the agreement between exact and mode truncated spectra looks considerably better than in the case of not normalized spectra.

Figures 3.4-3.6 show the functions $s_0(h)$, $s_1(h)$, $s_1(h)/s_0(h)$ determined by the lowest three energy levels in the v sector via the formulae (3.327), (3.328) in various ranges. Figure 3.5 and 3.6 also show the curves given by (3.307) and (3.308) on the left-hand side (red/grey line). $s_0(h)$ remains close to 1 and for large values of h it tends to a constant which can be expected to converge to 1 as $n_c \rightarrow \infty$. $s_1(h)$ also tends to a constant for large values of h which can be expected to increase to infinity as $n_c \rightarrow \infty$. The behaviour of $s_1(h)/s_0(h)$ and $s_1(h)$ are similar.

Figure 3.7.a shows the normalized mode truncated spectrum and the normalized exact spectrum rescaled by $s_0(h)$ and $s_1(h)$ in the v sector. No difference between the two is visible. In Table 3.2 values of the fifth normalized energy gap $\frac{k(3, h) + k(0, h)}{k(1, h) + k(0, h)}$ of the v sector are listed: the values in the non-truncated case are listed in the first column, the values in the mode truncated case are listed in the second column and the rescaled non-truncated values are listed in the third column (which would be the same as the values in the second column if the renormalization could be satisfied exactly).

Figure 3.7.b shows the normalized mode truncated spectrum and the normalized exact spectrum rescaled by $s_0(h)$ and $s_1(h)$ in the u sector. The $s_0(h)$, $s_1(h)$ obtained in the v sector were used for the rescaling, which corresponds to the assumption that $s_0(h)$ and $s_1(h)$ are the same for both sectors. The difference between the mode truncated and rescaled exact spectra is not visible in the figure.

We also see from Table 3.4 in which values of the fourth normalized energy gap $\frac{k(3, h) - k(0, h)}{k(1, h) - k(0, h)}$ of the u sector are listed that the rescaling together with the above assumption works well.

We have not tried to calculate s_0 and s_1 for the u sector because $\frac{E_2 - E_0}{E_1 - E_0}(h)$ is not invertible in this case. One way to circumvent this difficulty would be to use other energy levels E_i, E_j, E_k for which $\frac{E_i - E_k}{E_j - E_k}(h)$ is invertible.

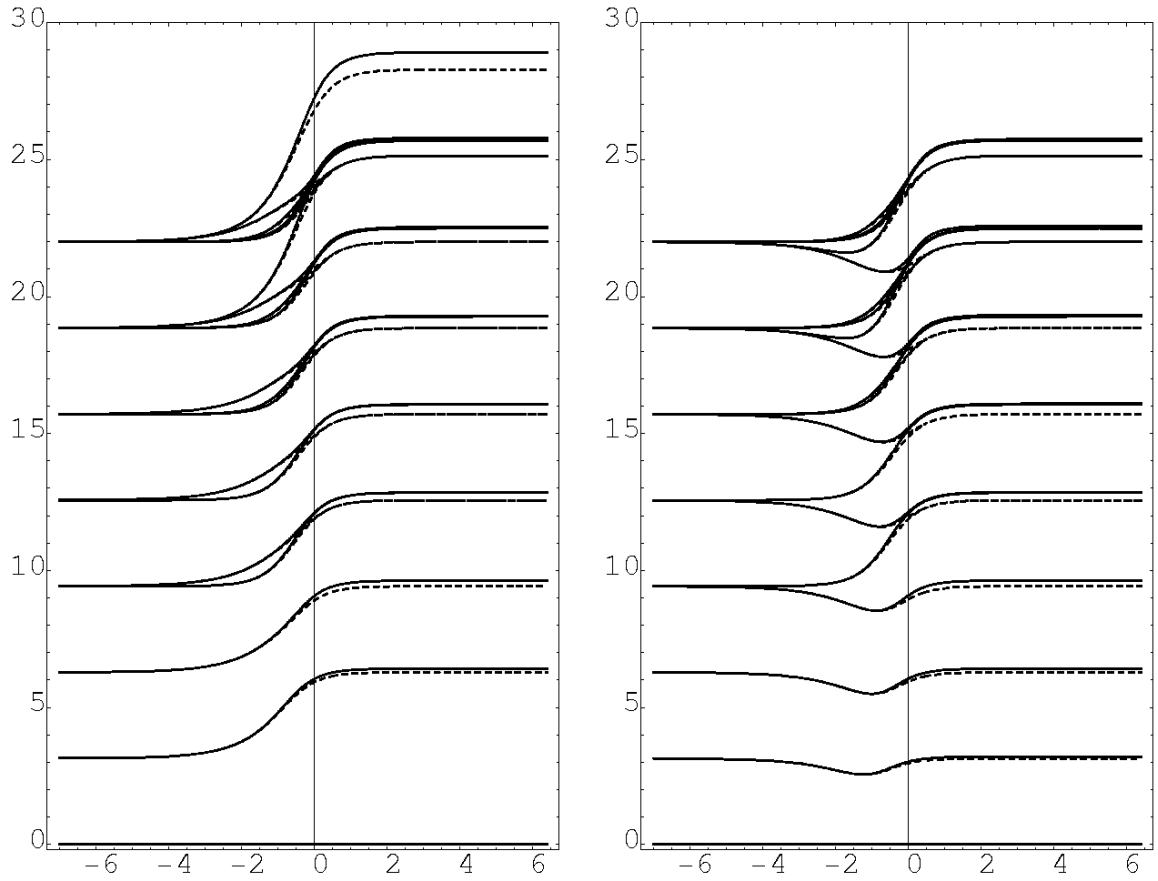


Figure 3.2: Exact (dashed lines) and mode truncated (solid lines) energy gaps $(E_i - E_0)$ in the v and u sectors respectively as a function of $\ln(h)$ at truncation level $n_c = 9$

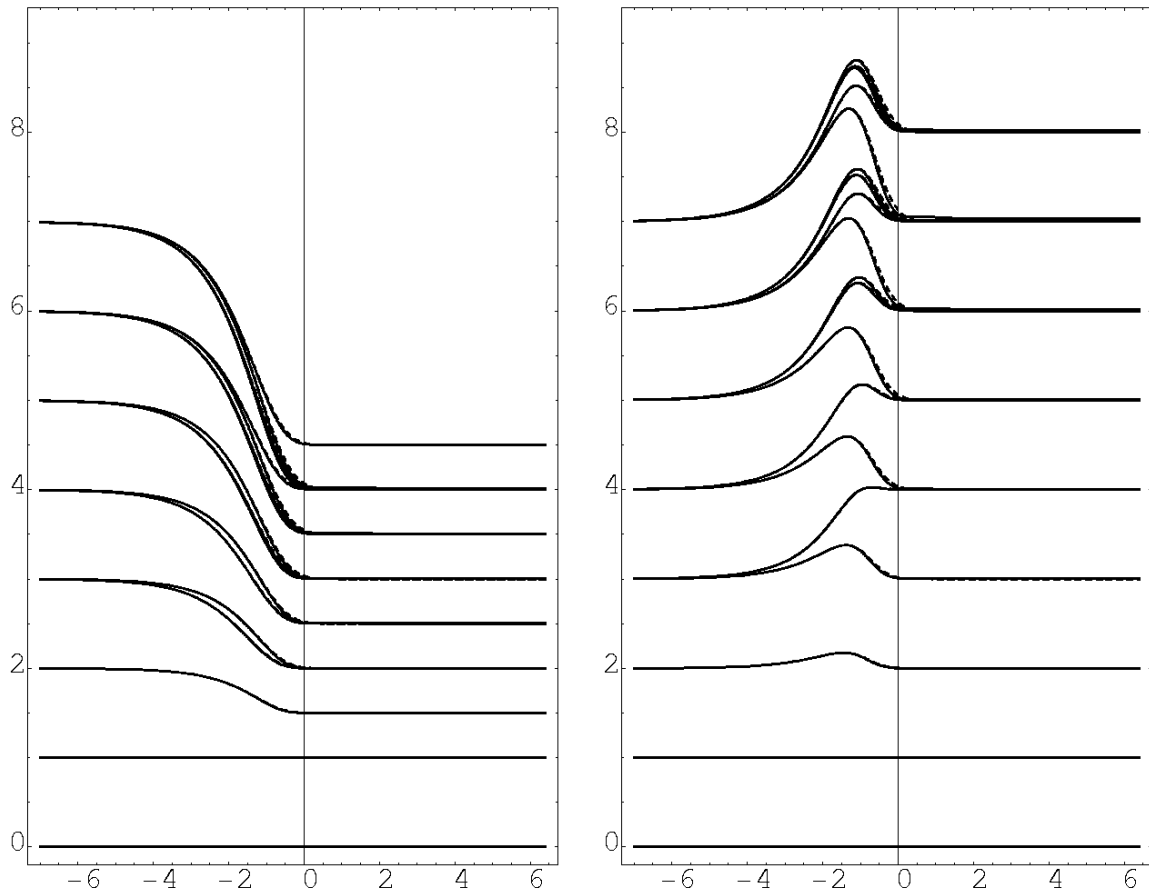


Figure 3.3: Exact (dashed lines) and mode truncated (solid lines) normalized spectra in the v and u sectors respectively as a function of $\ln(h)$ at truncation level $n_c = 9$

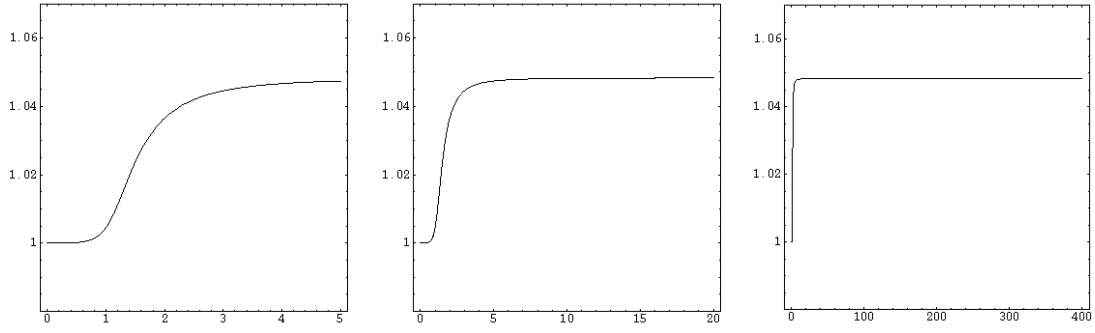


Figure 3.4: The function $s_0(h)$ for the v sector in the ranges $h \in [0, 3]$, $h \in [0, 20]$, $h \in [0, 400]$ and $s_0 \in [0.95, 1.05]$ at truncation level $n_c = 9$

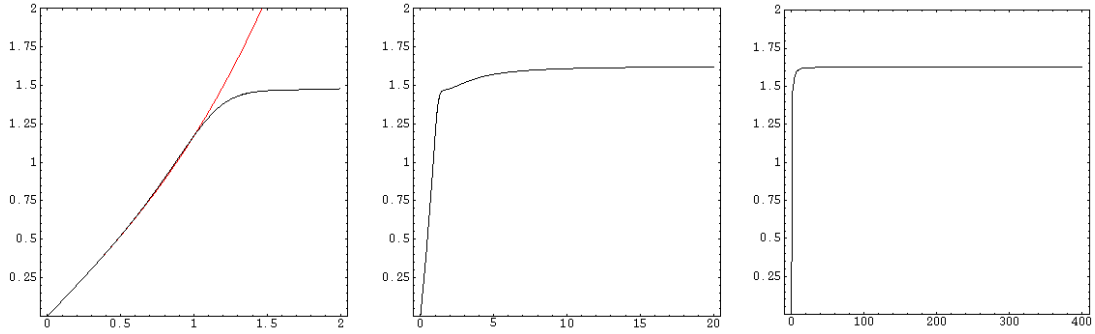


Figure 3.5: The function $s_1(h)$ for the v sector in the ranges $h \in [0, 2]$, $h \in [0, 20]$, $h \in [0, 400]$ and $s_1 \in [0, 2]$ at truncation level $n_c = 9$

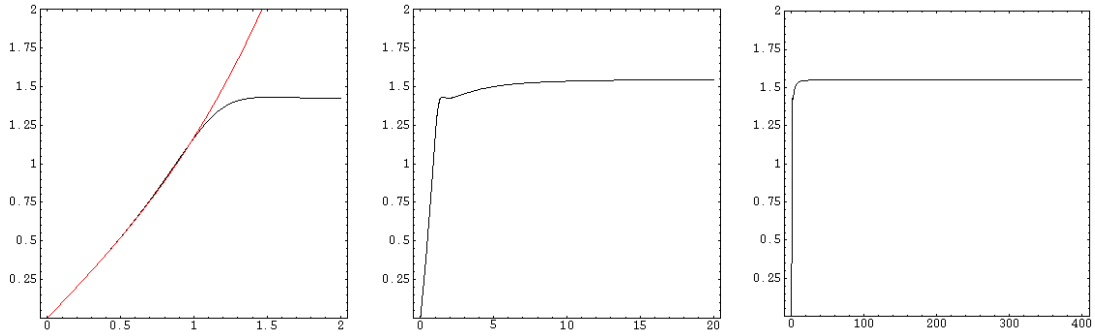


Figure 3.6: The function $s_1(h)/s_0(h)$ for the v sector in the ranges $h \in [0, 2]$, $h \in [0, 20]$, $h \in [0, 400]$ and $s_1/s_0 \in [0, 2]$ at truncation level $n_c = 9$

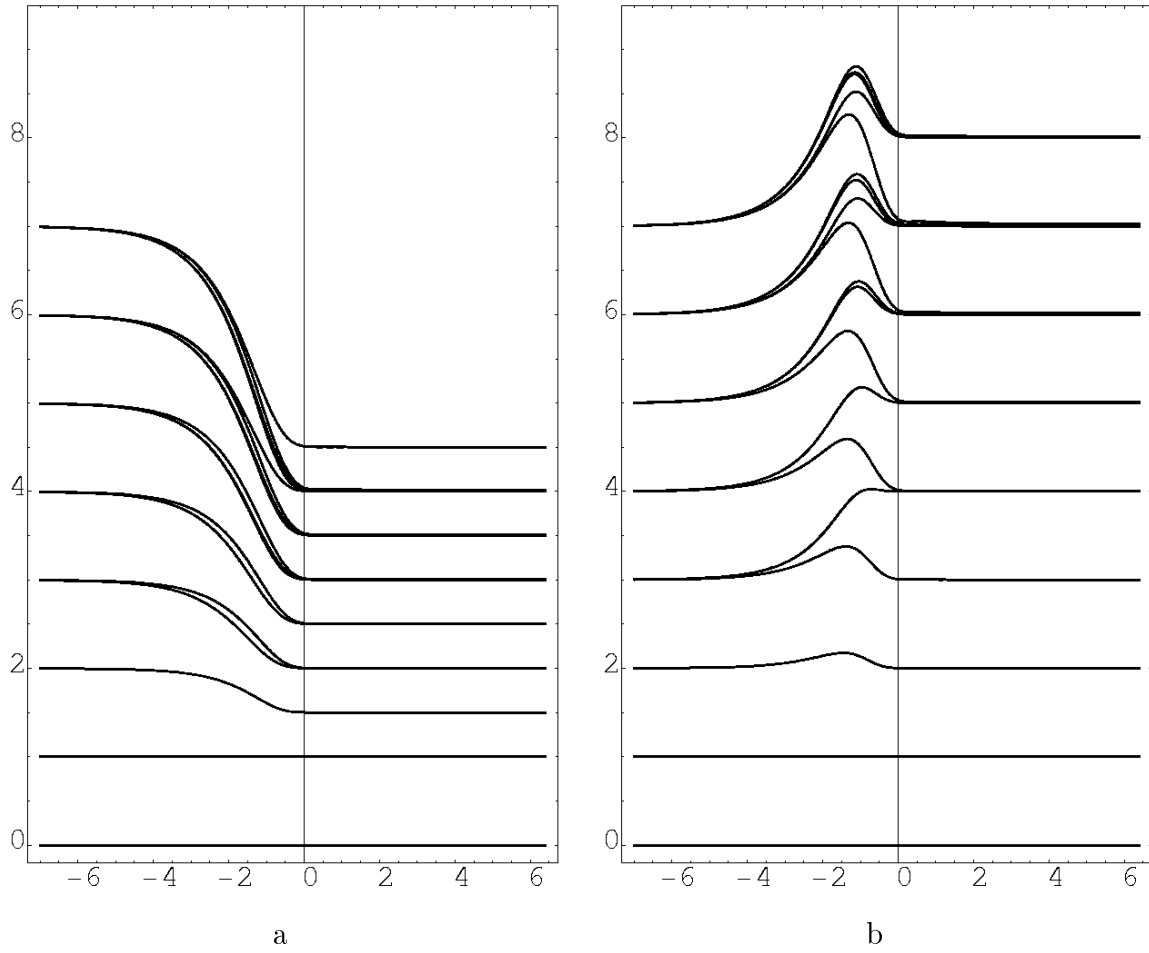


Figure 3.7: The mode truncated (solid lines) and rescaled exact (dashed lines) normalized spectra in the v and u sectors respectively as a function of $\ln(h)$ at truncation level $n_c = 9$

Table 3.2: The normalized energy gap $\frac{k(3,h)+k(0,h)}{k(1,h)+k(0,h)}$ in the v sector: exact, MT ($n_c = 9$) and rescaled exact values

| $\log(h)$ | Exact | MT | Rescaled exact |
|-----------|------------|------------|----------------|
| -7 | 2.997677 | 2.997677 | 2.997677 |
| -6 | 2.993681 | 2.993681 | 2.993681 |
| -5 | 2.982797 | 2.982797 | 2.982797 |
| -4 | 2.953071 | 2.953068 | 2.953068 |
| -3 | 2.8719584 | 2.8719043 | 2.8719043 |
| -2 | 2.66042177 | 2.6594328 | 2.6594328 |
| -1 | 2.25064420 | 2.24043886 | 2.24043637 |
| 0 | 2.00954942 | 2.00440950 | 2.00435155 |
| 1 | 2.00003474 | 2.00145821 | 2.00136637 |
| 2 | 2.00000008 | 2.00106850 | 2.00100783 |
| 3 | 2.0000000 | 2.0009872 | 2.0009201 |
| 4 | 2.0000000 | 2.0009756 | 2.0009202 |
| 5 | 2.0000000 | 2.0009740 | 2.0009187 |
| 6 | 2.0000000 | 2.0009738 | 2.0009185 |
| 6.4 | 2.0000000 | 2.0009738 | 2.0009185 |

Table 3.3: The energy gap $k(3, h) + k(0, h)$ in the v sector: exact and MT ($n_c = 9$) values

| $\log(h)$ | Exact | MT |
|-----------|-----------|-----------|
| -7 | 9.428427 | 9.428427 |
| -6 | 9.434703 | 9.434703 |
| -5 | 9.451803 | 9.451804 |
| -4 | 9.498544 | 9.498549 |
| -3 | 9.626826 | 9.626912 |
| -2 | 9.972034 | 9.973705 |
| -1 | 10.746173 | 10.770531 |
| 0 | 11.897034 | 12.101539 |
| 1 | 12.461229 | 12.740942 |
| 2 | 12.552003 | 12.833098 |
| 3 | 12.564424 | 12.845456 |
| 4 | 12.566107 | 12.847126 |
| 5 | 12.566335 | 12.847352 |
| 6 | 12.566366 | 12.847382 |
| 6.4 | 12.566368 | 12.847385 |

Table 3.4: The normalized energy gap $\frac{k(3,h)-k(0,h)}{k(1,h)-k(0,h)}$ in the u sector: exact, MT ($n_c = 9$) and rescaled exact values

| $\log(h)$ | Exact | MT | Rescaled exact |
|-----------|------------|------------|----------------|
| -7 | 3.002321 | 3.002321 | 3.002321 |
| -6 | 3.006305 | 3.006305 | 3.006305 |
| -5 | 3.017105 | 3.017105 | 3.017105 |
| -4 | 3.046201 | 3.046203 | 3.046203 |
| -3 | 3.1225067 | 3.1225559 | 3.1225559 |
| -2 | 3.29172833 | 3.29237422 | 3.29237405 |
| -1 | 3.32029283 | 3.31272102 | 3.31271418 |
| 0 | 3.01716419 | 3.00801374 | 3.00788791 |
| 1 | 3.00006366 | 3.00269022 | 3.00249222 |
| 2 | 3.0000000 | 3.0019707 | 3.0018400 |
| 3 | 3.0000000 | 3.0018211 | 3.0017004 |
| 4 | 3.0000000 | 3.0017997 | 3.0016804 |
| 5 | 3.0000000 | 3.0017968 | 3.0016776 |
| 6 | 3.0000000 | 3.0017964 | 3.0016773 |

Table 3.5: The energy gap $k(3, h) - k(0, h)$ in the u sector: exact and MT ($n_c = 9$) values

| $\log(h)$ | Exact | MT |
|-----------|----------|----------|
| -7 | 9.421132 | 9.421132 |
| -6 | 9.414873 | 9.414873 |
| -5 | 9.397906 | 9.397906 |
| -4 | 9.352150 | 9.352146 |
| -3 | 9.231143 | 9.231064 |
| -2 | 8.939485 | 8.938216 |
| -1 | 8.545045 | 8.541635 |
| 0 | 8.939748 | 9.084020 |
| 1 | 9.345985 | 9.558387 |
| 2 | 9.414002 | 9.626803 |
| 3 | 9.423318 | 9.635922 |
| 4 | 9.424580 | 9.637153 |
| 5 | 9.424751 | 9.637320 |
| 6 | 9.424774 | 9.637342 |

3.9.2 TCS scheme

Figure 3.8 shows the exact and TCSA spectra as a function of the logarithm of the coupling constant. The truncation level is $n_c = 14$, and the dimension of the Hilbert space is 110 in each sector. It is remarkable that there is strong deviation between the TCSA and exact spectra for large values of h . The behaviour of the TCSA energy gaps is $E_i(h) - E_0(h) \propto h$ for large values of h . Numerical values are listed in Table 3.7 for the fifth energy gap $k(3, h) + k(0, h)$ of the v sector and in Table 3.9 for the fifth energy gap $k(4, h) - k(0, h)$ of the u sector. The number of digits presented do not exceed the numerical precision.

Figure 3.9 shows the same spectra, but the lowest gap is normalized to 1, i.e. the functions $\frac{E_i(h) - E_0(h)}{E_1(h) - E_0(h)}$ are shown. It is remarkable that the agreement between exact and TCSA spectra looks better than in the case of not normalized spectra. The functions $\frac{E_i(h) - E_0(h)}{E_1(h) - E_0(h)}$ have finite limit as $h \rightarrow \infty$ and the degeneracy pattern in this limit appears to correspond to the $c = 1/2, h = 1/16$ representation of the Virasoro algebra. This correspondence improves as n_c is increased. As an illustration of this improvement we show the spectra at $n_c = 10$ in Figure 3.10. At any fixed finite value of h , however, the TCSA data are expected to converge to the exact values as $n_c \rightarrow \infty$.

Figures 3.11-3.13 show the functions $s_0(h)$, $s_1(h)$, $s_1(h)/s_0(h)$ in various ranges calculated in the same way as in the mode truncated case. The figures also show the curves given by (3.319) and (3.320) on the left-hand side (red/grey line). It is remarkable that $s_0(h) \propto h$ for large values of h . Calculations at other values of n_c show that the slope of $s_0(h)$ decreases as n_c is increased and it can be expected to converge to 0 as $n_c \rightarrow \infty$. $s_1(h)$ appears to tend to a constant for moderately large values of h . Calculations at other values of n_c show that this constant increases as n_c is increased and it can be expected to converge to infinity as $n_c \rightarrow \infty$. For large values of h , $s_1(h)$ decreases. $s_1(h)/s_0(h)$ reaches a maximum at $h \approx 1.6$ and then decreases to zero. Calculations at other values of n_c show that the maximum value and the value of h where it is reached increase as n_c is increased and it can be expected that both values converge to infinity as $n_c \rightarrow \infty$.

Figure 3.14.a shows the normalized TCSA spectrum and the normalized exact spectrum rescaled by $s_0(h)$ and $s_1(h)$. They show good qualitative agreement. Values of the fifth normalized energy gap $\frac{k(3, h) + k(0, h)}{k(1, h) + k(0, h)}$ of the v sector are listed in Table 3.6 as in the mode truncated case. These data show that the rescaling results significant improvement (which is especially noticeable if $\ln(h) > -2$).

Figure 3.14.b shows the normalized TCSA spectrum and the normalized exact spectrum rescaled by $s_0(h)$ and $s_1(h)$ in the u sector. The $s_0(h)$, $s_1(h)$ functions obtained in the v sector were used for the rescaling as in the mode truncated case. Table 3.8 shows

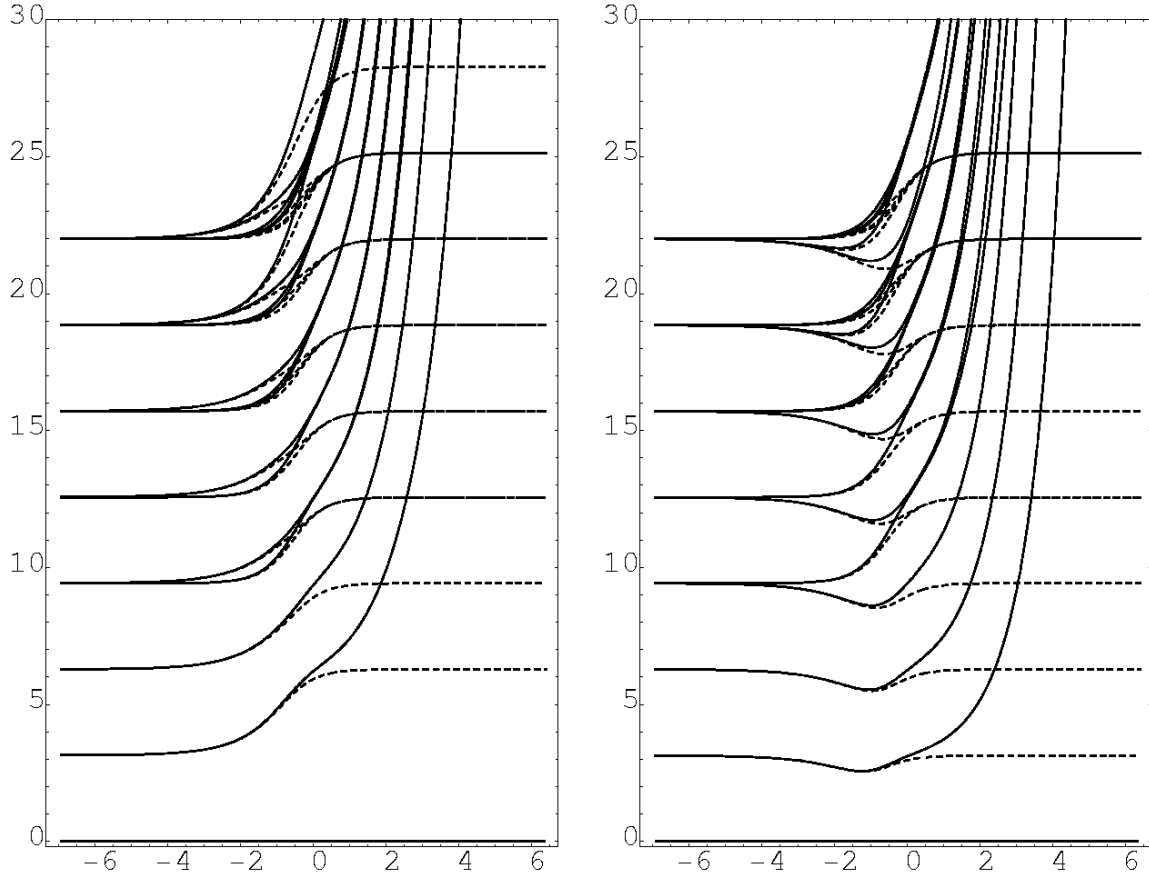


Figure 3.8: Exact (dashed lines) and TCSA (solid lines) energy gaps $(E_i - E_0)$ in the v and u sectors respectively as a function of $\ln(h)$ at truncation level $n_c = 14$

values of the fourth normalized energy gap $\frac{k(3,h)-k(0,h)}{k(1,h)-k(0,h)}$ of the u sector. We see from the table that the assumption that $s_0(h)$ and $s_1(h)$ are the same in both sectors does not give very good result in this case, although the situation might become better at higher truncation levels.

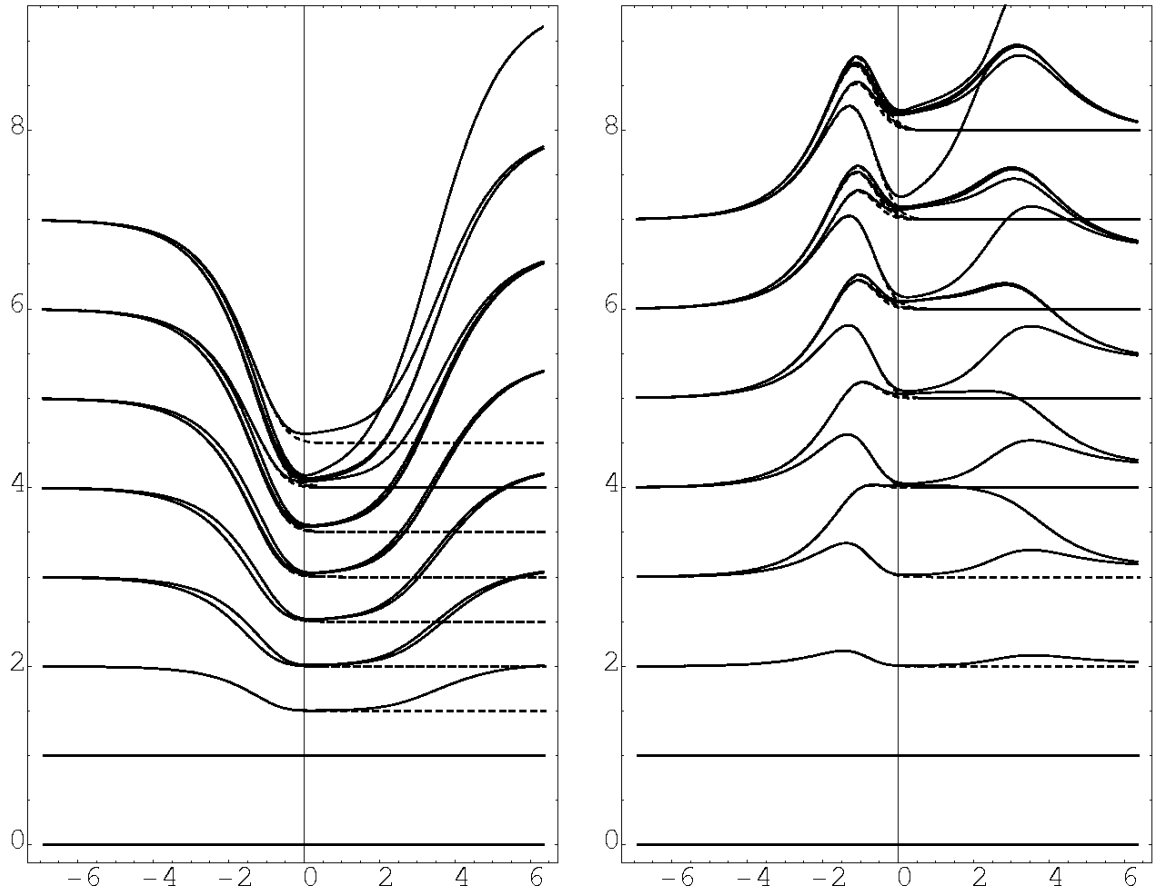


Figure 3.9: Exact (dashed lines) and TCSA (solid lines) normalized spectra in the v and u sectors respectively as a function of $\ln(h)$ at truncation level $n_c = 14$

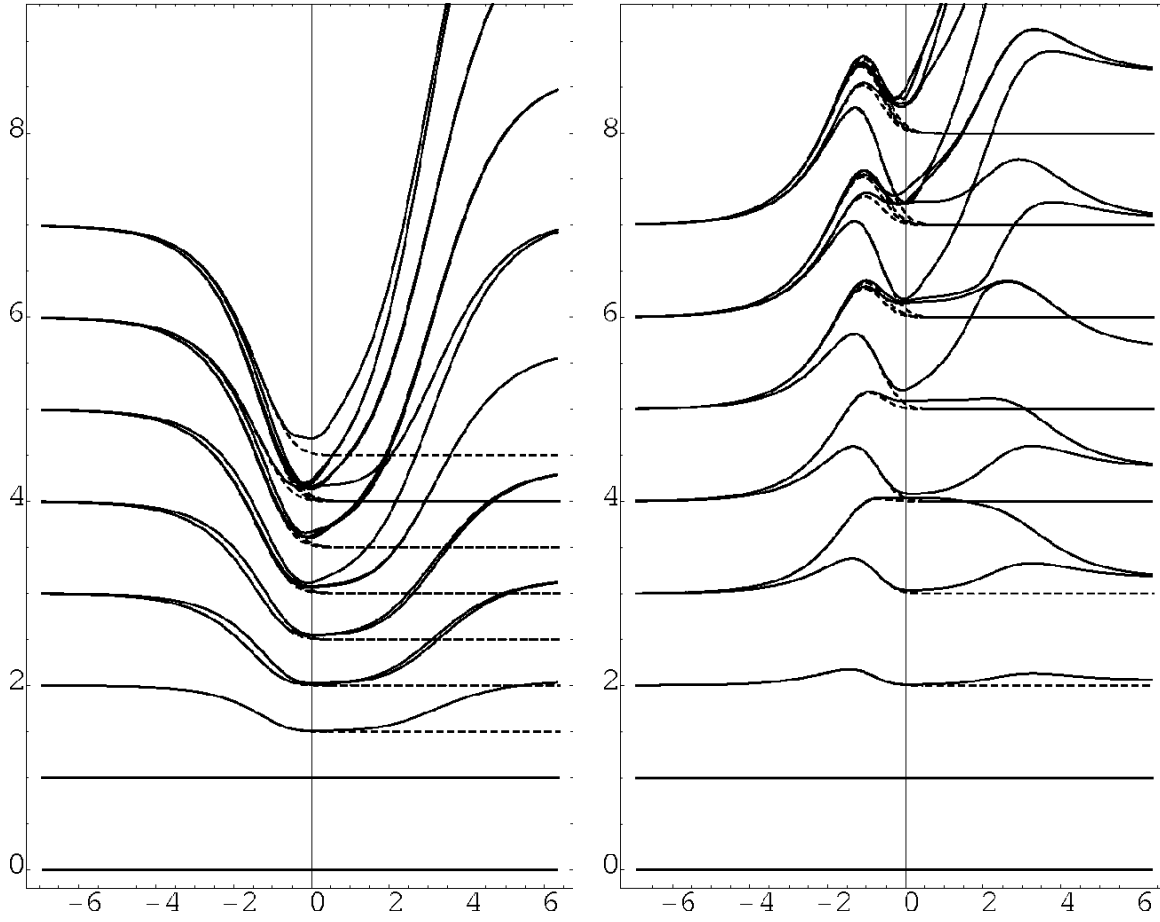


Figure 3.10: Exact (dashed lines) and TCSA (solid lines) normalized spectra in the v and u sectors respectively as a function of $\ln(h)$ at truncation level $n_c = 10$

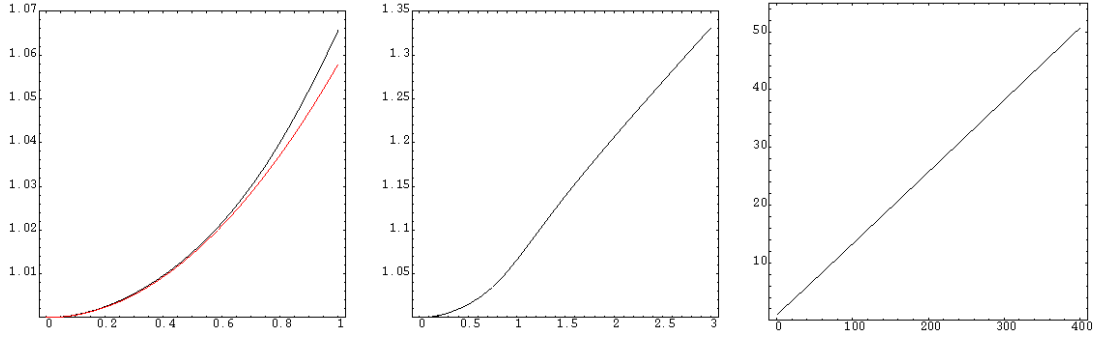


Figure 3.11: The function $s_0(h)$ for the v sector in the ranges $h \in [0, 1]$, $s_0 \in [1, 1.07]$; $h \in [0, 3]$, $s_0 \in [1, 1.35]$; $h \in [0, 400]$, $s_0 \in [1, 60]$ at truncation level $n_c = 14$

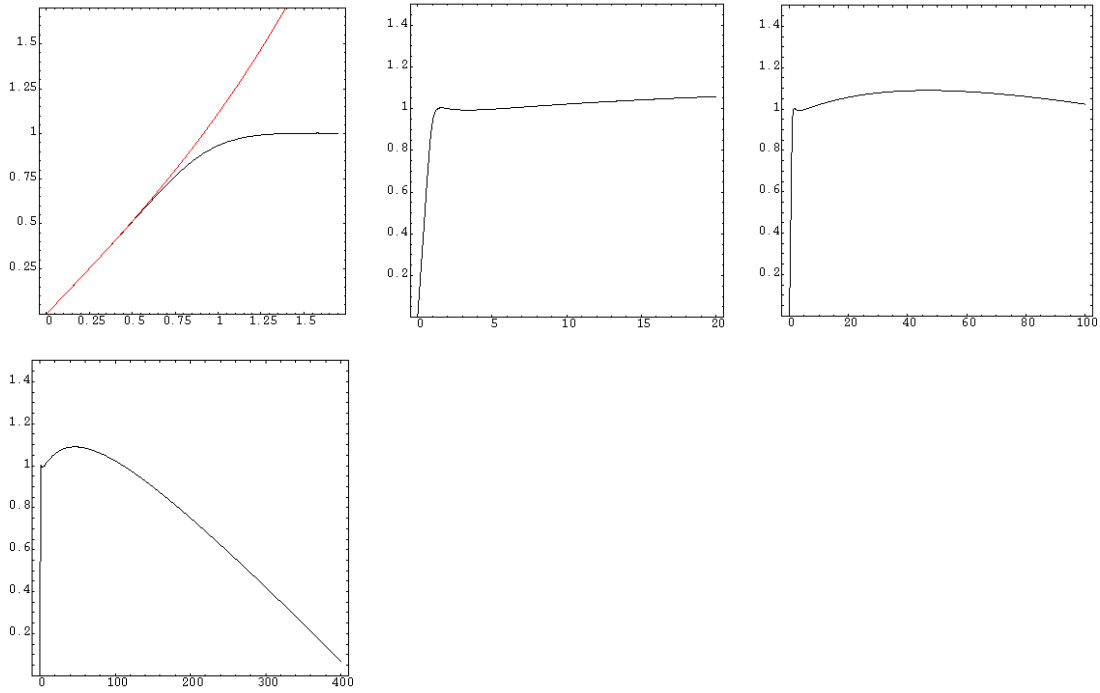


Figure 3.12: The function $s_1(h)$ for the v sector in the ranges $h \in [0, 1.75]$, $s_1 \in [0, 1.7]$; $h \in [0, 20]$, $s_1 \in [0, 1.5]$; $h \in [0, 100]$, $s_1 \in [0, 1.5]$; $h \in [0, 400]$, $s_1 \in [0, 1.5]$ at truncation level $n_c = 14$

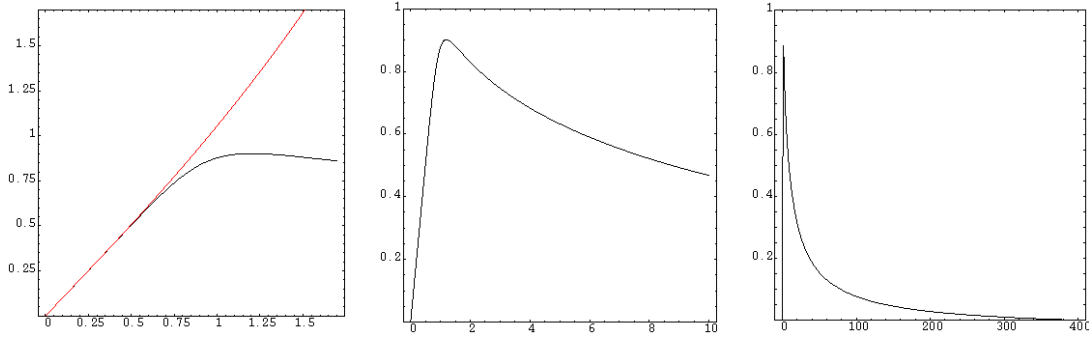


Figure 3.13: The function $s_1(h)/s_0(h)$ for the v sector in the ranges $h \in [0, 1.75]$, $s_1/s_0 \in [0, 1.75]$; $h \in [0, 10]$, $s_1/s_0 \in [0, 1]$; $h \in [0, 400]$, $s_1/s_0 \in [0, 1]$ at truncation level $n_c = 14$

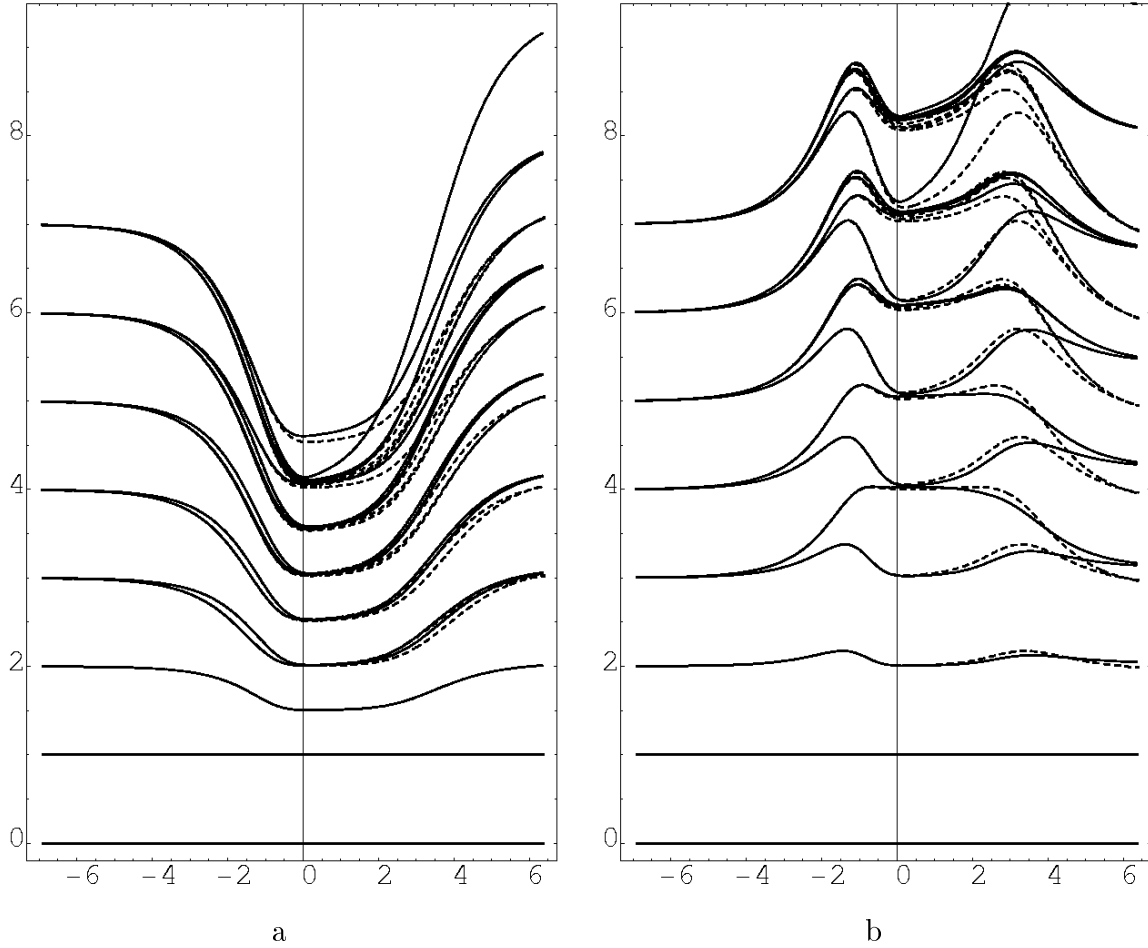


Figure 3.14: The TCSA (solid lines) and rescaled exact (dashed lines) normalized spectra in the v and u sectors respectively as a function of $\ln(h)$ at truncation level $n_c = 14$

Table 3.6: The normalized energy gap $\frac{k(3,h)+k(0,h)}{k(1,h)+k(0,h)}$ in the v sector: exact, TCSA ($n_c = 14$) and rescaled exact values

| $\log(h)$ | Exact | TCSA | Rescaled exact |
|-----------|------------|----------|----------------|
| -6 | 2.993681 | 2.993681 | 2.993681 |
| -5 | 2.982797 | 2.982797 | 2.982797 |
| -4 | 2.953071 | 2.953074 | 2.953073 |
| -3 | 2.8719584 | 2.871974 | 2.871961 |
| -2 | 2.66042177 | 2.660322 | 2.660236 |
| -1 | 2.25064420 | 2.2488 | 2.24837 |
| 0 | 2.00954942 | 2.01699 | 2.0177 |
| 1 | 2.00003474 | 2.028321 | 2.031631 |
| 2 | 2.00000008 | 2.101337 | 2.105516 |
| 3 | 2.0000000 | 2.33433 | 2.32573 |
| 4 | 2.0000000 | 2.670454 | 2.643480 |
| 5 | 2.0000000 | 2.916318 | 2.879339 |
| 6 | 2.0000000 | 3.037542 | 2.997132 |

Table 3.7: The energy gap $k(3, h) + k(0, h)$ in the v sector: exact and TCSA ($n_c = 14$) values

| $\log(h)$ | Exact | TCSA |
|-----------|-----------|-----------|
| -6 | 9.434703 | 9.434706 |
| -5 | 9.451803 | 9.451830 |
| -4 | 9.498544 | 9.498745 |
| -3 | 9.626826 | 9.628349 |
| -2 | 9.972034 | 9.983987 |
| -1 | 10.746173 | 10.840718 |
| 0 | 11.897034 | 12.51855 |
| 1 | 12.461229 | 15.0054 |
| 2 | 12.552003 | 20.7975 |
| 3 | 12.564424 | 36.1193 |
| 4 | 12.566107 | 77.0368 |
| 5 | 12.566335 | 187.694 |
| 6 | 12.566366 | 488.292 |

Table 3.8: The normalized energy gap $\frac{k(3,h)-k(0,h)}{k(1,h)-k(0,h)}$ in the u sector: exact, TCSA ($n_c = 14$) and rescaled exact values

| $\log(h)$ | Exact | TCSA | Rescaled exact |
|-----------|------------|----------|----------------|
| -7 | 3.002321 | 3.002321 | 3.002321 |
| -6 | 3.006305 | 3.006305 | 3.006305 |
| -5 | 3.017105 | 3.017105 | 3.017105 |
| -4 | 3.046201 | 3.046206 | 3.046198 |
| -3 | 3.1225067 | 3.122558 | 3.122504 |
| -2 | 3.29172833 | 3.292196 | 3.291849 |
| -1 | 3.32029283 | 3.31947 | 3.31865 |
| 0 | 3.01716419 | 3.0268 | 3.0315 |
| 1 | 3.00006366 | 3.03610 | 3.05522 |
| 2 | 3.0000000 | 3.11033 | 3.16799 |
| 3 | 3.0000000 | 3.27063 | 3.36158 |
| 4 | 3.0000000 | 3.28320 | 3.30254 |
| 5 | 3.0000000 | 3.203134 | 3.115763 |
| 6 | 3.0000000 | 3.152931 | 3.002865 |

Table 3.9: The energy gap $k(3, h) - k(0, h)$ in the u sector: exact and TCSA ($n_c = 14$) values

| $\log(h)$ | Exact | TCSA |
|-----------|----------|----------|
| -7 | 9.421132 | 9.421132 |
| -6 | 9.414873 | 9.414877 |
| -5 | 9.397906 | 9.397933 |
| -4 | 9.352150 | 9.352345 |
| -3 | 9.231143 | 9.232544 |
| -2 | 8.939485 | 8.949181 |
| -1 | 8.545045 | 8.61250 |
| 0 | 8.939748 | 9.4096 |
| 1 | 9.345985 | 11.3108 |
| 2 | 9.414002 | 16.0395 |
| 3 | 9.423318 | 29.8152 |
| 4 | 9.424580 | 69.5595 |
| 5 | 9.424751 | 179.6918 |
| 6 | 9.424774 | 480.0968 |

3.10 Scaling properties of the s_1/s_0 , s_1 and s_0 functions

In this section we describe results obtained mainly numerically for the n_c -dependence of the $s_1(n_c, h)/s_0(n_c, h)$, $s_1(n_c, h)$ and $s_0(n_c, h)$ functions. The value of L is fixed. $s_0(n_c, h)$ and $s_1(n_c, h)$ are calculated from the three lowest energy levels. In the TCSA case we considered $n_c = 11, 12, 13, 14$, in the MT case $n_c = 8, 9, 10, 11$.

In the MT scheme we found that the functions

$$n_c^{-1/2} \frac{s_1}{s_0}(n_c, hn_c^{1/2}) \quad (3.329)$$

$$n_c^{-1/2} s_1(n_c, hn_c^{1/2}) \quad (3.330)$$

$$n_c(s_0(n_c, hn_c^{1/2}) - 1) \quad (3.331)$$

are approximately independent of n_c . This is consistent with the perturbative formulae (3.307), (3.308). It should be noted that s_0 is very close to 1, therefore the scaling properties of s_0 , s_1 , s_1/s_0 written down above are not inconsistent.

In the TCSA scheme we found that the functions

$$n_c^{-\alpha} \frac{s_1}{s_0}(n_c, hn_c^\beta) \quad (3.332)$$

$$n_c^{-\alpha_1} s_1(n_c, hn_c^{\beta_1}) \quad (3.333)$$

$$s_0(n_c, hn_c^{\beta_2}) \quad (3.334)$$

are approximately independent of n_c with a suitable choice of the numbers α , β , α_1 , β_1 , β_2 . The precision of this independence, however, is not very high, especially for s_1/s_0 and s_1 . We obtained $\beta_2 \approx 1/2$, which is consistent with the perturbative formula (3.319). We also obtained that $\alpha \approx \beta$ and $\alpha_1 \approx \beta_1$, which is consistent with (3.319) and (3.320), however the value of α and α_1 appears to be around $1/3$, which deviates from the expectation based on (3.319) and (3.320). Moreover, the value of α and α_1 appears to depend on n_c , and on which three energy levels s_0 and s_1 are calculated from. One can also obtain different numbers if one takes different domains of the values of h into consideration. The values one can obtain for α and α_1 are between 0.3 and 0.5.

Generally one can expect that the functions $s_1(n_c, h)/s_0(n_c, h)$, $s_1(n_c, h)$ and $s_0(n_c, h)$ can be written in the form

$$s(n_c, h) = n_c^{\gamma_1} F_1(hn_c^{\delta_1}) + n_c^{\gamma_2} F_2(hn_c^{\delta_2}) + \dots \quad (3.335)$$

where $s(n_c, h)$ stands for $s_1(n_c, h)/s_0(n_c, h)$, $s_1(n_c, h)$ or $s_0(n_c, h)$, and γ_1 , δ_1 , γ_2 , δ_2 , \dots are constants. Some of the functions F_1 , F_2 , \dots may depend on the method used to calculate $s_1(n_c, h)/s_0(n_c, h)$, $s_1(n_c, h)$ and $s_0(n_c, h)$. (The functions F_1 , F_2 , \dots and the

exponents are generally different for s_1/s_0 , s_1 and s_0 , of course.) In the MT scheme one term appears to dominate clearly. For s_0 this term is the constant function 1, and the next term also appears to be much larger than the further terms. In the TCSA scheme it appears that there is one dominant term for s_0 , and a dominant term cannot be isolated for s_1/s_0 and s_1 at the values of n_c that we considered.

3.11 Discussion

We have investigated the validity of the approach (1.5) for the description of truncation effects in TCSA spectra. Comparison with a solvable truncation method called mode truncation shows that the remarkably regular behaviour of the TCSA spectrum for large h in the case of the model (1.2) is not universal (i.e. not independent of the truncation scheme). The numerical calculations show that (1.5) provides a good approximation of the truncated spectra in both the TCSA and the mode truncation scheme. This is confirmed by perturbative analytic calculations as well. The main difference between the mode truncated and TCSA spectra at large h seems to be explicable through the different behaviour of the function $s_0(n_c, h)$ in the two schemes. Difference between the $s_0(n_c, h)$ functions appears also in perturbation theory. We have shown analytically that in the mode truncation scheme the convergence of the truncated spectra to the exact spectra can be improved by one order in $1/n_c$ by the rescaling (1.5). This has also been shown in the TCSA scheme for low orders of perturbation theory in h .

We have also given a quantum field theoretic discussion of the model (1.2). In particular we have discussed the change of the boundary condition satisfied by the fermion fields as the coupling constant (or external boundary magnetic field) is increased. Such a change, which is emphasized in the literature, seems impossible naively — in our formulation at least. The paradox is resolved by the phenomenon that the fermion fields (more precisely their matrix elements between energy eigenstates) develop a discontinuity at the boundary if the coupling constant is nonzero.

It is still an open problem to present an explanation of the validity of the approach (1.5). Within the framework of (1.5) the behaviour of the TCSA spectrum at large h , in particular the second flow mentioned in the Introduction, is explained by the behaviour of s_0 and s_1 at large h : $s_0 \propto h$, s_1 is bounded from above, therefore s_1/s_0 tends to zero. It is a further problem to give an analytic derivation of this behaviour of s_0 and s_1 . In the future we intend to investigate the scaling properties of s_1/s_0 , s_1 and s_0 and the TCSA and MT spectra more thoroughly by taking higher values of n_c [115]. It would also be interesting to extend our results to other perturbed boundary conformal minimal models,

which show similar behaviour numerically to the model that we have studied. Certain results concerning other minimal models and scaling properties already exist [65, 61]; see also [59]. It is a further problem to classify the possible behaviours of truncated spectra at large h for various truncation schemes. Finally, the quantum field theoretic description of the model (1.2) could be developed further and extended to the massive case.

Chapter 4

A nonperturbative study of phase transitions in the multi-frequency sine-Gordon model

4.1 The multi-frequency sine-Gordon model

In this section the definition and basic properties of the multi-frequency sine-Gordon model (MSG) are described.

The action of the model is

$$\mathcal{A}_{MSG} = \int dt \int dx \left(\frac{1}{2} \partial_\mu \Phi \partial^\mu \Phi - V(\Phi) \right),$$

where

$$V(\Phi) = \sum_i^n \mu_i \cos(\beta_i \Phi + \delta_i)$$

is the potential, which contains n cosine terms. Φ is a real scalar field defined on the two-dimensional Minkowski space \mathbb{R}^{1+1} , $\beta_i \in \mathbb{R}$ are the frequencies, $\beta_i \neq \beta_j$ if $i \neq j$, μ_i are the coupling constants (of dimension mass² at the classical level) and $\delta_i \in \mathbb{R}$ are the phases in the terms of the potential.

Two cases can be distinguished according to the periodicity properties of the potential. The first one is the rational case, when $V(\Phi)$ is a trigonometric polynomial: the ratios of the frequencies β_i are rational and the potential is periodic. Let the period of the potential be $2\pi r$ in this case. The target space of the field Φ can be compactified:

$$\Phi \equiv \Phi + 2kr\pi,$$

where $k \in \mathbb{N}$ can be chosen arbitrarily. The model obtained in this way is called the k -folded MSG. The well-known classical sine-Gordon model corresponds to $n = 1$, $k = 1$.

The other case is the irrational one, when the potential is not periodic and no such folding can be made. The irrational case is much more complicated than the rational one, so we restrict our attention to the rational case. We remark here only that although $V(\Phi)$ always has a finite infimum, it does not necessarily admit an absolute minimum. The potential $V(\Phi)$ can always be written uniquely as a sum $V(\Phi) = V_1(\Phi) + V_2(\Phi) + \dots + V_k(\Phi)$, where the terms V_1, \dots, V_k are periodic but any sum of any of these terms is not periodic. $V(\Phi)$ has an absolute minimum if and only if $V_1(\Phi), \dots, V_k(\Phi)$ have a common absolute minimum. This occurs for special choice of the δ_i , if the values of β_i are given. In particular, if β_i/β_j are irrational for all $i \neq j$ and $\mu_i < 0$ for all i , then $V(\Phi)$ has a absolute minimum if and only if $\frac{\delta_i}{\beta_i} - \frac{\delta_j}{\beta_j} = \frac{2\pi b_i}{\beta_i} - \frac{2\pi b_j}{\beta_j}$ is satisfied with some numbers $b_i \in \mathbb{Z}$, which is equivalent to the case $\delta_i = 0$ for all i . See and [75] and [52] for further remarks on the irrational case.

At the quantum level the theory can be regarded as a perturbed conformal field theory:

$$\mathcal{A}_{MSG} = \mathcal{A}_{CFT} + \mathcal{A}_{pert} ,$$

where

$$\mathcal{A}_{CFT} = \int dt \int dx \frac{1}{2} \partial_\mu \Phi \partial^\mu \Phi ,$$

which is the action of the free scalar particle of zero mass, and

$$\mathcal{A}_{pert} = \int dt \int dx (-V(\Phi)) = -\frac{1}{2} \int dt \int dx \sum_{i=1}^n (\mu_i e^{i\delta_i} V_{\beta_i} + \mu_i e^{-i\delta_i} V_{-\beta_i}) ,$$

where V_ω denotes the vertex operator

$$V_\omega =: e^{i\omega\Phi} : ,$$

which is a primary field with conformal dimensions

$$\Delta_\omega^\pm = \Delta_\omega = \frac{\omega^2}{8\pi}$$

in the unperturbed (conformal) field theory. The upper index \pm corresponds to the left/right conformal algebra and $: :$ denotes the conformal normal ordering. The dimensions of the coupling constants at the quantum level are

$$[\mu_i] = (mass)^{2-2\Delta_i} , \quad \Delta_i \equiv \Delta_{\beta_i} .$$

The perturbing operators are relevant only if

$$\beta_i^2 < 8\pi , \tag{4.1}$$

we restrict ourselves to this case. We also assume that

$$\beta_i^2 < 4\pi ,$$

which is a necessary and sufficient condition for the model to be free from ultraviolet divergencies in the perturbed conformal field theory framework [114, 75, 52].

The model has a massgap in general, and it is clear that phase transitions occur in the classical version of the model as the coupling constants are tuned (assuming that $n > 1$). It is also expected that there are topologically charged solutions/states in the model [75]. We shall investigate the sector with zero topological charge, which is sufficient for our purposes. We also restrict ourselves to 1-folded models ($k = 1$), as it is natural to expect that in infinite volume a folding number $k \neq 1$ results simply in a k -fold multiplication of the spectrum corresponding to $k = 1$.

4.2 The Truncated Conformal Space Approach for the multi-frequency sine-Gordon model

The following fields are primary fields in the folded free boson as a conformal field theory:

$$V_{p,\bar{p}}(z, \bar{z}) =: \exp[ip\phi_{CFT}(z) + i\bar{p}\bar{\phi}_{CFT}(\bar{z})] : .$$

$V_{p,\bar{p}}(z, \bar{z})$ has conformal dimensions $\Delta^+ = \frac{p^2}{8\pi}$, $\Delta^- = \frac{\bar{p}^2}{8\pi}$, where $p = \frac{n}{r} + 2\pi rm$, $\bar{p} = \frac{n}{r} - 2\pi rm$, $n, m \in \mathbb{Z}$, and the free boson field Φ_{CFT} is

$$\Phi_{CFT}(x, t) = \phi_{CFT}(x - t) + \bar{\phi}_{CFT}(x + t) .$$

\mathcal{H}_{CFT} is spanned by the states $|p, \bar{p}\rangle = \lim_{z, \bar{z} \rightarrow 0} V_{p,\bar{p}}(z, \bar{z})|0\rangle$ ($|0, 0\rangle \equiv |0\rangle$) and $a_{n_1} \dots \bar{a}_{m_1} \dots |p, \bar{p}\rangle$, where a_{n_i} and \bar{a}_{m_i} are creating operators of Fourier modes of Φ_{CFT} . The mode creating operators increase the conformal weight by 1. The conformal generators L_0 and \bar{L}_0 are diagonal in this basis. We refer the reader to [73] for more details on the quantization of the folded free boson in finite volume.

The basis of the TCSA Hilbert space is obtained by taking those elements $|v\rangle$ of the basis above which satisfy the truncation condition

$$\frac{\langle v | \frac{L}{2\pi} H_{CFT} | v \rangle}{\langle v | v \rangle} < e_{cut} .$$

e_{cut} is the dimensionless upper conformal energy cutoff and L is the volume of space. We restrict ourselves to the sector with zero topological charge ($p = \bar{p}$), this being the sector

containing the ground state(s) and the relevant information for the problem treated in this chapter. We can also restrict to zero momentum states i.e. to states satisfying the condition $(L_0 - \bar{L}_0)|v\rangle = 0$. (The operator $L_0 - \bar{L}_0$ commutes with H and H_{CFT} as well). We remark that e_{cut} also serves as an ultraviolet cutoff.

The matrix elements of H between two elements $|a\rangle$ and $|b\rangle$ of the basis of \mathcal{H}_{CFT} above are given by

$$\begin{aligned} \left(\frac{H}{M}\right)_{ab} &= \frac{2\pi}{l} \left(L_0 + \bar{L}_0 - \frac{c}{12}\right)_{ab} \\ &+ \frac{2\pi}{l} \sum_{j=1}^n \text{sgn}(\mu_j) \kappa_j \left(\frac{M_j}{M}\right)^{x_j} \frac{l^{x_j}}{2(2\pi)^{x_j-1}} e^{i\delta_j} (V_{\beta_j, \beta_j}(1, 1))_{ab} \delta_{\Delta_a - \bar{\Delta}_a, \Delta_b - \bar{\Delta}_b} \\ &+ \frac{2\pi}{l} \sum_{j=1}^n \text{sgn}(\mu_j) \kappa_j \left(\frac{M_j}{M}\right)^{x_j} \frac{l^{x_j}}{2(2\pi)^{x_j-1}} e^{-i\delta_j} (V_{-\beta_j, -\beta_j}(1, 1))_{ab} \delta_{\Delta_a - \bar{\Delta}_a, \Delta_b - \bar{\Delta}_b} , \end{aligned} \quad (4.2)$$

where M is a mass scale of the theory given below, $l = LM$ is the dimensionless volume, $x_j = 2 - 2\Delta_j$, $\Delta_j \equiv \Delta_{\beta_j}$; $\Delta_a, \bar{\Delta}_a, \Delta_b, \bar{\Delta}_b$ are the conformal weights of the states $|a\rangle$ and $|b\rangle$, c is the central charge of the conformal theory ($c = 1$ in the present case), and we have made a replacement corresponding to

$$|\mu_j| = \kappa_j M_j^{x_j} .$$

The ‘interpolating’ mass scale M is

$$M = \sum_j \eta_j M_j ,$$

where

$$\eta_j = \frac{|\mu_j|^{1/x_j}}{\sum_i |\mu_i|^{1/x_i}} \quad (4.3)$$

are the dimensionless coupling constants (of which only $n - 1$ are independent). (4.3) implies that $\eta_j \in [0, 1]$, $\sum_j \eta_j = 1$. M depends smoothly on the η_j -s. The precise expression for κ is not essential for our problem, we need only that κ depends on Δ only and that it is dimensionless. Following [52] we used the formula of [116]:

$$\kappa_j = \frac{2\Gamma(\Delta_j)}{\pi\Gamma(1 - \Delta_j)} \left(\frac{\sqrt{\pi}\Gamma(\frac{1}{x_j})}{2\Gamma(\frac{\Delta_j}{x_j})} \right)^{x_j} .$$

In the classical limit $\Delta_j = 0$ and $x_j = 2$.

The formula (4.2) is written in terms of dimensionless quantities, and the volume (l) dependence of H/M is also explicit. We refer the reader to [105] and [50, 52, 110, 89] for further explanation of (4.2). It should also be noted that the above basis for the Hilbert

space is not the one generated by the standard L_N elements of the Virasoro algebra, which is used in general for TCSA, but the one generated by the mode creating operators. In this (orthogonal) basis the matrix elements $(V_{\beta_j, \beta_j}(1, 1))_{ab}$ and $(V_{-\beta_j, -\beta_j}(1, 1))_{ab}$ are relatively easy to calculate.

It is clear from (4.2) that TCSA gives an exact result if $l \rightarrow 0$ (assuming (4.1)) and this limit of the theory is the conformal theory (the massless free boson), and the accuracy of the TCSA spectrum decreases at fixed e_{cut} as $l \rightarrow \infty$. For very large values of l the l -dependence of the spectrum of the TCSA Hamiltonian operator is power-like and it is determined by the l^{x_j-1} coefficients in (4.2). The TCSA Hamiltonian operator cannot be considered as good approximation for these values of l .

We denote the (dimensionless) energy levels of H/M in volume l by $e_i(l)$, $i = 0, 1, 2, \dots$, and $e_0 \leq e_1 \leq e_2 \leq \dots$ is assumed if not stated otherwise. We shall draw conclusions about the spectrum at $l = \infty$ from the behaviour of the functions $e_i(l)$ for low values of i and moderately large values of l .

4.3 Phase structure in the classical limit

4.3.1 Phase structure of the two-frequency model in the classical limit

The Lagrangian density takes the following form in the two-frequency case:

$$\mathcal{L} = \frac{1}{2} \partial_\mu \Phi \partial^\mu \Phi - \mu \cos(\beta \Phi) - \lambda \cos(\alpha \Phi + \delta) ,$$

where

$$\frac{\beta}{\alpha} = \frac{n}{m} \neq 1 ,$$

n and m are coprimes (and the folding number equals to one).

The following proposition about the properties of $V(\Phi)$ can be used to determine the phase structure:

Assume that $\mu, \lambda \neq 0$. Then the following three cases can be distinguished:

a.) If the function $V(\Phi)$ is symmetric with respect to the reflection $\Phi \mapsto 2\Phi_0 - \Phi$, where Φ_0 is a suitable constant, and $n, m > 1$, then V has two absolute minima, which are mapped into each other by the reflection. We remark that it depends on the value of δ whether V has this symmetry or not, and it is easy to give a criterion for the existence of this symmetry in terms of n, m and δ .

b.) If V is symmetric with respect to a reflection as in case a., but $n = 1$ or $m = 1$, then V has one or two absolute minima depending on the values of μ and λ . In this case, assuming that $n = 1$, V can be brought to the form

$$V(\Phi) = -|\mu| \cos(\beta\Phi) + |\lambda| \cos(m\beta\Phi)$$

by an appropriate shift of Φ . V has two absolute minima if $|\lambda/\mu| > 1/m^2$, and one absolute minimum if $|\lambda/\mu| \leq 1/m^2$. The two absolute minima are mapped into each other by the reflection. The second derivative of V is nonzero at the minima if $|\lambda/\mu| \neq 1/m^2$, but it is zero if $|\lambda/\mu| = 1/m^2$. In the latter case, the fourth derivative of V at the minimum is nonzero. The two minima of V merge and the value of the second derivatives of V at the two minima tends to zero as $|\lambda/\mu|$ approaches $1/m^2$ from above.

c.) If V does not satisfy the requirements of a) and b), then V has a single absolute minimum.

We omit the proof of this proposition, which is elementary, although long and not completely trivial because of the arbitrariness of n and m .

If μ or λ equals to zero, then V is periodic and has m or n absolute minima, respectively. See [110] for a detailed investigation of these (integrable) limiting cases.

The phases of the classical model are determined by the behaviour of the absolute minima of $V(\Phi)$ as the value of the coupling constants vary. In particular, the proposition above implies that the phase structure of the two-frequency model is the following:

The model exhibits an Ising-type second order phase transition at the critical value

$$\eta_c = \frac{m}{1+m}$$

of the dimensionless coupling constant $\eta = \sqrt{|\mu|}/(\sqrt{|\mu|} + \sqrt{|\lambda|})$ if $n = 1$ and V has the \mathbb{Z}_2 -symmetry introduced above. This critical point separates two massive phases with unbroken and spontaneously broken \mathbb{Z}_2 -symmetry. Equivalent statement can be made if $m = 1$. If V is not symmetric, then there is only one massive phase with nondegenerate ground state. If $m, n \neq 1$ and V is symmetric, then there is one massive phase with doubly degenerate ground state (i.e. the reflection symmetry is spontaneously broken). In the limiting cases $\eta = 0$ and $\eta = 1$ the model is massive and has spontaneously (and completely) broken \mathbb{Z}_n or \mathbb{Z}_m symmetry.

4.3.2 Phase structure of the three-frequency model in the classical limit

A complete description of the behaviour of the absolute minima of V for all values of the parameters becomes excessively difficult in the three- and higher-frequency cases, so we restrict our attention to particular values. The potential in the three-frequency case is

$$V(\Phi) = \mu_1 \cos(\beta_1 \Phi) + \mu_2 \cos(\beta_2 \Phi + \delta_2) + \mu_3 \cos(\beta_3 \Phi + \delta_3) . \quad (4.4)$$

We choose the frequency ratios $3 : 2 : 1$, i.e.

$$\beta_1 = \beta , \quad \beta_2 = \frac{2}{3}\beta , \quad \beta_3 = \frac{1}{3}\beta .$$

This three-frequency model has a tricritical point if and only if $\delta_2 = \delta_3 = 0$ (and also in a few equivalent cases), in this case V is symmetric with respect to the reflection $\Phi \mapsto -\Phi$. In the tricritical point the absolute minimum of V can be located only at 0 or π . The two cases are equivalent, we consider the case when the location of the absolute minimum is 0 . The tricritical point in this case is located at

$$\frac{\mu_1}{\mu_2} = -\frac{1}{6} , \quad \frac{\mu_1}{\mu_3} = \frac{1}{15} .$$

In this point $V^{(6)}(0) \neq 0$. (The upper index $^{(6)}$ denotes the sixth derivative with respect to Φ .) $V^{(6)}(0) > 0$ requires $\mu_1, \mu_3 < 0$ and $\mu_2 > 0$. We restrict ourselves to this domain and to the values $\delta_2 = \delta_3 = 0$.

The phase diagram is shown in Figure 4.1. The points of the diagram correspond to the values of the pair (η_1, η_2) of dimensionless parameters. The allowed values constitute the left lower triangle, the straight line joining $(0, 1)$ and $(1, 0)$ corresponds to $\eta_3 = 0$. The tricritical point is denoted by t , it is located at

$$\left(\frac{1}{1 + \sqrt{6} + \sqrt{15}} , \frac{\sqrt{6}}{1 + \sqrt{6} + \sqrt{15}} \right) \approx (0.1365, 0.3345) .$$

At t V has one single and absolute minimum (at $\Phi = 0$). Phase transition occurs when the lines 5 and 3 shown in the phase diagram are crossed. Second order Ising-type phase transition occurs on 5 and first order phase transition occurs on 3. The domain $A \cup B \cup F$ corresponds to a massive \mathbb{Z}_2 -symmetric phase (with unique ground state). The domain $E \cup C$ corresponds to a massive phase with spontaneously broken \mathbb{Z}_2 -symmetry. Characteristic shapes of the potential in the various domains and on the various lines of the phase diagram can be seen in Figure 4.2. Data applying to the quantum case are also shown in Figure 4.1, they will be explained in subsequent sections.

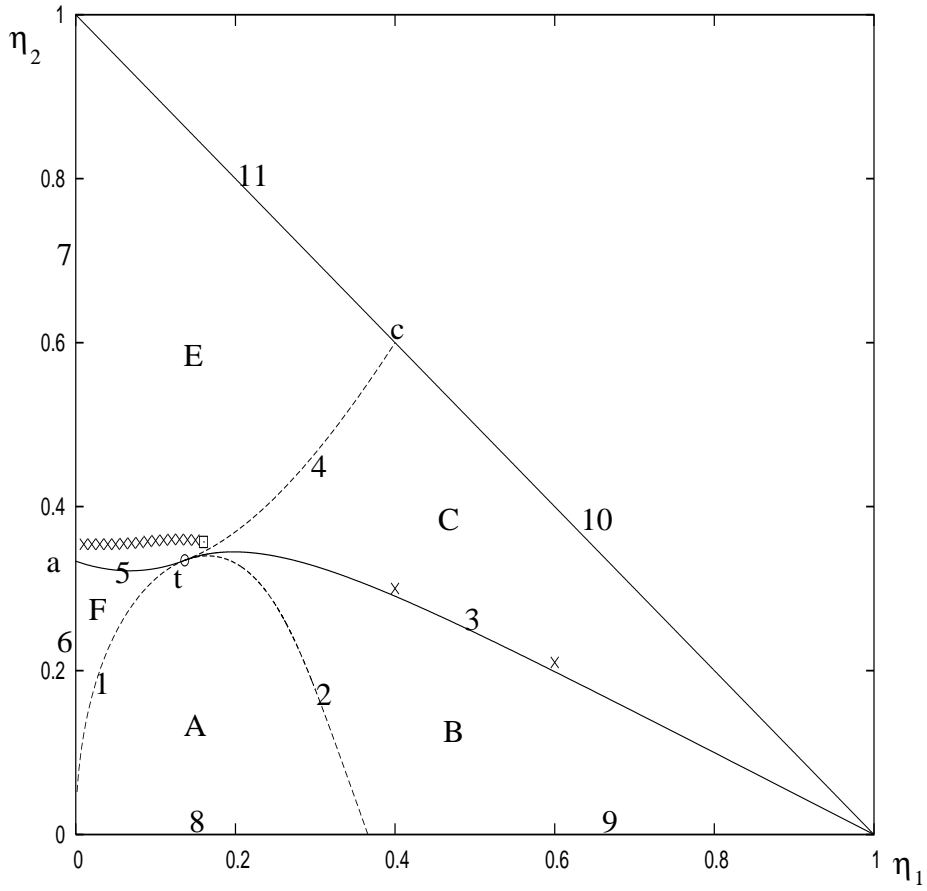


Figure 4.1: Phase diagram of the classical three-frequency sine-Gordon model at $\beta_1/\beta_2/\beta_3 = 3/2/1$, $\delta_1 = \delta_2 = \delta_3 = 0$, $\mu_1, \mu_3 < 0$ and $\mu_2 > 0$. The crosses and the square correspond to certain quantum theory values described in Section 4.6.

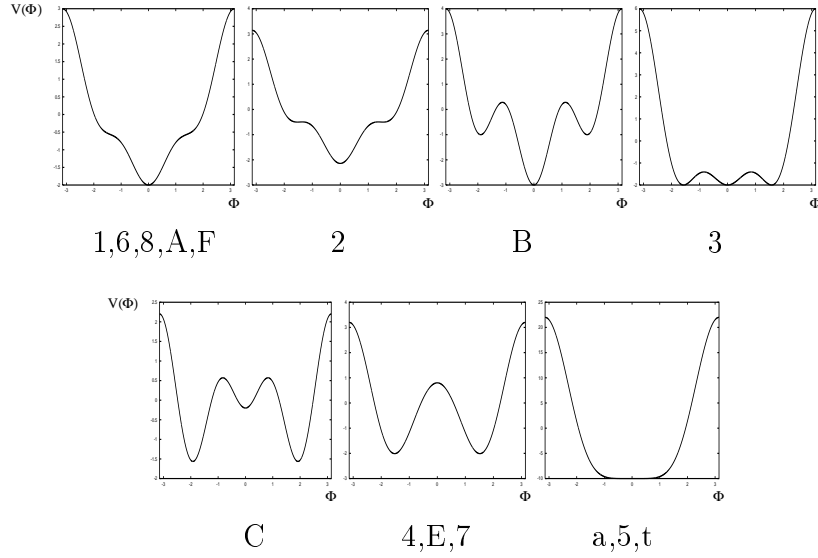


Figure 4.2: Characteristic shapes of the potential

4.3.3 n -frequency model in the classical limit

Let us take the n -frequency model with $\beta_i = i\beta$, $i = 1 \dots n$, and $\delta_i = 0$. In this case there exist unique values of μ_i/μ_1 , $i = 2 \dots n$ so that $V(x)$ has a single global minimum at $x = 0$ and has no other local minima, and $V''(0) = 0$, $V'''(0) = 0$, \dots , $V^{(2n)}(0) = 0$ also hold. The values of μ_i/μ_1 are determined by the latter equations. The point corresponding to these values of μ_i/μ_1 is an n -fold multi-critical point in the phase space. The neighbourhood of this multi-critical point contains m -fold multi-critical points for any integer $0 < m < n$.

These statements can be proved using well known properties of analytic functions and the fact that V is a trigonometric polynomial. We omit the details of the proof.

4.4 Signatures of 1st and 2nd order phase transitions in finite volume

The considerations in this section apply to the quantum case.

The behaviour of the spectrum is governed by the $l \rightarrow 0$ limiting conformal field theory for small values of l , so $e_n(l) - e_0(l) \sim 1/l$. Massive phases in infinite volume are characterized by the existence of a massgap and the behaviour $\lim_{l \rightarrow \infty} (e_n(l) - e_0(l)) = C_n$, where $C_n \geq 0$ are constants. $C_n = 0$ if $0 \leq n \leq d$ and $C_n > 0$ if $n > d$, if the ground state has d -fold degeneracy in infinite volume. In a phase with spontaneously broken symmetry the spectrum is degenerate in the $l \rightarrow \infty$ limit, in finite volume the degeneracy is lifted (at least partially) due to tunneling effects. The resulting energy split between

the degenerate vacua vanishes exponentially as $l \rightarrow \infty$.

In the critical points (in infinite volume) the massgap vanishes and the Hilbert space contains a sector that corresponds to the conformal field theory specifying the universality class of the critical point. We consider this sector in the following discussion. In finite but large volume near the critical point this sector of the theory can be regarded as the $l \rightarrow \infty$ limiting conformal theory perturbed by some irrelevant and relevant operators. The corresponding TCSA Hamiltonian operator takes the (generic) form

$$H = \frac{2\pi}{L} \left((L_0)_{IR} + (\bar{L}_0)_{IR} - \frac{c_{IR}}{12} + \sum_{\psi} \frac{g_{\psi} L^{2-2\Delta_{\psi}}}{(2\pi)^{1-2\Delta_{\psi}}} \psi(1,1) \right), \quad (4.5)$$

where the ψ are the perturbing fields of weight $(\Delta_{\psi}, \Delta_{\psi})$, g_{ψ} are constants. This picture (proposed in [52]) gives the following volume dependence of energy levels (in the first order of conformal perturbation theory):

$$e_{\Psi}(l) - e_0(l) = \frac{2\pi}{l} (\Delta_{IR,\Psi}^+ + \Delta_{IR,\Psi}^-) + \sum_{\psi} A_{\Psi}^{\psi} l^{1-2\Delta_{\psi}}, \quad (4.6)$$

where $\Delta_{IR,\Psi}^+$ and $\Delta_{IR,\Psi}^-$ are the conformal weights of the state Ψ in the $l \rightarrow \infty$ limiting CFT, A_{Ψ}^{ψ} are constants that also depend on the particular energy eigenstate Ψ . The presence of irrelevant perturbations ($1 - 2\Delta_{\psi} < -1$) is due to the finiteness of the volume, whereas the presence of the relevant perturbations ($1 - 2\Delta_{\psi} > -1$) is caused by the deviation of the parameters from the critical value. The effect of the truncation is not taken into consideration in (4.5).

The location of the critical points can be determined using the criterion of vanishing massgap. A more precise method that also allows the determination of the universality class of the critical point (i.e. the $l \rightarrow \infty$ limiting CFT) is the following: we make an assumption that the critical point is in a certain universality class. This assumption predicts the set of ψ -s, the values of $\Delta_{IR,\Psi}^+$ and $\Delta_{IR,\Psi}^-$, and the values of the Δ_{ψ} -s in (4.6). We take leading terms of the series on the r.h.s. of (4.6) and determine the value of the $(\Delta_{IR,\Psi}^+ + \Delta_{IR,\Psi}^-)$ -s and of the A_{Ψ}^{ψ} -s by fitting to the TCSA energy data obtained at several values of l . The magnitude of the A_{Ψ}^{ψ} -s corresponding to the relevant perturbations measures the deviation from the critical point, so if the assumption on the universality class is right, then by tuning the coupling constants one should be able to find a (critical) value at which these A_{Ψ}^{ψ} -s are small, the TCSA data are described well by (4.6) (terms from higher orders of perturbation theory can also be included if necessary) in a reasonably large interval of the values of l , and the values of the $(\Delta_{IR,\Psi}^+ + \Delta_{IR,\Psi}^-)$ -s obtained from the TCSA data agree with the assumption with good precision. The interval where (4.6) describes the TCSA data well is called the scaling region. This region may be (and in

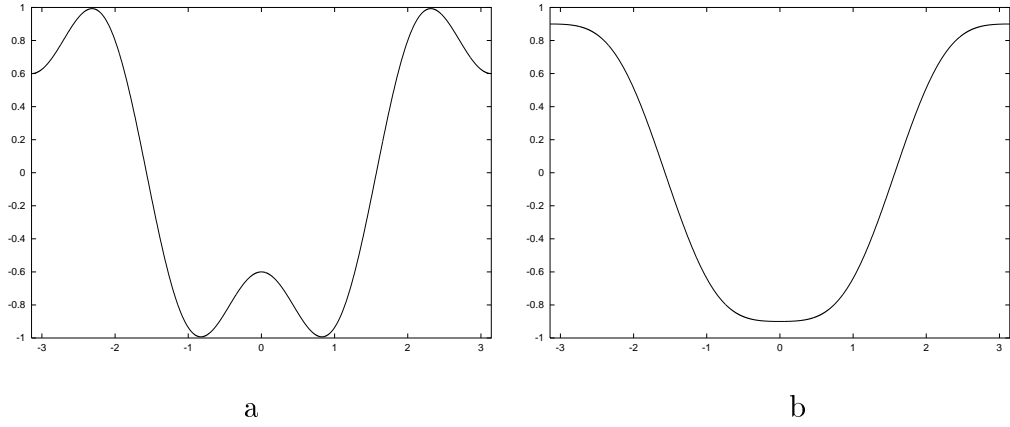


Figure 4.3: Typical shape of $V(\Phi)$ in the broken and in the unbroken symmetry phase

fact is) different for different energy levels. We remark that it is also possible to make a theoretical prediction for $e_0(l)$, which allows to extract c_{IR} from the TCSA data for $e_0(l)$ in principle [52]. However, experience ([52]) shows that the accuracy of the TCSA data is not sufficient to determine c_{IR} precisely in this way, so we did not attempt to extract c_{IR} directly from the TCSA data.

In the classical case a first order phase transition occurs when the absolute minimum of the potential becomes a relative minimum and a previously relative minimum becomes absolute. In the quantum case this phase transition is characterized by the presence of ‘runaway energy levels’ with asymptotic behaviour $e(l) \sim cl$ for large l in the neighbourhood of the transition point, where c is a constant that tends to zero as the transition point is approached. The multiplicity of the ground state also changes as the transition point is passed if the two phases have different symmetry properties. We remark that runaway energy levels are present in general whenever a model has unstable vacua.

4.5 The phase diagram of the two-frequency model in the case $\frac{\alpha}{\beta} = \frac{1}{3}$, $\delta = \frac{\pi}{3}$

We assume that $\lambda, \mu > 0$, and use the parameter

$$\tilde{\eta} = \frac{\lambda^{x_\beta}}{\mu^{x_\alpha} + \lambda^{x_\beta}}$$

instead of η in this case to conform with [52].

The classical model with $\alpha/\beta = \frac{1}{3}$, $\delta = \frac{\pi}{3}$ exhibits an Ising type phase transition at $\tilde{\eta} = 3^4/(1 + 3^4)$.

Considering the quantum case we proceed along the lines of [52] in this section. The numerical nature of the TCSA makes it necessary to choose a finite number of values for β and l at which calculations are done. One should choose as large values for l as possible, the $l \rightarrow \infty$ limit being of interest. However, the accuracy of TCSA decreases as l grows. The accuracy can be improved by taking higher e_{cut} , but this increases the size of the TCSA Hamiltonian matrix and the time needed for diagonalization. Experience shows that accuracy decreases for values of β near to $\sqrt{4\pi}$ (this is the value where UV divergences appear in conformal perturbation theory) although the speed of convergence of the spectrum to the $l \rightarrow \infty$ asymptotic values increases, and the speed of convergence becomes very low for values of β near to 0. Taking these properties of the TCSA into consideration and following [52] we performed calculations at the values $\beta = 8\sqrt{\pi}/7$, $4\sqrt{\pi}/3$, $8\sqrt{\pi}/5$. We also note that the accuracy of the TCSA spectra is severely decreased if V has several (local) minima.

Figure 4.3.a and 4.3.b show the shape of the classical potential in the phases with broken and unbroken \mathbb{Z}_2 -symmetry, respectively. Figures 4.4.a-4.4.g show TCSA spectra obtained at $\beta = 4\sqrt{\pi}/3$ at various values of $\tilde{\eta}$. The TCSA Hilbert space had dimension 3700, the first 12 energy levels are shown in the figures. The highest values of l are chosen so that the truncation error still be small (the massgap remain constant). However, the effect of truncation is perceptible in Figure 4.4.b for instance. It can be seen that in the domain $\tilde{\eta} < 0.92$ the ground states and the first massive states are doubly degenerate. (They are triply degenerate at $\tilde{\eta} = 0$.) ‘Runaway’ energy levels (of constant slope) corresponding to the single local minimum of the potential can also be seen (especially clearly in Figure 4.4.b). In the domain $\tilde{\eta} > 0.98$ the spectra are massive, but the ground state and the first massive state are nondegenerate. In the intermediate domain (especially for $\tilde{\eta} \sim 0.95$) the structure of the spectrum changes, no massgap and degeneracy can clearly be seen. We obtained similar spectra at $\beta = 8\sqrt{\pi}/5$ and $\beta = 8\sqrt{\pi}/7$ as well. As we did not see ‘runaway’ energy levels that would have signaled first order phase transition in the transitional domain of $\tilde{\eta}$ we analyzed the data by looking for a second order Ising type phase transition at some critical values $\tilde{\eta}_c(\beta)$.

The Ising model contains three primary fields: the identity with weights $(0,0)$, the ϵ with weights $(1/2, 1/2)$, and σ with weights $(1/16, 1/16)$. Since the DSG model exhibits the \mathbb{Z}_2 -symmetry for all values of $\tilde{\eta}$, the \mathbb{Z}_2 -odd σ and its descendants cannot appear as perturbations in the Hamiltonian operator (4.5). The only relevant field compatible with the \mathbb{Z}_2 -symmetry is ϵ (the contribution of the identity cancels in the relative energy levels). The presence of a relevant perturbation ϵ in the Hamiltonian operator leads to a correction B_Ψ or $B_\Psi + C_\Psi l$ to $e_\Psi(l) - e_0(l)$. The term $C_\Psi l$ is of second order in

conformal perturbation theory. The leading irrelevant perturbation (compatible with the \mathbb{Z}_2 -symmetry) is the first descendant of ϵ , this gives a correction $A_\Psi l^{-2}$ to $e_\Psi(l) - e_0(l)$ (in first order). Thus we expect that in a large but finite volume range, near $\tilde{\eta}_c(\beta)$, the volume dependence of the energy levels is described well by the formula

$$e_i(l) - e_0(l) = \frac{2\pi}{l} D_i + A_i l^{-2} + B_i + C_i l . \quad (4.7)$$

We fitted this function to the lowest energy levels obtained by TCSA and determined the ‘best’ $\tilde{\eta}_c(\beta)$ value by tuning $\tilde{\eta}$ in the transition region and looking for whether $e_2(l) - e_0(l)$ continues to decrease along the complete l range ($\lim_{l \rightarrow \infty} (e_2(l) - e_0(l)) = 0$ only at $\tilde{\eta}_c(\beta)$), and B_i and C_i are as small as possible. The result is shown in Table 4.1. The fitting was done in the volume ranges $l = 10 - 105$, $l = 55 - 105$; $l = 10 - 140$, $l = 100 - 190$; $l = 20 - 200$, $l = 150 - 390$. The errors presented come from the fitting process and do not contain the truncation errors which are generally larger.

The first two energy levels above the ground state correspond to the operators σ and ϵ in the Ising model. These operators have conformal weights $\Delta^\pm = 1/16$ and $\Delta^\pm = 1/2$, so the exact values for D_1 and D_2 are

$$D_1 = 0.125 , \quad D_2 = 1 .$$

The results of the fits agree quite well with this prediction.

The TCSA data obtained at the estimated values of $\tilde{\eta}_c$ using a truncated space with dimension 4800, 5300 and 5100 are shown in Figure 4.5. These figures show energy levels multiplied by $l/(2\pi)$ as functions of l . The constant lines corresponding to the Ising model values of D_i are also shown in these figures.

To summarize, evaluating the TCSA data we found that the phase transition is second order and Ising type at the values of β chosen. We remark that it is not possible to distinguish a second order transition from a (very) weakly first order transition by TCSA.

For values of β near 0 second order phase transition can be expected, because the model is semi-classical in this region and so the correction to the classical potential in the effective potential is expected to be small.

A correction to the classical potential in the effective potential of frequency $2\beta/3$ is possible in principle. A correction with this frequency is —unlike in the case of $\alpha/\beta = 1/2$ — relevant for any values of β , and it can be verified by elementary calculation that it may change the order of the transition outside the semiclassical region if its coefficient is sufficiently large (see also [117, 52]). However, the accuracy of TCSA did not allow us to perform calculations at values about $\beta^2 > 8\pi/3$ and to check the nature of phase transition in this domain.

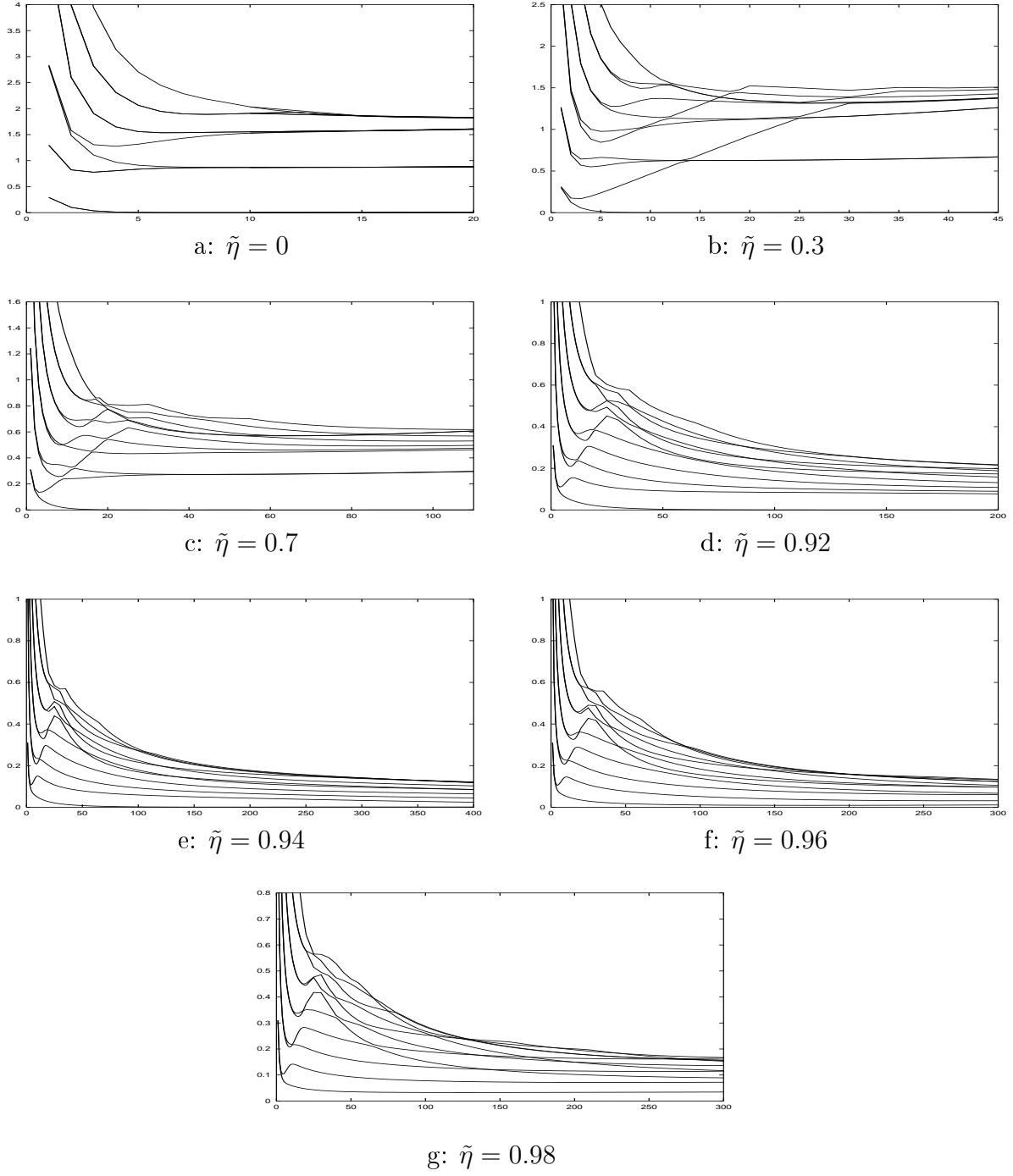


Figure 4.4: Change of the spectrum as $\tilde{\eta}$ varies from 0 to 1 at $\beta = 4\sqrt{\pi}/3$. The first 12 energy levels (including the ground level) relative to the ground level are shown as functions of l .

Table 4.1: The results of fitting (4.7) to the first two excited levels for various values of β at the estimated critical value of $\tilde{\eta}$

$$\beta = 8\sqrt{\pi}/5, \tilde{\eta} = 0.944$$

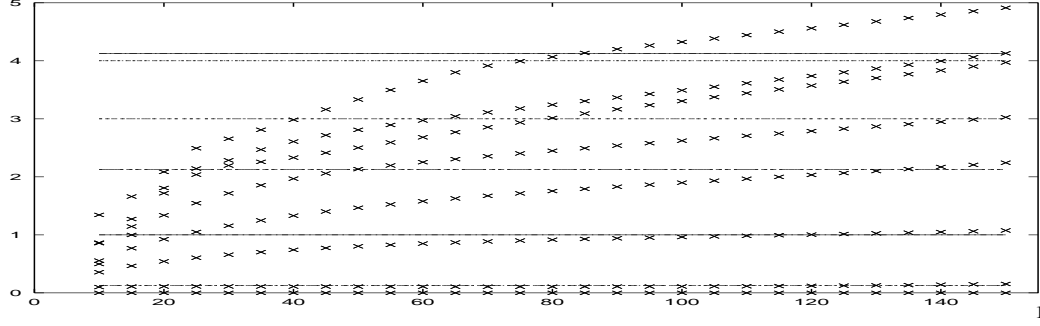
| State | D_i | A_i | B_i | C_i |
|---------|--------------------|-----------------|----------------------|--|
| $i = 1$ | 0.138 ± 0.0005 | -2.0 ± 0.02 | -0.0046 ± 0.0001 | $2.98 \cdot 10^{-5} \pm 9 \cdot 10^{-7}$ |
| $i = 2$ | 1.00 ± 0.01 | -74 ± 2 | 0.004 ± 0.001 | $9 \cdot 10^{-6} \pm 4 \cdot 10^{-6}$ |

$$\beta = 4\sqrt{\pi}/3, \tilde{\eta} = 0.955$$

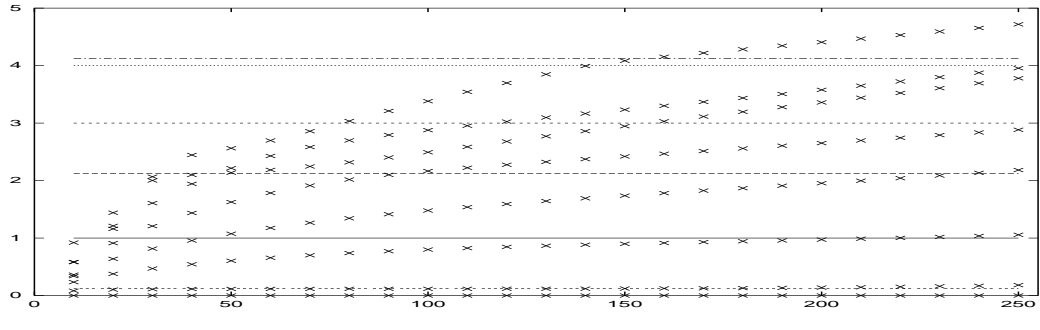
| State | D_i | A_i | B_i | C_i |
|---------|-------------------|-------------------|----------------------|--|
| $i = 1$ | 0.125 ± 0.001 | -2.63 ± 0.025 | -0.0002 ± 0.0001 | $3 \cdot 10^{-7} \pm 1 \cdot 10^{-6}$ |
| $i = 2$ | 1.04 ± 0.02 | -152 ± 6 | 0.0014 ± 0.0009 | $-1.5 \cdot 10^{-5} \pm 2 \cdot 10^{-6}$ |

$$\beta = 8\sqrt{\pi}/7, \tilde{\eta} = 0.961$$

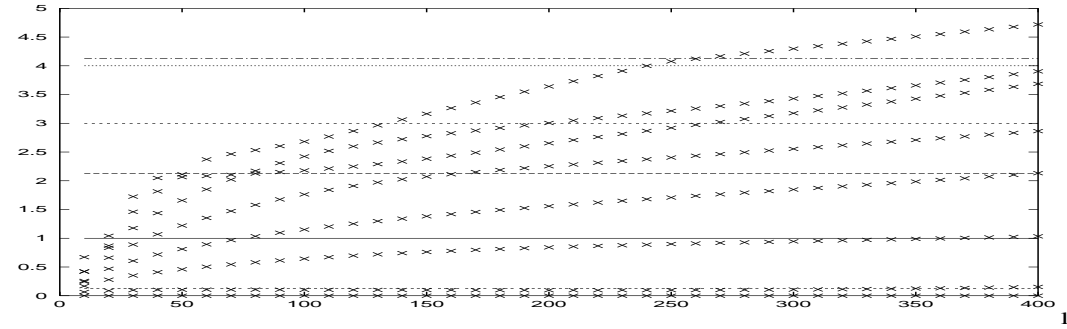
| State | D_i | A_i | B_i | C_i |
|---------|-------------------|----------------|----------------------|---|
| $i = 1$ | 0.125 ± 0.001 | -4.4 ± 0.1 | -0.0009 ± 0.0001 | $4 \cdot 10^{-7} \pm 5 \cdot 10^{-7}$ |
| $i = 2$ | 1.00 ± 0.02 | -252 ± 9 | 0.0002 ± 0.0004 | $4.3 \cdot 10^{-6} \pm 6 \cdot 10^{-7}$ |



$$[e_i(l) - e_0(l)] \cdot l/2\pi \text{ at } \beta = 8\sqrt{\pi}/5 \text{ and } \tilde{\eta} = 0.944$$



$$[e_i(l) - e_0(l)] \cdot l/2\pi \text{ at } \beta = 4\sqrt{\pi}/3 \text{ and } \tilde{\eta} = 0.955$$



$$[e_i(l) - e_0(l)] \cdot l/2\pi \text{ at } \beta = 8\sqrt{\pi}/7 \text{ and } \tilde{\eta} = 0.961$$

Figure 4.5: TCSA spectra as functions of l at the estimated critical values of $\tilde{\eta}$

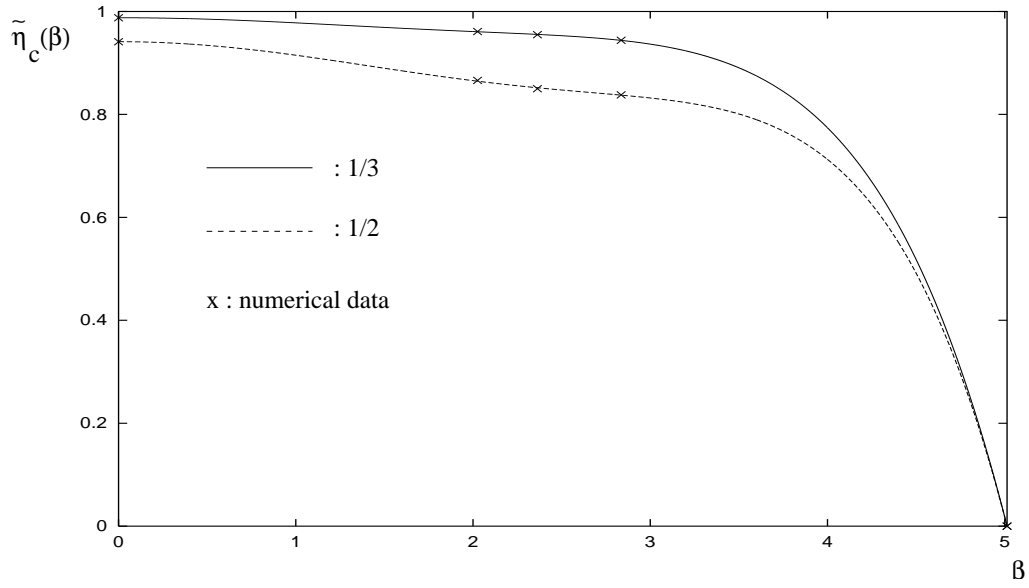


Figure 4.6: The phase diagram of the two-frequency model at $\alpha/\beta = 1/2$ and $\alpha/\beta = 1/3$

The phase diagram in the $(\beta, \tilde{\eta})$ plane based on the data obtained by TCSA can be seen in Figure 4.6. We took into consideration that $\tilde{\eta}_c(0) = 3^4/(1+3^4) \approx 0.988$ is exactly known $\beta = 0$ being the classical limit, and at $\beta = \sqrt{8\pi}$ the term with frequency β in the potential becomes irrelevant and thus for $\beta \rightarrow \sqrt{8\pi}$ the other term and so the symmetric phase is expected to dominate, so $\lim_{\beta \rightarrow \sqrt{8\pi}} \tilde{\eta}_c(\beta) = 0$. The figure shows the three values of $\tilde{\eta}_c$ obtained from the TCSA data and the two values at $\beta = 0$ and $\beta = \sqrt{8\pi}$. The continuous line is obtained by fitting an even polynomial (note that $\tilde{\eta}_c(\beta) = \tilde{\eta}_c(-\beta)$) to these values and is shown in order to get an idea of the phase transition line. The model is in the symmetric phase above the line and in the phase with broken symmetry below the line. The data obtained by [52] for the $\alpha/\beta = 1/2$ case are also shown, the dashed line is fitted to these data.

4.6 Phase diagram of the three-frequency model

We take the same values of the parameters of (4.4) as in section 4.3.2, namely $\beta_1 = \beta, \beta_2 = \frac{2}{3}\beta, \beta_3 = \frac{1}{3}\beta, \delta_2 = \delta_3 = 0, \mu_1, \mu_3 < 0, \mu_2 > 0$, and investigate the quantum model in this case.

4.6.1 The tricritical point

The tricritical Ising model contains 6 primary fields with the following conformal weights:

$$(0, 0), \left(\frac{1}{10}, \frac{1}{10}\right), \left(\frac{3}{5}, \frac{3}{5}\right), \left(\frac{3}{2}, \frac{3}{2}\right), \quad (4.8)$$

and

$$\left(\frac{3}{80}, \frac{3}{80}\right), \left(\frac{7}{16}, \frac{7}{16}\right). \quad (4.9)$$

The fields corresponding to (4.8) are even and those corresponding to (4.9) are odd with respect to parity, so only the fields corresponding to (4.8) and their descendants can contribute to the Hamiltonian operator (4.5). Thus the volume dependence of the energy levels near the tricritical point should be described well for large l by

$$e_{\Psi}(l) - e_0(l) = \frac{2\pi}{l}(\Delta_{IR,\Psi}^+ + \Delta_{IR,\Psi}) + A_{\Psi}l^{-0.2} + B_{\Psi}l^{0.8} + \dots,$$

where only the leading terms are kept. Searching for the tricritical point we fitted the function

$$\frac{2\pi}{l}D_i + A_i l^{-0.2} + B_i l^{0.8} \quad (4.10)$$

of l to the data obtained by TCSA for $e_i(l) - e_0(l)$ near the estimated location of the tricritical point. Best fits are shown in Table 4.2. (The errors presented come from the fitting process and do not contain the truncation errors which are generally larger.) The fitting was done in the volume ranges $l = 50 - 230$, $l = 110 - 230$, the dimension of the truncated Hilbert space was 13600. The results of the fitting support the existence of a tricritical point located (approximately) at $\eta_1 = 0.163$, $\eta_2 = 0.3518$. The exact values of D_1 and D_2 in the tricritical Ising model are

$$D_1 = 0.075, \quad D_2 = 0.2.$$

The numerical results agree quite well with this prediction. The TCSA spectrum obtained at the tricritical point is shown in Figure 4.7. The values of D_i predicted by the tricritical Ising model are also shown in the figure. The dashed lines and + signs are used for odd parity states, the continuous lines and \times signs are used for even parity states.

We used a modified version of the TCSA program exploiting the \mathbb{Z}_2 -symmetry of the model by taking even and odd basis vectors and taking the Hamiltonian operator on the even and odd subspaces separately, which reduces the total time needed for diagonalization and thus allows to take higher e_{cut} values.

The TCSA data for the first two excited states fit quite well to the prediction of the tricritical Ising model, the energy levels of the next two excited states also show correspondence with the prediction. Clear correspondence cannot be seen for higher levels.

Table 4.2: The results of fitting (4.10) to the first two excited levels in the estimated tricritical point

| State | D_i | A_i | B_i |
|---------|-------------------|---------------------|---|
| $i = 1$ | 0.074 ± 0.004 | -0.0060 ± 0.001 | $2.8 \cdot 10^{-5} \pm 5 \cdot 10^{-6}$ |
| $i = 2$ | 0.196 ± 0.01 | -0.006 ± 0.002 | $2.4 \cdot 10^{-5} \pm 6 \cdot 10^{-6}$ |

$$\beta = 8\sqrt{\pi}/7, \eta_1 = 0.163, \eta_2 = 0.3518$$

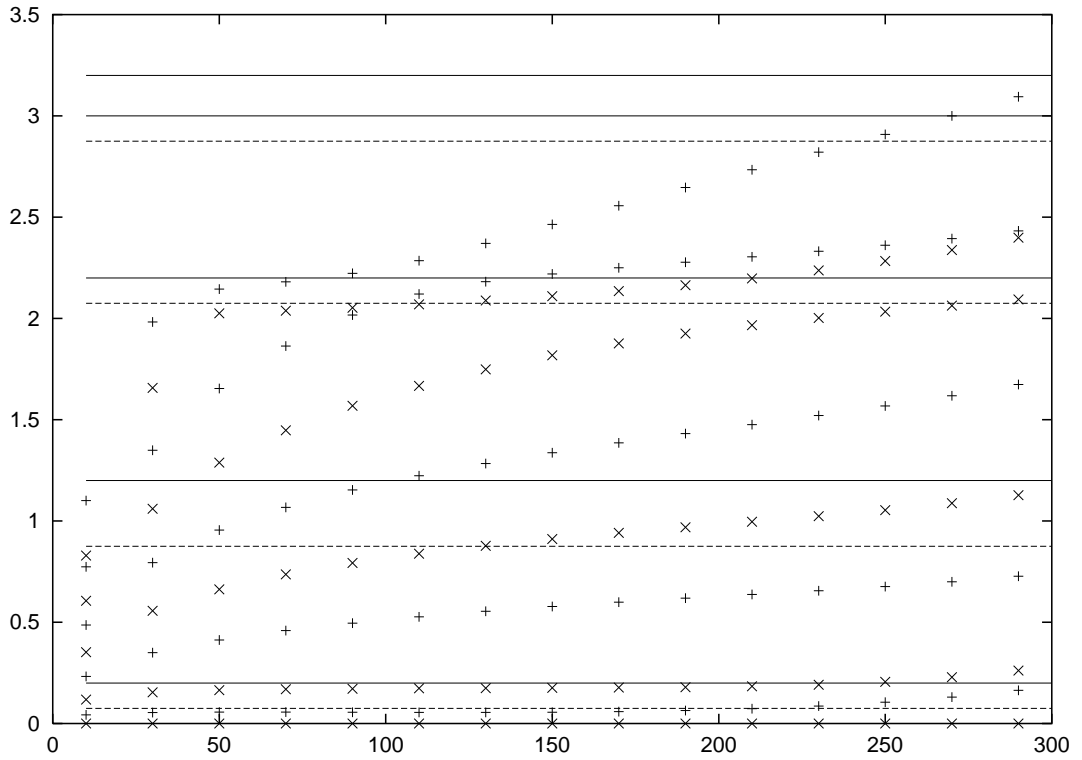


Figure 4.7: $[e_i(l) - e_0(l)] \cdot l/2\pi$ as functions of l obtained by TCSA at $\beta = 8\sqrt{\pi}/7$, $\eta_1 = 0.163$, $\eta_2 = 0.3518$

Table 4.3: Points of the critical line found by TCSA

| η_1 | η_2 | η_1 | η_2 | η_1 | η_2 | η_1 | η_2 |
|----------|----------|----------|----------|----------|----------|----------|----------|
| 0.01 | 0.354 | 0.06 | 0.355 | 0.11 | 0.359 | 0.16 | 0.357 |
| 0.02 | 0.354 | 0.07 | 0.3555 | 0.12 | 0.36 | 0.163 | 0.3565 |
| 0.03 | 0.354 | 0.08 | 0.356 | 0.13 | 0.36 | | |
| 0.04 | 0.354 | 0.09 | 0.3575 | 0.14 | 0.3595 | | |
| 0.05 | 0.354 | 0.1 | 0.3585 | 0.15 | 0.359 | | |

4.6.2 The critical line

The points of the critical line we found using TCSA are listed in Table 4.3. The value of η_1 was chosen and fixed in advance, and then η_2 was estimated in the same way as described in Section 4.5. These points are also marked in Figure 4.1 by crosses. The dimension of the truncated Hilbert space was 10269 in these calculations, which corresponded to $e_{cut} = 17$. The value of β was $8\sqrt{\pi}/5$. Figures 4.8.a-l show the TCSA spectra (especially the lowest lying energy levels) obtained in these points as well as the values of D_i corresponding to both the critical and the tricritical Ising model. Crosses are used for odd parity states, squares are used for even parity states. It can be seen that moving on the critical line in the phase space towards the tricritical endpoint the finite volume spectrum changes continuously. In the $\eta_1 < 0.11$ domain the spectra (especially the first two levels) correspond clearly to phase transitions in the Ising universality class. At $\eta_1 = 0.11$ the first excited level already appears to correspond to the prediction of the tricritical Ising model, whereas the second excited level still has the behaviour predicted by the Ising model. It would be very interesting to know the large volume behaviour (and infinite volume limit) of the first excited level, but the precision of TCSA does not allow to determine it. What we can see is that there is no sign in the TCSA data that the first excited level follows the predictions of the Ising model in the large volume limit. In the domain $0.11 \leq \eta_1 \leq 0.16$ there is a spectacular rearrangement of the higher energy levels (already observable in the $\eta_1 < 0.11$ domain), and at $\eta_1 = 0.16$ the second excited level also appears to correspond to the prediction of the tricritical Ising model. We regard therefore the point $\eta_1 = 0.16$, $\eta_2 = 0.357$ to be the tricritical endpoint of the critical line, this point is marked by a square in Figure 4.1. (We did not aspire to determine the value of η_1 more precisely for this value of β .) Each figure shows the spectrum in the volume interval $l = 0 \dots 200$, and for the large values $l \approx 200$ the truncation error is always conspicuous.

The value of l where the truncation errors become large gets smaller and smaller as

the tricritical point is approached, which corresponds to the fact that a tricritical point as renormalization group fixed point is more repelling than an Ising type one. Increasing η_1 further the behaviour corresponding to the tricritical point would rapidly disappear from the finite volume spectrum.

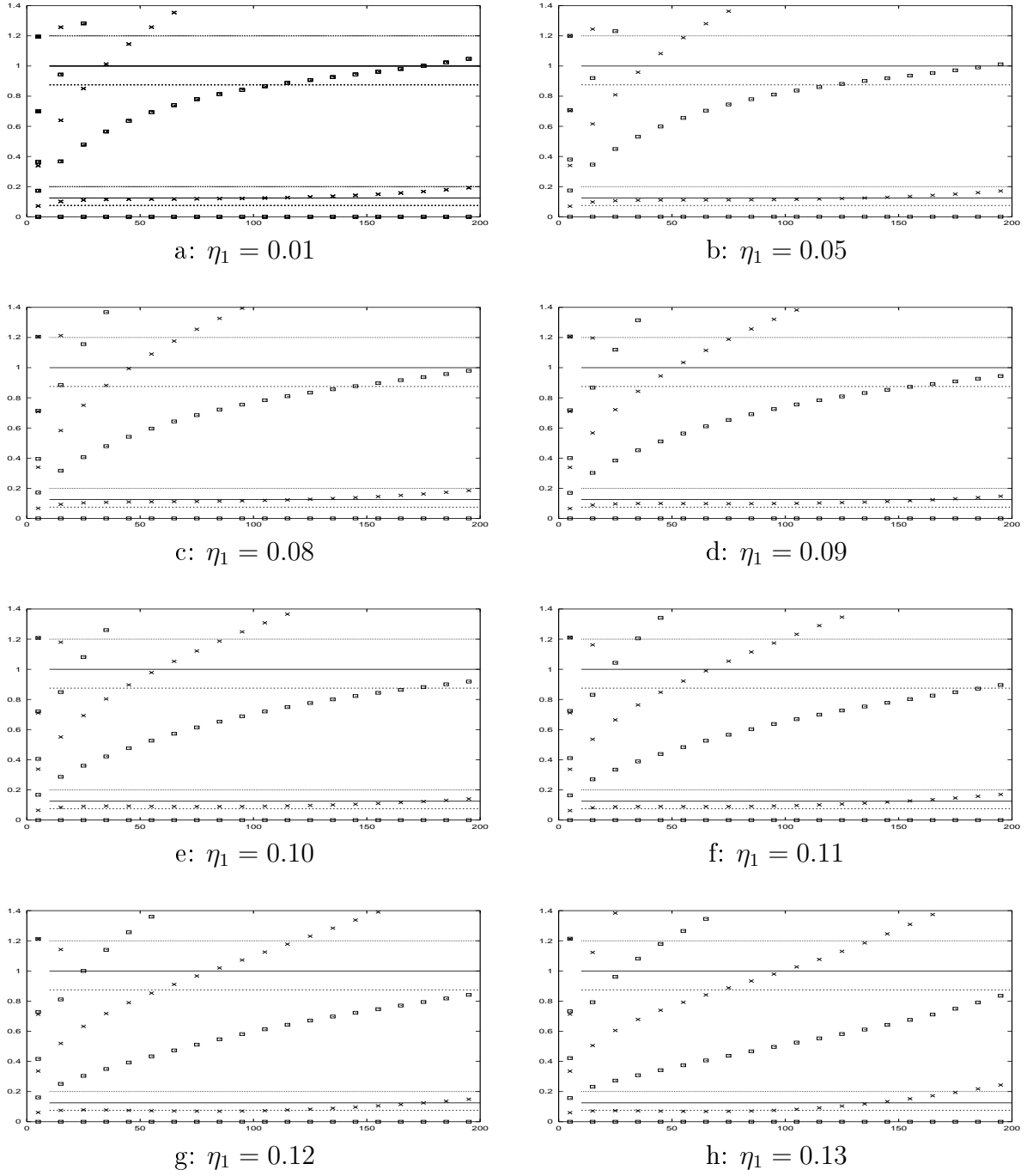


Figure 4.8: $[e_i(l) - e_0(l)] \cdot l / 2\pi$ as functions of l obtained by TCSA at $\beta = 8\sqrt{\pi}/5$ and at various points (η_1, η_2) lying on the critical line, the predictions of the critical Ising model (continuous horizontal lines) for D_i , the predictions of the tricritical Ising model (dashed horizontal lines) for D_i

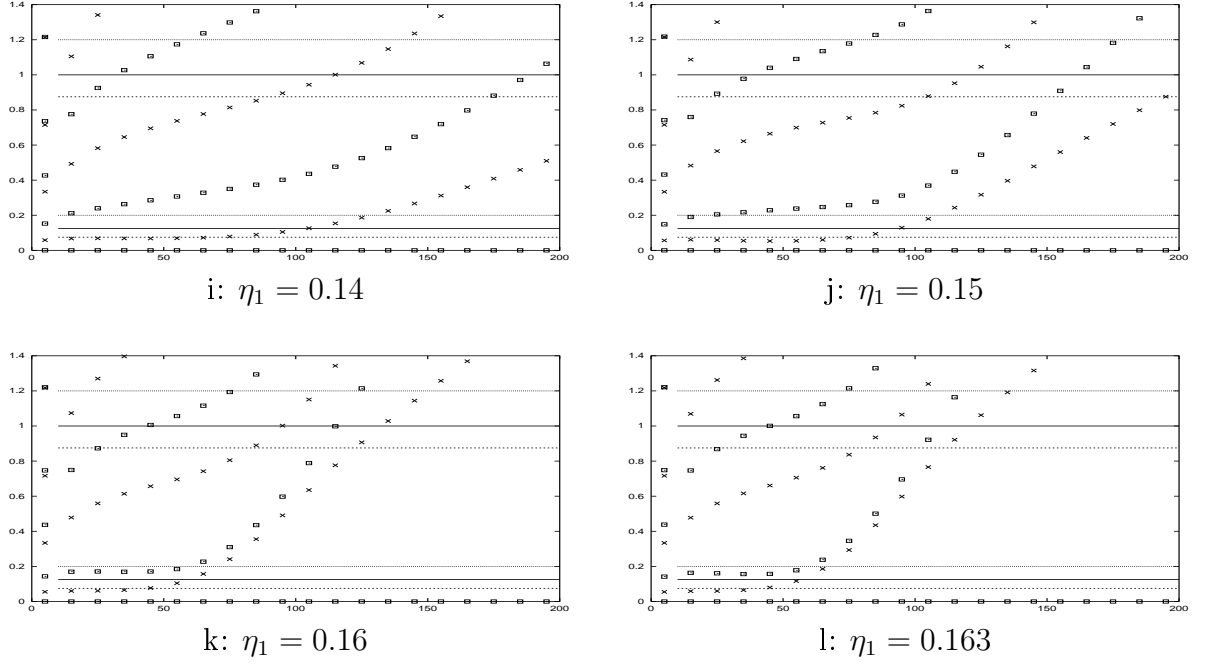


Figure 4.8 continued

4.6.3 The line of first order transition

Figures 4.9.a-j show TCSA spectra obtained at $\eta_1 = 0.6$ and at various values of η_2 between 0.17 and 0.30. The energy levels are shown as compared to the lowest level. The dimension of the truncated Hilbert space was 6597 in these calculations, which corresponded to $e_{cut} = 16$. The value of β was $8\sqrt{\pi}/5$. Dashed lines are used for odd parity levels and continuous lines for even parity levels.

At $\eta_2 = 0.17$ (and also for $\eta_2 < 0.17$) the ground state is unique for all values of l , whereas doubly degenerate runaway levels can also be seen. At $\eta_2 = 0.19$, however, the ground level is doubly degenerate for small values of the volume but becomes nondegenerate in large volume, i.e. there is a value of l where the doubly degenerate runaway level and the single level cross each other. The slope of the runaway levels become smaller and smaller as η_2 is increased, and the crossing point also moves towards larger and larger values. At $\eta_2 = 0.3$ the ground state is already doubly degenerate for all values of l and nondegenerate runaway levels are present. These features indicate that a first order phase transition occurs at an intermediate value of η_2 . The behaviour of the finite volume spectra around the transition point seen in the figures implies that a precise determination of the transition point from the TCSA data in a direct way would require precise data for large values of l . For this reason we did not aspire to find many points of the line

of first order phase transition, we did TCSA calculations only at $\eta_1 = 0.4$ and $\eta_1 = 0.6$, and we roughly estimated the location of the first order phase transition at these values. Our estimation based on the TCSA data are $\eta_2 = 0.30$ and $\eta_2 = 0.21$. These points are also marked in Figure 4.1 by crosses. The Figures 4.9.a-j show the first 20 levels in the domain $l = 0 \dots 200$. Unfortunately the truncation effect is large in most of this domain of l , however we expect that those qualitative features of the spectra which we allude to are correct.

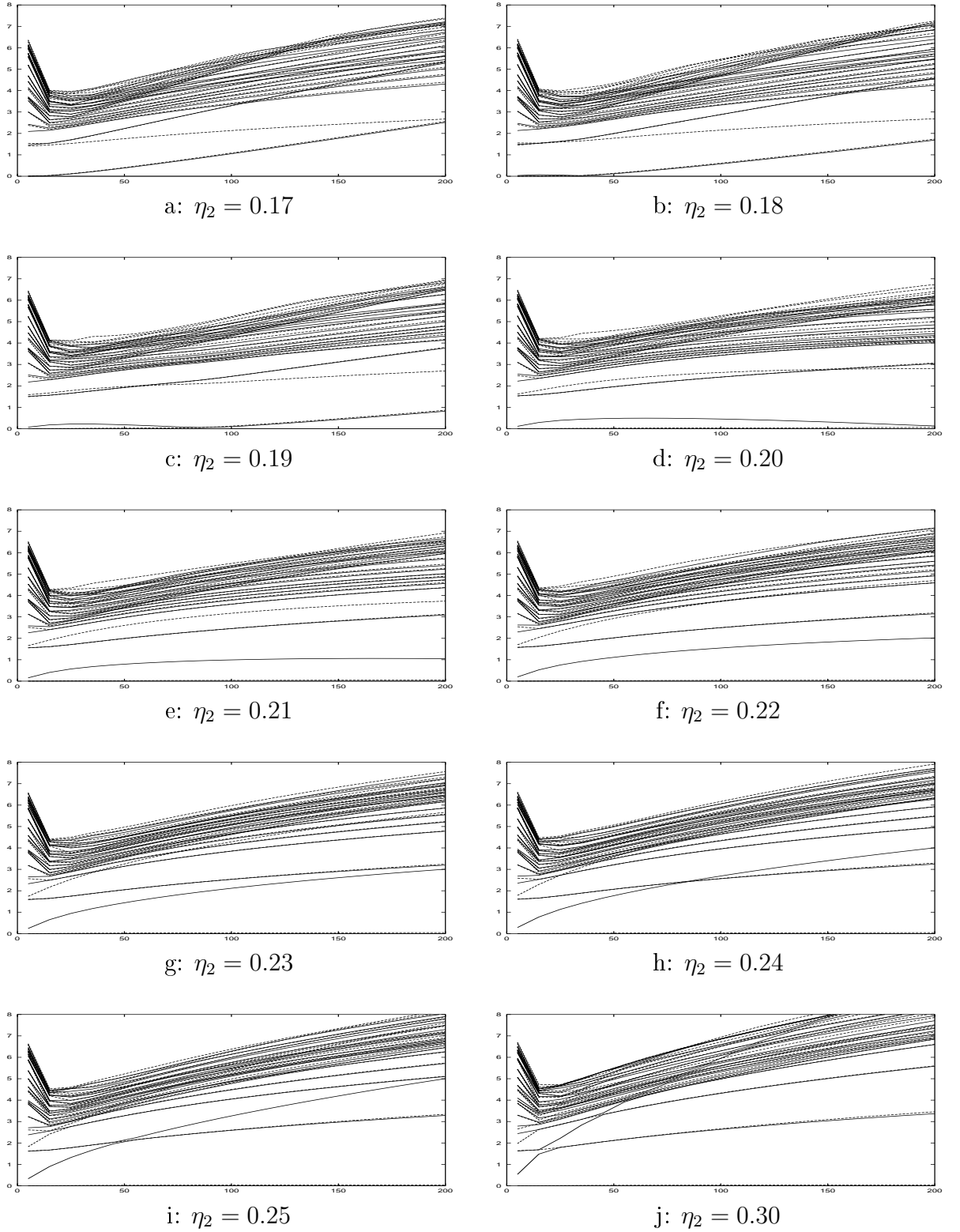


Figure 4.9: $[e_i(l) - e_0(l)]$, $i = 0 \dots 19$ as functions of l obtained by TCSA at $\beta = 8\sqrt{\pi}/5$, $\eta_1 = 0.6$ and at various values of η_2

4.7 Discussion

We have investigated selected special cases of the multi-frequency sine-Gordon theory, especially the structure of their phase space, continuing the work begun in [52]. Concerning the classical limit we found that the only possible phase transition in the (rational) two-frequency case is a second order Ising-type transition. The three-frequency model has some new qualitative features compared to the two-frequency model: a tricritical point which is at the end of a critical line can also be found, and first order transition is possible as well. The phase space of the n -frequency model contains n -fold critical points, otherwise we do not expect new qualitative features compared to the three-frequency model.

The numerical (TCSA) calculations in the quantum case yielded the following results: we found the same type of phase transitions as in the classical case, in particular we were able to determine the second order Ising nature and the location of the phase transition in the two-frequency model with good precision. The accuracy of the TCSA also allowed us to find the tricritical point in the three-frequency case, which we regard the main result of this chapter. It demands more numerical work than the two-frequency model for the following reasons: the two-frequency model has only one-dimensional phase space, whereas the phase space is two-dimensional in the three-frequency model; and the tricritical point as a renormalization group fixed point is more repelling than the Ising-type critical point, so one has to take larger truncated space to achieve good precision. Furthermore, in the three-frequency case we found several points of the critical line and observed how the TCSA spectrum changes as the tricritical endpoint is approached. It would be interesting to investigate this at considerably better precision. Although the focus was mainly on the tricritical point, we also investigated the first order phase transition in the three-frequency model and we found that the first order nature can be established by TCSA, but the location of the transition can be determined much less accurately than that of the second-order transition. We expect that multi-critical points in the universality classes of further elements of the discrete unitary series could be found in the higher-frequency models, but increasing numerical accuracy would be needed, because these multi-critical points are more and more repelling. Finally, we remark that the quantum corrections did not alter the nature of the phase transitions in any of the cases we investigated, and the location of transition points is almost the same in the classical and quantum theory. The investigation of the multi-frequency model with irrational frequency ratios is still an open problem. We also remark that the particle content of the multi-frequency sine-Gordon model could also be investigated by the method of semiclassical quantization [118].

Acknowledgements

I would like to express my gratitude to my supervisor László Palla for his advice and constant support during my research. I am also grateful to Gábor Takács and Zoltán Bajnok for many illuminating discussions. I thank Gustav Delius for an illuminating discussion on the boundary supersymmetry algebra, and the Mathematics Department at King's College London, where I spent ten months, for hospitality. I also thank Gérard Watts for acting as a supervisor while I was at King's College London. Finally, I express my gratitude for the invaluable support that was provided to me by the Theoretical Physics Research Group of the Hungarian Academy of Sciences at the Theoretical Physics Department of Eötvös University. I acknowledge support by the Hungarian fund OTKA (T037674), by the Research Training Network "EUCLID" (contract HPRN-CT-2002-00325) of the EU at various times, and by the Marie Curie Training Site (MCFH-2001-00296) "Strings, Branes and Boundary Conformal Field Theory" of the EU at King's College London.

Bibliography

- [1] W.E. Thirring: A soluble relativistic field theory, *Ann. of Phys* **3**, 1958, 91-112
- [2] J. Schwinger: Field Theory Commutators, *Phys. Rev. Lett.* **3**, 1959, 296-297
- [3] J. Schwinger: Gauge Invariance and Mass. II, *Phys. Rev.* **128**, 1962, 2425-2429
- [4] H. Bethe: On the theory of metals: eigenvalues and eigenfunctions of linear atomic chains, *Z. Phys.* **71**, 1931, 205
- [5] L. Onsager: Crystal statistics I: a two-dimensional model with an order-disorder transition, *Phys. Rev.* **65**, 1944, 117-149
- [6] B. Berg, M. Karowski, P. Weisz: Construction of Green functions from an exact S matrix, *Phys. Rev.* **D19**, 1979, 2477
- [7] M. Karowski, P. Weisz: Exact Form-Factors In (1+1)-Dimensional Field Theoretic Models With Soliton Behavior, *Nucl. Phys.* **B139**, 1978, 455
- [8] P.H. Weisz: Exact Quantum Sine-Gordon Soliton Form-Factors, *Phys. Lett.* **B67**, 1977, 179
- [9] A.B. Zamolodchikov: Integrable field theory from conformal field theory, *Adv. Studies in Pure Math.* **19**, 1989, 641-674
- [10] A.B. Zamolodchikov: Integrals of motion in scaling three state Potts model field theory, *Int. J. Mod. Phys.* **A3**, 1988, 743-750
- [11] A.B. Zamolodchikov: Higher order integrals of motion in two-dimensional models of the field theory with a broken conformal symmetry, *JETP Lett.* **46**, 1987, 160-164
- [12] G.Zs. Tóth: N=1 boundary supersymmetric bootstrap, *Nucl. Phys.* **B676**, 2003, 497-536, hep-th/0308146

- [13] G.Zs. Tóth: A non-perturbative study of phase transitions in the multi-frequency sine-Gordon model, *J. Phys.* **A37**, 2004, 9631-9650, hep-th/0406139
- [14] I. Affleck, A.W.W. Ludwig: Critical theory of overscreened Kondo fixed points, *Nucl. Phys.* **B360**, 1991, 641-696
- [15] I. Affleck, A.W.W. Ludwig: Exact conformal field theory results on the multichannel Kondo effect: single-fermion Green's function, self energy, and resistivity, *Phys. Rev.* **B48**, 1993, 7297
- [16] P. Fendley, A.W.W. Ludwig, H. Saleur: Exact conductance through point contacts in the $\nu = 1/3$ fractional quantum Hall effect, *Phys. Rev. Lett.* **74**, 1995, 3005, cond-mat/9408068; Exact non-equilibrium transport through point contacts in quantum wires and fractional quantum Hall devices, *Phys. Rev.* **B52**, 1995, 8934, cond-mat/9503172; Exact non-equilibrium DC shot noise in Luttinger liquids and fractional quantum Hall devices, *Phys. Rev. Lett.* **75**, 1995, 2196, cond-mat/9505031
- [17] R. Chatterjee: Exact Partition Function and Boundary State of 2-D Massive Ising Field Theory with Boundary Magnetic Field, *Nucl. Phys.* **B468**, 1996, 439-460, hep-th/9509071
- [18] H. Saleur: Lectures on nonperturbative field theory and quantum impurity problems, in the proceedings of the 1998 Les Houches Summer School, cond-mat/9812110; Lectures on non perturbative field theory and quantum impurity problems: Part 2, cond-mat/0007309
- [19] S. Ghoshal, A. Zamolodchikov: Boundary S matrix and boundary state in two-dimensional integrable quantum field theory, *Int. J. Mod. Phys.* **A9**, 1994, 3841-3886, Erratum-ibid. **A9** 4353, hep-th/9306002
- [20] Z. Bajnok, L. Palla, G. Takács, G.Zs. Tóth: The spectrum of boundary states in sine-Gordon model with integrable boundary conditions, *Nucl. Phys.* **B622**, 2002, 548-564, hep-th/0106070
- [21] P. Mattsson: Integrable quantum field theories in the bulk and with a boundary, PhD thesis, University of Durham, UK, 2000, hep-th/0111261
- [22] P. Mattsson, P. Dorey: Boundary spectrum in the sine-Gordon model with Dirichlet boundary conditions, *J. Phys.* **A33**, 2000, 9065-9094, hep-th/0008071

- [23] G.W. Delius, G.M. Gandenberger: Particle reflection amplitudes in $a_n^{(1)}$ Toda field theories, *Nucl. Phys.* **B554**, 1999, 325-364, hep-th/9904002
- [24] E. Corrigan, A. Taormina: Reflection factors and a two-parameter family of boundary bound states in the sinh-Gordon model, *J. Phys.* **A33**, 2000, 8739-8754, hep-th/0008237
- [25] E. Corrigan, G.W. Delius: Boundary breathers in the sinh-Gordon model, *J. Phys.* **A32**, 1999, 8001-8014, hep-th/9909145
- [26] Z. Bajnok, L. Palla, G. Takács: On the boundary form factor program, *Nucl. Phys.* **B750**, 2006, 179-212, hep-th/0603171
- [27] M. Jimbo, R. Kedem, H. Konno, T. Miwa, R. Weston: Difference equations in spin chains with a boundary, *Nucl. Phys.* **B448**, 1995, 429-456
- [28] T. Kojima, Y.H. Quano: Difference equations for the higher rank XXZ model with a boundary, *Int. J. Mod. Phys.* **A15**, 2000, 3699-3716, nlin.si/0001038, Y.H. Quano: Difference equations for correlation functions of Belavin's $Z(n)$ symmetric model with boundary reflection, *J. Phys.* **A33**, 2000, 8275, hep-th/0003276, Y.H. Quano: Difference equations for correlation functions of $A^{**}(1)(n-1)$ face model with boundary reflection, *J. Phys.* **A34**, 2001, 8445-8464, hep-th/0102100
- [29] B. Hou, K. Shi, Y. Wang, W. Yang: Bosonization of quantum sine-Gordon field with boundary, *Int. J. Mod. Phys.* **A12**, 1997, 1711-1741, hep-th/9905197
- [30] K. Schoutens: Supersymmetry and factorized scattering, *Nucl. Phys.* **B344**, 1990, 665-695
- [31] D. Bernard, A. LeClair: Residual quantum symmetries of the restricted sine-Gordon theories, *Phys. Lett.* **B227**, 1989, 417
- [32] C. Ahn, D. Bernard, A. LeClair: Fractional supersymmetries in perturbed coset CFTs and integrable soliton theory, *Nucl. Phys.* **B346**, 1990, 409-439
- [33] C. Ahn: Complete S-matrices of supersymmetric sine-Gordon theory and perturbed superconformal minimal model, *Nucl. Phys.* **B354**, 1991, 57-84
- [34] T.J. Hollowood, E. Mavrikis: The $N=1$ supersymmetric bootstrap and Lie algebras, *Nucl. Phys.* **B484**, 1997, 631-652, hep-th/9606116

- [35] K. Schoutens, M. Moriconi: Reflection matrices for integrable $N=1$ supersymmetric theories, *Nucl. Phys.* **B487**, 1997, 756-778, hep-th/9605219
- [36] Z. Bajnok, L. Palla, G. Takács: Spectrum of boundary states in $N=1$ SUSY sine-Gordon theory, *Nucl. Phys.* **B644**, 2002, 509, hep-th/0207099
- [37] R.I. Nepomechie: Supersymmetry in the boundary tricritical Ising field theory, *Int. J. Mod. Phys.* **A17**, 2002, 3809, hep-th/0203123
- [38] C. Ahn, W. Koo: Exact boundary scattering matrices of the supersymmetric sine-Gordon theory on a half line, *J. Phys.* **A29**, 1996, 5845-5854, hep-th/9509056
- [39] C. Ahn, W. Koo: Supersymmetric sine-Gordon model and the eight-vertex free fermion model with boundary, *Nucl. Phys.* **B482**, 1996, 675-695, hep-th/9606003
- [40] L. Chim: Boundary S-matrix for the tricritical Ising model, *Int. J. Mod. Phys.* **A11**, 1996, 4491-4512, hep-th/9510008
- [41] P. Dorey: Exact S-matrices, in Conformal Field Theories and Integrable Models, Proceedings of the Eötvös Graduate Course p. 85, Budapest 1996, edited by Z. Horváth and L. Palla, Springer Verlag, ISBN: 3540636188, hep-th/9810026
- [42] G. Mussardo: Off critical statistical models: factorized scattering theories and bootstrap program, *Phys. Rept.* **218**, 1992, 215-379
- [43] E. Abdalla, M.C.B. Abdalla, K.D. Rothe: Non-perturbative methods in 2 dimensional quantum field theory, World Scientific, 1991
- [44] O.A. Castro Alvaredo: Bootstrap methods in 1+1 dimensional quantum field theories: the homogeneous sine-Gordon model, PhD thesis, University of Santiago de Compostela, Spain, 2001, hep-th/0109212
- [45] V. Riva: Semiclassical methods in 2D QFT: spectra and finite size effects, PhD thesis, SISSA Trieste, Italy, 2004, hep-th/0411083
- [46] P. Christe, M. Henkel: Introduction to Conformal Invariance and Its Applications to Critical Phenomena, Lecture Notes in Physics, Springer-Verlag
- [47] Alexander B. Zamolodchikov, Alexei B. Zamolodchikov: Factorized S-matrices in two dimensions as the exact solutions of certain relativistic quantum field models, *Ann. Phys.* **120**, 1979, 253-291

- [48] G.W. Delius, N.J. MacKay: Quantum group symmetry in sine-Gordon and affine Toda field theories on the half-line, *Commun. Math. Phys.* **233**, 2003, 173-190, hep-th/0112023
- [49] G.W. Delius, A. George: Quantum group symmetry of integrable models on the half-line, “Sao Paulo 2002, Integrable theories, solitons and duality”, unesp2002/042, 2002, hep-th/0212300
- [50] G. Feverati, F. Ravanini, G. Takács: Truncated conformal space at $c=1$, nonlinear integral equation and quantization rules for multi-soliton states, *Phys. Lett.* **B430**, 1998, 264-273, hep-th/9803104
- [51] B. Pozsgay, G. Takács: Characterization of resonances using finite size effects, *Nucl. Phys.* **B748**, 2006, 485-523, hep-th/0604022
- [52] Z. Bajnok, L. Palla, G. Takács, F. Wágner: A nonperturbative study of the two-frequency sine-Gordon model, *Nucl. Phys.* **B601**, 2000, 503-538, hep-th/0008066
- [53] M. Kormos: Boundary renormalisation group flows of unitary superconformal minimal models, *Nucl. Phys.* **B744**, 2006, 358-379, hep-th/0512085
- [54] A. Recknagel, D. Roggenkamp, V. Schomerus: On Relevant Boundary Perturbations of Unitary Minimal Models, *Nucl. Phys.* **B588**, 2000, 552-564, hep-th/0003110
- [55] K. Graham, G.M.T. Watts: Defect lines and boundary flows, *JHEP* **0404**, 2004, 019, hep-th/0306167
- [56] S. Fredenhagen: Organizing Boundary RG Flows, *Nucl. Phys.* **B660**, 2003, 436-472, hep-th/0301229
- [57] F. Lesage, H. Saleur, P. Simonetti: Boundary flows in minimal models, *Phys. Lett.* **B427**, 1998, 85-92, hep-th/9802061
- [58] A. Cappelli, G. D’Appollonio, M. Zabzine: Landau-Ginzburg description of boundary critical phenomena in two-dimensions, *JHEP* **0404**, 2004, 010, hep-th/0312296
- [59] J.L. Cardy, M. Lässig, G. Mussardo: *The scaling region of the tricritical Ising model in two-dimensions*, *Nucl. Phys. B* **348**, 1991, 591-618
- [60] G.M.T. Watts, private communication, 2004

- [61] G. Feverati, K. Graham, P.A. Pearce, G. Zs. Tóth, G. Watts: *A Renormalisation group for TCSCA*, talk presented by G. Watts at the workshop “Integrable Models and Applications: from Strings to Condensed Matter”, Santiago de Compostela, Spain, 12-16 September 2005, hep-th/0612203
- [62] J. Cardy: Boundary Conditions, Fusion Rules And The Verlinde Formula, *Nucl. Phys.* **B324**, 1989, 581
- [63] J. Cardy, D. Lewellen: Bulk and boundary operators in conformal field theory, *Phys. Lett.* **B259**, 1991, 274-278
- [64] I. Affleck, A.W.W. Ludwig: Universal Noninteger “Ground-State Degeneracy” in Critical Quantum Systems, *Phys. Rev. Lett.* **67**, 1991, 161-164
- [65] G. Feverati, K. Graham, P.A. Pearce, G.M.T. Watts, in preparation
- [66] R. Chatterjee: Exact Partition Function and Boundary State of Critical Ising Model with Boundary Magnetic Field, *Mod. Phys. Lett.* **A10**, 1995, 973-984, hep-th/9412169
- [67] R. Chatterjee, A. Zamolodchikov: Local Magnetization in Critical Ising Model with Boundary Magnetic Field, hep-th/9311165
- [68] A. LeClair, G. Mussardo, H. Saleur, S. Skorik: Boundary energy and boundary states in integrable quantum field theories, *Nucl. Phys.* **B453**, 1995, 581-618, hep-th/9503227
- [69] A. Konechny: Ising model with a boundary magnetic field: An example of a boundary flow, *JHEP* **0412**, 2004, 058, hep-th/0410210
- [70] R. Konik, A. LeClair, G. Mussardo: On Ising correlation functions with boundary magnetic field, *Int. J. Mod. Phys.* **A11**, 1996, 2765-2782, hep-th/9508099
- [71] I. Runkel: Boundary Problems in Conformal Field Theory, PhD thesis, King’s College London, UK, 2000
- [72] P. Dorey, I. Runkel, R. Tateo, G.M.T. Watts: g-function flow in perturbed boundary conformal field theories, *Nucl. Phys.* **B578**, 2000, 85-122, hep-th/9909216
- [73] P. Di Francesco, P. Mathieu, D. Sénéchal: Conformal Field Theory, Graduate Texts in Contemporary Physics, Springer-Verlag

- [74] G.Zs. Tóth: A study of truncation effects in boundary flows of the Ising model on a strip, *J. Stat. Mech.* P04005, 2007, hep-th/0612256
- [75] G. Delfino, G. Mussardo: Non-integrable aspects of the multi-frequency sine-Gordon model, *Nucl. Phys.* **B516**, 1998, 675-703, hep-th/9709028
- [76] H.M. Babujian, A. Fring, M. Karowski, A. Zapletal: Exact form factors in integrable quantum field theories: the sine-Gordon model, *Nucl. Phys.* **B538**, 1999, 535-586, hep-th/9805185
- [77] F.A. Smirnov: Form-factors in completely integrable models of quantum field theory, *Adv. Ser. Math. Phys.* **14**, 1992, 1-208
- [78] P. Ginsparg: *Applied Conformal Field Theory*, 1989 Fields, Strings and Critical Phenomena (Les Houches, Session XLIX, 1988) ed E Brézin and J Zinn-Justen (Elsevier), hep-th/9108028
- [79] D. Lewellen: Sewing constraints for conformal field theories on surfaces with boundaries, *Nucl. Phys.* **B372**, 1992, 654-682
- [80] I. Runkel: Structure constants for the D series Virasoro minimal models, *Nucl. Phys.* **B579** 2000, 561-589, hep-th/9908046
- [81] I. Runkel: Boundary structure constants for the A series Virasoro minimal models, *Nucl. Phys.* **B549**, 1999, 563-578, hep-th/9811178
- [82] V.B. Petkova, J.-B. Zuber: Conformal boundary conditions and what they teach us, Lectures given at Eotvos Summer School in Physics: Nonperturbative QFT Methods and Their Applications, Budapest, Hungary, 14-18 August 2000. Published in Budapest 2000, Non-perturbative QFT methods and their applications, 1-35, hep-th/0103007
- [83] R.E. Behrend, P.A. Pierce, V.B. Petkova, J.-B. Zuber: Boundary conditions in rational conformal field theories, *Nucl. Phys.* **B570**, 2000, 525-589, hep-th/9908036
- [84] R.E. Behrend, P.A. Pierce, V.B. Petkova, J.-B. Zuber: On the classification of bulk and boundary conformal field theories, *Phys. Lett.* **B444**, 1998, 163-166, hep-th/9809097
- [85] R.E. Behrend, P.A. Pierce, J.-B. Zuber: Integrable boundaries, conformal boundary conditions and A-D-E fusion rules, *J. Phys.* **A31**, 1998, L763-L770, hep-th/9807142

- [86] K. Graham, I. Runkel, G.M.T. Watts: Renormalisation Group Flows of Boundary Theories, 4th Annual European TMR Conference on Integrability, Nonperturbative Effects and Symmetry in Quantum Field Theory, Paris, France, 7-13 Sep 2000, hep-th/0010082
- [87] K. Graham, I. Runkel, G.M.T. Watts: Boundary Renormalisation Group Flows of Minimal Models, Non-perturbative QFT methods and their applications: proceedings of the 24th Johns Hopkins Workshop on Current Problems in Particle Theory, Budapest, Hungary, World Scientific, 2000, 95-113
- [88] P. Dorey, M. Pillin, A. Pocklington, I. Runkel, R. Tateo, G.M.T. Watts: Finite Size Effects in Perturbed Boundary Conformal Field Theories, 4th Annual European TMR Conference on Integrability, Nonperturbative Effects and Symmetry in Quantum Field Theory, Paris, France, 7-13 Sep 2000, hep-th/0010278
- [89] F. Ravanini: Finite size effects in integrable quantum field theories, Eotvos Summer School in Physics: Nonperturbative QFT Methods and Their Applications, Budapest, Hungary, 14-18 August 2000, Published in Budapest 2000, Non-perturbative QFT methods and their applications, 199-264, hep-th/0102148
- [90] S.R. Coleman, H.J. Thun: On the prosaic origin of the double poles in the sine-Gordon S matrix, *Comm. Math. Phys.* **61**, 1978, 31
- [91] P. Dorey, R. Tateo, G.M.T. Watts: Generalisations of the Coleman-Thun mechanism and boundary reflection factors, *Phys. Lett.* **B448**, 1999, 249-256, hep-th/98100098
- [92] Z. Bajnok, G. Böhm, G. Takács: On perturbative quantum field theory with boundary, *Nucl. Phys.* **B682**, 2004, 585-617, hep-th/0309119
- [93] Z. Bajnok, G. Böhm, G. Takács: Boundary reduction formula, *J. Phys.* **A35**, 2002, 9333-9342, hep-th/0207079
- [94] L. Castillejo, R.H. Dalitz, F.J. Dyson: Low's scattering equation for the charged and neutral scalar theories, *Phys. Rev.* **101**, 1956, 453-458
- [95] Z. Bajnok, C. Dunning, L. Palla, G. Takács, F. Wágner: SUSY sine-Gordon theory as a perturbed conformal field theory and finite size effects, *Nucl. Phys.* **B679**, 2004, 521-544, hep-th/0309120

- [96] E.K. Sklyanin: Boundary Conditions for Integrable Models, *Funct. Anal. Appl.* **21**, 1987, 164-166
- [97] R.I. Nepomechie: The boundary supersymmetric sine-Gordon model revisited, *Phys. Lett.* **B509**, 2001, 183-188, hep-th/0103029
- [98] A. MacIntyre: Integrable boundary conditions for classical sine-Gordon theory, *J. Phys.* **A28**, 1995, 1089, hep-th/9410026
- [99] C. Ahn, R.I. Nepomechie: Exact solution of the supersymmetric sinh-Gordon theory on a half line, *Nucl. Phys.* **B586**, 2000, 611-640, hep-th/0005170
- [100] E. Corrigan, P.E. Dorey, R.H. Rietdijk and R. Sasaki: Affine Toda field theory on a half-line, *Phys. Lett.* **B333**, 1994, 83, hep-th/9404108
- [101] P. Bowcock, E. Corrigan, P.E. Dorey and R.H. Rietdijk: Classically integrable boundary conditions for affine Toda field theories, *Nucl. Phys.* **B445**, 1995, 469, hep-th/9501098
- [102] E. Corrigan: Integrable models with boundaries and defects, UK-Japan Winter School on Geometry and Analysis Towards Quantum Theory, Durham, England, 6-9 Jan 2004, math-ph/0411043
- [103] A. George: The massive Klein-Gordon field coupled to a harmonic oscillator at the boundary, *J. Phys.* **A38**, 2005, 7399-7418, hep-th/0412067
- [104] P. Baseilhac, G.W. Delius, A. George: Coupling the sine-Gordon theory to a mechanical system at the boundary, nlin.si/0201007
- [105] V.P. Yurov, Al.B. Zamolodchikov: Truncated conformal space approach to scaling Lee-Yang model, *Int. J. Mod. Phys.* **A5**, 1990, 3221-3246
- [106] P. Dorey, A. Pocklington, R. Tateo, G.M.T. Watts: TBA and TCSA with Boundaries and Excited States, *Nucl. Phys.* **B525**, 1998, 641-663, hep-th/9712197
- [107] V.P. Yurov, Al.B. Zamolodchikov: Truncated fermionic space approach to the critical 2-D Ising model with magnetic field, *Int. J. Mod. Phys.* **A6**, 1991, 4557-4578
- [108] Zamolodchikov A B, *Thermodynamic Bethe Ansatz In Relativistic Models. Scaling Three State Potts And Lee-Yang Models*, 1990 *Nucl. Phys. B* **342** 695-720
- [109] T.R. Klassen, E. Melzer: Kinks in Finite Volume, *Nucl. Phys.* **B382**, 1992, 441-485, hep-th/9202034

- [110] Z. Bajnok, L. Palla, G. Takács, F. Wágner: The k-folded sine-Gordon model in finite volume, *Nucl. Phys.* **B587**, 2000, 585-618, hep-th/0004181
- [111] P. Fendley, H. Saleur: Deriving boundary S matrices, *Nucl. Phys.* **B428**, 1994, 681-693, hep-th/9402045
- [112] Z. Bajnok, L. Palla, G. Takács: Boundary states and finite size effects in sine-Gordon model with Neumann boundary condition, *Nucl. Phys.* **B614**, 2001, 405-448, hep-th/0106069
- [113] J.S. Caux, H. Saleur, F. Siano: The two-boundary sine-Gordon model, *Nucl. Phys.* **B672**, 2003, 411-461, cond-mat/0306328
- [114] T.R. Klassen, E. Melzer: Spectral flow between conformal field theories in 1+1 dimensions, *Nucl. Phys.* **B370**, 1992, 511-550
- [115] G.Zs. Tóth, G.M.T. Watts, in preparation
- [116] Al.B. Zamolodchikov: Mass scale in the sine-Gordon model and its reductions, *Int. J. Mod. Phys.* **A10**, 1995, 1125-1150
- [117] M. Fabrizio, A.O. Gogolin, A.A. Nersesyan: Critical properties of the double-frequency sine-Gordon model with applications, *Nucl. Phys.* **B580**, 2000, 647-687, cond-mat/0001227
- [118] G. Mussardo, V. Riva, G. Sotkov: Semiclassical Particle Spectrum of Double Sine-Gordon Model, *Nucl. Phys.* **B687**, 2004, 189-219, hep-th/0402179
- [119] T. Quella: Asymmetrically gauged coset theories and symmetry breaking D-branes: New boundary conditions in conformal field theory, PhD thesis, Humboldt University, Berlin, Germany, 2003

Summary of the main results

In my thesis I study problems in three areas of $1 + 1$ -dimensional quantum field theory. These investigations are described in three largely independent chapters.

In Chapter 2 I deal with the boundary bootstrap for the scattering theory of supersymmetric massive integrable quantum field theories with a boundary in a special framework in which the blocks of the full S-matrix and reflection matrix are assumed to take the form of a product of a supersymmetric and a non-supersymmetric factor. I give a description of supersymmetry in the presence of a boundary, i.e. when the space is the half-line. I present rules for the determination of the representations in which higher level boundary bound states transform, and for the determination of the supersymmetric one-particle reflection matrix factors for the higher level boundary bound states. These rules apply under the assumption that the bulk particles transform in the kink or in the boson-fermion representation. I also present examples for the application of these rules to specific models.

In Chapter 3 I investigate the effect of the Hilbert space truncation applied in the numerical method called truncated conformal space approach (TCSA) on boundary flows in the case of the critical Ising model on a strip with magnetic perturbation on one of the boundaries. The main goal is to show that the effect of truncation on the spectrum can be taken into consideration approximately by a change of the coefficients of the terms in the Hamiltonian operator. I present the results of numerical and perturbative calculations, which support this idea. I also present a comparison with another truncation method which preserves the solvability of the model. The changing of the coefficients appears to work for this truncation method as well. The comparison reveals that certain qualitative properties of the flows of the truncated spectra depend on the particular truncation method applied. The chapter includes an exact quantum field theoretic solution of the model under consideration, in particular the calculation of the spectrum and the matrix elements of the fields. I also propose a description of the model as a perturbation of its infinite coupling constant limit. I present the description of the spectrum by the Bethe-Yang equations, which gives the exact result in this case.

In Chapter 4 I investigate the phase diagrams of the two- and three-frequency sine-Gordon models by the TCSA method. The focus is mainly on the finding of a tricritical point in the case of the three-frequency model. I give substantial evidence that this point exists. I also find several points of the critical line in the phase diagram and present TCSA data showing the change of the finite volume spectrum along the critical line as the tricritical endpoint is approached. I find a few points of the line of first order transition as well.

A fő eredmények összefoglalása

Doktori értekezésemben az $1 + 1$ -dimenziós kvantumtérelmélet három részterületéhez tartozó problémákkal foglalkozom. Ennek megfelelően az értekezés három lényegében független részre oszlik.

A 2. fejezetben a szuperszimmetrikus peremes integrálható kvantumtérelméletek szóráselméletét tanulmányozom egy speciális konstrukció keretei között, amelyben a teljes S-mátrix és reflexiós mátrix blokkjai egy szuperszimmetrikus és egy nem szuperszimmetrikus rész szorzataként állnak elő. Tárgyalom a szuperszimmetria definícióját perem jelenléte esetén, továbbá megadok olyan szabályokat, amelyek segítségével meghatározhatók az egyes magasabb energiájú határkötött állapotokon megvalósuló ábrázolások, és az ezen állapotokról történő részecskeviszazaverődés mátrixának szuperszimmetrikus részei. Ezek a szabályok abban az esetben alkalmazhatóak, amikor az elmélet részecskéi a kink vagy a bozon-fermion ábrázolás szerint transzformálódnak. A szabályok alkalmazását konkrét példákon is bemutatom.

A 3. fejezetben a levágott konform tér közelítés (TCSA) nevű numerikus módszer alkalmazásakor végzett levágásnak a peremes renormálási csoport folyamokra való hatását tanulmányozom egy konkrét modell, a határon mágneseszen perturbált, szakaszon értelmezett kritikus Ising modell esetén. A kitűzött cél annak az elképzelésnek az igazolása, hogy a levágás hatása a spektrumra figyelembe vehető a Hamilton operátorban szereplő tagok együttthatóinak megváltoztatásával. Ismertetem az általam végzett numerikus és perturbatív számolások eredményeit, amelyek alátámasztják ezt az elképzelést. Elvégeztem az említett számolásokat egy olyan levágási eljárás esetén is, amelyik az eredeti modell egzakt megoldhatóságát nem szünteti meg. Az együttthatók megváltoztatása ebben az esetben is alkalmasnak látszik a levágás hatásának figyelembe vételére, továbbá kiderül, hogy (levágás alkalmazása után) a folyamatok kvalitatív viselkedése függ az alkalmazott levágási eljárástól. Megadom a vizsgált modell egy egzakt kvantumtérelméleti megoldását, amely magába foglalja többek között a spektrum és a terek mátrixelemeinek kiszámítását. Javaslom a modellnek egy a végtelen csatolású határeset perturbációjaként való leírását. Elvégzem a spektrum kiszámítását a Bethe-Yang egyenletekkel is.

A 4. fejezetben a két- és háromfrekvenciás sine-Gordon modell fázisszerkezetének a TCSA módszerrel való feltérképezésével foglalkozom. A fő eredmény ebben a fejezetben egy trikritikus pont megtalálása. Emellett megkeresem annak a kritikus vonalnak számos pontját, amelyiknek a végén a trikritikus pont található, és bemutatom a véges térfogatbeli spektrum változását a kritikus vonal mentén a trikritikus pont felé haladva. Megkeresem a fázisdiagramban található elsőrendű fázishatár néhány pontját is.